Study on Cellulose Hydrogel Films Regenerated From Natural Plant Bagasse and Their Bio and Cytocompatible Properties for Tissue Engineering

（天然植物バガス廃棄物から再生したセルロースハイドロゲルフイルムと再生医学のための生体ならびに細胞適合性特性に関する研究）

Tovar-Carrillo Karla Lizette
(トバールカリージョ カーラ リゼッテ)

Energy and Environmental Science
Nagaoka University of Technology

March 2014

Acknowledgments

I wish to express my deepest gratitude to Dr. Takaomi Kobayashi of the Department of Material Science and Technology, Nagaoka of Technology, Nagaoka, Japan, for his for his continuous support, supervision, guidance and encouragement throughout my study during the period from September 2010 to Mach 2014.

I would also like to thank Assist. Prof. Motohiro Tagaya for his kindly support, comments and suggestions during doctoral program.

I would like to express a very special thank you to Dr. Rosa Saucedo for her support and help to accomplish this goal in my life. I will like to also express my gratitude to Dr. Armando Zaragoza for all his help and advises.

I am also extremely grateful to The University of Cd. Juarez, en Mexico, for supporting me favorable conditions when I studied in Japan.

Last but not least, I send my special thanks and love to my family and friends. Their continuous support and encouragement were the inspiration and motivation for me, even during tough times in the Ph.D pursuit.

Karla Lizette Tovar Carrillo

Contents

Chapter 1 General Introduction

1.1 Biomass Polymer hydrogels

Since the pioneering work of Wichterle and Lim in 1960 on crosslinked hydroxyethyl methacrylate (HEMA) hydrogels [1], great interest to biomaterial scientists have been focused for many years. The large interesting characters are their hydrophilic nature and potential to be compatible materials [2-9]. In addition, later in the 1980s, Yamas et. al. [10] incorporated natural polymers such as collagen and shark cartilage into hydrogels for use as artificial burn dressings. As shown in Table 1-1, hydrogels based on both natural and synthetic polymers have continued to applying interest for encapsulation of cells [11-14]. Then, most recently such hydrogel has become especially attractive to "tissue engineering" as matrices for repairing and regenerating a wide variety of tissue and organs [9-15]. Hydrogels consisted of hydrophilic polymer networks which can absorb from 10-20% up to thousands of times to their dry weight in water. Various hydrogels originated from natural polymers have been used in hyaluronate [16,17] alginate [18], starch [19], chitosan, and their derivatives [20,21], and cellulose [22-26], These due to their potential application, their safety, hydrophilicity, biocompatibility and biodegradability. Among them, hyaluronic acid (HA) is well-known polysaccharide and composed of the repeating disaccharide units D-glucuronic acid and *N*-acetyl-D-glucosamine. It is one of the glycosaminoglycan (GAG) components in natural extracellular matrices (ECM) and plays an important role in many biological processes, such as lubrication, matrix assembly, cell proliferation, and differentiation [70,71]. ECM is the network which provides structural and biochemical support to the surrounding cells. Here, HA is nonimmunogenic and biodegradable, making it attractive in tissue engineering. The abundant hydroxyl and carboxyl groups of HA can

be modified to amine, hydrazide, thiol, acrylate, and phenol functionality [25-27]. The mechanical and degradation properties of HA-based hydrogels are adjusted with the molecular weight, the degree of functionalization, and the polymer concentration [28,29]. Additionally, HA and its derivatives have been clinically used as medical products for altering the properties of the resulting materials, including modifications leading to hydrophobicity and biological activity. Living derivatives of HA can form new covalent bonds in the presence of cells, tissues, and therapeutic agents. In most cases, living HA derivatives are required for clinical and preclinical uses in 3D cell cultures and in vitro cell delivery. Chitosan that is a partially deacetylated derivative of chitin, comprised of glucosamine and *N*-acetylglucosamine residues, has a chemical structure having similarity to GAGs in the ECM of cartilage, as related biofunctions in cartilage regeneration, chitosan is known to be enzymatically degraded in vivo by lysozyme, which is found in cartilage [29-32]. Chitosan-based hydrogels were developed from acidified chitosan solutions by neutralization with basic glycerophosphate [33,34]. Chemical modifications of chitosan with different hydrophilic moieties are used to produce water-soluble chitosan derivatives [35-37]. Water-soluble chitosan derivatives can be used to prepare hydrogels either by physical or chemical crosslinking. Studies have demonstrated that chitosan-based hydrogels supported and enhanced both chondrogenesis and osteogenesis in vitro [38,39] and in vivo [40]. Due to their hemostatic properties, chitosan is a natural polymer as known in the medical world for wound management; it is derived from chitin, accelerates bone formation and has regenerative effect on connective gum tissue. Chitosan can be used to prevent or treat wound and burn infections, and also be applied as slow-released drug-delivery vehicle for growth factors to improve wound healing. It is widely preferred because of its hemostatic, antimicrobial, nontoxic, biocompatible and biodegradable properties. Alginate, a natural-occurring anionic

polysaccharide composed of 1,4-linked β-D-mannuronate (M) and 1,4-linked α-L-guluronate (G) residues. Such polysaccharide is well-known for its gelling features with reversible crosslinking via ionic interactions between carboxylic groups and bivalent cations like Ca^{2+}. An alginate gels strength decreases ~40% within the first 9 days in vitro [41]. Covalent by crosslinking alginates are being explored by oxidative coupling [42] and Schiff-base formation [41]. Dextran, a glucose homopolysaccharide consisting of α-(1→6)-linked glucan with branches attached to the O-3 of the backbone chain units, is commercially available in a wide range of molecular weights. This polymer is soluble in water forming low viscosity solutions. Dextran can be chemical modified to introduce aldehyde groups [43] and other functional groups, such as (meth) acrylates [44,45], thiols [46], phenols [47], maleimide [48], and vinyl sulfones [99]. Dextran hydrogels are used for sustained protein and drug delivery [46,50] and, by incorporating specific cell-adhesive peptides, in tissue engineering scaffolds [51]. Nowadays, these fibers have become important materials for wound dressing because they have unique gel forming characteristics. The gelation structure keeps the area between the dressing and the wound moist, consequently assisting the healing process. Such fiber is widely used for manufacturing modern dressing materials and suitable for using on medium to heavily oozing wounds and cavities. Dressings made from alginate fiber are bio absorbable and non-adherent, so that it can easily be removed from a wound without causing any pain or discomfort. Often, this dressing is used to treat diabetic foot ulcers.

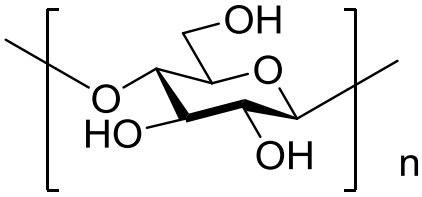

Figure 1.1. Cellulose chemical structure

Among them, cellulose (Fig. 1.1) is the most abundant renewable resource on earth [47-49]. Moreover, numerous new functional materials from cellulose are being developed over a broad range of applications because of the increasing demand for environmentally friendly and biocompatible products [40,41]. Recent literature has been cited their advances on cellulose-based hydrogel materials including pure cellulose, cellulose composite, and cellulose hybrid hydrogels [32].

Rapid progress has been made in recent years in the field of biomedical materials, which utilize both natural and synthetic polymers. Thus, cellulose-based materials can be used in a variety of applications, including wound closure, drug delivery systems, novel vascular grafts, or scaffolds for in vitro or in vivo tissue engineering. As mentioned, biopolymers are important in all aspects of medicine, surgery and healthcare. These biomaterials require only simple technologies to process them, and research in the field of biopolymers is constantly making process. In biopolymers, several polysaccharides including hyaluronic acid, dextran, and alginate have interesting physical and biological applications. Cellulose, a polysaccharide has already been used quite successfully as scaffold for cell adhesion, proving that it could become a high-value product in the field of tissue engineering, as seen in Table 1-2. Numerous new functional materials from cellulose are being developed over a broad range of applications, because of the increasing demand for environmentally friendly and biocompatible products. The general belief is that biodegradable polymer materials prepare from cellulose will reduce the need for synthetic polymer production at a lower cost, thereby producing a positive effect in the future, both environmentally and economically.

Table 1-1. Polymers used to synthesize hydrogels matrices

Polymers used to synthesize hydrogel matrices	
Natural Polymers and their derivatives (± Crosslinkers)	
Anionic polymers: Hyaluronic acid (HA), Laginic acid, pectin, carrageenan, chondroitin sulfate, dextran sulfate	[12-16]
Cationic polymers: chitosan, polylysine	[15-18]
Amphipathic polymers: collagen (and gelatin), carboxymethyl chitin, fibrin	[11-14]
Neutral polymers: dextran, agarose, pullulan	[12-15]
Synthetic polymers (± Crosslinkers)	
Polyesters: PEG-PLA-PEG, PEG-PLGA-PEG, PEG-PCL-PEG, PLA-PEG-PLA, PHB, P (PF-$_{CO}$-EG) ± acrylate end groups, P(PEG/PBO terephthalate)	[10-13]
Other polymers: PEG-bis-(PLA-acrylate), PEG±CDs, PEG-g-P(AAm-co-Vamine), PAAm, P(NIPAAm-co-AAc0, P(NIPAAm-co-EMA), PVAc/PVA, PNVP, P(MMA-co-HEMA), P(AN-co-allyl sulfonate), P(biscarboxy-phenoxy-phosphazene), P(GEMA-sulfate)	[11-14]
Combinations of natural and synthetic polymers	
P(PEG-co-peptides), alginate-g-(PEO-PPO-PEO), P(PLGA-co-serine), collagen-acrylate, alginate-acrylate, P(HPMA-g-peptide), P(HEMA/Matrigel), HA-g-NIPAAm	[12-16]

Table 1-2. Cellulose-based hydrogels.

	Methods	Hydrogel	Applications
Hydrogels prepared direct from Native cellulose	LiCl/dimethylacetamide (DMAc) system.	Natural cellulose films	Industry, medical applications [28]
	NMMO system	Natural cellulose films, fibers, food castings, membranes, sponges, beads.	Industry, food companies [26-28]
	ILs system	Flexible gels obtained	Industry [28]
	Alkaly/urea ot Thiourea aqueous systems	Weak gels can be obtained	Industry [25-27]
	BC hydrogels	Films, membranes and gels	Medical applications [26-27]
Hydrogels from cellulose derivatives	Physical cross-linking	Methyl cellulose (MC) Hydroxypropyl cellulose (HPMC) Hydroxypropylmethyl cellulose (HPMC) Carboxymethyl cellulose (CMC)	To prepare biomedical matrices. To coat the surface of polystyrene dish to cultivate embryonic cells [25-28]
	Chemical cross-linking	HPC with epichloronhyndrin (ECH) CMC/HEC	Drug delivery systems, pharmaceutical [26]

Table 1-2. *Continued*

Type of preparation	Methods	Hydrogel	Applications
Cellulose-polymer composite hydrogels	Blend with natural polymers	MC blend with hyaluronan	Delivery drug system, Tissue engineering [25]
		Cellulose-sodium alginate	
	Blend with PVA	PVA/ECH	Drug delivery system, medical applications [26-27]
		BC/PVA	
	Polyelectrolyte complexes	CMC/Chitosan	Hydrogels can bend toward either anode o cathode [25,26]
		Polyvinylamine (PVAm)/CMC	
	Interpenetrating Polymer Networks (IPNs)	BC/poly acrylamide	Used as vehicles for controlled delivery of ciprofloxacine [27]
		Poly (*N*,*N*-dimethylacrylamide/cellulose	
Cellulose inorganic hybrid hydrogels	Biphasic calcium phosphate mixed with HMPC	Si-HMPC	Bone substitute and also developed for filling bone [26,27]
	BC as template for formation of calcium	Calcium-deficient hydroxyapatite (CdHAP)	Precursor similar to natural bone apatite [26,27]
	Heparin with cellulose	Heparin/Cellulose/Charcoal	Blood compatibility of activated charcoal [25-27]

As mentioned, hydrogels based on natural polymers and cellulose has been elaborated for medical applications. It some cases, it has been observed that the obtained hydrogels showed poor mechanical properties forcing to crosslink for solving this problem or synthesizing derivatives as well as composites, and affecting in some cases the biocompatibility of the obtained material. Hydrogels elaborated with natural cellulose show poor mechanical properties, but has bio and cytocompatibility without the presence of cross linkers or any other chemical modification reducing the possibility of adverse reactions in the body.

1.2 Cellulose as sustainable materials

In nature, cellulose is the structural material for plant cell wall. This is reason for that cellulose is an environmentally friendly and renewable biomaterial as sustainable materials. Two statistical data can give us the idea that how important this biomaterial is to our daily life. It constitutes around 1.5×10^{12} tons of the total annual biomass production and approximately 2% (3.2 million tons in 2003) are used for production of cellulose regenerate fibers and films. It is known that cellulose is the main structural material in plant cell wall [32], which contributes 45% of wood mass. The less abundant components are hemicellulose and lignin. The former takes about 35% in hardwoods and 25% in softwoods, while the latter takes up 21% in hardwoods and 25% in softwoods respectively [33,34].

As sustainable cellulose, for example, agave bagasse waste is very interesting for regeneration in Mexico [33]. Agave bagasse is the residual fiber remaining after cooked agave heads are shredded, milled and the sugar water-extracted. The bagasse is primarily the rind and

fibrovascular bundles dispersed throughout the interior of the agave head. It represents about 40% of the total weight of the milled agave on a wet weight basis.

Tequila industry represents economic importance in Mexico. For example, The Tequila Company Corralejo, is one of the most important tequila companies in Mexico. This company use blue agave plant primarily in the area surrounding the city of Tequila located at northwest of Guadalajara, and in the highlands (Los altos) of the north western Mexican state of Jalisco. Mexican laws state that tequila can be produced only in the state of Jalisco and limited regions in the state of Guanajuato, Michoacán, Nayarit and Tamaulipas.

Research work on the use of agro-industrial waste is needed because of the serious economic and environmental problems caused by the disposal of these resources. The possibility of utilizing at least part of agave bagasse as an efficient ruminant feed could have a major impact on livestock production practices in areas where tequila is produced. The availability of energy to the close physical and chemical association between structural carbohydrates and lignin and the crystalline arrangement of the cellulose polymer in plant cell walls.

The bagasse fibers could also be used to produce a wide variety of other products such as filters, sorbents, geotextiles, fiberboards, packing, molded products or in combination with other resources. The purpose of the present study was to investigate the use of agave bagasse pith as a possible animal feed and the fiber for fiberboard production.

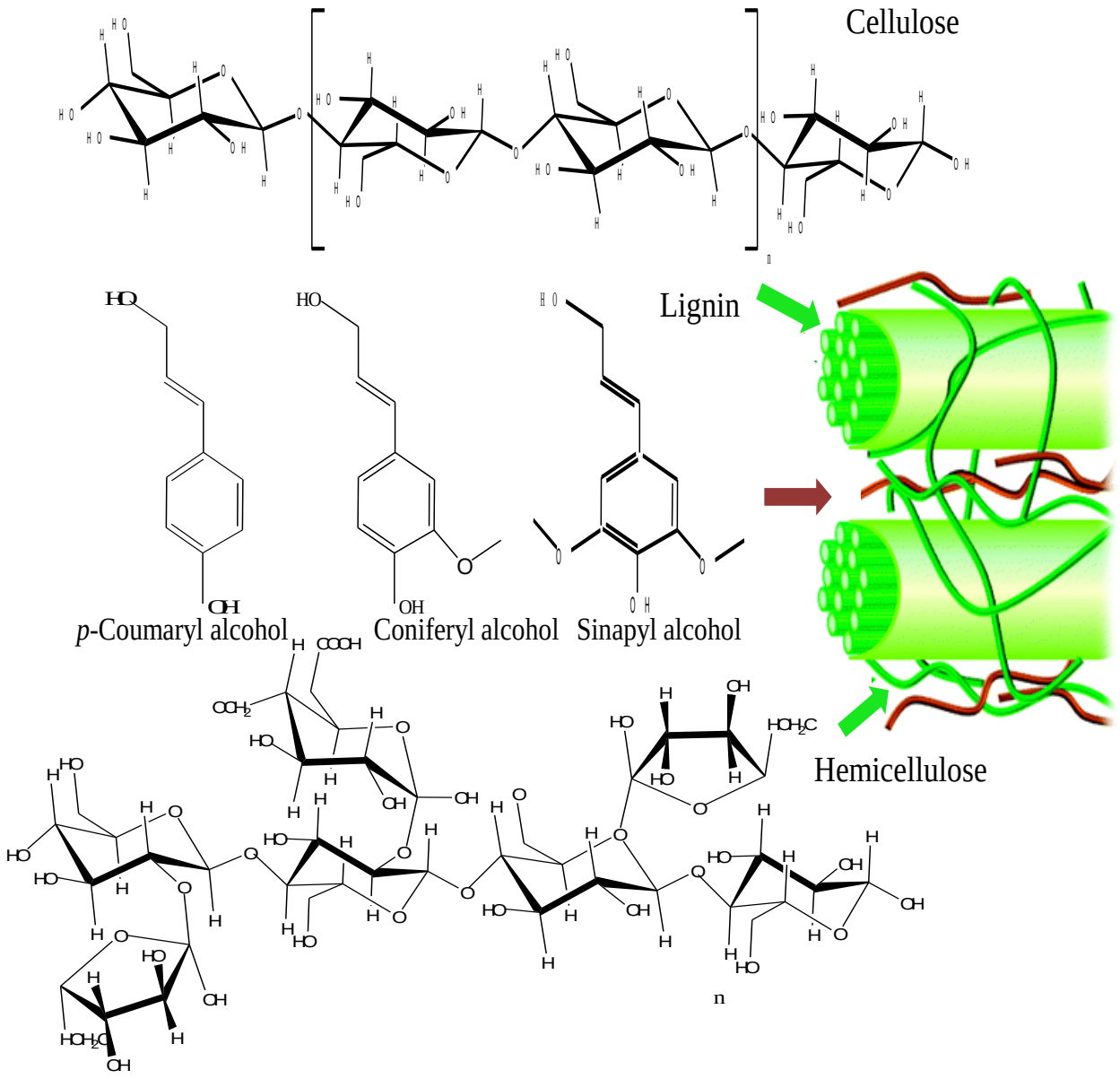

Figure 1.2 Components of primary cell wall.

As shown in Figure 1.2, cellulose has the basic molecular unit in $C_6H_{10}O_5$ and constructed by so called anhydroglucose unit (AGU). The cellulose molecule is linked in the form of β-1, 4-glucan. The polymer chain length is expressed as the number of AGUs or degree of polymerization, DP.

Generally, 20-30 repeating units give all the cellulose properties. Figure 1.3 shows elementary cellulose fibrils and the different levels of organization in the cell wall of the plants [29].

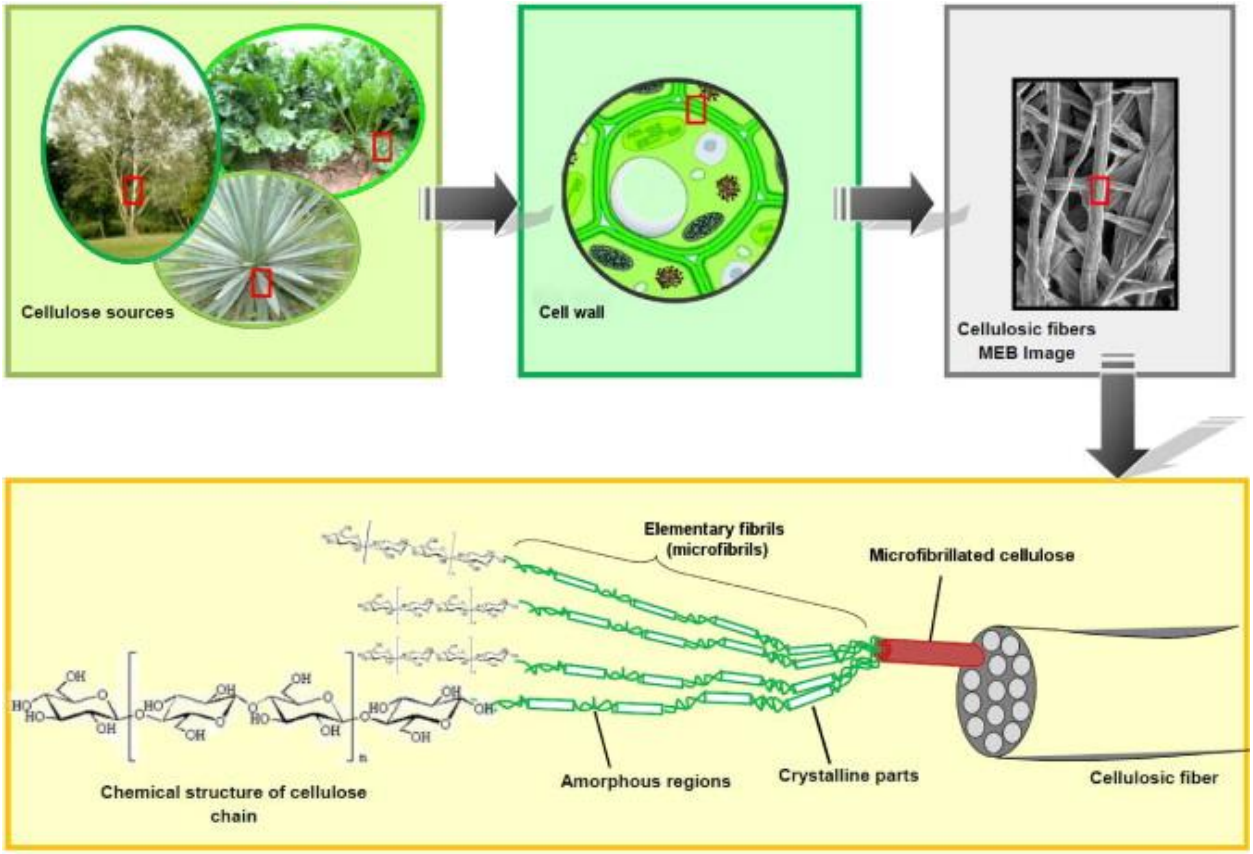

Figure 1.3. Elementary cellulose fibrils and the different levels of organization in the cell wall of plants [28,29].

Cellulose fibers, as pulp fibers are the fibrous residue remaining after the mechanical chipping of pulp wood and the chemical treatment design to remove lignin in other impurities from the cellulose fibers. The two main classes of trees yielding cellulose fibers are softwoods or coniferous trees and hardwoods or deciduous trees. The cellular structure of both types of trees is a highly complex subject, but some general features are common to both types. The bulk of

wood pulp cellulose comes from xylem. The xylem is the part of a tree which has ceased to grow and provides mechanical strength and conveys sap to the growing portions of the tree. The xylem provides the main bulk of tree trunks and larger branches. The structure consists of elongated parallel cells with cell walls that have been thickened by the deposition of layers of cellulose and strengthened by lignin. In the cellulose extraction of wood, which consists of chemical action with mechanical agitation, most of the lignin and other impurities are dissolved, and the fiber structure is disintegrated longitudinally. Such fibrous material is in the form of flat ribbons, usually with flattened internal canals. The structure of the cell wall is somewhat porous due to the strong chemical attack and removal of lignin. The fibers of conifers wood are the remains of cellular elements known as tracheids which are elongated single vessels which are formed by the fusion of rows of shorter cells. Cellulose fibers, depending on the part of the plant from which they are taken, can be classified as; grasses and reeds (bamboo and sugarcane), leaf fibers (as sisal and referred as hard fibers), Bast fibers (as kenaf), seed and fruit hairs (as cotton and coconut) and wood fibers (as wooden pulp). These fibers consist of several fibrils that run along the length of the fiber. In vascular plants, the average chain length is determined by the structural purpose of the cellulose in the plant cell wall and the species of the plant. As shown in Figure 1.3, the cell wall in cellulose consists of highly crystalline and regular regions of pure cellulose interspaced with small regions of irregular or amorphous cellulose. These amorphous regions usually contain small amounts of impurities. Present theory describes the beta-linked glucose chains in the crystalline regions as forming flat ribbons with the glucose rings of each chain lying in the same plane while the hydroxyl groups on the glucose molecules protrude above and below the plane of the cellulose ribbon. Bundles of these cellulose ribbons are called microfibrils. The microfibrils vary in width from 0.008 to 0.03 μm and are approximately half as thick as they are

wide. The microfibril bundles are held together by hydrogen bonds formed between the protruding hydroxyl groups of the flat glucose molecules. The hydrogen bonding in these microfibrils is very strong with the microfibrils remaining intact except under several processing conditions. It is noted that, the main structural unit of cellulose in the plant wall consists of these cellulose microfibrils bonded together in a polymeric matrix. In filament-wound rocket motor casings, the filaments are bonded together by polymer resins. The microfibrils are covalently bonded together by various polymeric sugars and proteins (Fig. 1.3). The covalent bonded microfibrils are often found grouped into fibrils. These cellulose fibrils are generally between 0.05-0.3 μm in diameter with an average diameter of approximately 0.15 μm and up to 20 cm or more in length. The presence of the fibrils and their length, and the exact composition and the amount of the fibril bonding materials are determined primarily by plant species and function, with the microfibrils serving as the main building unit of the fibrils. These fibrils then form the various structured features found in the plant cell.

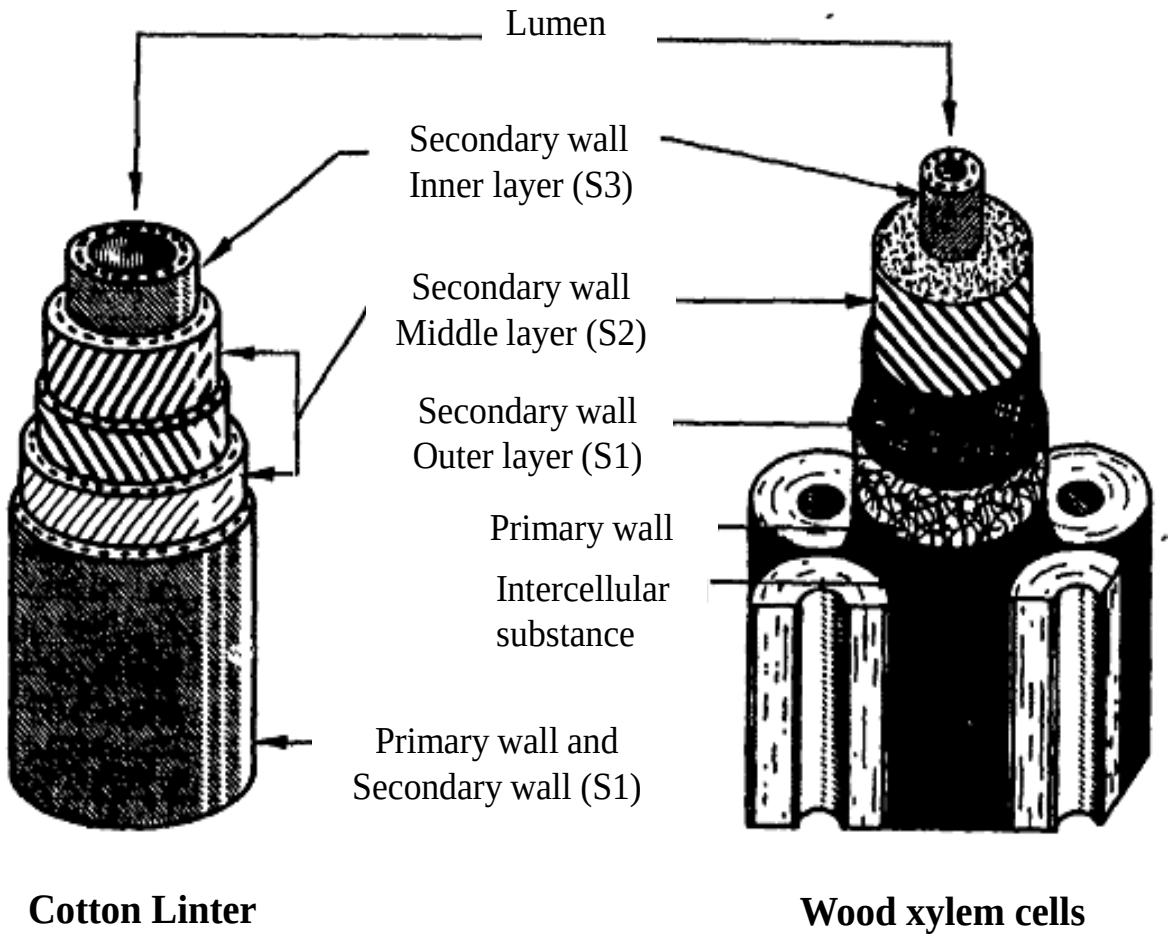

Figure 1.4. Model of basic cell wall structures of cotton and wood cells showing structures of cell walls [31].

The figure 1.4 shows basic drawing for cell wall structure of cotton and wood cells. The plant cells grow first by forming primary or outer wall after the nucleus has divided during cell division (mitosis). This primary cell wall consists of layered cellulose fibrils. In cotton linters, this primary wall consists of dense spiral wrapped layers of cellulose fibrils. In wood cells, the primary cell wall is formed of matted fibrils resembling matted felt and is usually coated with an outer protective or bonding layer. In cotton fibers, a waxy cuticle to protect the exposed cell wall,

as cotton fibers in the cotton ball consist of single individual row of plant cells which are coated by intercellular materials that connect adjoining cell walls together. As a general rule, each secondary cell wall is formed of alternating angles of spiral wrapped cellulose fibrils. The angles of the spiral wrapping and the thickness of these layers are determined by the species, the maturity of the cell, and growth conditions.

As the plant matures to full size, the successive layers of fibrils in most cell walls are thought to slowly unwind and become more and more parallel. Thus, cotton linters possess a highly defined, spiral wrapped pattern of the fibrils while the fibrils in wood pulp fibers, which consist mainly of mixture of mature xylem cell, appear almost parallel.

As the plant reaches its maximum length and maturity two main processes occurs, the first is the deposition of lignin, as drawn in Figure 1.2. Lignin is a complex polymer of condensed, substituted phenols. It is water insoluble and highly resistant to chemical attack. Lignin is the major binder for the cellulose in the cell wall and provides the strength and rigidity of woody tissues. The amount of lignin deposited will control the flexibility of the cell wall. Other materials deposited during maturation involve hemicellulose, pectin, and some proteins. This process occurs in both trees and in the woody portions of cotton plants. The cotton fibers contain little lignin and are thus very flexible. The end result is a plant cell with a rigid cell wall composed of elongated cellulose fibrils surrounding a hollow center that is used to convey sap to the growing regions of the plant. In wood pulp fiber, the dry weight of the fibers is 40-60 percent cellulose prior to processing while cotton linter contains 70-97 percent cellulose by dry weight.

Like cotton and woods, there are wide varieties of fibers that can be used as cellulose source. These include wood fibers, such as team-exploded fibers, and a variety of agro-based fibers in stems, stalks, bast and seed hairs. These fibers are abundantly available throughout the world and

come from renewable resources [31-34]. Other large source are recycling agro fiber-based products such as paper, waste wood, and point source agricultural residues such as rice hulls from rice processing plant [32].

The properties of these fibers are strongly influenced by many factors (Table 1-3), particularly chemical composition and internal fiber structure, which differ between the different parts of the plant as well as between different plants. The most efficient cellulose fibers are those with high cellulose content coupled with low fibril angle, such as cellulose content of more than 60% and fibril angle in the range of 7-12° to the fiber axis [29-32].

Cellulose fibers present many advantages compared to synthetic fibers which make them attractive for different applications such as cellulose source. The come from abundant and renewable resources at low cost which ensures a continuous fiber supply and a significant material cost saving [32-34].

Table 1-3. Mechanical properties of some cellulose fibers.

Fiber	Diameter (μm)	Density (g/cm^3)	Moisture content (%)	UTS[1] (MPa)	Modulus (GPa)	
Cotton		1.5		500-880	0.05	
Jute	200	1.45	12	460-533	2.5-13	
Coir	100-450	1.15	10-12	131-175	4-6	
Banana	80-250	1.35	10-12	529-754	7.7-20.8	
Sisal	50-200	1.45	11	568-640	9.4-15.8	
Conifer		1.50		1100	100	
Kraft fiber		1.54		1000	40	
Sunhemp	48	0.673		200-300	2.68	
Pineapple	20-80	1.44		413-1627	34.5	
Palm leaf	240			98.14	2.22	
Kenaf	200	1.47		157.38	12.62	
Kusha grass	390			150.59	5.69	[31-34]

The cellulose microfibrils bundles are held together by hydrogen bonds formed between the protruding hydroxyl groups. The hydrogen bounding in these microfibrils is very strong and remains intact except under several processing conditions such as, elevated temperatures, strong solvents, acids, and bases. The microfibrils are bonded together by various polymers sugars and proteins. These covalent bonded microfibrils are often found grouped into fibrils. When cellulose is obtained from natural fibers, one of the first steps is to remove all the possible amount of fiber impurities as lignin, hemicellulose and others. After this process cellulose fibrils are the main constitute of the natural fiber full of protruding hydroxyl groups. The structure of these aggregates has been described in terms of a "fringed" micellar structure. Figure 1.5 shows a schematic possibility for such an aggregate, composed of laterally aligned chains, forming a rather compact and probably geometrically anisotropic core, immiscible with the solvent. The "coronas" at both ends of the particle consist of solvated amorphous cellulose chains. Formation of fringed micellar structure is backed by experimental evidence. For example, increasing cellulose concentration results in a pronounced increase in molar mass of the particle, although its dimensions increase only slightly. The geometric anisotropy of the central part of the micelle is expected to be associated with optical anisotropy. Additionally, it may be visualized by an appropriate experimental technique. Both expectations have been confirmed by use of shear-induced birefringence, and electron microscopy [33]. The number of chain molecules, forming the aggregate, and the thickness of the coronas increase as a function of increasing both cellulose concentration, and the interfacial tension between the particle core and the solvent system [32-34]. Parts (B) and (C) of Figure 1.5 refer to mono-disperse solutions of a small DP (B), and large DP (C) cellulose molecules. The former part shows that the length of the short cellulosic chain is practically equal to its persistent length; there is neither coiling, nor interactions between the

chains. In Figure 4c, the flexibility of the long chain polymer permits the formation of strong intra-molecular hydrogen bonds, provided that the OH groups reside for some times within a "critical distance" from each other, sufficient for the van der Waals interactions to operate [34].

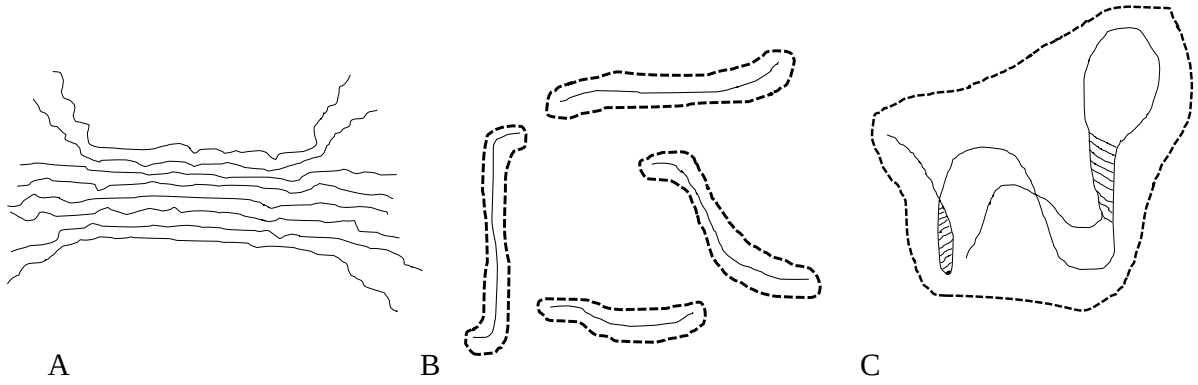

Figure 1.5. Schematic representation of cellulose structures in solution: Part A shows the "fringed" micellar structures. Parts B and C show possible chain conformation of celluloses of different DP. For high molecular weight cellulose, C, intra-molecular hydrogen bonding is possible.

For the same cellulose, the accessibility of the hydroxyl groups increases as function of decreasing solution concentration. For different celluloses, at the same concentration, only the outer surface of the fringed micelle core is accessible, the area of this part decreases as function of increasing DP and Ic. Researchers have been indicated the presence of aggregates in the LiCl/DMAc solvent system, whose size depends on the pre-treatment employed, DP, concentration of LiCl, and presence of water. Molecularly dispersed cellulose solutions are obtained at low polymer- and high LiCl concentrations [35]. Non-cellulosic materials may lead to further aggregation. Whereas hardwood Kraft pulps were found to be completely soluble in

this solvent system, soft-Kraft pulps were not, due to relatively higher contents of mannan, lignin, and nitrogen-containing compounds (originated from degraded proteins). One of the reasons that mercerization may lead to better derivatization results, is the effect of sodium hydroxide-mediated removal of non-cellulosic material on the physical state of cellulose in solution.

Figure 1.6 shows

a)

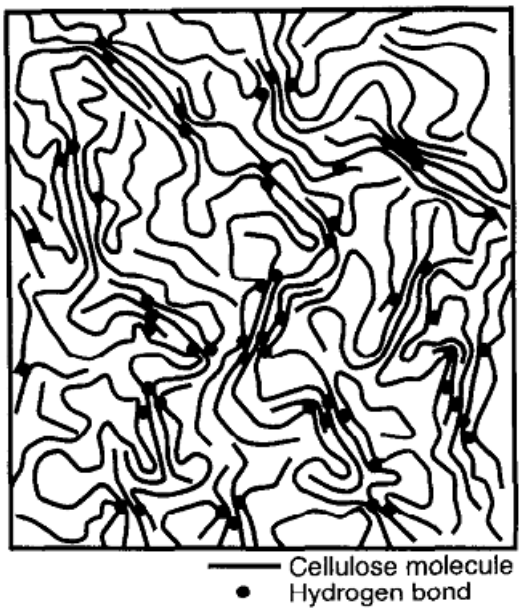

b)

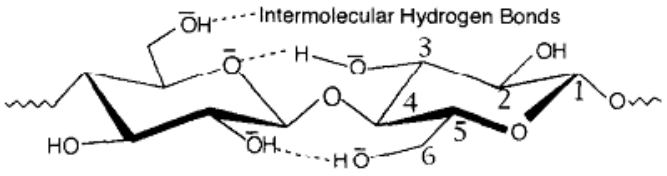

Intra; OH at C-2 and OH at C-6
OH at C-3 and O in the neighboring ring.
Inter; OH at C-2, C-3 and C-6

Figure 1.6. a) Schematic model proposed for amorphous cellulose, b) cellulose structure involving either intra- or intermolecular hydrogen bonding.

1.3 Difficulty in dissoluble cellulose

In the fabrication of cellulose-based materials, there is a key process which is destroying the hydrogen bonds. If we prepare cellulose hydrogels, it is necessary to be that cellulose can be prepared from a cellulose solution. Because cellulose has many hydroxyl groups which can form

hydrogen bonding linked network easily. The basic requirement for cellulose dissolution is that the solvent is capable to interacting with the hydroxyl groups of the AGU, so is to eliminate, at least partially, the strong inter-molecular hydrogen-bonding between the polymer chains. Cellulose is hard to dissolve due its stiffness, it contains hydrophilic and hydrophobic parts, but due its stiffness it cannot adjust its conformation to reduce the contact between hydrophobic parts and water. For this reason, is very difficult to dissolve cellulose in common solvents. However, for preparing cellulose hydrogel, lack of appropriate solvents delays the development for the preparation of cellulose hydrogels [28-31]. Figure 1.7 shows different approaches of cellulose dissolution. There are two basic schemes for cellulose dissolution: (i) Where it results from physical interactions between cellulose and the solvent; (ii) where it is achieve via chemical reaction, leading to covalent bond formation "derivatizing solvents".

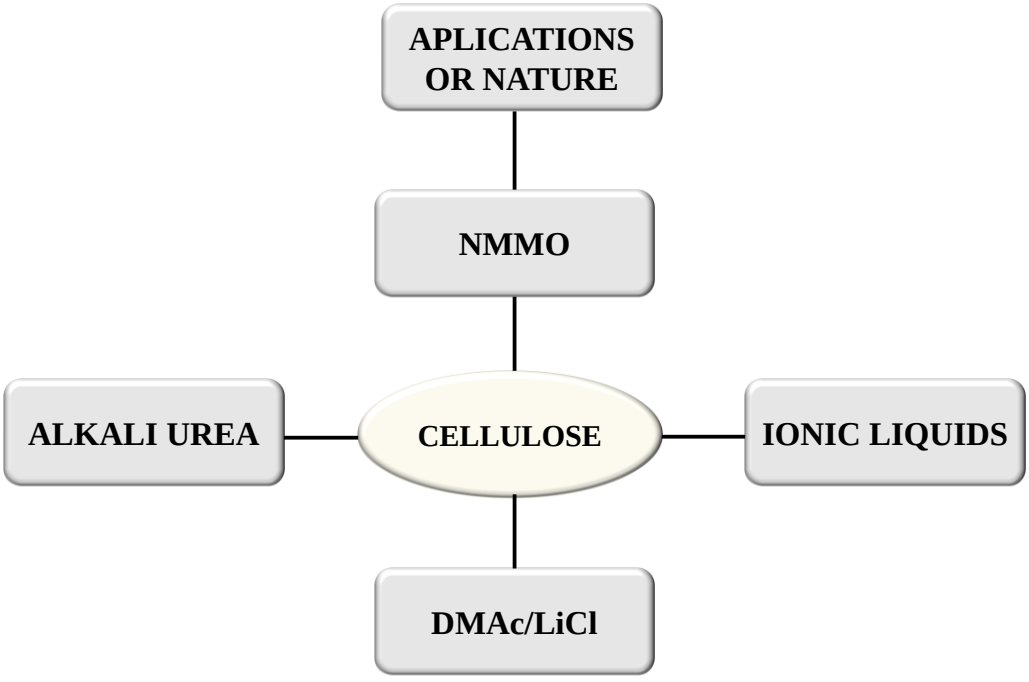

Figure 1.7. Different approaches for dissolution of cellulose.

Table 1-4 lists some conventional solvents for cellulose. Sulfuric acid hydrolysis is now widely used to yield cellulose whisker microcrystals [35]. It is believed that sulfuric acid destroys the amorphous regions of the cellulose fibers and allows the grafting of sulfate groups on the surface. This can stabilize the aqueous whisker suspensions by electrostatic repulsion [35-37]. Alkali chemicals including LiOH and NaOH can be used to swell and activate cellulose. Alkaline Xanthogeneration is also well known as traditional viscose rayon process [35,36], but became the high toxicity. Therefore, it is gradually replaced by other process. For an example, in lyocell production, *N*-methylmorpholine-*N*-oxide (NMMO) is a solvent to be used in partially industrialized process. In general, alkali hydroxide solutions possess some of these requirements, e.g., those of cost, ease of recycling, and high polarity. Indeed, a clear solution was obtained when microcrystalline cellulose was swollen by 8 to 9 wt% aqueous solution of NaOH [35-38]. However, it is difficult to dissolve substantially all cellulose having a high degree of polymerization (DP>300) in an alkali aqueous solution. Consequently, aqueous NaOH solutions are not suitable for technical applications [35-39], and only cellulose with lower molecular weight could be dissolved in this solvent. Kamide et al. reported that steam-exploted chemical wood pulps could be dissolved in aqueous 9% NaOH at -5 to 5°C without the addition of carbon disulfide [39]. Moreover, some limitations of NaOH-based aqueous systems have been observed on the preparation of solutions from wood pulps [35-40].

Due to that the intermolecular hydrogen bonds are present in cellulose, the effectively destruction of intermolecular hydrogen bonding is essential for successful applications of cellulose. It is known that intermolecular hydrogen bonding of polysaccharides can be broken by using urea [33,34]. Interestingly, NaOH and especially urea broke intermolecular hydrogen

bonding of polysaccharides, allowing enhancement of water-solubility. The addition of organic compounds such as urea or thiourea to NaOH solution could have substantial impact on cellulose solubility. However, this system could diminish cellulose molecular weight [38-40]. More extensive work has been carried out on binary, or ternary mixtures, which will be designed as solvent "systems". The most investigated ones include inorganic or organic electrolytes in strongly dipolar aprotic solvents. Examples are LiCl in DMAc [32-34], in *N*-methyl-2-pyrrodinone [35-36], in 1,3-dimethyl-2-imidazolidinone [35-37], and tetra-n-butyl ammonium fluoride trihydrate in DMSO (TBAF/DMSO) [37-38]. Among them, the solvent system LiCl/DMAc has been most extensively employed because it is capable of dissolving different celluloses including samples of high DP for example in cotton linters and bacterial cellulose.

Table 1-4. Conventional and new cellulose solvents

Solvents	**Method and condition**	**Cellulose**	**Reference**
8-10 wt% NaOH	Direct dissolution, 4°C	Treated cellulose[a], DP = 330	Kamide et al. (1984)
7-9 wt% NaOH	Direct dissolution	Treated cellulose[b], DP = 330	Yamane et al. (1996)
8-9 wt% NaOH	Freeze-thaw	MCC, DP = 200	Isogai and Atalla (1998)
6 wt% NaOH/4 wt% urea	Freeze-thaw	Cotton linter, DP = 690	Zhou and Zhang (2000)
7 wt% NaOH/12 wt% urea	Direct dissolution, - 10°C	Cotton linter, DP = 700	Cai and Zhang (2005)
9.5 wt% NaOH/4.5 wt% thiourea	Direct dissolution, - 4°C to -5°C	Cotton linter, DP = 620	Ruan et al. (2004)
9 wt% NaOH/1 wt% PEG	Freeze-thaw	Cellulose powder, DP = 810	Yan and Gao (2008)
12-18 wt% NaOH 16-28 wt% urea	Two-step, -2 to 5°C	Cotton linter, DP = 570	Qi et al. (2011)
12-18 wt% NaOH 4-6 wt% thiourea	Two-step, -2 to 5°C	Cotton linter, DP =570	Qi et al. (2011)
14-18 wt% thiourea 2-4 wt% PEG	Two-step, -2 to 5°C	Avicel, DP = 570	Qi et al. (2011)

1.3.1. DMA/LiCl system through cellulose swelling process.

In the DMAc/LiCl system, the activation step is crucial for destroying the hydrogen bonded in the polymer chains into the most relaxed conformation. In order to enhance the diffusion kinetics of the solvent to the tightly packed crystalline regions. This process spends mainly allowing sufficient time for chains to unfold chemical cellulose. Experimentally, the most effective activation methods prior to dissolution in DMAc/LiCl was indicated to be described in the two US patents [40].

This can be achieved by the following processes:

a) Water activation firstly is needed to be followed by DMAc exchange. At this time, water swells to loose cellulose structure. The inter-and intramolecular hydrogen bonds are replaced by hydrogen bonds with water.

b) DMAc introduced subsequently impedes the inter- and intra-hydrogen bonds to be re-forming. The exchange works as solvation with water on the cellulose solution.

c) Water activation in LiCl/DMAc/H_2O by fractional distillation to less than 4% water.

d) Liquid ammonia activation followed by DMAc exchange.

After the activation phase, the cellulose substrate is ready to dissolve in DMAc/LiCl. By report review [41], it was showed that the experimental conditions tested by different authors. It was apparently mentioned that the relative proportion of LiCl and cellulose was critical for optimal dissolution. So, “ideal” concentrations of LiCl by weight of cellulose were reporting ranging between 2 and 12% [41-43] for cotton and wide variety of wood fibres such as softwood and hardwood in Kraft pulps. As result, 8% LiCl was found the least amount necessary to achieve

complete dissolve at lower LiCl concentrations. In contrast, reports using LiCl concentrations above 12% to above 15% the DMAc became to be supersaturated with the salt, leading that the celluloses tended to precipitate out of the solution. Sjoholm et al. found the concentration of LiCl to be critical in the formation of aggregates upon dissolution of wood pulp and cotton linter, independently of the sample concentration [39].

For hardwood Kraft pulp, the proportion of the cellulose aggregation increased, when the concentration of LiCl increased from 6% to 8% and from 8% to 10% wt [40-42]. Over the years, various dissolution mechanisms for cellulose in DMAc/LiCl were proposed as following: 1) A $[DMAc_n+Li]^+$ macrocation must exist. 2) In the ion cluster with cellulose, the Cl^- anion is dissociated from the Li^+ cation by intercalating with one or more DMAc molecules. 3) The Li^+ cation interacts with the carbonyl group oxygens of the DMAc molecules. 4) The Cl^- anion disrupting the hydrogen bonds of cellulose can create hydrogen-bond-type interactions with the hydroxyl group hydrogens of cellulose. 5) The macrocation must have weak interactions with the cellulose oxygens. But, these processes should be mentioned to be no conclusive evidence. Until today, the interactions between Li^+ cation and the glycosidic oxygen were indicated in the solution system described though semi-empirical MNDO computer models. This type of interaction between cation and various disaccharides in the gas phase [41-43].

Firstly, the solvate chromic experiments, the interaction between the Cl^- anion and cellulose contributes approximately 80% to the dipole-dipole type interactions between DMAc and cellulose, while the interactions between the $[DMAc_n+Li]^+$ macrocation and cellulose are approximately at 10%. Figure 1.8 shows the structure of cellulose/solvent system complexes has been described by several schemes, differing essentially in the role played by the Li+ and Cl^- ions. In structure a), the complex between Li+ and the oxygen of the solvent CO groups results

in formation of a macro-cation [Li(DMAC)]+, leaving the Cl^- free to form hydrogen bonding with the OH group of the AGU. The repulsion among macro-cations formed allows solvent penetration within the natural polymer chains. Alternatively, the lithium ion binds simultaneously to the OH group of cellulose and the solvent, the latter binding can occur either with the CO group of DMAc, structure b), or with the CO group and the amide nitrogen, structure c).

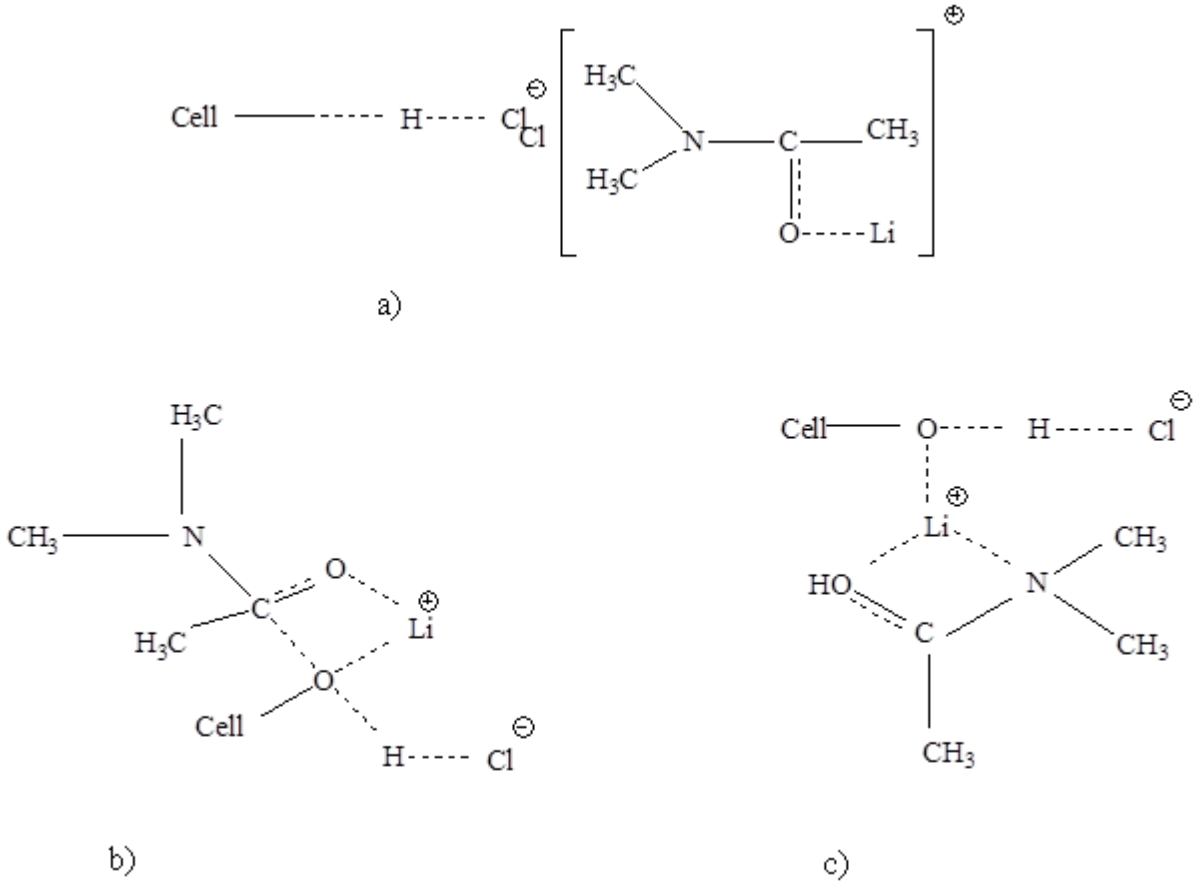

Figure 1.8. Structures suggested for explaining the interactions of cellulose with LiCl/aprotic solvent systems. Redrawn from [41-43]; for simplicity, partial charges are not shown.

1.4 Wet phase separation of polymer film preparation

The idea for the fabrication of films by wet immersion method rose after the study of the reported methods for the obtaining of films from cellulose solutions. It was observed that by using phase immersion method the shape and thickness of the films could be controlled. Moreover, transparent and strong films could be obtained without the addition of any chemical or cross-linker. In a system of two immiscible liquids, usually water (or an aqueous solution) and an organic liquid (an oil), there are two general types of dispersions which can be formed depending on the conditions of the system. A water-in-oil (W/O) dispersion is a dispersion formed when the aqueous phase is dispersed in the organic phase and an oil-in-water (O/W) dispersion is a dispersion which is formed when the organic phase is dispersed in the aqueous phase. Phase inversion is the phenomenon whereby the phases of a liquid-liquid dispersion interchange that the dispersed phase spontaneously inverts to become the continuous phase and vice versa under conditions determined by the system properties, volume ratio and energy input [44-46]. In phase inversion is a process whereby a polymer is transformed in a controlled manner from a liquid to a solid state. The process of solidification is very often initiated by the transition from one liquid state into two liquids (liquid-liquid demixing). At a certain stage during demixing, one of the liquid phases (the high polymer concentration phase) solidifies so that a solid matrix is formed. By controlling the initial stage of phase transition, the film morphology can be controlled. The concept of phase inversion covers arrange of techniques such as, precipitation by solvent evaporation, precipitation by controlled evaporation, thermal precipitation, immersion precipitation and precipitation from vapours phase [45-47].

It was known that precipitation from the vapour phase method was used as early as 1918 by Zsigmondy. A cast film, consists of a polymer and a solvent, is placed in a vapour atmosphere where the vapour phase consist of a nonsolvent saturated with a solvent. The high solvent concentration in the vapour phase prevents the evaporation of solvent from the cast film. As a result, film formation occurs because of the penetration (diffusion) of nonsolvent into the cast film. This lead to a the formation of a film from dissoluble polymer in solvent.

It was reported that, phase inversion method was used for the preparation of cellulose hydrogels to obtain transparent and thin films. For example, novel hydrogels based on sodium carboxymethylcellulose (NaCMC) and hydroxyethyl cellulose (HEC) crosslinked with divinyl sulfone (DVS) were obtained, possessing swelling capabilities and high water retention capacities. These significant results have been achieved by inducing a microsporous structure in the hydrogel, by means of the phase inversion technique in acetone. Here acetone was used as non-solvent for cellulose.

Moreover, cellulose acetate dissolved in DMAc/LiCl has been used to elaborate films as rate controlling membrane for transdermal use. Unfortunately, for the elaboration of a film with good mechanical properties the use of plasticizers is needed. It has been reported that the use of plasticizers diminish the biocompatibity of the obtained films. For this, the use of natural plants as cellulose source to elaborate films without crosslinker.

1.5 Scaffolds and cell adhesion materials for tissue engineering

In the rapidly changing scientific world, contributions of scientists and engineers are leading to major new solutions of significant medical problems. The ultimate goal of tissue engineering is to replace, repair or enhance the biological function or damage, absent or dysfunctional elements of a tissue or an organ. Engineered tissues are produced by using cells that are manipulated trough their extracellular environment to develop living biological substitutes for tissues that are lacking or malfunctioning [48-51].

There are three ways in which materials have been shown to be useful in tissue engineering:

(1) Inducing migration of tissue regeneration.

(2) Using to encapsulate cells and acting as inmmunoisolation barrier.

(3) Using as a matrix to support cell growth and cell organization.

The materials to be used as scaffolds in tissue engineering must fulfill a number of complex requirements, such as biocompatibility, biodegradability, appropriate porous structure, mechanical properties and suitable surface chemistry. Because of their nontocicity, biocompatibility and biodegradability, biopolymers become the most attractive materials to produce tissue engineering scaffolds, as they are very versatile materials.

The application of biomaterials in tissue engineering is a truly interdisciplinary endeavor, involving several experts in chemistry, chemical engineering, cell biology, matrix biochemistry, biomechanics, and clinical medicine. In many cases scientists highly focused expertise in one discipline and cross boundaries into the new area. The recent shift in their emphasis is away from biomaterials and towards tissue engineering, as illustrated in Figure 1.9. There was a steady growth over the last 40 years in the annual number of papers with “biomaterials” as a key word of tittle word. The phrase “tissue engineering” was not cited in the literature until the mid-1980s and during the 1990s. There was an explosion of interest in this emerging field. Indeed, by the dawn of the new millennium, there were more papers being published using the term “tissue engineering” than “biomaterials.” If research activity provides an insight into the future technology, then tissue engineering will undoubtedly revolutionize the disease treatment in the near future.

As a material science, biomaterials are related with the physical properties, and both chemical composition and structure. As a medical science, their goals are the improvement of the human health and quality of life [52-53].

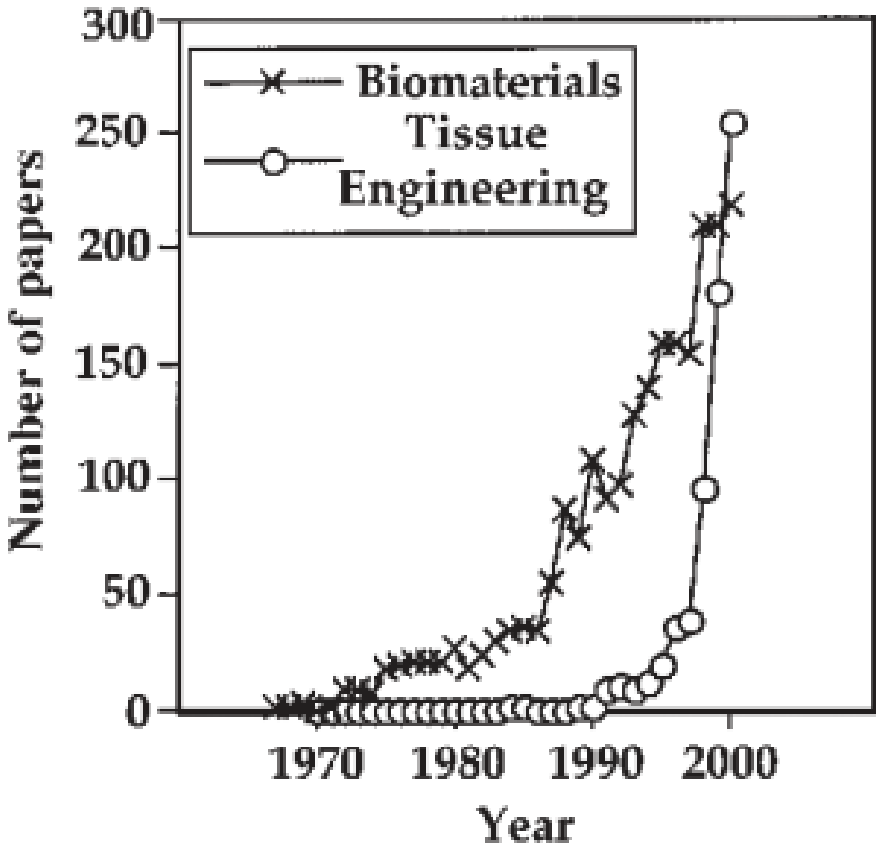

Figure 1.9. Publication rates in biomaterials and tissue engineering.

Some of the commonly used biomaterials are explained in Table 1-5. According to biological responses, biomaterials can be classified as bio-tolerant, (bone cement, stainless steel, and cobalt-chrome alloy), bio-inert (alumina, zirconia, carbon materials and titanium) and bioactive materials (calcium phosphate ceramics, hydroxyapatite (HA), and glass ceramics). Ceramics, metals, polymers and composite materials are classified on the basis of their chemical composition.

Table 1-5. Examples of biomaterials applications

Cardiovascular implants	Heart and valves	
	Vascular grafts	
	Pacemakers	
	Stents	[49]
Plastic and reconstructive implants	Breast augmentation or reconstruction	
	Maxilofacial reconstruction	
	Penile implant	[50]
Orthopedic prostheses	Knee join	
	Hip join	
	Fracture fixation	[51]
Opthalmic systems	Contact lenses	
	Intraocular lenses	[52]
Neural implants	Cochlear implant	
	Dialyzers	
	Plasmapheresis	[53]
Divices for controlled drug delivery	Coating for tablets or capsule	
	Transdermal systems	
	Microcapsules	
	Implants	[54]
General surgery	Sutures	
	Staples	
	Adhesives	
	Blood substitutes	[55]
Diagnosis	Fiber optics for endoscopy	[52]

Ceramics specially design ceramics materials. In other words, bioceramics have been used for the repair, reconstruction, and replacement of diseased or damaged parts of the body since 1960s. Polycrystalline (Alumina or HA), bioactive glass, bioactive glass-ceramic or bioactive composite (Polyethylene-HA) are the main examples of bioceramics. Principal characteristics of bio-inert ceramics are wear resistance, minimal biological response, stiffness; strength and toughness especially in total join replacements. Bioactive ceramics show porous and crystalline structures and they are also biocompatible. However, ceramics materials are brittle and difficult to produce and they have no resilence properties. In fact, low tensile strength and fracture toughness limit the usage of bioactive ceramics [49-55]. As seen in Table 1-6, for examples in metals implants possess the property of being able to endure tensile stresses. Metals are mainly used in load bearing parts of the body. Typical examples of highly loaded implants are hip and known endoprostheses, plates, screws, nails and dental implants. In addition, metallic biomaterials are applied to unloaded and functional devices such as cages for pumps, valves and heart pacemakers, conducting wires, etc [10]. Generally, metals are characterized with toughness and ductility. On the other hand, the main drawbacks of these materials are corrosion and density [50-53]. Polymers are used mainly in tissue engineering, implantation of medical devices, production of artificial organs and prostheses, ophthalmology, dentistry, repair of bone and drug delivery systems. Polymethylmethacrylate (PMMA), polyethylene (PE), polypropylene (PP), polytetrafluoroethylene (PTFE) and Teflon are some examples of polymers used in the medical applications. The main advantages of polymers are elasticity and easiness in the production. However, mechanical properties and some deformations-degradation problems have been observed in the medical applications.

Table 1-6. Materials for use in the body

Materials	Advantages	Disadvantages	Examples
Polymers (nylon, silicon, polyester, etc)	Resilient Easy to fabricate	Not strong Deforms with time May degrade	Blood vessels, sutures, ear, nose, Soft tissues [52].
Metals (Ti and its alloys Co-Cr alloys, stainless Steels)	Strong tough ductile	May corrode, dense, difficult to make	Join replacement, bone plates and screws, dental root implant, pacer, and suture [55]
Ceramics (Aluminum Oxide, calcium phosphates, including hydroxyapatite carbon)	Very biocompatible Inert strong in compression	Difficult to make Brittle Not resilient	Dental coating Orthopedic implants Femoral head of hip [56]
Composites (carbon-carbon, wire or fiber reinforced, bone cement)	Compression strong	Difficult to make	Joint implants Heart valves [57]

It is understand that, the main goal of tissue engineering is to produce new tissue where it is needed. Therefore, knowledge of the structure and functional limits of the regenerated tissue is essential. The cell type should be suitable for the implanted site, but the cultivated cells should be provided to the greater surface area in the scaffold [54-56].

Thus, biomaterials in tissue-engineered substitutes serve as a structural component and provide the proper three-dimensional (3D) architecture of the construct. The scaffold should prefer to provide the 3D matrix for guided cell proliferation and control the shape of the bioartificial device. Principally, a scaffold should have high porosity and have suitable pore sizes, and the pores should be interconnected [55-58].

1.5.1. Scaffold design.

Scaffolds designed for tissue engineering should mimic the site where they will be implanted as closely as possible. Here, the scaffold should support cell growth. All tissues have their own architecture. Table 1-7 summarizes polymer families used for the synthesis of scaffolds. For example, organs, such as liver, kidney, and bone have parenchymal and stromal components. The parenchyma is the physiologically active part of the organ, and the stroma is the framework to support the organization of the parenchyma [54-56]. There is another example to provide a bone defect with a stroma substitute. In this case, the spaces are morphologically suitable for osteons and vascularization enables the biological response to be supported. This enhances the regenerative process [56]. For ideal cortical bone scaffold, several studies have been performed to reveal the optimal pore size. The results vary from 40 μm for polyethylene scaffolds to 50-100 μm [54,58] and 500-600 μm for ceramics scaffolds [59]. In fact, pore size for optimal tissue ingrowth may be material-specific, not only cell-specific. Several criteria in the scaffold are presented and can define the ideal material for tissue-engineering scaffold. The material should be biocompatible, absorbable, and easily and reproducibly processable. In addition, it is necessary that can interact with the surface of the material and cells and tissues [50]. The material should not transfer antigens, and it should be immunologically inert [54]. Among on the

criteria, biocompatibility becomes a phenomenological concept, and is for the essential property. This is the reason for biomaterials can be applied as scaffold for the tissue engineering. For instance, the inner surface of an implanted vascular graft or blood pump must be blood-compatible in artificial heart, while its outer surface has to be tissue-compatible. In other words, the material surfaces must not exert any adverse effects upon blood or tissue, or upon other biological elements at the interfaces. In important factors (Table 1-4), physical or physical-chemistry capability including mechanical strength, permeation, or sieving characteristics, is another important requirement for the candidate of biomaterials. It is well known that cuprammonium rayon maintains its dominant position as the most popular material for hemodialysis to artificial kidney. It is known as good mechanical strength that cuprarayon can be fabricated into much thinner membranes than synthetic polymer membranes.

In addition, hydrophilicity and hydrophobicity of materials are to be the most fundamental properties in order to control whenever they are utilized as biomedical devices. It is well-known that protein adsorption is the first event when any of the body fluids encounters artificial materials.

1.5.2 Biocompatibility factors including cells on the materials

Figure 1.10 shows the sequence of events after a surface has suddenly been placed in a biological environment containing cells. The first molecules to reach the surface (time scale of order ns) are water molecules. Water is known to interact and bind at the surface depending on the surface properties. The properties of the surface water "shell" are an important factor influencing proteins and other molecules that arrive a little later. These water-soluble biomolecules can be on

hydration with water shells by an interaction through the interface. Thus, the interface influences the fundamental kinetic process and the thermodynamics of water.

When the cells arrive at the surface they “see” a protein-covered surface whose proteins layer has properties that were initially determined by the preformed water shells. Thus, when we talk about cell-surface interactions, it is ultimately an interaction between cells and surface bound proteins or other biomolecules. Figure 8 illustrates surface-water, surface-water including protein and surface-water-proteins and cells.

The first molecules to reach the surface are water molecules (ns time scale). The water shell that is formed affect the protein interaction starting on the micro to millisecond time scale, and continuing for much longer times. The water shell on the surface affects the protein interaction. Eventually cells reach the surface. Their surface interaction takes place via the protein coating whose properties is determined by the surface and water layer properties [60].

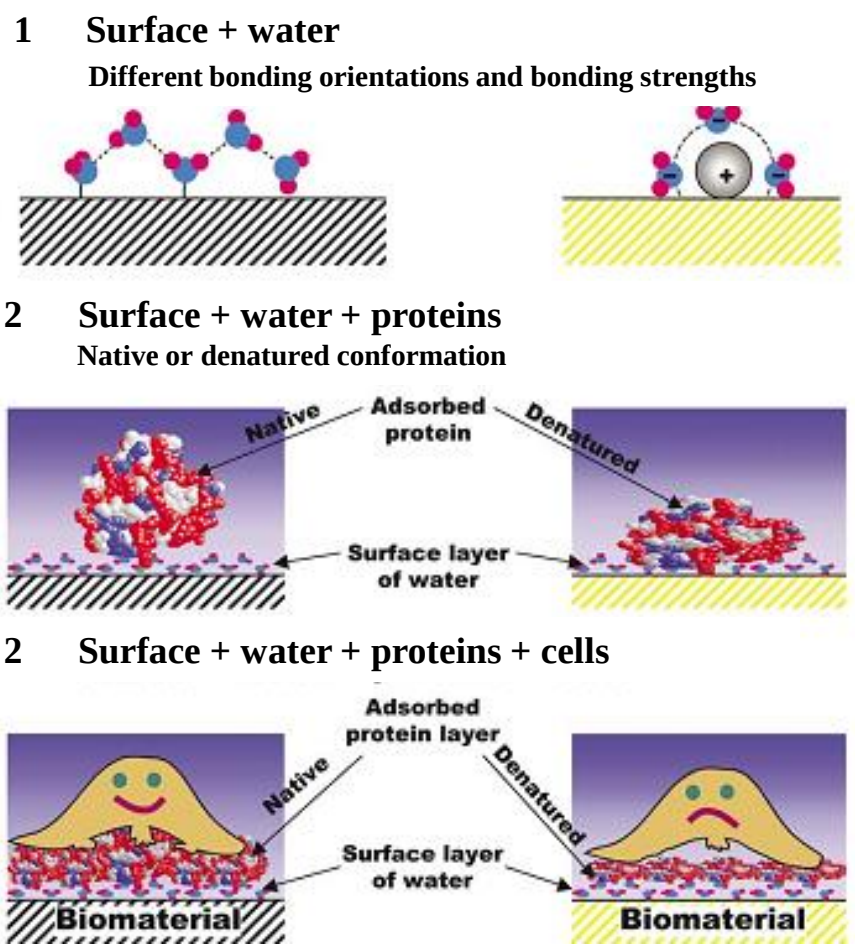

Figure 1.10 Schematic illustrations of the successive events following after implantation of a medical implant.

As a result, for the candidates, the most commonly used scaffold materials are the natural polymers such as chitosan [24-28], collagen [25-27], and hyaluronic acid [25-28] with its derivatives, ceramics such as hydroxyapatite [28-31], transformed coral [32], and synthetic bioabsorbable polymers like PGA and PLGA copolymers [33] as described. However, in the case of cellulose, there are fewer studies in uses of scaffold materials since problems are found as a proper dissolvent for the fabrication. However, sometimes chemical modification of cellulose [51-53] is needed to overcome the difficulty in the scaffold requiring.

1.5.3 Material view for tissue engineering.

A biomaterial is defined as any natural or synthetic substance engineered to interact with biological systems to direct medical treatment. To meet the needs of the biomedical community, materials composed of everything from metals and ceramics to glasses and polymers have been researched. Polymers possess significant potential because flexibility in chemistry gives rise to materials with great diversity of physical and mechanical properties.

Although natural polymers such as collagen have been used biomedically for thousands of years, research into biomedical applications of synthetic degradable polymers is relatively new, starting in the 1960s [49]. As biomaterials are applied in the clinical setting, numerous issues arise that cannot be adequately identified and addressed in previous *in vitro* and model *in vivo* experiments. The host response to both tissue engineering and drug delivery devices depends on the chemical, physical, and biological properties of the biomaterials.

A number of different polymers applied for the preparation of biomaterials possess bonds that are susceptible to hydrolysis including esters, anhydrides, acetals, carbonates, amides, urethanes, and phosphates. One of the major features that conveys significant impact on the capacity of these polymeric families to function as biomaterials is their relative degradation rates and erosion mechanisms. Table 1-7 shows different polymers families used for the preparation of biomaterials.

Table 1-7. Summary of different polymeric families' applications, advantages and disadvantages

Polymer	Applications	Advantages	Disadvantages	Structure
Polyphosphazenes	Tissue Engineering; Vaccine Adjuvant	Synthetic Flexibility: Controllable Mechanical Properties.	Complex Synthesis	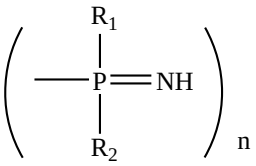
Polyanhydrides	Drug Delivery; Tissue Engineering	Sigbificant Monomer Flexibility; Controllable Degradation Rates	Low-molecular Weights; Weak Mechanical Properties	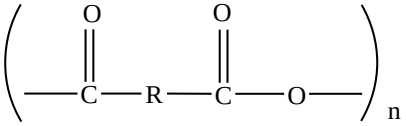
Polyecetals	Drug Delivery	Mild pH Degradation Products; pH sensitive Degradation	Low Molecular Weights; Complex Synthesis	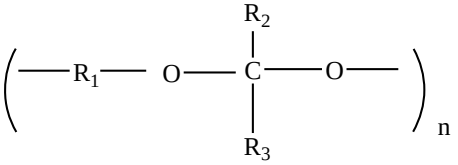
Poly(ortho esters)	Drug Delivery	Controllable Degradation Rates; pH Sensitive Degradation	Weak Mechanical Properties; Complex Synthesis	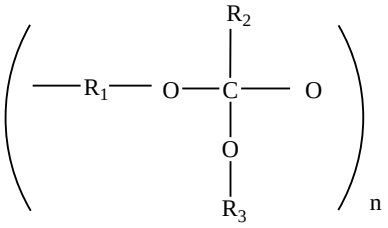
Polyphosphoesters	Drug delivery; Tissue Engineering	Biomolecule Compatibility; Highly Biocompatible Degradation Products	Complex Synthesis	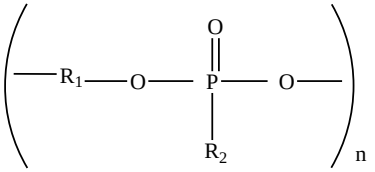

Table 1-7. *(Continued)*

Polymer	Applications	Advantages	Disadvantages	Structure
Polycapropactone	Prostheses; Tissue Engineering	Highly Processable; Many Commercial Vendors Available	Limited Degradation	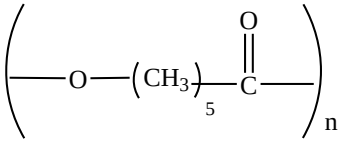
Polyurethanes	Prostheses; Tissue Engineering	Mechanically Strong; Handle Physical Stresses Well	Limited Degradation; Require Copolymerization with other polymers	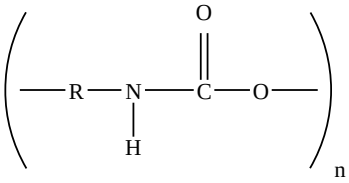
Polylactide	Tissue Engineering Drug delivery	Highly Processable; Many Commercial Vendors Available	Limited Degradation; Highly Acidic Degradation Products	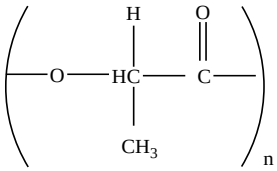
Polycarbonates	Drug Delivery Tissue Engineering Fixators	Chemistry-Dependent Mechanical Properties Surface Eroding	Limited Degradation; Require Copolymerization with other polymers	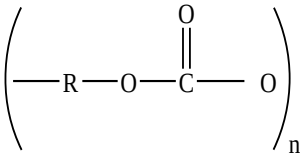
Polyamides	Drug Delivery	Conjugatable Side Group; Highly Biocompatible Degradable Products	Very Limited Degradation; Charge Induced Toxicity	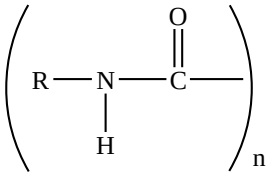 [44]

On these materials, the scaffolds studied included gels, foils, foams, membranes, including capillary membranes, textiles, tubes, microspheres and beads, porous block or specialized 3D shapes. Other methods applied also included non-woven technology [44], freeze drying [54], rapid prototyping [50], 3D printing, and phase separation [56-60]. One approach to tissue engineering involves seeding of a high density of uniformly distributed cells on three-dimensional (3D) polymeric scaffolds and cultivating the resulting cell-polymer constructs under conditions that permit the formation of tissues [61-63]. The scaffold provides defined structures for cell attachment and tissue development, and the bio-reactor provides control over the biochemical and physical factors in the cell environment. Moreover, evaluation of engineering tissues is clearly necessary to examine their properties and to determine that how close they are to those of the original tissue being engineered. Microscopy encompasses a group of techniques that allows the assessment of many parameters, including information on the cells themselves, on their viability, density, proliferation statues, morphology, their capacity for protein synthesis, and their cell activity. Microscope techniques such as scanning electron microscopy (SEM), atomic force microscopy (AFM) have been used to analyze cell adhesion, spreading and morphology, and light and fluorescent microscopy [59-62].

1.5.4 Relationship between cell compatibility and materials

For example, fibrin microbeads (FMB) has been used as biodegradable carries for culturing cells and for accelerating wound healing. Synthetic and naturally occurring polymers are an important element in new strategies for producing engineered tissue. Several approaches in the elaboration of materials for wound healing have been tested with fibroblast to evaluate their cytotoxixity. Most tissue-derived cells are anchorage dependent and require attachment to a solid surface for

viability and growth, as the case of fibroblasts. Fibrin was shown to be chemotactic to human fibroblast, macrophages, and endothelial cells needed for wound healing -process. To observe the healing process, imaging cells on the prepared scaffold was performed light and fluorescent microscopy using a standard fluorescent microscopy system [67]. In addition, visualization and quantifying cellular contact with materials is a critical step in the evaluation of cell-material interaction both in vitro and in vivo. The microscale texture of an implanted material can have a significant effect on the behavior of cells in the region of the implant. In recent study, porous polymer membranes containing certain structural features and fiber/strands were associated with enhanced new vessel growth [69]. The behavior of cultured cells on surface with edges, grooves, or other textures is different than behavior on smooth surfaces. In many cases, cells oriented and migrated along fibers or ridges in the surface, a phenomenon called contact guidance from early studies on neural cell cultures [70-71]. Fibroblasts have also been observed to orient on grooved surfaces [72], particularly when the texture dimension are 1 to 8 μm [73]. The degree of cell orientation depended on both the depth [74] and pitch [75] of the grooves. Substrates with peaks and valleys also influenced the function of attached cells. Polydimethylsiloxane (PDMS) surfaces with 2- to 5-μm texture maximized macrophage spreading [76]. Similarly, PDMS surfaces with 4- or 25-μm^2 peaks uniformly distributed on the surface provide better fibroblast growth than did 100-μm^2 peaks or 4- or 25-, or 100-μm^2 valleys [77].

For cells attached to a solid substrate, cell behavior and function depend on the characteristics of the substrate. Consider, for example, the experiments describes by Folkman and Moscona (1978), in which cells were allowed to settle onto surfaces formed by coating conventional tissue culture polystyrene (TCPS) with various dilutions of poly(2-hydroxyethyl methacrylate) (pHEMA). As the amount of pHEMA added to the surface increased, the surface become less adhesive and cell

spreading decreased; spreading was quantified by measuring the average cell height on the surface. Following a similar experiments, a number of groups have examined the relationship between chemical or physical characteristics of the substrate and behavior on function at attached cells [78-88]

For more surfaces, adhesion requires the presence of serum and, therefore, this optimum is probably related to the ability of proteins, such as fibronectin [89], to adsorb to the surface. In the presence of serum, adhesion is enhanced on positively charged surfaces [90]. Fibroblast spreading has been correlated with surface free energy, but the rate of fibroblast growth on polymer surface appears to be relatively independent of surface chemistry [90-93]. Cell viability may also be related to interactions with the surface [94]. The migration of surface-attached fibroblast [95], endothelial cells [96], and corneal epithelial cells [97] has been measured as function of polymer surface chemistry; rates of cell migration depend on the nature of the surface, although no general trends have emerged. Collagen synthesis in fibroblast has been correlated with contact angle, with higher rates of collagen synthesis per cell for the most hydrophobic surfaces [98-102]. Moreover, it is well know that collagen is the major protein in animals. It has an extended history of use in the medical field primary due to its ability to polymerize in vitro into strong fibers that can be fabricated into a number of forms. Collagen has been utilized for a variety of clinical purposes including wound treatment, hemostasis, and soft tissue augmentation. Soluble collagen has been used as a subcutaneous implant for repairing dermatological defects such as acne scars, glabellar furrows, excision scars and other soft tissue defects. Unfortunately, the use of collagen Type 1 for wound dressing have limited commercial success because of the difficulty of the physical form of the dressing, making difficult to apply to deep wounds. For these reasons, researches have been focused to polymers from natural plants as cellulose.

1.6 Cellulose used as scaffold for medical applications.

Cellulose, a naturally occurring polymer produced by plants, as well as by microorganisms, is the β (1→4) polymer of anhydroglucose (Fig.). In the biomedical field, cellulose and its derivatives have been extensively used for decades. The biocompatibility of several cellulosics is well established (4-7 paper polysaccharides as scaffolds). Baquey and coworkers have pioneered and considerably contributed to this field of study by firstly proposing the use of regenerated cellulose hydrogels (RCH) for orthopedic applications. Cellulose Regenerated by the Viscose process (CRV) was patented and thoroughly investigated. Briefly, the starting cellulose material is most usually found in refined wood pulp and is converted into alkali cellulose by steeping in sodium hydroxide, which is then aged. Alkali cellulose is then converted into sodium cellulose xanthate with carbon disulfide, and finally the xanthate is dissolved in dilute alkali, and viscose is regenerated thereof. The high swelling materials obtained by this method were widely used for decades [102-104]. As implantable material in orthopedic surgery, as sealing material for the femoral component in hip prostheses, in place of the acrylic cement, as well as dyaphyseal obturator [90-100]. It was envisaged to take advantage not only of its biostability and good matching with mechanical properties of cortical bone but also of its hydroexpansivity, allowing therefore a satisfactory fixation to hard tissue [91-99]. This material has been shown to satisfy most of biocompatibility requirements. It is cytocompatible although it seemed not to allow proliferation of bone cells, after an initial attachment of the cells.

The applicability of cellulose phosphate (CP) as a biomaterial for orthopedic applications was then investigated to improve the osseo integration of cellulose. CP has been used for decades in the treatment of Ca^{2+} metabolism-related diseases, such as renal stones, due to its high Ca binding capacity, associated with lack of toxicity and indigestibility [90,103]. CP is not cytotoxic,

independently of the phosphate content. However, CP promoted poor rates of cell attachment, proliferation and differentiation, which are attributed to the negative charge, associated with the high hydrophilicity of the cellulose derivatives [91]. On the contrary, unmodified and slightly oxidized RCH promoted high rates of cell attachment, proliferation and differentiation. In this case, an apatite layer was observed between the cellulose surface and the cell layer, which was attributed to the synthesis of extracellular matrix by the osteoplastic cells [93]. Some studies also suggest no effect on bone induction by oxidized cellulose [99].

1.7 Scope of present investigation

This thesis is described from viewpoints of novel cellulose hydrogel films prepared from waste bagasses and applied for tissue engineering when their biocompatible and cytotoxic properties are included. Thus, this consists of eight chapters as following. Chapter 1 has presented an brief introduction to related topics to hydrogels, cellulose and tissue engineering. Especially, this chapter introduced hydrogels composed of cellulose biopolymers used for the scaffold film in tissue engineering. Chapter 2 relates to the effect of sodium hypochlorite treatment of agave tequilana weber bagasse fibers for preparation of cyto and biocompatible hydrogel films. In this chapter, preparation method and resultant effect are mentioned by using Waste bagasse of *Agave tequilana*-Weber fibers for cellulose fibers and hydrogel films, respectively, when the bagasse is chemically treated with sodium hydroxide to elaborate hydrogel films. Analysis of the morphology of the films after adherent NIH3T3 fibroblast is cultivated; the treatment effect is examined in behaviors of the fibrobrast cultivation related with the projected cell area, aspect ratio and long axis. Chapter 3 describes fibroblast compatibility on scaffold hydrogels prepared from agave tequilana weber bagasse for tissue regeneration. This chapter, gaves the cellulose fibers that are used to elaborate a transparent and flexible cellulose hydrogel films and investigated with the scaffold properties for tissue regeneration as tested by *in vitro* assays of fibroblast cells. Using dimethylacetamide/lithium chloride (DMAc/LiCl) system is possible to study the treatment effect of bagasse fibers to the cellulose and resulted hydrogel films in the point of the LiCl concentration in the DMAc solution. Result are obtained that LiCl influences aggregation of cellulose fibers in phase inversed process to foam the hydrogel films. It is concluded that the prepared agave films show better cytocompatibility than the referenced PS

dish used as control. Detailed study with AFM images presents that the ordered and aggregated fiber orientation in the films relates with fibroblast cells spreading *in vivo* cultivation. Chapter 4 shows bamboo fibers elaborating cellulose hydrogel for medical applications. In this chapter, several cellulose fibers involving bamboo fibers are used to study as source to hydrogel films for cell cultivation scaffold. In addition to bamboo, this chapter presents fibroblast growing in several cellulose hydrogels made of agave, kenaf and conifer. The species of the cellulose source and the tissue regeneration of the fibroblast are investigated in preparation of three different dissolving methods with NaOH-based, NaOH/urea aqueous solutions and DMAc/LiCl solution. The obtained results of the DMAc/LiCl show a higher cytocompatibility for the cell cultivation scaffold. Chapter 5 relates to wooden pulp cellulose hydrogels having cyto and biocompatible properties. This chapter focuses in the cell grown on the hydrogel films of pulp wood celluloses. The results are presented that the cellulose hydrogel films prepared from wooden pulp exhibited good cytocompatibility for application of tissue engineering. Chapter 6 includes biohydrogels interpenetrated with hydroxyethyl cellulose and wooden pulp for biocompatible materials. This chapter describes the elaboration interpenetrated hydrogel films using pulp fibers and hydroxyethyl cellulose to determinate the effect on cytocompatibility. Finally, Chapter 7, conclusion of my doctoral thesis is summarized in addition with suggestions for future works addressed by the uses of natural fibers to elaborate films for medical applications.

1.5 References

[1] O. Wichterle, D. Lim, “Hydrophilic gels in biologic use”, Nature, 1960, 185, pp. 117.

[2] A. S. Hoffman, G. Schmer, C. Harris, W. G. Kraft, “Covalent binding of biomolecules to radiation-grafted hydrogels on inert polymer surfaces”, Trans. Am. Soc. Artif. Intem. Organs, 1972, 18, pp. 10.

[3] B. D. Ratner, A. S. Hoffman, “Synthetic hydrogels for biomadical applications”, ACS Symposium Series, 1976, 31, pp. 1.

[4] N. A. Peppas, “Hydrogels in Medicine and Pharmacy”, CRC Press, Boca Raton, FL, 1987, I-III.

[5] K. Park, W.S.W. Shalaby, H. Park, “Biodegradable Hydrogels for Drug Delivery”, Technomic, Lancaster, PA, 1993.

[6] K. Ulbrich, V. Subr, P. Podperova, M. Buresova, “Synthesis of novel hydrolytically degradable hydrogels for controlled drug release”, J. Controlled Release, 1995, 34, pp. 155.

[7] F. Lim, A. M. Sun, “Microencapsulated islets as bioartificial pancreas”, Science, 1980, 210, pp. 908.

[8] M. V. Sefton, M. H. May, S. Lahooti, J. E. Babensee, “making microencapsulation work: conformal coating immobilization gels and in vitro performance”, J. Controlled Release, 2000, 65, pp. 173.

[9] H. Gin, B. Dupuy, A. Baquey, C. Baquey, D. Ducassou, “Lack of resposnsiveness to glucose of microencapsulated Islet

Of Langerhans after three weeks implantation in the rat-influence of complement”, J. Microencapsul, 1990, 7, pp. 341.

[10] F. Y. Hsu, S. W. Tsai, F. F. Wang, Y. J. Wang. "The collagen-containing alginate/poly (L-lysine)/alginate microcapsules", Artif. Cells Blood Substit. Immobil. Biotechnol. 2000, 28, pp.147.

[11] J. P. Dillon, X. J. Yu, A. Sridharan, J. P. Ranieri, R. V. Bellamkonda, "The influence of physical structure and charge on neurite extensión in a 3D hidrogel scaffold", J. Biomater. Sci. Polym, 1998, 9, pp. 1049.

[12] Y. L. Cao, A. Rodriguez, M. Cacanti, C. Ibarra, C. Arevalo, C. A. Vacanti, "Comparative study of the use of PGA, calcium alginate and pluronics in the engineering og autologous porcine cartillage", J. Biomater, Sci. Polym, 1998, 9, pp. 475.

[13] V. F. Sechriest, Y. J. Miao, C. Niyibizi, A. Westerhausen-Larson, H. W. Matthew, C. H. Evans, F. H. Fu, J. K. Suh, "GAG-augmented polysaccharide hydrogel: a novel biocompatible and biodegradable material to support chondrogenesis", J. Biomed. Mater. Res, 1999, 49, pp.534.

[14] M. Yamamoto, Y. Tabata, T. Ikada, "Growth factor release from gelatin hydrogel for tissue engineering", J. Bioact. Compat. Polym, 1999, 14, pp. 474.

[15] L. G. Griffith, "Polymeric biomaterials", Acta Mater, 2000, 48, pp. 263.

[16] D. Campoccia, P. Doherty, M. Radice, P. Brun, G. Abatangelo, D. F. Williams, "Semisynthetic resorbable materials from hyaluroran esterification", Biomaterials, 1998, 19, pp. 2101.

[17] G. D. Prestwich, D. M Marecak, J. F. Marecak, K. P. Vercruyse, M. R. Ziebell, "Contrlled chemical modification of hyaluronic acid", J. Controlled Release, 1998, 53, pp. 93.

[18] L. S. Nair, C. T. Laurencin, "Biodegradable polymers as biomaterials, " Prog. Polym. Sci, 2008, 33, pp. 1059.

[19] J. E. Morris, R. Fischer, A. S. Hoffman, “Affinity precipitation of proteins with polyligands”, Anal. Biochem, 1993, 41, pp. 991.

[20] X. Liu, L. Ma, Z. Mao, C. Gao, “Chitosan-based biomaterials for tissue repair and regeneration”, Adv. Polym. Sci, 2011, 244, pp. 81.

[21] L. L. Llooyd, J. F. Kennedy, P. Methacanon, M. Paterson, C. J. Knill, “Carbohydrates polymers as wound management aids”, Carbohydr. Polym, 1998, 37, pp. 315.

[22] M. I. Vazquez, R. De Lara, J. Benavente, “Chemical surface diffusional, electrical and lelastic characterization of two different dense regenerated cellulose membranes”, J. Colloids. Interface, Sci, 2008, 328, pp. 331.

[23] K. J. Edgar, C. M. Buchanan, J. S. Debenham, P. A. Rundquist, B. D. Seiler, M. C. Shelton, D. Tindall, “ Advanced in cellulose ester performance and application”, Prog. Polym. Sci, 2001, 26, pp. 1605.

[24] A. L. Dupont, C. Egasse, A. Morin, F. Vasseur, “Comprehensive characterization of cellulose and lignocellulose degradation products in aged papers: Capillary zone electrophoresis of low molar mass organic acids, carbohydrates, and aromatic lignin derivatives”, Carbohydr. Polym, 2007, 68, pp. 1.

[25] C. N. Saika, T. Goswani, A. C. Ghosh, Esterification of high α cellulose extracted from Hibiscus cannabinus L”, Ind. Crops. Prod, 1995, 4, pp. 233.

[26] A. Svensson, E. Nicklasson, T. Harrah, B. Panilatis, D. L. Kaplan, M. Brittgerg, P. Gatenholm, “Bacterial cellulose as a potential scaffold for tissue engineering of cartilage”, Biomaterials, 2005, 26, pp.419.

[27] Ruozi, B.; Parma, B.; Crace, M. A.; Tosi, G.; Bondioli, L.; Vismara, S.; Forni, F.; Vendelli, M. A. Collagen based modified membranes for tissue engineering: influence of type and molecular weight of GAGs on cell proliferation. *Int. J. Pharm.* **2009**, *378*, 108.

[28] Stamatials, D. T.; Papendurg, B. J.; Girones. M.; Saiful, S.; Bettahalli, S. N. M.; Schmitmeter, S.; Wessling, M. Medical applications of membranes: Drug delivery, artificial organs tissue engineering. *J. Memb. Sci.* **2008**, *38*, 1.

[29] Hoenich, N. A. Update on the biocompatibility of hemodialysis membranes. *Hong Kong J. Nephrol.* **2004**, *6*, 74.

[30] Puppi, D.; Chiellini, F.; Piras, A. M.; Chiellini, E. Polimeric materials for bone and cartilage repair. *Prog. Polym. Sci.* **2010**, *35*, 403.

[31] Sikareepaisan, P.; Ruktanonchai, U.; Supaphol, P. Preparation and characterization of asiaticoside-loaded alginate films and their potential for use as effectual wound dressings. *Carbohy. Polyms*. **2011**, *83*, 1457.

[32] B. Mulder, J. Schel, A. M. Emons, "How the geometrical model for plant cell wall formation enables the production of a random texture," Cellulose, 2004, 11, pp. 395.

[33] D. Klemm, B. Philipp, T. Heinze, U. Heinze, W. Wagenknecht, "Comprehensive Cellulose Chemistry", Wiley-VCH, Weinheim, 1995, vol.1.

[34] A. C. O'Sullivan, "Cellulose: the structure slowly unravels", Cellulose, 1997, 4, pp. 173.

[35] J. Cai, L. Zhang, "Rapid dissolution of cellulose in LiOH/urea and NaOH/urea aqueous solutions", Macromol. Biosci, 2005, 5, pp. 539.

[36] D. Ruan, L. Zhang, J. Zhou, H. Jin, H. Chen, "Structure and properties of novel fibers spun from cellulose in NaOH/thiourea aqueous solution", Macromol. Biosci, 2004, 4, pp. 1105.

[37] L. Yan, Z. Gao, "Dissolving of cellulose in PEG/NaOH aqueous solution", Cellulose, 2008, 15, pp. 789.

[38] H. Zhang, J. Wu, J. Zhang, J. He, "1-Allyl-3-methylimidazolium chloride room temperature ionic liquid: a new and powerful nondericatizing solvent for cellulose", Macromolecules, 2005, 38, pp. 8272.

[39] C. L. MacCormick, P. A. Callais, B. H. Hutchinson, "Solution studies of cellulose in lithium chloride and N, N-dimethylacetamide", Macromolecules, 1958, 18, pp. 2394.

[40] T. Heinze, R. Dicke, A. Koschella, A. H. Kull, E. A. Klohr, W. Koch, "Effective preparation of cellulose derivatives in a new simple cellulose solvent", 2000, 201, pp.627.

[41] T. R. Dawsey, C. L. McCormick, "The lithium chloride/dimethylacetamide solvent for cellulose: a literature review", J. Appl. Polym. Sci, 1996, 60, pp. 63.

[42] A. M. Striegel, "Theory and applications of DMAc/LiCl in the analysis of polysaccharides", 1997, 34, pp. 267.

[43] E. Sjoholm, K. Gustafsson, B. Eriksson, W. Brown, A. Colmsjo, "Aggregation of cellulose in lithium chloride/N,N-dimethylacetamide", Carbohydr. Polym, 2000, 41, pp. 153.

[44] C. W. Patrick, A. G. Mikos, L. V. McIntire, "Frontiers in Tissue Engineering", Pergamon, Oxford, UK, 1998, pp.700.

[45] R. M. Nerem, A. Sambanis, “Tissue engineering: from biology to biological substitutes”, Tissue engineering, 1995, 1, pp. 3.

[46] E. C. Shors, R. E. Holmes, “Porous hydroxyapatite, in An Introduction to Bioceremics (Hench, L. L., Wilson, J., eds), World Scientific, Singapore, 1993, pp. 181-198.

[47] J. J. Klawitter, S. F. Hulbert, “Application of porous ceramic for the attachment of load bearing orthopedic applications”, J. Biomed. Mater. Symp, 1971, 2, pp. 161.

[48] J. J. Klawitter, J. G. Bagwell, A. M. Weinstern, B. W. Sauer, J. R. Pruitt, “An evaluation of bone growth into porous high density polyethylene” J. Biomed. Mater. Res. 1976, 10, pp. 311.

[49] P.S. Eggli, W. Muller, R. K. Schenk, “Porous hydroxyapatite and tricalcium phosphate cylinders with two different pore size implanted in the cancellous bone of rabbits”, Clin. Orthop. Relat. Res, 1988, 232, pp. 127.

[50] L. G. Cima, J. P. Vacanti, C. Vacanti, D. Ingber, D. Mooney, R. Langer, “Tissue engineering by cell transplantation using degradable polymer substrates”, J. Biomech. Eng, 1991, 113, pp. 143.

[51] P. A. Albertsson, “Partition of Cell Particles and Macromolecules”, 3rd Ed. Wiley, New York, 1986.

[52] H. Water, “Method of Cell Separation”, Vol. 1, Plenum, New York, 1977, pp. 307.

[53] T. Sato, “Concentrated Solutions of Liquid-Crystalline Polymers”, Advanced in Polymer Science, Springer, 1996, 126, pp.8.

[54] R. C. Thomson, A. G. Mikos, E. Beahm, J. C. Lemon, W. C. Satterfied, T. B. Aufdemorte, " Guided tissue fabrication from periosteum using performed biodegradable polymer scaffolds", Biomaterials, 1999, 20, pp. 2007.

[55] C. A. Vacanti, R. Langer, B. Schloo, J. P. Vacanti, " Synthetic polymers seeded with chondrocytes provide a template for new cartilage formation", Plast. Reconstr. Surg, 1991, 88, pp. 753.

[56] C. R. Chu, R. D. Coutts, M. Yoshioka, F. L. Harwood, A. Z. Monosov, D. Amiel, " Articular cartilage repair using allogeneic perichondrocyte seeded biodegradable porous polylactic acid (PLA): A tissue-engineering study", J. Biomed. Mater. Res, 1995, 29, pp. 1147.

[57] P. X. Ma, B. Schloo, D. Mooney, R. Langer, "Development of biomechanical properties and morphogenesis of in vitro tissue engineered cartilage", J. Biomed. Mater. Res, 1995, 29, pp. 1587.

[58] C. T. Laurencin, M. A. Attawia, H. E. Elgendy, K. M. Herbert, "Tissue engineered bone-regeneration using degradable polymers: the formation of mineralized matrices", Bone, 1996, 19, pp. 93.

[59] D. J. Mooney, D. F. Baldwin, N. P. Suh, J. P. Vacanti, R. Langer, "Novel approach to fabricate porous sponges of poly(D,L-lactic-co-glycolic acid) without the use of organic solvents", Biomaterials, 1996, 17, pp.1417.

[60] D. J. Mooney, C. L. Mazzoni, C. Breuer, K. McNamara, D. Hern, J. P. Vacanti, "Stabilized polyglycolic acid fibre-based tubes for tissue engineering", Biomaterials, 1996, 17, pp.115.

[61] M. Sittinger, D. Reitzel, M. Dauner, H. Hierlemann, C. Hammer, E. Kastenbauer, "Resorbable polymers in cartilage engineering: affinity and biocompatibility of polymer fiber structures to chondrocytes", J. Biomed. Mater. Res, 1996, 33, pp.57.

[62] E. Wintermantel, J. Mayer, J, Blum, K. L. Eckert, P. Luscher, M. Mathey, "Tissue engineering scaffolds using superstructures", Biomaterials, 1996, 17, pp.83.

[63] M. S. Widmer, P. K. Gupta, L. Lu, R. K. Meszlenyi, G. R. D. Evans, K. Brandt, "Manufacture of porous biodegradable polymer conduits by an extrusion process for guided tissue regeneration", Biomaterials, 1998, 19, pp.945.

[64] P. Angele, R. Kujat, M. Nerlich, J. Yoo, V. Goldberg, B. Johnstone, "Engineering of osteochondral tissue with bone marrow mesenchymal progenitor cells in a derivatized hyaluronan-gelatin composite sponge", Tissue Enginerring, 1999, 5, pp.545.

[65] M. Doser, "Criteria for the selection of biomaterials for tissue engineering", Polymers for Medical Technologies, 37th Tutzing-Symposion of Dechema, 1999, 8, pp.11.

[66] B. Kreklau, M. Sittinger, M. B. Mensing, C. Voigt, G. Berger, G. Burmester, "Tissue engineering of biphasic joint cartilage transplants", Biomaterials, 1999, 20, pp.1743.

[67] S. V. Madihally, H. W. T. Matthew, " Porous chitosan scaffolds for tissue emgineering", Biomaterials, 1999, 20, pp.1133.

[68] A. Dedlich, C. Perka, O, Schultz, R. Spitzer, T. Haupl, G. R. Burmester, "Bone engineering on the basis of periosteal cells cultured in polymer fleeces", Journal of Materials Science, 1999, 10, pp.767.

[69] B. A. Huibregtse, B. Johnstone, V. M. Goldberg, A. I. Caplan, "Effect of age and sampling site on the chondro-osteogenic potential of rabbit marrow-derived mesenchymal progenitor cells", J. Orthop. Res, 2000, 18, pp.18.

[70] T. C. Laurent, J. R. Fraser, Hyaluran, *FASEB J*, 1992, 6, pp.2397.

[71] K. Kawasaki, M. Ochi, Y. Uchio, J. Hyaluronic acid enhances proliferation and chondroitin sulfate in cultured chomdrocytes embedded in collagen gels. Cell. Physiol, 1999, 179, pp.142.

[72] P. Bulpitt, D. Aeschlimann, New strategy for chemical modification of hyaluronic acid: preparation of functionalized derivatives and their use in the formation of novel biocompatible hydrogels. J. Biomed. Mater. Res. 1999, 47, pp.152.

[73] X. Zheng, Y. Lui, F. S, In situ crosslinkable hyaluronan hydrogels for tissue engineering. Biomaterials, 2004, 25, pp.1339.

[74] M. Kurisawa, J. E. Chung, Y. Y. Yang, Oxidative coupling of epigallocatechin gallate amplifies antioxidant activity and inhibits xanthine oxidase activity. Chem. Commun, 2005, 2005, pp.4312.

[75] D. L. Nettles, T. P. Vail, M. T. Morgan, Photocrosslinkable hyaluronan as a scaffold for articular cartilage repair. Ann Biomed Eng, 2004, 32, pp.391.

[76] J. A Burdick, C. Chung, X, Jia, Controlled degradation and mechanical behavior of photopolymerized hyaluronic acid networks. Biomacromolecules, 2005, 6, pp.386.

[77] C. Chung, J. Mesa, M. A. Randolph, J. Biomed. Mater. Res. A, 2006, 77A, pp.518.

[78] H. Onishi, Y. Machida, Biodegradation and distribution of water-soluble chitosan in mice. Biomaterials, 1999, 20, pp.175.

[79] J. M. Moss, M. P. Van Damme, W. H. Murphy, Purification, characterization, and biosynthesis of bovine cartilage lysozyme isoforms. Arch. Biochem. Biophys, 1997, 339, pp.172.

[80] J. K/ Suh, H. W. T. Matthew. Application of chitosan-based polysaccharide biomaterials in cartilage tissue engineering: a review. Biomaterials, 2000, 21, pp.2589.

[81] A. Di Martino, M. Stittinger, M. V. Risbud, Chitosan: a versatile biopolymer for orthopaedic tissue-engineering. Biomaterials, 26, pp.5983.

[82] I.Y. Kim, S. J. Seo, H. S. Moon, Chitosan and its derivatives for tissue engineering applications. Biotechnol. Adv, 2008, 26, pp.1

[83] J. Wu, Z. G. Su, A thermo and pH-sensitive hydrogel composed of quaternized chitosan/glycerophosphate. Int. J. Pharm, 2006, 315, pp.1

[84] A. Chenite, C. Chaput, D. Wang, Novel injectable neutral solutions of chitosan form biodegradable gels in situ. Biomaterials, 2000, 21, pp.2155

[85] Y. Hong, Z. Mao, H. Wang, Covalently crosslinked chitosan hydrogel formed at neutral pH and body temperature. J. Biomed. Mater, Res, A. 2006, 79A, pp.913.

[86] N. Bhattarai, H. R. Ramay, J. Gunn, PEG-grafted chitosan as an injectable thermosensitive hydrogel for sustained protein release. J. Contr. Release, 2005, 103, pp.609.

[87] K. Ono, Y. Saito, H. Yura, Photocrosslinkable chitosan as a biological adhesive. J. Niomed. Mater. Res, 2000, 49, pp.289.

[88] E. Marsich, M. Borbogna, I. Donati, Alginate/lactose-modified chitosan hydrogels: A bioactive biomaterials for chondrocyte encapsulation. J. Biomed. Mater, Res, A. 2008, 84A, pp.364.

[89] V. F. Sechriest, Y. J. Miao, C. Niyibizi, GAG-augmented polysaccharide hydrogel: A novel biocompatible and biodegradable material to support chondrogenesis. J. Biomed. Mater. Res, 2000, 49, pp.534.

[90] C. D Hoemann, J. Sun, A. Legare, Tissue engineering of cartilage using an injectable and adhesive chitosan-based cell-delivery vehicle. Osteoarthritis Cartilage, 2005, 13, pp.318.

[91] M. S. Shoichet, R. H. Li, M. L. White, stability of hydrogels used in cell encapsulation: An in vitro comparison of alginate and agarosa. Biotechnol. Bioeng, 1996, 50, pp.374.

[92] S. Sakai, k. Kawakami, Synthesis and characterization of both ionically and enzymatically cross-linkable alginate. Acta Biomater, 2007, 3, pp.495.

[93] J. Maia, L. Ferreira, R. Carvalho, Synthesis and characterization of new injectable and degradable dextran-based hydrogels. Polymer, 2005, 46, pp.9604.

[94] S. H. Kim, C. Y. Won, C. C. Chu,Synthesis and characterization of dextran-based hydrogels prepared by photocrosslinking. Carbohydr, Polym, 1999, 40, pp.183.

[95] S. G. Levesque, R. M. Lim, M. S. Shoichet, Macroporous interconnected dextran scaffolds of controlled porosity for tissue-engineering applications. Biomaterials, 2005, 26, pp.7436.

[96] C. Hiemstra, L. J. Vander, Z. Zhong, Rapidly in Situ-forming degradable hydrogels from dextran thiols through Michael addition. Biomacromolecules, 2007, 8, pp.1548.

[97] R. Jin, C. Hiemstra, Z. Zhong, Enzyme-mediated fast in situ formation of hydrogels from dextran-tyramine conjugates. Biomaterials, 2007, 28, pp.2791.

[98] S. G. Levesque, M. S. Synthesis of enzyme-degradable, peptide-cross-linked dextran hydrogels. Shoichet, Bioconjug, Chem, 2007, 18, pp.874.

[99] C. Hiemstra, L. J. Vander, Z. Zhong, Novel in situ forming, degradable dextran hydrogels by Michael addition chemistry: synthesis, rheology, and degradation. Macromolucules, 2007, 40, pp.1165.

[100] T. Coviello, P. Matricardi, C. Marianecci, J. Polysaccharides hydrogels for modified release formulations. Control. Release, 2007, 119, pp.5.

[101] S. G Levesque, M. S. Shoichet. Synthesis of cell-adhesive dextran hydrogels and macroporous scaffolds. Biomaterials, 2006, 27, pp.5277.

[102] S. J. Bryant, K. S, Anset, J. Biomater. Hydrogel properties influence ECM production by chondrocytes photoencapsulated in poly (ethyleneglycol) hydrogels. Mater. Res, 2002, 59, pp.63.

[103] S. J. Bryant, K. S, Anset, J. Controlling the spatial distribution of ECM components in degradable PEG hydrogels for tissue engineering cartilage. Biomater. Mater. Res. A, 2003, 64A, pp.70.

[104] P. J. Martens, S. J. Bryant, K. S. Anseth, Tailoring the degradation of hydrogels formed from multivinyl poly (ethylene glycol) and poly (vinyl alcohol) macro,ers for cartilage tissue engineering. Biomacromolecules, 2003, 4, pp.283.

Chapter 2

Effect of chemical treatment of *Agave Tequilana W*eber bagasse fibers used to elaborate cyto and biocompatible hydrogel films

Abstract: Waste bagasse of *Agave tequilana*-Weber fibers were chemically treated with sodium hydroxide, sulfuric acid and bleached with sodium hypochlorite to prepare cellulose solution to elaborate hydrogel films. The concentration of the sodium hypochlorite used in the chemical treatment affected the color of the fibers by changing from brown to white. Dimethylacetamide/lithium chloride (DMAc/LiCl) was used as solvent to prepare cellulose solutions. The transparent hydrogel films were obtained by phase inverse method advantageously without chemical cross-linker. It was found that the resultant hydrogels showed increment in tensile from 40 N/mm^2 to 56 N/mm^2 with the increasing of sodium hypochlorite concentration from 1 to 10 vol%, respectively. Regarding to biocompatibility properties of the hydrogel films, platelet adhesion, clotting time and protein adsorption were investigated. Analysis of the morphology of adherent NIH3T3 fibroblast indicated that the projected cell area, aspect ratio and long axis gradually increased with the increment of sodium hypochlorite content in the agave treatment. It was presented that the chemical treatment affects cell adhesion and morphology and remain lignin content in the brown fibers.

2.1 Introduction

Sisal fiber is one of the most widely used natural fibers and is very easily cultivated. Nearly 4.5 million of tons of sisal fiber are produced every year throughout the world [1, 2]. As well as sisal fiber, agave bagasse is the residual fiber remaining after agave heads are cooked, shredded, and milled, and then, sugars were extracted to leave agave bagasse. Figure 2.1 shows agave tequilana Weber plant.

Figure 2.1. Agave tequilana Weber plant.

Agave tequilana Weber is used in Mexico for the fabrication of tequila. The diverse varieties of agave found throughout Mexico have been used since time immemorial to make different alcoholic beverages. Tequila manufacture in a traditional distillery, begins with the cooking of agave tequilana Weber azul plant heads to hydrolyze the polymers present in the plant, mainly inulin, into fermentable sugars. Agave tequilana Weber azul is cultivated only in very restricted regions established as protected territories by the tequila denomination of origin as shown in Figure 2.2.

Figure 2.2. States of Mexico with agave tequilana Weber for the elaboration of tequila.

The bagasse is primarily the rind and fibro vascular bundles dispersed throughout the interior of the agave head. The bagasse was found way after mechanical pith, separation and sun-drying, in the manufacture of mattresses, furniture and packing materials. However, this waste product is destined to be incinerated. In recent years, the tequila market has growth and been developed due to the recently recognized "tequila origin denomination" by the European Union. This tendency means that even more bagasse would be on the disposal problems in the Tequila Companies [1-6]. Serious economic and environmental problems have been caused by the disposal of this resource. Therefore, the necessity of the development of new technologies to solve this problem is evident for the effective re-uses. Due to this, research work on the use of agro-industrial waste

is needed. Several research works have been conducted using bagasse from *Agave tequilana* Weber *azul* to offer an alternative use for this product [7-10]. However, none is offered us a final solution in useful application. It is known that the agave bagasse contains cellulose source as useful biomass. It is well known that cellulose is the most abundant renewable resource on earth. Moreover, numerous new functional materials from cellulose are developing over a broad range of applications because of the increasing demand for environmentally and friendly biocompatible products [11-13]. In addition, cellulose having abundant hydroxyl groups can be used to prepare thin films easily with fascinating structures and properties. On the other hand, it is worth noting that hydrogels have wide potential applications in the fields of food, biomaterials, agriculture, water purification, and etc [14-16]. Recently, scientists have devoted much energy to the development novel hydrogels for new applications such as tissue engineering. For example, a number of polysaccharides such as carrageenan, dextran sulfate, and collagen have been studied because they can be degraded to nontoxic products and then easily assimilated by the body [17-19]. In addition, various hydrogels from natural polymers have been fabricated by using hyaluronate, cellulose, chitosan and its derivatives, showing a potential application in biomaterials field because of their safety, hydrophilicity, biocompatibility and biodegradability [20-23]. However, very limited work has been performed by using cellulose fibers for hydrogel uses. In our previous report we found that cellulose hydrogel films prepared from agave fiber showed good bio and cytocompatibility [10]. However, it was found that the chemical treatment of the agave fibers affected the properties of the obtained solutions and the elaborated hydrogels. Base on this manner, we focus our study on the effect of chemical treatment of the agave fibers on the cytocomnpatibility of the obtained hydrogel films.

Thus, on our strategy, cellulose hydrogel films were successfully prepared without additional chemical modification and by phase inversion method. The hydrogel films prepared from agave bagasse fibers were studied in their cytotoxicity and biocompatibility was reported [10]. However, there are still several unknown events on the agave fibers about the treatment products for the hydrogels in the tissue engineering.

Therefore, the present study describes cyto and biocompatible hydrogel films of waste agave bagasse treated with different concentration of sodium hypochlorite (NaOCl) during the chemical processes. The present work studied cell morphology and adhesion to assess the relative biocompatibility of cellulose hydrogel films prepared with agave fibers treated with different concentration of sodium hypochlorite. The aim of this study was to demonstrate the effect of the chemical treatment procedure for agave cellulose on cytocompatibility of the obtained hydrogel film. The obtained results showed that chemical treatment of the agave fibers played an important role in the dissolution of cellulose in the DMAc/LiCl system helping to remove lignin and other compounds from agave fibers leaving higher cellulose content. It was found that the chemical treatment improved cytocompatibility of the obtained hydrogel films.

2.2 Experiments

2.2.1 Materials

Tequilana Webber bagasse was provided from Corralejo Tequila Company, Guanajuato, Mexico. *N N,* dimethyl acetamide (DMAc) was purchased from TCI, Tokyo, Japan, and stored for more than 5 days over potassium hydroxide before used. Ethanol (C_2H_5OH), lithium chloride (LiCl), sodium hydroxide (NaOH), and sodium hypochlorite (NaOCl) were purchased from Nacalai Tesque. Inc. Lithium chloride was dried at 120°C for 12 h in a vacuum oven before

used. For protein adsorption studies, Bicinchoninic acid (BCA) kit was purchased from Sigma Aldrich Japan. Poor platelet plasma (PPP Sigma Aldrich), fetal bovine serum (FBS), and bovine serum albumin (BSA) were purchased from Sigma Aldrich. Phosphate-buffered saline (PBS, Dullbecco Co., Ltd), 0.05 w/v% trypsin-0.053 M-ethylenediaminetetraacetate (trypsin-EDTA, Gibco), and formaldehyde (37 vol %, Wako Co., Ltd.) were used as received. NIH 3T3 mouse embryonic fibroblast cells were purchased from BioResource Center, Japan.

2.2.2 Agave fiber treatment

The agave fibers were washed 3 times with distillated water to remove traces of sugars from tequila manufacturing process and dried in vacuum oven at 50°C. As a first part of the treatment, 3 g of agave fibers were immersed in 1000 mL of 10 wt% NaOH solution and stirred for 12 h at 100°C, until a black liquor solution was obtained [23,24]. Then, the fibers were washed 5 times with abundant distilled water to eliminate residues of NaOH remaining in the fibers. Then, agave fibers were immersed in 1000 mL of distilled water and stirred at room temperature until pH 7 was obtained. After that, the fibers were added to 1000 mL solution of 4 vol% H_2SO_4 stirring for 2 h at 100°C. Then, the fibers were washed 5 times with abundant distilled water to eliminate residues of H_2SO_4 solution in the fibers. At this point, there was still brown color in the fibers as shown in Figure 1. Then, varying the concentration of NaOCl in the range of 1.0, 2.5, 5.0, 7.5 and 10 vol% was carried out a bleach process for the treatment of the agave fibers. The agave fibers were immersed in 1000 mL of NaOCl solution and stirred for 2 h at room temperature. Finally, the treated agave fibers were washed 5 times with abundant distillated water and dried under vacuum for 2 days.

2.2.3 Preparation of hydrogel films.

The treated fibers (1 wt%) were dissolved in DMAc solution with 6 wt% LiCl of concentration by following three steps of solvent exchange [25]. The treated agave fibers were suspended in 300 mL of distilled water and stirred overnight to allow swelling of the fibers. Afterwards, water was removed from the suspension by an adapter glass filter under vacuum. Ethanol (300 mL) was added to the swelled fibers and the mixture was stirred for 24 h. Then, ethanol was removed and the treated fibers were added to 300 mL of DMAc and stirred overnight. Finally, LiCl and DMAc were added to the swelled agave fibers in order to adjust the concentration of the solution to 1 wt%. The mixture was stirred at room temperature for 3 days until a viscous solution was obtained.

For hydrogel films preparation, 10g of the agave solution was poured into a glass tray (10 cm diameter), and kept for 12 h in a container filled with 20 mL of ethanol. After this, a transparent hydrogel film was obtained (Figure 1). The resulting film was washed with ethanol 3 times and then put it on shaking bath for 24 h to remove remain DMAc. Then, the hydrogel film was immersed in distilled water and kept at 4°C overnight in a plastic container with PBS. This procedure was repeated 2 times.

2.2.4 Evaluation of cellulose hydrogels

Shear viscosity of cellulose solutions was measured after agave fibers were dissolved during three days and before the coagulation of hydrogel films. Shear viscosity measurements were carried out by using a B type viscometer (Tokyo). Equilibrium water contents (EWC) of the resultant hydrogel films were determined by weighting the wet and dry samples and calculated with dry base. Samples (5 x 5 mm^2) were cut from the films and previously dried with vacuum

and kept in desiccator for 48 h. Then, the samples were then swollen in PBS for 36 h. After this, the samples were removed and wrapped with filter paper in order to remove the excess of PBS. The weight of hydrated samples was then determined. The percent EWC of hydrogels was calculated based on EWC= ($(W_h - W_d)/ W_d$) x 100, where the values of W_h is the weight of the hydrated samples and W_d is the dry weight of the sample. For each specimen, four independent measurements were done and averaged. In the case of tensile strenght and elongation measurements, hydrogel film were previously dried under vaccum for 48 h. Hydrogel samples (50 x 10 mm) were used and the experiments were carried out by a LTS -500N - S20 (Minebea, Japan), which was a universal testing machine equipped with a 2.5 kN cell. The hydrogel film specimens were cut in size with a length of 50 mm and a width of 10 mm. The hydrogel film at different concentration of NaOCl was tested 3 times. Only samples which ruptured near mid-specimen length were considered for the calculation of tensile strength (N/mm^2) and elongation (%). Viscoelasticity of the hydrogel films with 2 cm in diameter with 5 mm in thickness was determinate by Auto Paar-Reoplus equipment (Auton Paar Japan, Tokyo) in wet conditions at 37°C. FT-IR spectroscopy was applied to examine components by using FT-IR 4100 series (Jasco Corp. Japan). In the case of the hydrogel film sample, the film was set up in CaF_2 window (30 mm diameter; thickness 2 mm, Pier Optics Co. Ltd). Then, 2 μL of distillated water was dropped to the film. Then, another window was pressed to cover the wet film. From the FT-IR spectra, a deconvolution analysis of the OH stretching was carried out. Where the center of the fixed peaks from the original OH stretching bands obtained in the spectra data were decomposed into Gaussian components. The peak centers and the curve were then fitted using OriginPro 8.5.1 [26].

2.2.5 Biocompatibility experiments

In the case of protein adsorption hydrogel films with 5 mm in diameter were incubated in phosphate buffered solution (PBS) for 24 h and then, immersed in 1 mL of PBS containing BSA (1g/ml) for 4 h at 37°C. FBS experiments, 1 mL of Dulbecco's modified Eagle's medium (DMEM) enriched with 10% of FBS was used. Subsequently, the hydrogel films were rinsed slightly with PBS. Then, the hydrogel films were immersed in 2 mL of 2 wt% of dodecyl sulfate (SDS) solution and shaken for 2 h to remove the adsorbed protein. The amounts of absorbed protein were then determined by using a Micro BCA protein assay with spectrophotometer at 562 nm. The six measurements were averaged to obtain a reliable value.

For the Lee White Clotting Time (LWTC) test, the platelet poor plasma (PPP) was used [27]. The hydrogels films (5 mm x 5 mm) where placed into plastic containers and 200 μL of PPP were dropped and maintained at 37^{O}C. Simultaneously, with the addition of $CaCl_2$ the time on the chronometer was started and the solution was mixed well. After 20 s passed, clotting time was recorded with a chronometer. The tests were repeated three times for each experiment. The measurements of sic experiments were averaged. For the platelet adhesion measurements, all the appliance, reagents and films (5 mm x 5 mm) were sterilized by 75 vol % Ethanol for 3 h before the experiments. Then, the samples were immerged in PBS buffer for 24 h and placed in disposal plastic tubes. In each tube 200 μL of platelet rich plasma (PRP) was dropped, and then the samples were incubated at 37^{O}C for 90 min. Following this, the hydrogel films were rinsed three times with PBS (37^{O}C) and the adhered platelets were fixed on the film surface with 1 mL 2.5% w/w glutaraldehyde/PBS at 4^{O}C for 2 h. Finally, the samples were immerged in PBS for 5 min. The tests were repeated three times for each sample. Five experiments were averaged. For the observation and counting of adherent platelets dehydration, the samples were carried out as

follows. The first dehydration was performed in a series of ethanol/PBS mixtures with increasing ethanol concentrations (25, 50, 75, and 100 wt% for 15 min in each mixture). Then, a second dehydration with a series of alcohol iso-amyl acetate/PBS mixtures was carried out with increasing iso-amyl acetate concentrations from 25 to 100 wt% for 15 min in each mixture. After freeze-drying, the platelet-attached films were analyzed by scanning electron microscope (SEM).

2.2.6 Cell culture and cell seeding.

The samples were sterilized twice with 70 vol% and 50 vol% of ethanol for 30 min, respectively. Then rinsed twice in PBS for 30 min and finally swelled in DMEM for 1 h before the seeding procedure. NIH 3T3 mouse embryonic fibroblast cells were cultured under at 37°C in 95% relative humidity under 5% CO_2 environment. The culture medium was on 90% DMEM as supplement with 10% FBS and 1% penicillin/streptomycin. The cells were seeded on the hydrogel films samples in polystyrene tissue culture dish (PS dish), at a density of $8x10^3$ cells cm^{-2}. The cells were used for image and characterization purposes after 4 to 72 h culture. The samples were imaged using inverse microscope (Olympus CKX41, Japan) for the measurement of aspect ratio, long axis and cell density. To measure cell area, the cell boundaries were marked using Cellsens software. Approximately 50 cells were analyzed per image. For each sample six images were analyzed to obtain an unbiased estimate of the cell density and morphology. Herein, the presented results were based on three independent experimental runs. The measurements were assessed statistically using a one-way analysis of variance (ANOVA) test followed by the Student's t Test with a significance criterion of $p < 0.05$.

2.3 Results and Discussion.

2.3.1 Effect of sodium hypochlorite treatment of the agave fibers.

Table 2.1 shows shear viscosity of the agave cellulose solutions in the DMAc/LiCl system. The cellulose solutions originated from agave fibers treated with different concentration of NaOCl showed a significant difference in shear viscosity value around 158 Cp and 200 Cp for 0 wt% and 10 wt% of NaOCl, respectively. This could be attributed to the macrocation form in the system DMAc/LiCl which interacts with cellulose molecules and acts as crosslinker [28]. After the increment of NaOCl, another components as lignin and hemicellulose could be remove and the constituent of the fibers is mainly cellulose. Therefore, the fibers could interact more with the solvents. In addition, Kennedy et. al. [29] reported that the treatment used to remove lignin in wood pulps created voids and a wide distribution of pores. Such microporous structure eases the liquids and solvent used in DMAc/LiCl system. This could increase the interactions between cellulose fibers and the macrocation formed increasing the viscosity of the obtained solution. These suggested that the higher degree of the NaOCl in the treatment could remove more lignin from the agave fibers.

Table 2.1. Properties of agave cellulose hydrogel films.

	Agave DMAc/LiCl solution		Hydrogel films		
NaOCl Content (vol%)	Shear viscosity (cp) 6 rpm	60 rpm	Equilibrium Water Content dry base	Elongation (%)	Tensile strength (N/mm^2)
0.0	158	155	371	8	38
1.0	160	158	361	10	40
2.5	165	162	352	14	43
5.0	170	168	332	17	46
7.5	180	178	322	22	52
10.0	190	197	292	25	56

Mean ± standard deviation (SD) for $n \geq 30$ units.penetration by activation

As shown in Figure 2.3, remarkable color change of the agave fibers was observed when the concentration of NaOCl was varied from 0 to 10 vol%. The brown color of the agave fibers at 0 vol% concentration could be changed to be bleached, as the concentration was increased throughout 10 vol%. As shown in Figure 2.3 (b) difference in color was observed in the cellulose solutions depending of the NaOCl concentration used. Brown color was observed in the solution obtained with 0 vol% of NaOCl, yellowish with 5 vol% and colorless cellulose solution was obtained with 10 vol% of NaOCl.

In order to confirm the treatment of the agave fibers UV spectra and FT-IR spectra were measured. Figure 2.4 shows UV spectra of the hydrogel films prepared with agave fibers treated with different concentration of NaOCl. It was observed that at lower NaOCl used, the intensity of absorbance peak at 280 nm assigned to lignin, decreased with increasing of NaOCl concentration in the treatment [30]. Moreover, at 10 vol% of NaOCl any trace of lignin could not be detected in the obtained film.

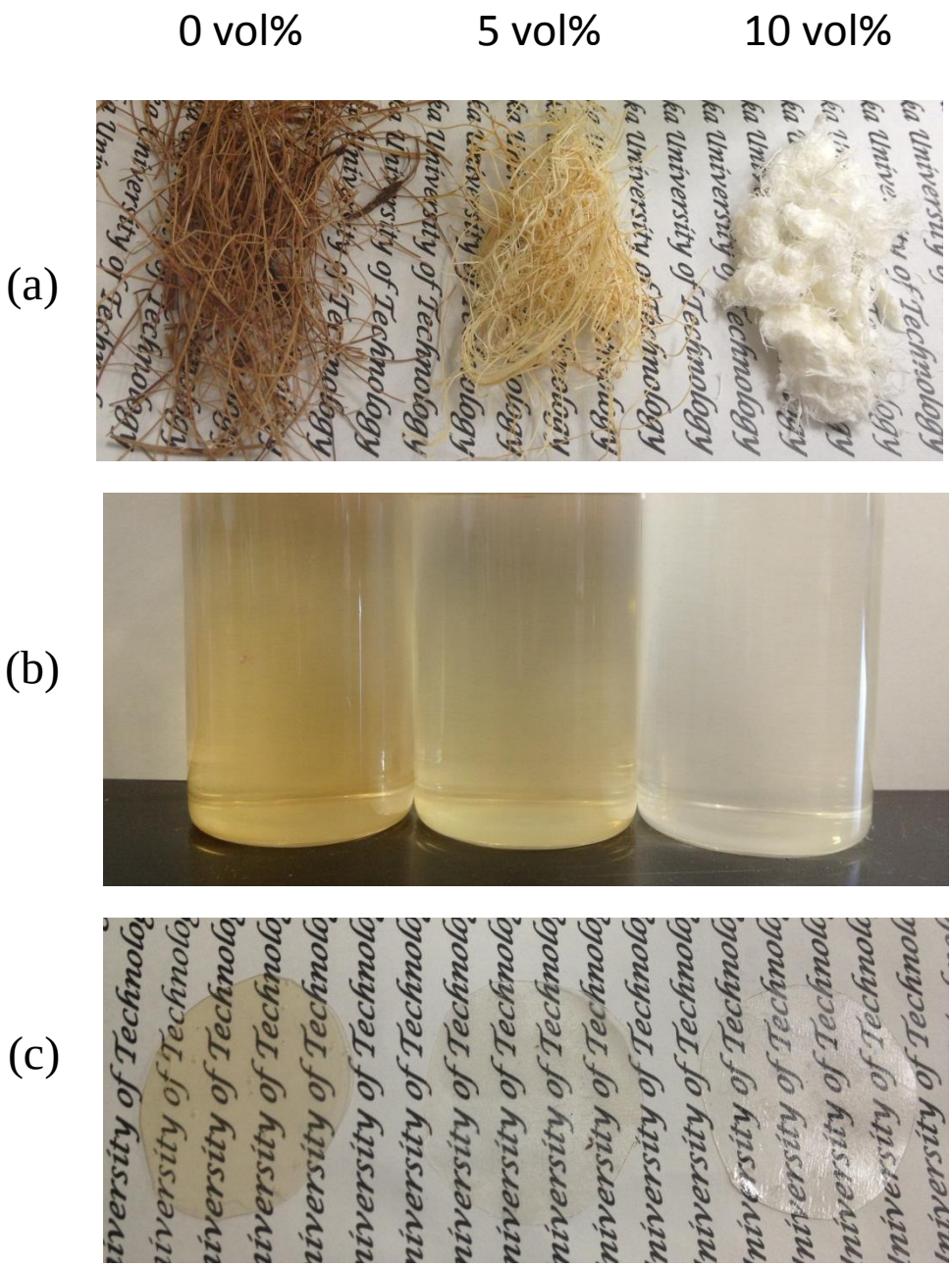

Figure 2.3. (a) Agave fibers treated with different concentration of NaOCl (0, 5 and 10 vol%), (b) agave solutions prepared with the agave fibers treated, and (c) the obtained agave hydrogel films in dry conditions.

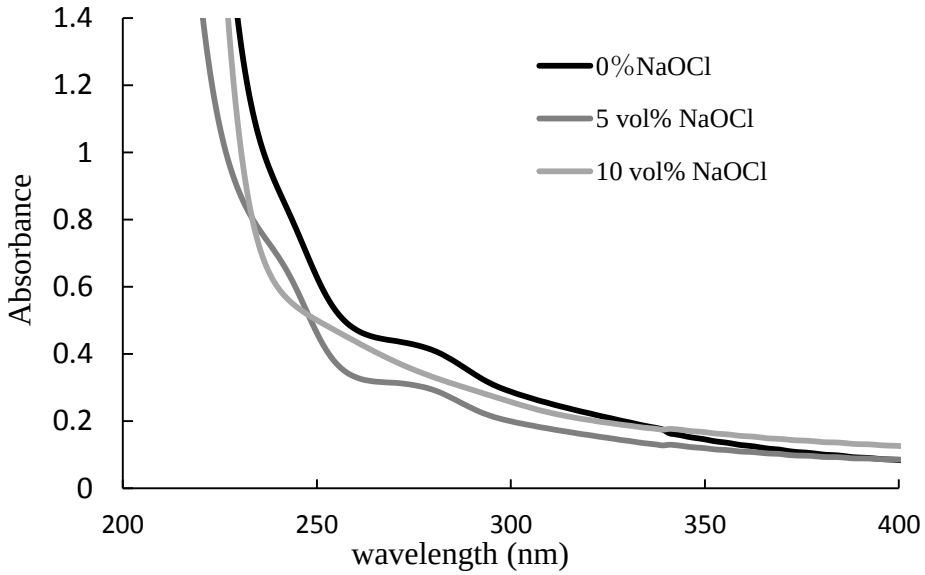

Figure 2.4. Absorption spectra of cellulose hydrogel films prepared with agave fibers by NaOCl treatments in different concentration.

The FT-IR spectra in Figure 2.5 showed remarkable differences between the obtained agave fibers before and after the NaOCl treatments. Moreover, these spectra data presented that the broad peak centered at 3400 cm^{-1} was due to the stretching vibrations of bonded and non-bonded hydroxyl groups as water in the samples. This meant that the presence of the hydroxyl groups in the fibers might interact with the sorrounded water, supporting the preparation of the agave solutions for the elaboration of the hydrogel films. The C-O-C and C-O vibrations of polysaccharides content in the initial agave bagasse samples were found in the region between 1200 cm^{-1} and 900 cm^{-1}. The appeared peaks around 1510 and 1520 cm^{-1} showed the presence of lignin and lignocellulose in the initial agave fibers. The use of high concentration of NaOCl for the treatment of agave fibers a decreased the intensity of the peaks at 1510 and 1520 cm^{-1} observed in the spectra. This clearly indicated that the amount of lignin on the agave fibers was successfully decreased by the chemical treatments with NaOCl. In addition, the IR spectra were

changed at 1473, 1417, 1367, 1315, 1263 and 1230 cm^{-1} by the tretament. The peaks at 1473, 1417 and 1367 were assigned to C-H and –O-C- bending and around 1315, 1263 and 1230 cm^{-1} were assigned to H-C and C-O bending. Futhermore, the weak band at 1160 cm^{-1} and 1080 cm^{-1} could be asigned to polysaccharides as reported by Grude et al. [30,31] As indicated by the FT-IR spectra in Figure 2.2 (b), the hydrogel film prepared from 10 vol% of NaOCl treatment exhibed higher O-H streching band near 3200-3500 cm^{-1}. This was due to higher contents of O-H group resulted from cellulose. However, in the case of 0 and 5 vol%, additional peaks of lignin was observed, meaning that the lignin contained had a tendency for interfering with the hydrogen bonding.

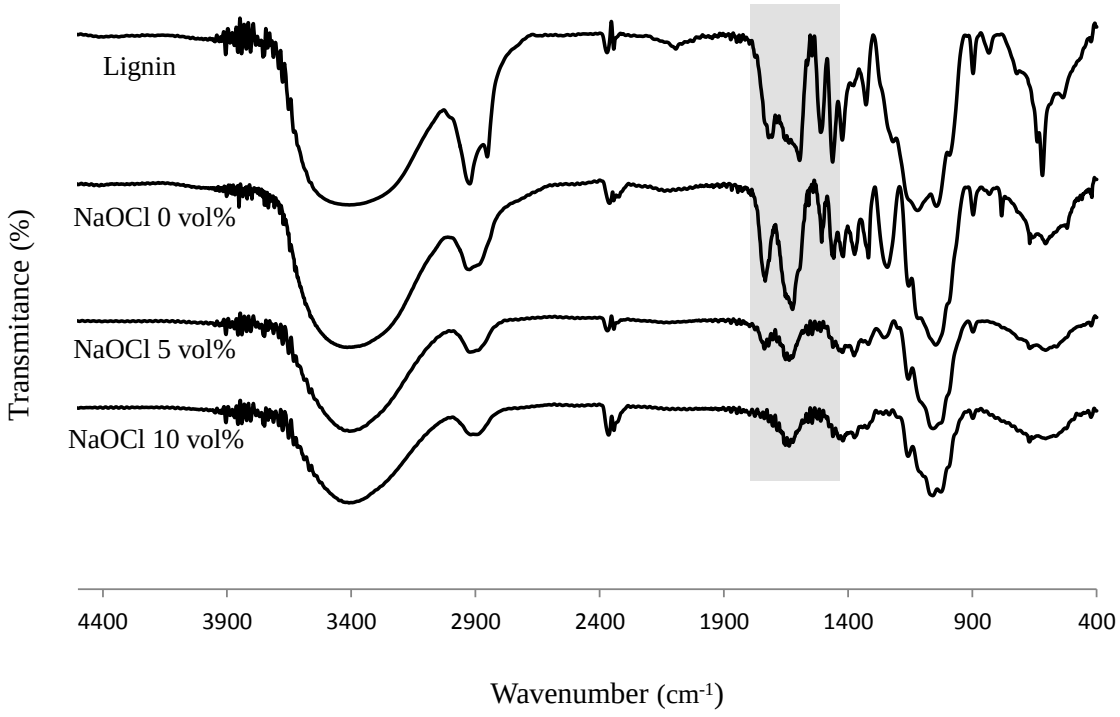

Figure 2.5. FT-IR spectra of cellulose films prepared with agave fibers by NaOCl treatments in different concentrations.

As shown in Table 2.1, the value of EWC significantly decreased with increase of the NaOCl concentration in the treatment of the agave fibers. All of the samples reached to the equilibrium after 36 h in the swelling process. The hydrogel films had 37% and 29% of EWC, as the concentration of NaOCl was 1 vol% and 10 vol%, respectively. The higher elongations and tensile strength of the resultant hydrogel films were observed in the films that were prepared from fibers treated at 10 vol% of NaOCl. With increasing of NaOCl concentration from 1 to 10 vol% tensile strength and elongation values increased from 40 N/mm^2 to 56 N/mm^2 and from 10.3 to 24.6%.

Figure 2.6 shows viscolelasticity of each hydrogel film. As strain was increased in the sample film, the value of G' decreased for the hydrogel film in 0 vol% suggesting that the deformation of the hydrogel films was started in the strain. When the strain reached 80%, each hydrogel film showed 280, 750 and 1300 Pa of G'. There was similar tendency of G' in function of strain% of the film, but the higher values of G' were observed in hydrogel films with 10 vol% of NaOCl attribuited to more elastic strian than at 0 vol% of NaOCl. G'' value of each hydrogel film exhibited almost one order lower than G'. In each case of lower strain 1%, the G'' value was increased and then decreased gradually at 10 vol% strain.

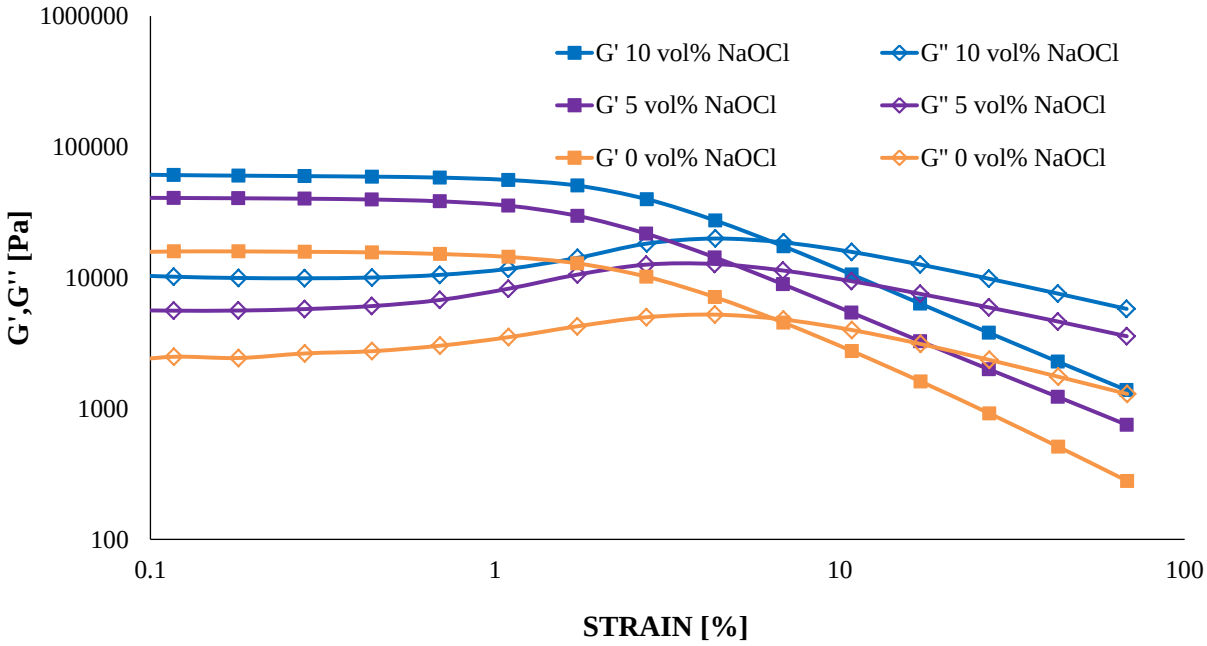

Figure 2.6. Viscoelasticity of the swelled hydrogel films prepared with agave fibers treated with different concentration of NaOCl.

In order to analyze the interaction of the obtained agave hydrogel films with the water molecules we analyzed the hydrogel films by peak deconvolution in the FT-IR spectra. From the data the peak positions were determined by using second derivative method. These spectra were decomposed into Gaussian components by curve fixed positions [26]. Figure 2.7 exhibits the fixed courves of a) NaOCl 0 vol% and b) NaOCl 10 vol%. Here, the peak 1 was assigned to free water molecules. Peak 2 was assigned to free OH groups of the polysaccharides chains. Peaks 3 and 4 were assigned to strong intermolecular bonding between water molecules and free OH groups of the polysaccharide chain. Peak 5 was assigned to strong hydrogen bond interactions between water and the OH groups from the polymer chain. In addition, the fixed curve of CH stretching was included in the spectra. For the deconvoluted spectra, peak 6 was assigned to CH

stretching band. As it was observed in Figure 5 a) and b) a remarkable difference was observed in the peaks 1, 2 and 3 with the change in the NaOCl concentration in the treatment of the agave fibers. As it was expected, with the increasement of NaOCl concentration the intensity of the peaks 2 and 3 increased due to the exposing of cellulose fibrils in the agave fibers after the bleaching process. Moreover, the decrease of free water as shown in the intensity of peak 1, could be attribuited to the increase of the interaction of free water with the OH groups in the fiber. As it was espected, this was more evident in fibers treated with higher concentration of NaOCl. Due to the content in the higher content of cellulose in treated fibers which rapedily interacts with free water molecules. These results could give evidence of the used of NaOH to remove lignin and others components from agave fibers.

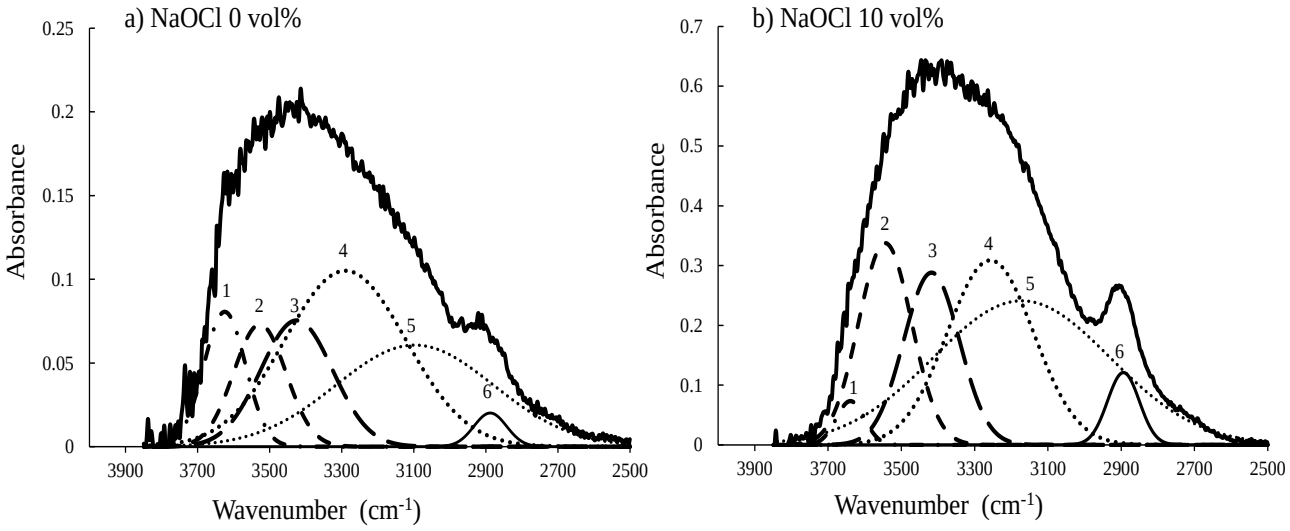

Figure 2.7. Deconvolution of OH and CH stretching region for the wet hydrogel films of the agave fibers treated with (a) NaOCl 0 vol% and (b) NaOCl 10 vol%.

2.3.2 Biocompatibility and cytotoxicity of agave hydrogel films.

Since the agave hydrogel films presented higher cyto and biocompatibility based in our previous report [10], our interesting focused on the effect of NaOCl treatment on their properties, which are very important on the application of the hydrogel films for tissue engineering. Therefore, the biocompatible properties of the hydrogel films prepared from different concentrations of NaOCl treatment were examined. Table 2.2 shows protein adsorption, platelet adhesion and clotting time for each hydrogel film prepared from different concentration of NaOCl. The values of adsorption of BSA and FBS *in vitro* for each hydrogel film increased with the increase of the NaOCl concentration for the treatment. These results were consistent to Salem et. al, they reported that it was observed that BSA and FBS tended to bind onto stiffer surfaces [32]. In additions, this significant difference was also observed in the obtained protein adsorption result compared with our previous report [10]. These results were consistent with the different observation in the viscoelasticity measurements. Moreover, after the hydrogel samples were in contact with PPP, the clotting time was significantly affected by the NaOCl concentration used. As seen in Table 2.2, the value of clotting time decreased with increasing of the NaOCl concentration. This result could be supported with the results of the protein adsorption. In the protein adsorption, it was easy to consider that the increase of protein serum adsortion might enhance the formation of a fibrin rich cloth on the hydrogel film. For this reason, if the protein serum adsorption decreased, the time for the formation of the cloth will incresead. In addition, protein adsorption on the hydrogel film surface also influence cell adhesion. The cell density on the hydrogel films was evaluated by counting adhered fibroblast on the hydrogel surface. Figure 2.8 shows that all the samples revealed differences in the number of adherent cells on hydrogel films as NaOCl concentration of agave fibers was changed, these differences were

Table 2.2. Biocompatibility properties of agave cellulose hydrogel films

NaOCl content (wt%)	Protein adsorption (μg/cm²) BSA	FBS	Platelet adhesion (Platelet/μm²)	Clotting time (s)
0.0	2	13	921	60
1.0	3	15	965	58
2.5	5	17	1022	56
5.0	8	26	1156	53
7.5	9	32	1303	49
10.0	11	35	1487	47

Mean ± standard deviation (SD) for $n \geq 125$ units.

significant (ANOVA, $p < 0.05$). For this reason, after 4 h of cultivation the number of adherent cells showed slight difference compared with PS dish used as control. This was significant in all the hydrogel samples after 4, 24 and 72 h of incubation (Student's t-test, $p < 0.05$, n = 6). An increased in the number of adherent cell was observed as NaOCl concentration increased. This increase was significant after 48 and 72 h of incubation (Student's t-test, $p = < 0.05$, n = 6). These differences were observed between NaOCl 7.5 vol% and NaOCl 10 vol% after 48 hours of

cultivation (Student's t-test, $p = < 0.05$, n = 6). In the case of NaOCl 0 vol% and NaOCl 2.5 vol%, a slight increase in the number of adherent cells was found after 48 h of cultivation, these differences were only significant after 72 h of cultivation compared with NaOCl 10 vol% (Student's t-test, $p = < 0.05$, n = 6). The results revealed that all the hydrogel samples used showed better cytocompatibility than the commercial culture dish (PS dish) used as control. These results confirm the expected suppress of fibroblast adhesion with the changed of the NaOCl concentration in the treatment of the agave fibers due to decrease of protein adsorption comparing with our previous report [10]. Moreover, the higher cell number was observed on hydrogel surface with the higher contact angle. Similar results were obtained by Tamada et al. [33], and Salem et al. [32], observing that fibroblast adhered better to stiffer surfaces with a contact angle around 52°. It was found that the softness and stiffness of the scaffold might regulate the adhesion between cellular-extracellular matrix molecules as well as surface wettability. Based on this, the observed difference in cell density between NaOCl 10 vol% and NaOCl 0 vol% could be attributed to the change with water content, contact angle, and the decrease of the hydrogel stiffness due to change in the NaOCl concentration in the treatment of agave fibers. One reason could be due to the diminishing of the hydrogel stiffness as shown in Figure 2.6 for viscolelasticity of the hydrogel films, which also affected wettability of the hydrogel films. It is important to consider that these affected the focal adhesions containing clusters of integrin transmembrane adhesion receptors that bind the extra cellular matrix proteins like fibronectin adsorbed to the materials surface. The obtained results revealed that cell density was sensitive to the concentration of NaOCl treatment.

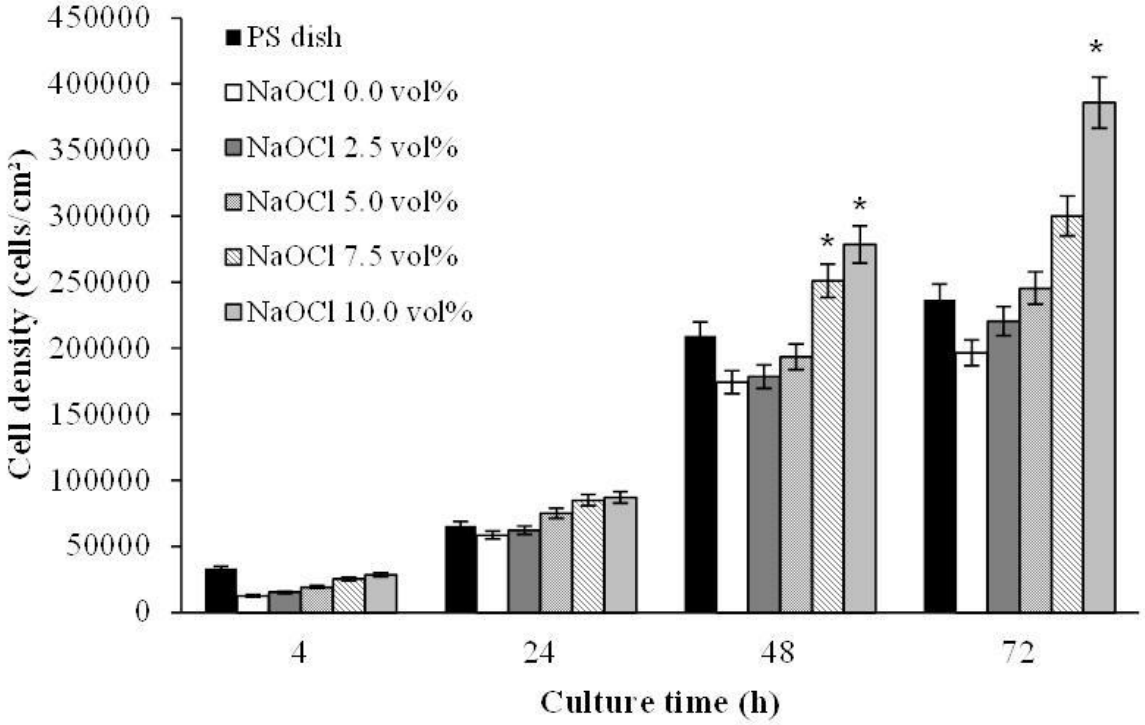

Figure 2.8. Cell number on agave hydrogel film surfaces as function of culture time, NaOCl used for the agave fiber treatment was varied from 0 to 10 vol%. An asterisk indicates statistically significant different from the PS dish used as control ($p < 0.05$). Mean ± SEM ($n = 6$).

As presented in Table 2.2 for protein adsorption, the chemical treatment of the agave fiber changed the scaffold property for better cell adhesion of the fibroblast. In order to observe such behaviour of fibroblast growing for the hydrogel films, phase-contrast light microscope images of fibroblasts on the pulp hydrogel films surface were acquired to determine the effect on cell adhesion and morphology. The cell morphology on the hydrogels films revealed a remarkable difference on adherent fibroblast morphology as shown in Figure 2.9, (a) PS dish, and hydrogel films (b-d). The cell initially adhered at 4 hours after the cell seeding. When the higher NaOCl concentration was used in the agave fibers treatment (d), the fibroblast surely adhered and grew

on the hydrogel film in comparison with picture (b) for lower concentration NaOCl. It is also important to remark that the observed shape of adherent fibroblast on Figure 2.9 (d) was significantly anisotropic. This meant that the hydrogel film provided better environment for the cell adhesion even at early timepoint of the cell cultivation on the hydrogel films showing potential medical applications.

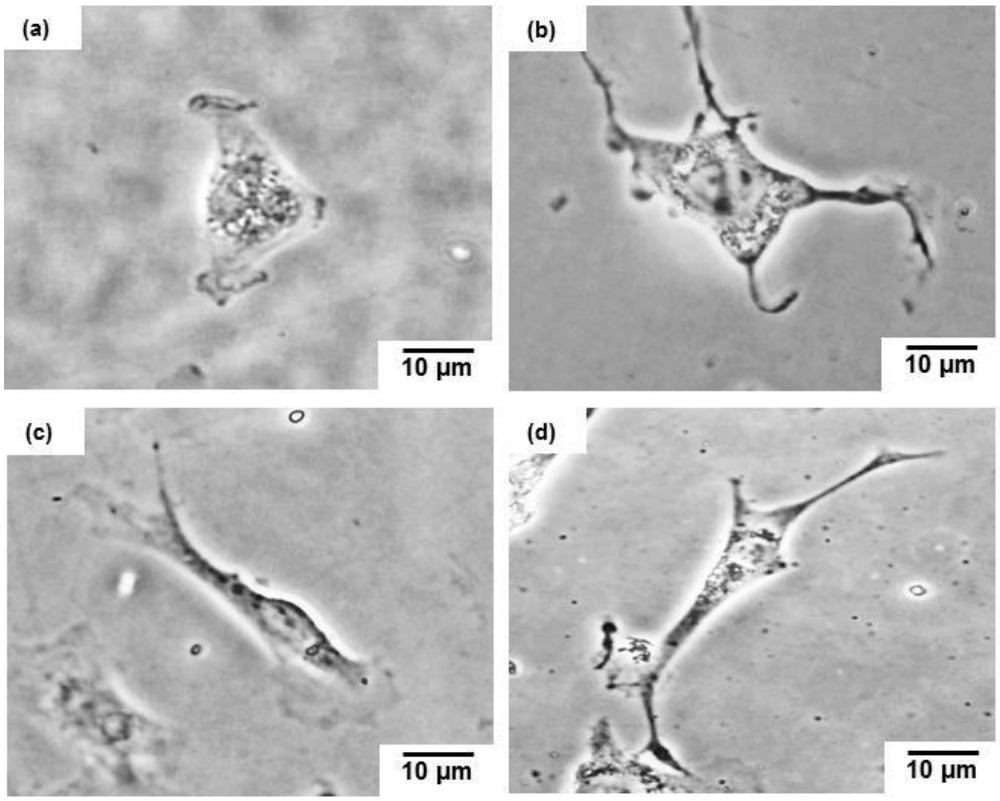

Figure 2.9. Phase-contrast light images (a) commercial PS dish used as control, hydrogel films prepared with agave fibers treated with (b) 0 vol% of NaOCl, (c) 5 vol% of NaOCl, and (d) 10 vol% of NaOCl. The culture time was 4 h.

In addition, cell morphology results are shown in Figure 2.10. It was observed that the values of cell area, aspect ratio, and length of the long axis were higher at 10 vol% NaOCl concentrations in the treatment; these differences were significant (ANOVA, $p < 0.05$). After 48

h of cultivation cell area, aspect radio and long axis showed differences compared with PS dish used as control. This was significant in all the hydrogel samples (Student's t-test, p <0.05, n=6). An increased in cell area was observed as NaOCl concentration increased. This increase was significant for PS dish and NaOCl 1 vol% (Student's t-test, p <0.05, n=6), and for NaOCl 5 vol% and 7.5 vol% (Student's t-test, p <0.05, n=6). Moreover, the remarkable differences on aspect ratio results were observed when NaOCl concentration increased. These differences were significant comparing NaOCl 1 vol% and NaOCl 10 vol% (Student's t-test, p <0.05, n=6). These results confirmed the expected differences of long axis with the increment of NaOCl. These differences were significant with PS dish compared with NaOCl 1 vol% and NaOCl 10 vol% (Student's t-test, p <0.05, n=6). These results were consistent with the reported by Salem, et al. [32] they observed diminished of the projected cell area for MC3T3-E1 pre-osteoblasts on less smooth surfaces. Therefore, for the fibroblast, the diminish of projected cell area, aspect ratio and long axis could be the negative effect in focal adhesion due to smooth surface observed on hydrogel films prepared with fibers treated with lower NaOCl concentration, as showed in Table 2.1 and Figure 2.6. In addition, it is reported that because adhesion and spreading of anchorage-dependent cells are prerequisite for cell viability and proliferation [19,32], the reduction of the projected area on smoother surfaces might be expected to result in lower cell densities, especially at early timepoints in the cell culture.

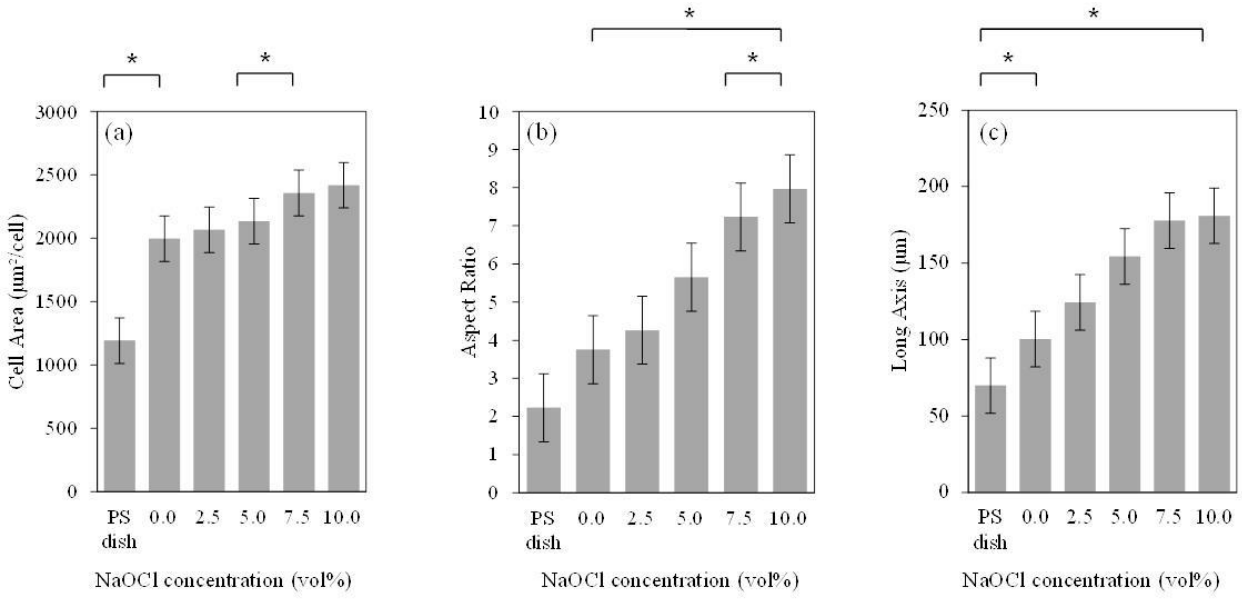

Figure 2.10. Effect of variation of NaOCl content during the treatment of agave fibers for the preparation of hydrogel films on (a) cell area, (b) aspect ratio, and (c) length of long axis. An asterisk indicates statistically significant different from the PS dish used as control ($p < 0.05$). Mean ± SEM ($n = 6$).

2.4 Conclusion

The present paper described the effect of NaOCl treatment in the agave cellulose on biocompatibility and cytocompatibility of hydrogel film. It was proved that the NaOCl concentration used for the agave fiber treatment strongly affected the mechanical properties of the hydrogel films. It was concluded that the cytotoxicity and biocompatibility properties were remarkably influenced by the degree of the NaOCl concentration used the treatment. Thus, the presence of lignin was due to the soft chemical treatment of agave fibers retarded the formation of the interaction hydrogen bonding networks of the resultant cellulose in the hydrogel film. This

might be influenced in the protein adsorption for the fibroblast cells at initial stage. In addition, the presence of lignin component also showed less effect on the cultivation of the cell on the film scaffold. In conclusion, the present paper could emphasis on the chemical treatment method with purification of the agave fibers for further tissue engineering.

2.5 References

[1] Y. Li, Y. W Mai, L. Ye, Sisal fibre and its composites: a review of recent developments, Compos. *Sci. Technol*. 60 (2000) 2037-2048.

[2] G. Iñuguez-Covarrubias, S. E. Lang, R. M. Rowel, Utilization of by-products from the tequila industry. Part 1: potential value of agave tequilana weber azul leaves, *Bioresour. Technol*. 77 (2001) 25-40.

[3] G. Iñuguez-Covarrubias, R. Diaz-Teres, R. Sanjuan-Dueñas, J. Anzaldo-Hernandez, R. M. Rowel, Utilization of by-products from the tequila industry. Part 2: potential value of agave tequilana weber azul leaves, *Bioresour. Technol*. 77 (2001) 101-111.

[4] A. Branco, J. D. Santos, M. Pimente, J. T. Osuno, L. S. Lima, J. M. David, $_{D}$-Mannitol from Agave sisalana biomass waste, *Ind Crops Prod*. 32 (2010) 507-512.

[5] A. M. Hamisso, A. Lodi, M. Seffen, E. Finocchio, R. Botter, A. Converti, Asorption of Cd (II) and Pb (II) from aqueous solution onto Agave Americana fibers, *Chem. Eng. J.*, 159 (2010) 67-76.

[6] A. R. Martin, M. A. Martins, O. R. da Silva, L. H. Motto, Studies on the thermal properties of sisal fiber and its constituents, *Thermochim. Acta.* 506 (2010) 14-22.

[7] G. R. Filho, S. D. Ribeiro, C. da S. Meireles, L. G. Da silva, R. Ruggiero, M. F. F. Junior, D. A. Cerqueira, R. M. N. Assuncao, M. Zeni, P. Polleto, Release of doxycycline through cellulose acetate symmetric and asymmetric membrane produced from recycled agroindustrial residue: sugarcane bagasse, *Ind. Crop. Prod.* 33 (2011) 566-576.

[8] C. N. Saika, T. Goswami, A. C. Ghosh, Esterification of high α cellulose extracted from hibiscus cannabinus. *Ind. Crops. Prod.* 4 (1995) 233-241.

[9] J. L. Guimaraes, E. Frollini, C. G. da Silva, F. K. G. Wypych, Characterization of banana, sugarcane bagasse and sponge gourd fibers of Brazil, *Ind. Crops. Prod.* 30 (2009) 407-415.

[10] K. L. Tovar-Carrillo, M.; Tagaya, T. Kobayashi, Fibroblast compatibility on scaffold hydrogels prepared from Agave tequilana weber bagasse for tissue regeneration, *Ind & Eng. Chem. Res.* 60 (2013) 11607-11673.

[11] M. I. Vazquez, R. De Lara, J. Benavente, Chemical surface diffusional, electrical and elastic characterization of two different dense regenerated cellulose membranes, *J. Colloid. Interface. Sci.* 328 (2008) 331-338.

[12] K. J. Edgar, C. M. Buchanan, J. S. Debenham, P. A. Rundquist, B. D. Seiler, M. C. Shelton, D. Advances in cellulose ester performance and application, *Prog. Polym. Sci.* 26 (2001) 1605-1611.

[13] A. L. Dupont, C. Egasse, A. Morin, F. Vasseur, Comprehensive characterization of cellulose and lignocellulose degradation products in aged papers: Capillary zone

electrophoresis of low molar mass organic acids, carbohydrates, and aromatic lignin derivatives, *Carbohydr. Polym*. 68 (2007) 1-8.

[14] A. Svensson, E. Nicklasson, T. Harrah, B. Panilaitis, D. L. Kaplan, M. Brittberg, P. Gatenholm, Bacterial cellulose as a potential scaffold for tissue engineering of cartilage, *Biomaterials.* 26 (2005) 419-425.

[15] L. L. Lloyd, J. F. Kennedy, P. Methacanon, M. Paterson, C. J. Knill, Carbohydrates polymers as wound management aids, *Carbohydr. Polym.*, 37 (1998) 315-319.

[16] H.; Yamaoka, T.; Ogasawara, H.; Nishizawa, T.; Takahashi, T.; Nakatsuka, I.; Koshima, K.; Nakamura, H.; Kawaguchi. U.; Chung, T.; Takato, K. Hoshi, Cartilage tissue engineering using human auricular chondrocytes embedded in different hydrogel materials, *J. Biomed. Mater. Res. A,* 78 (2006) 1-8.

[17] R. Langer, J. P. Vacanti, Tissue engineering, *Science.* 260 (1993) 920-926.

[18] A. Sionkowske, Current research on the blends of natural and synthetic polymers as new biomaterials: Review*, Prog. Polym. Sci.* 36 (2011) 1254-1261.

[19] H. Chen, L. Yuan. W. Song, Z. Wu, D. Li, Biocompatible polymer materials. Role of protein-surface interactions, *Prog. Polym. Sci.* 33 (2008**)** 1059-1065.

[20] L. S. Nair, C. T. Laurencin, Biodegradable polymers as biomaterials, *Prog. Polym. Sci.* 32 (2007) 762-767.

[21] L. J. Gibson, Biomechanics of cellular solids. Biomechanics of cellular solids, *J. Biomech.* **2005**, *38*, 377.

[22] X. Liu, L. Ma, Z. Mao, C. Gao, Chitosan-based biomaterials for tissue repair and regeneration, *Adv. Polym. Sci.* 244 (2011)81-87.

[23] D. T. Pokhrel, T. Viroraghavan, Treatment of pulp and paper mill wastewater a review, S*ci. Total. Environ.* 333 (2004) 37-43.

[24] B. Lindma, G. Karlstrom, L. Stigsson, On the mechanism of dissolution of cellulose, *J. Mol. Liq.* 156 (2010) 76-81.

[25] A. M. Striegel, Theory and applications of DMAc/LiCl in the analysis of polysaccharides, *Carbohydr. Polym.* 34 (1997) 267-273.

[26] J. A Venegas-Sanchez, M Tagaya, T. Kobayashi, Effect of ultrasound on the aqueous viscosity of several wáter-soluble polymers, *Polym. J.* 45 (2013) 1-9.

[27] B. Walkowiak, A. Kesy, L. Michalec, Microplate reader- a convenient tool in studies of blood coagulation, *Thromb Res. 87* (1997) 95-102.

[28] E. Sjoholm, K. Gustafsson, B. Eriksson, W. Brown, A. Colmsjo, Agregation of cellulose in lithium chloride/N,N-dimethylacetamide, *Carbohydr Polym*, 41 (2000) 153-159.

[29] J.K.; Kennedy, Z. S.; Rivera, C. A.; White, L.L.; Lloyd, F. P. Warner, Molecular weight characterization of underivatised cellulose by GPC, *Cellulose Chem. Technolo.* 24 (1990)319-325.

[30] J. Wu, K. Fukuzawa, J. Ohtani, Lignin analysis in some tropical hardwoods using ultraviolet microscopy, *Res. Bull. Of College Exp.* For., Hokkaido Univ. 47 (1990) 353-361.

[31] F. W Langkilde, A. Skantesson, Identification of celluloses with Fourier-Transform (FT) mid-infrared, FT-Raman and Near-infrared spectroscopy, *J. Pham. Biomed. Anal.* 13 (1995) 409-415.

[32] A. K. Salem, S. J. Tendler, C. J. Roberts, Interactions of 3T3 fibroblasts and endothelial cells with defined pore features, *J. Biomed. Mater. Res.* 61 **(2002)** 212-218.

[33] Y. Tamada, Q. Ikada, Effect of preadsorbed proteins on cell adhesion to polymer surface, *J. Colloid. Interface. Sci.* 155 (1993) 334-341.

Chapter 3

Fibroblast compatibility on scaffold hydrogels prepared from *Agave tequilana* Webber bagasse for tissue regeneration

Abstract: Agave fibers were used to elaborate a transparent and flexible cellulose hydrogel films used as scaffold for tissue regeneration and tested by *in vitro* assays with NIH 3T3 fibroblast cells. Using dimethylacetamide/lithium chloride (DMAc/LiCl) system was possible to obtain cellulose solutions and hydrogel films were prepared by phase inverse method without cross-linker. The concentration of LiCl in the DMAc solution was varied from 4 to 12 wt%. The resultant hydrogel films showed water contents in the range of 239% to 323% and enough film strength of 50 N/mm^2 to 66 N/mm^2, when the LiCl was changed from 4 to 12 wt% concentrations, respectively. The prepared agave cellulose films showed better cytocompatibility than the PS dish used as control. AFM images showed that the hydrogel films with lower LiCl apparently contained ordered and aggregated fiber orientation. This comparison suggested that the segmental microstructure in the hydrogel films influenced fibroblast cells spreading.

3.1 Introduction

It is worth noting that hydrogels have wide potential applications in the fields of food, biomaterials, agriculture, water purification, and etc [1-4]. Recently, scientists have devoted much energy to the developing of novel hydrogels for tissue engineering applications showing biodegradable nature [2-4]. This has a purpose in polymers occurring in new strategies for producing engineered tissue on synthetic or natural materials as scaffold. Several classes of

polymers have proved to be most useful in biomedical applications including situations in intimate contact with cells and tissues for prolonged periods. But, to select appropriated polymers for tissue engineering, it is necessary to understand the influence of the polymer such as surface and mechanical properties on cell viability, growth and function. In time, researchers have noted that synthetic polymers have offered limited properties for biological cell growing on the scaffold. For example, hydrogels having polyethylene glycol (PEG) segments showed advantages in the ability for its preparation and properties since the scaffold contained adjustable mechanical properties, which could be introduced by synthetic approaches. Unfortunately this scaffold type still could not provide an ideal environment to support cell adhesion and tissue formation due to their bio-inert nature [5-7]. Therefore, one strategy in researches has been working with natural polymers, in order to improve the properties to support cell adhesion and tissue formation on the material surface. In addition, because of their, hydrophilicity, biocompatibility and biodegradability, biopolymers were easily assimilated in the body [8]. Various hydrogels from natural polymers were fabricated by using hyaluronate [9-10], chitosan, and its derivatives [11,12], and cellulose [13-17], which there is a potential application in biomaterials field, many possibilities are remained in biopolymers. Among them, cellulose is the most abundant renewable resource on earth, and may become a main chemical resource in the future [18-22]. Therefore, this sustainable material in plants has numerous functional possibilities and can be expected in development to a broad range of applications especially demand for environmentally friendly and biocompatible products. In our strategy for cellulose having abundant hydroxyl groups, pure hydrogels of cellulose are tried to fascinating. Moreover, *agave tequilana* Weber *azul*, is an economically important plant cultivated in central Mexico for the production of tequila. More than 800 thousand tons of agave bagassees have been disposed as

waste product per year. This becomes as an important problem for the disposal of the bagasse agave and has been attention to regeneration to useful material [23]. Within these waste products, bagasse from *Agave tequilana* Weber *azul* is found that until now, several research works have been performed to offer an alternative use for this waste product, while none is offered us a final solution, due to the necessity of the development of new technologies to solve this problem [24-26].

In the present study, waste agave was used to obtain a biomass hydrogel and then the hydrogel films could be applied as scaffold on tissue regeneration. Although few attempts were made to extract compounds from bagasse of sugarcane and banana, any research works in biomass cellulose using agave bagasse are still less in biomedical application. Base on this background, the research in a*gave* bagasse could apply in sustainable waste product for tissue regeneration. As a frontier research, the present work in natural cellulose polymer can provide important evidence on tissue regeneration. The elaboration of hydrogel films from agave bagasse and cytotoxic nature was firstly reported in the present paper, showing possibility in tissue regeneration application.

3.2 Experiments

3.2.1 Materials

Tequilana Webber bagasse was provided from Corralejo Tequila Company, in Penjamo, Guanajuato, Mexico. *N,N*-Dimethylethylendiamine (DMAc) was purchased from TCI, Tokyo, Japan, and stored for more than 5 days over potassium hydroxide before used. Lithium chloride was dried at 80°C for 12 h in a vacuum oven before uses. Ethanol, sodium hydroxide, sodium hypochlorite and sulfuric acid were purchased from Nacalai Tesque. Inc. For protein adsorption

studies, Bicinchoninic acid (BCA) kit was purched from Sigma Aldrich, Japan. Fetal bovine serum (FBS), and bovine serum albumin (BSA), purchased from Sigma Aldrich, phosphate-buffered saline (PBS, Dullbecco Co., Ltd), 0.05 w/v% trypsin-0.053 M-ethylenediaminetetraacetate (trypsin-EDTA, Gibco), formaldehyde (37 vol %, Wako Co., Ltd.) were used. NIH3T3 mouse embryonic fibroblast cells purchased from BioResource Center (Japan).

3.2.2 Agave fiber treatment

The agave fibers were watched 3 times with distillated water to remove traces of sugars from tequila manufacturing process, and then dried in an oven at 50°C. For the treatment of the agave fibers, 3 g of agave fibers were immersed in 1000 mL of 10 vol% NaOH solution and stirred for 12 h at 100°C, until a black liquor solution was obtained [27]. Then, the fibers were washed with abundant distilled water 5 times to eliminate residues of NaOH solution remain in the fibers. The agave fibers were immersed in 1000 mL of distilled water with stirring at room temperature until pH 7 was obtained. After the fibers were filtrated, 1000 mL of 4% H_2SO_4 solution were added and kept under stirring for 2 h at 100°C. Then, the fibers were washed with abundant distilled water 5 times to eliminate residues of H_2SO_4 solution. Then, 10 vol% of NaOCl solution was used as bleach agent to obtain a light colour fibers for the preparation of cellulose solution. The agave fibers were immersed in 1000 mL of NaOCl solution and stirred at room temperature for 2 h. Finally, the treated agave fibers were washed 5 times with abundant distillated water and dried under vacuum for 2 days. The treated agave fibers were used for following process in preparation of the agave cellulose in DMAc/LiCl solution. The treated fibers (1g) were suspended in 300 mL of distilled water and stirred overnight to allow thorough

swelling of the fibers. After water was removed from the suspension by an adapter glass filter under vacuum, ethanol (300 mL) was added to the swelled fibers and the mixture was stirred for 24 h. The 300 mL of ethanol were removed, and the treated fibers were added to 300 mL of DMAc. The DMAc-fibers were then left overnight under the stirred condition. Dry LiCl and DMAc were added to the swelled agave fibers to obtain a 1 wt% concentration of the treated agave solution. The mixture was stirred at room temperature for 3 days until a viscous solution was obtained. At this time, the LiCl concentration was changed in 4, 6, 8, 10 and 12 wt% in the agave cellulose solutions [28]. For preparations of hydrogel films, 10g of the solution was poured into a glass tray (10 cm diameter), and kept for 12 h in a container filled with 20 mL of ethanol in order to coagulate and obtain films by using phase inverse method. After the phase inverse method, transparent hydrogel film was obtained in the glass tray, as shown in Figure 1. The resulting film was wasted by ethanol 3 times, and then put it on shaking bath for 24 h to remove remain DMAc. Then, the hydrogel film was immersed in distilled water over night and kept in phosphate buffered saline (PBS) at 4°C in a plastic container; this procedure was repeated 2 times.

3.2.3 Evaluation of fibroblast adhesion on agave hydrogel films.

The samples were sterilized with ethanol 50 and 70 vol% of concentration twice for 30 min, then rinsed twice with PBS 30 min, and finally swelled in DMEM for 2 h before the seeding procedure. NIH 3T3 mouse embryonic fibroblast cells were cultured at 37°C, 95% relative humidity and 5% CO_2 environment. The culture medium was 90% Dulbecco's modified Eagle's medium (DMEM) supplemented with 10% fetal bovine serum (FBS) and 1% penicillin/streptomycin. The cells were seeded on the agave films samples in polystyrene tissue

culture dish (PS) 35 x 10 mm, at a density of $8x10^3$ cells cm^{-2}. PS dish was used as control. The cells were used for imaging and characterization purposes after 72 h of culture. The samples were imaged using inverse microscope (Olympus CKX41). The images were analyzed for cell elongation and directionality using Cellsens software digital imaging software. To measure cell area the cell boundaries were marked. Aspect ratio, long axis and cell density were also measured. Approximately 50 cells were analyzed for each sample, and five images were analyzed to obtain an unbiased estimate of the cell density and morphology. The results presented herein were based on three independent experimental runs.

3.2.4 Evaluation of biocompatibility and other properties of hydrogel films.

In the case of protein adsorption the hydrogel films (5 mm x 5 mm) were incubated in PBS solution for 24 h and then immerged in 1 mL of PBS solution containing bovine serum albumin (BSA) (1g/mL) for 4 h at 37°C. For fetal bovine serum (FBS) experiments, 1 mL of Dulbecco's modified Eagle's medium (DMEM) enriched with 10% of FBS was used. Subsequently, the hydrogel films were rinsed slightly with PBS, FBS solution, and distilled water. Then, the hydrogel films were immersed in 2 mL of 2 wt% dodecyl sulfate (SDS) solution and shaken for 2h to remove the adsorbed protein. The amounts of absorbed protein were then calculated by using a spectrophotometer at 562 nm. At least, eight measurements were averaged to get a reliable value.

In the coagulation time, a modified Lee-White method was used in vitro [28]. For the Lee White Clotting Time (LWTC) tests, the hydrogel films (5 mm x 5 mm) were incubated with 0.2 mL of platelet poor plasma (PPP) at 37°C in disposable plastic tubes. Simultaneously, with addition of $CaCl_2$ the time was started and the solution was mixed well. After 20s passed, the

time of clot formation was recorded with a chronometer [28]. The tests were repeated three times for each sample. At least eight measurements were averaged. For the platelet adhesion measurements, all of the appliance, reagents, and films (5 mm x 5 mm) were sterilized by 75 vol% of ethanol for 3 h before the experiments. Then, the samples were immersed into BSA buffer for 24 h and placed in disposable plastic tubes. In each tube 200 µL of platelet rich plasma (PRP) was dropped, then the samples were incubated at 37°C for 90 min. on following this, the hydrogel films were rinsed three times with PBS at 37°C and the adhered platelet were fixed with 1 mL of 2.5 wt% of glutaraldehyde/PBS at 4°C for 2 h. Finally, the hydrogel films were immersed into the PBS for 5 min and dehydrated twice as followed. The first dehydration was carried out with a series of ethanol/PBS mixtures with increasing ethanol concentration (25, 50, 75, and 100 wt%), samples were immersed for 15 min in each mixture. The second dehydration was performed with iso-amyl acetate/PBS mixtures. After freeze-drying the treated samples, the platelet-attached films were coated with gold layer for the SEM measurements and count the adherent platelet.

Water content of the resultant hydrogel films were determined by weighing dry and wet samples by following procedure. Disk samples with 5 mm of diameter were cut from cast films and dried in vacuum oven for 24 h and weighed. Then, samples were emerged in distilled water for 36 h then; specimens were removed from water and wrapped with filtered paper on the surface in order to remove excess of water, and then weighed. Finally, the water content was calculated with the weights of the wet (W_1) and dried (W_0) hydrogel films.

$$\text{Water content (\%)} = (W_1 - W_0)/ W_0 \times 100$$

The tensile and elongation tests of the swelled films in PBS for 24 hours were carried out using hydrogel samples (50 x 10 mm) on a LTS -500N - S20 (Minebea, Japan), which was a

universal testing machine equipped with a 2.5 kN cell. Strips with a length of 50 mm and a width of 10 mm were cut from the hydrogel films with a razor blade. One set of samples, for each percentage of LICl varied was tested, and each set was repeated 3 times. Only samples which ruptured near mid-specimen length were considered for the calculation of tensile strength. The value of the tensile strength (N/mm^2) and elongation (%) were calculated with following equations:

$$\text{Tensile strength} = \text{Maximum Load} / \text{cross section area}$$

$$\text{Elongation} = (\text{Final length at maximum load/initial length}) \times 100,$$

The viscoelasticity of the hydrogel films with 2 cm of diameter and having 5 mm of thickness was carried out by Auto Paar, Reoplus equipment, in wet conditions at 25°C. For the contact angle measurements, three samples of the resultant hydrogel films were measured using a contact angle goniometer (Kyowa Interface Science). A piece of 2 cm x 2 cm of hydrogel films was stuck on a glass slide and mounted on the goniometer. A total of 3μL of double distilled water was dropped on the air side surface of the films at room temperature. The contact angle was measured after 10s passed from the droplet process. At least eight measurements were averaged to obtain a reliable value. These data are listed in Table 1 for the agave hydrogel films prepared from different LiCl concentration in the DMAc solution. Moreover, the AFM was used to analize the topography of scaffolds of the agave hydrogels. The AFM measurements were performed with samples (10 x 10 mm) in wet conditions. The agave samples were immersed in PBS for 24h before the measurements. Using a cantilever (SI-DF3-A) AFM was performed with a spring contact of 3.0 N/m. The conditions of resonance frequency of 33 kHz, and a level length of 450 μm, was used.

3. 3 Results and Discussion.

3.3.1 Preparation of agave hydrogel films.

Figure 3.1 shows pictures of (a) Agave fibers before treatment, (b) agave fibers after treatment, (c) transparent dry hydrogel film and (d) transparent wet hydrogel film. The bleached agave fibers showed similar FT-IR spectra with typical cellulose as shown in the chemical structure in Figure 3.1 (b). In order to prepare hydrogel films of the agave fibers (b), the fibers were dissolved in DMAc solution having 4-12 wt% of LiCl after solvent exchange between water and ethanol and then ethanol and DMAc. The obtained hydrogel films (c) were used for cyto and biocompatibility measurements.

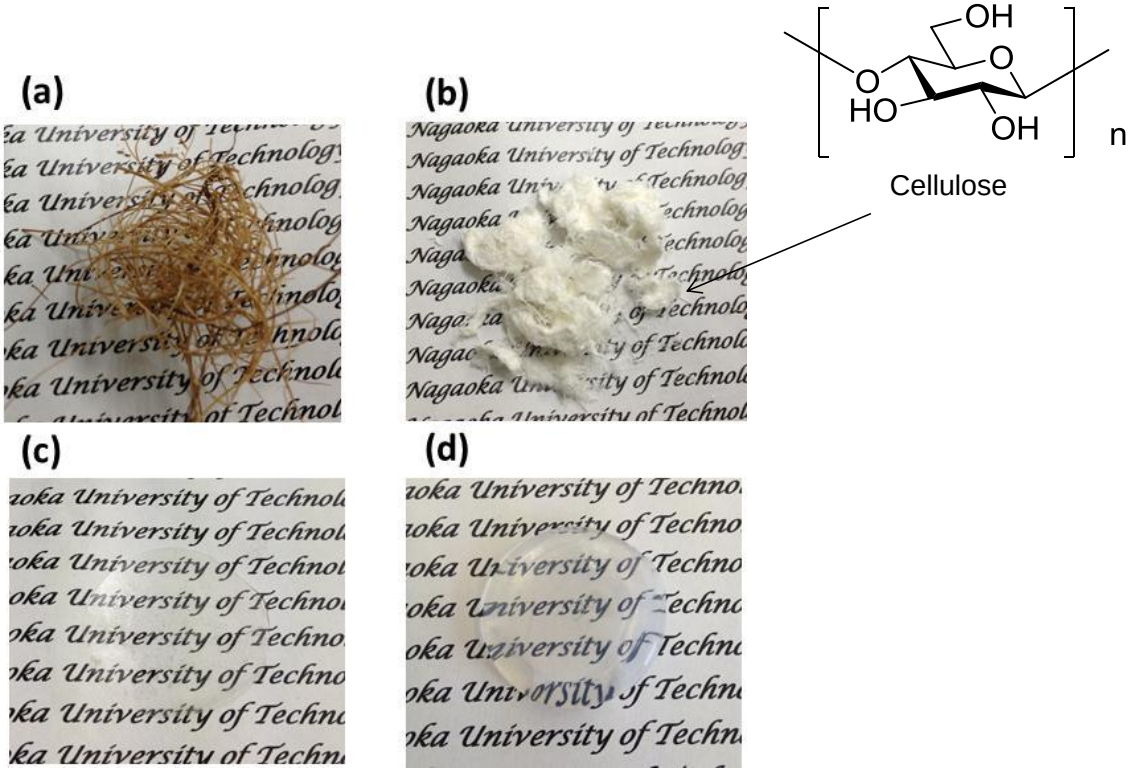

Figure 3.1.Agave fibers and hydrogel films images. (a) Agave fibers before treatment, (b) Agave fibers after treatment and cellulose chemical structure, (c) Agave hydrogel film in dry conditions and (d) Agave hydrogel film in wet conditions.

3.3.2 Evaluation of fibroblast adhesion on agave hydrogel films.

In order to determinate cytotoxicity of the agave hydrogel films NIH 3T3 fibroblasts were used. Since fibroblast cell is a type of cell that can synthesize the extracellular matrix for animal tissue and the most common cells of conective tissue in animal, the investigation of the cytotoxic nature of the agave hydrogels was meaningful for tissue regeneration. For the measurement of cell density on the agave hydrogel films, phase-contrast light microscope images of fibroblasts on the hydrogel film surface were acquired to determine the effect on cell adhesion and morphology. For fibroblast adhesion the hydrogel films prepared with 4, 6, 8, 10 and 12 wt% of LiCl were compared in view of pictures. Figure 3.2 presents the cell density of the fibroblast cells on the agave hydrogel films prepared from the agave fibers varying LiCl concentration. In all cases, the results obtained in the hydrogel films were higher than the observed on PS dish used as control surface. With increasing duration time, the cell density became gradually to increase. After 72 h passed, the amounts of the cell density in the 4 wt% LiCl were actually higher. As indicated by Tamada and Salem, fibroblast was found to have a maximum adhesion on the surface of hydrophilic and soft films [29,30]. According with the obtained results, the fibroblast cells preferred soft surface for proliferation. On the other hand, in the present work, the difference in the cell density between the hydrogels prepared with 4 wt% and 12 wt% of LiCl was seen in Fig. 3.2. This seemed to be related to the softness of the hydrogels. As shown in Table 1, the softness of the hydrogel films changed with the variation of the LiCl concentration the softness in the hydrogel film prepared from lower LiCl might promote adhesion of fibroblasts. This could be attributed to that at lower content of LiCl case the softness and stiffness of the films might regulate the adhesion between cellular- extracellular matrix molecules. In addition, in tissue regeneration degradable biomaterials are desirable to replace by newly formed tissue

upon regeneration, however, there are applications where slow or no degradation are desirable. The hydrogel degradation was tested by weighting the film for 3 days. However, there were no changes in the hydrogel films during the cell culture time using fibroblasts. This meant that no degradation of the scaffold during the cell culture was observed.

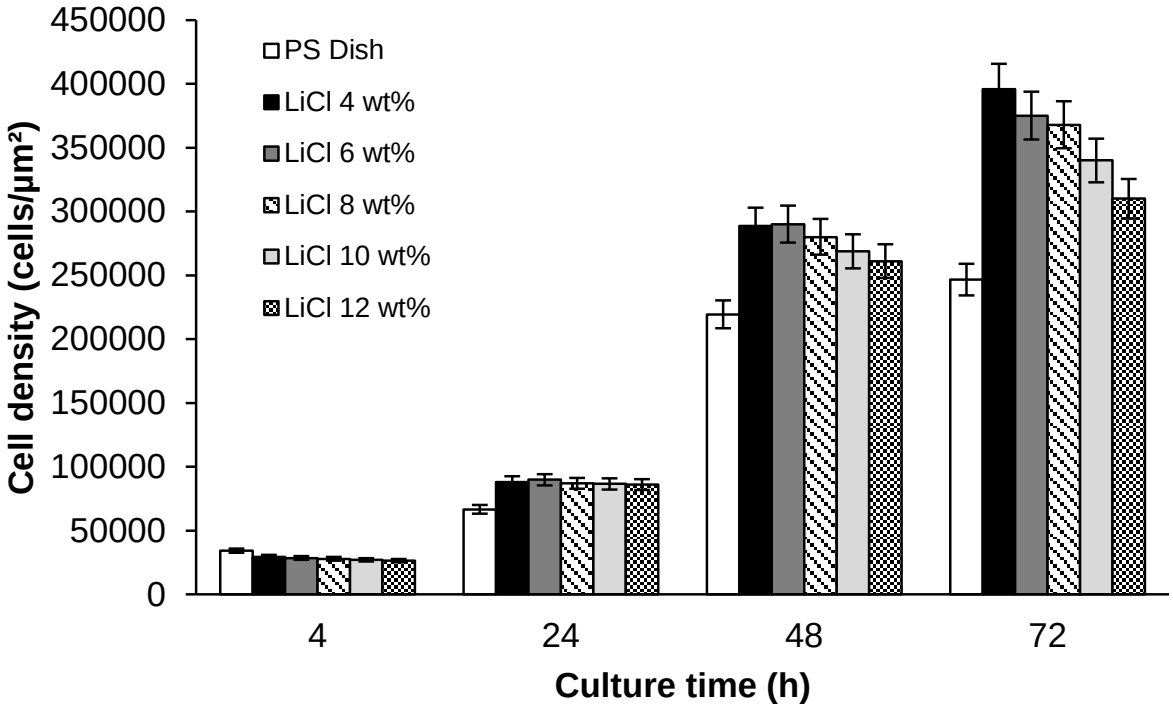

Figure 3.2. Cell density of hydrogel films containing different LiCl concentration.

Figure 3.3 (on the top) shows reflectance optical microscope images of the agave hydrogel films prepared with different LiCl content without cell adhesion, and in the bottom phase-contrast light images revealed a growing pattern of the adhered NIH 3T3 cells on the agave hydrogel films. The red arrows on the reflectance optical microscope images indicated the orientation of the cellulose fibers in the hydrogel films. In order to relate the cell growing pattern in the hydrogel films and the growth direction of fibroblast on the films phase-contrast light microscope images

were taken. When the reflectance and phase-contrast images were compared, the results revealed that the cell spreading followed the fiber arrangement pattern as shown in the pictures for the hydrogel films. At near 6 wt% of LiCl concentration, it was seen that the presence of the aggregated cellulose promoted circular patterns as domains. Higher portions of fibroblasts growing following a pattern were observed on films in this LiCl case at cell culture times of 12 days. In Figure 3.4, results of cell morphology on the hydrogels films revealed a remarkable difference on fibroblast morphology for the hydrogel films (d-i) and commercial PS dish (a-c). For example, in the hydrogel film for the 6 wt% LiCl (d-f), the fibroblast surely adhered and grown on the hydrogel film, as observed in the images. After 4 hours of cell culture, the image (d) showed longer axis shape of the frown cells as compared with those adhered on the PS Dish at the same condition. Moreover, the boundaries of the adhered cells on cellulose films seemed to be tightly adhered on the hydrogel surface, showing a diffuse shape. In addition, anisotropic shape was observed in the first hours of the cell culture, when the hydrogel films were used in the scaffold on the cell growing. Relative to the hydrogel film, the fibroblast shape observed on the reference PS dish was mainly round at 4 hours, as seen in (a). This indicated that the cell could not tightly adhere to the surface of the commercial dish. Comparing with fibroblast shape shown in (d) and (g) for the hydrogels films prepared from 6 wt% and 12 wt% of LiCl cases, respectively. The cells growing at 4 hours in the cultivation showed higher cytocompatibility in (d). When the LiCl was increased in the DMAc solution to 12 wt%, the resultant cell shape showed lower aspect ratio and long axis with lower cell density on the hydrogel films. This might be due to the decreased swelling and softness of the sample film as shown in Table 3.1. These results revealed that the hydrogel films made of the agave cellulose provided a better surface for fibroblast growing, depending upon hydrogel properties.

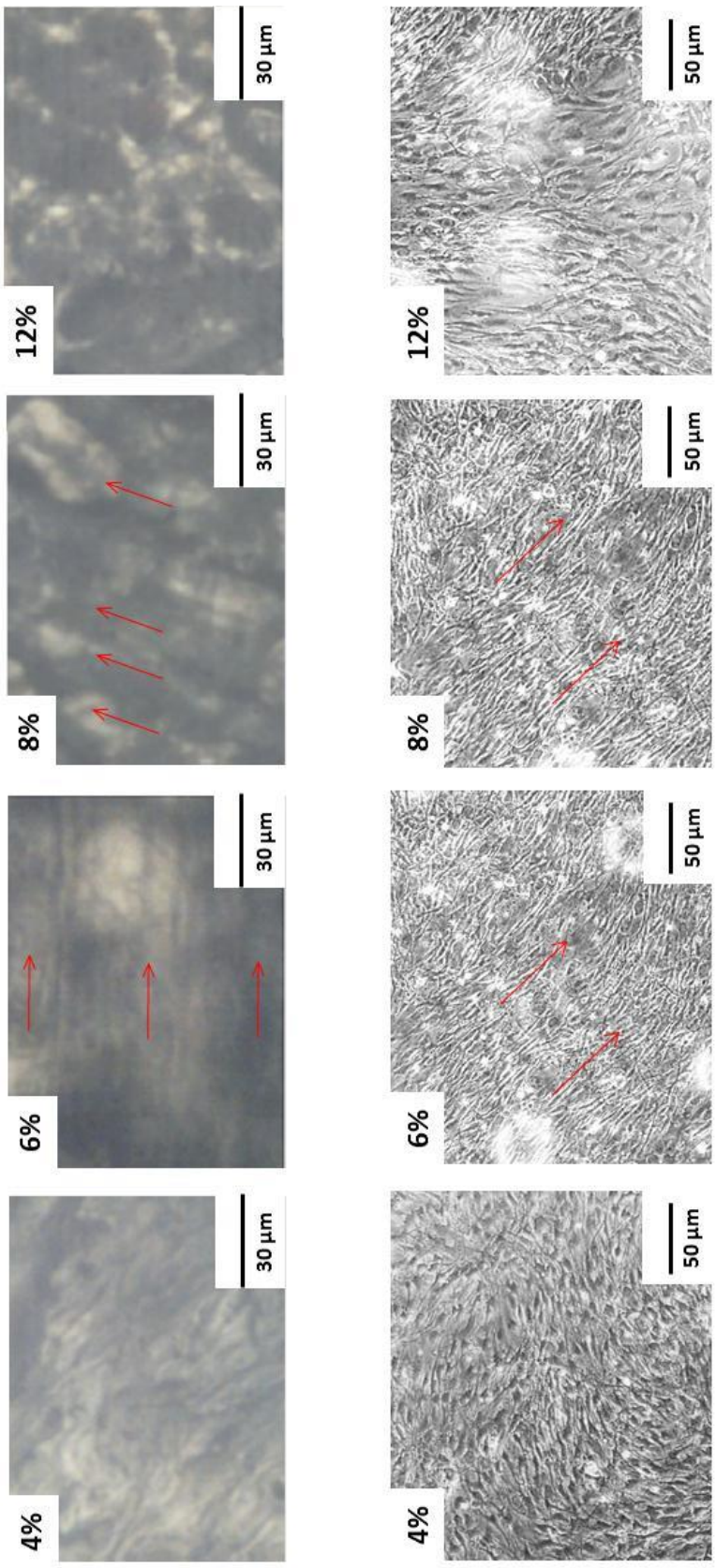

Figure 3.3. On the top, reflectance optical microscope images of hydrogel films with different content of LiCl. Above, Phase-contrast light images of hydrogel films of hydrogel films with different content of LiCl with a cell culture time of 48 hours.

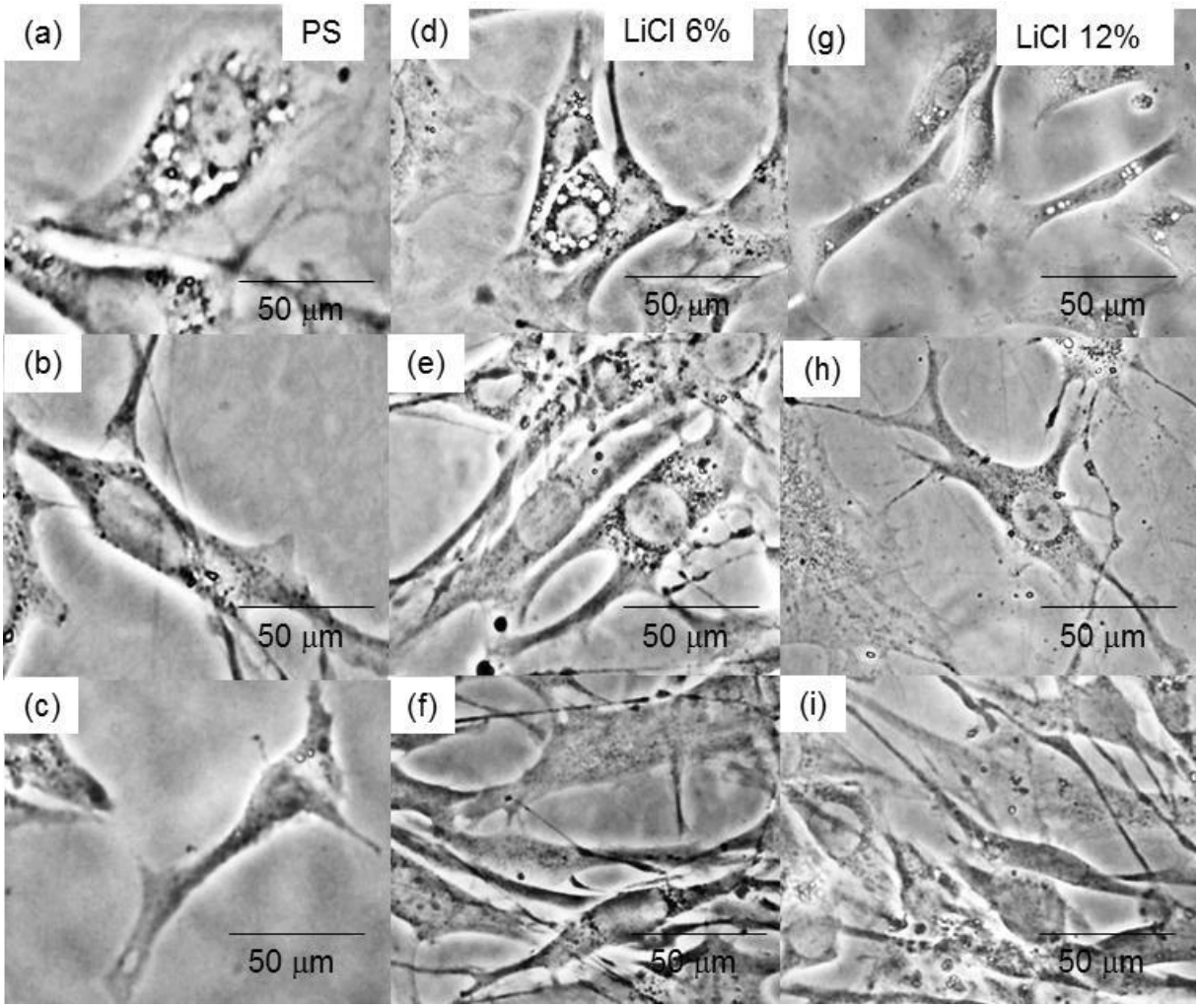

Figure 3.4. Phase-contrast light images of hydrogel films (a-c) commercial PS dish as control, (d-f) hydrogel films prepared with 6 wt% of LiCl, (g-i) hydrogel films prepared with 12 wt% of LiCl. The cell culture time was (a,d,g) 4 hours, (b,e,h) 24 hours and (c,f,i) 48 hours.

Table 3.1. Properties of agave cellulose hydrogel films.

LiCl content (wt%)	Water content (%)	Elongation (%)	Tensile strength (N/mm^2)	Contact angle
4	325	14.3	50	48
6	296	24.6	56	51
8	262	28.7	62	57
10	252	36.0	65	61
12	239	38.4	66	64

3.3.3 Biocompatibility of agave hydrogel films.

In addition with cytotoxic nature, biocompatibility is one important factor for the application in tissue engineering. Therefore, as Table 2 lists biocompatibility and cytotoxicity properties are presented. It is well known that protein adsorption is the first stage of the interactions between substrate and the body [20]. Therefore, it is interesting in the present work to examine more protein adsorption to the hydrogel films for BSA and FBS. As seen in table data, adsorption of BSA and FBS was examined *in vitro* for each hydrogel film. In the hydrogel films prepared by different LiCl content of the DMAc solution, the amounts of BSA on the hydrogels films increased with the increase of the LiCl content. However, the results observed in the case of FBS expressed opposite tendency to the BSA. Also, the adsorbed amounts of the FBS on the hydrogel films were higher than those of BSA. It was known that BSA proteins tended to bind onto hydrophobic surface, meanwhile FBS preferred to hydrophilic surface [29]. In the present work, the BSA adsorption tended to suppress cell adhesion as the LiCl concentration was higher and the obtained results showed that FBS adsorption became higher in all cases. In these

cases, it could be considered that the predominant adsorption in BSA and FBS might be due to hydrogel nature depending upon the LiCl contents.

Furthermore, blood compatibility of the hydrogel films was also studied. Herein, after the hydrogel samples were in contact with platelet poor plasma (PPP), the time of cloth formation was measured. The results in Table 3.2 demostrated that the time of the cloth formation was affected by the LiCl contents in the DMAc solution. As seen, the value of the time of cloth formation increased with decrease of the LiCl content used. This phenomenon could be supported with the results of the FBS adsorption. In protein adsorption capacity of the hydrogel films, it was easy to consider that the fibrogen adsortion might be enhancing to form a fibrin rich cloth. In the case of the afinity of the materal surface, blood components should become important issue.

Table 3.2. Biocompatibility and cytotoxicity properties of agave hydrogel films.

LiCl content (wt%)	Protein adsorption (mg/μm^2) PBS	FBS	Platelet adhesion (Platelet/μm^2)	Cloth time (s)	Aspect ratio (72 h)	Cellular area (μm^2)
4	7	30	1201	50	11.04	2036.76
6	9	35	1487	47	11.49	2953.94
8	13	29	1654	44	10.49	2615.82
10	19	27	1793	40	8.24	2093.83
12	23	28	1836	35	8.81	1800.86

Thus, in the adhesion process, it is necessary for platelets and fibroblast to grow to be larger molecules such as fibrogen platelet adhesion was tested. The results revealed that platelet adhesion was lightly supressed at lower LiCl content in the DMAc solution. In addition, higher number of platelet was observed on the surface of the hydrogel films prepared with 12 wt% LiCl. In contrast, the number of platelet adhesion on the surface of the films prepared with 4 wt% LiCl slightly decreased as compared with the hydrogel film samples with 12 wt% of LiCl. Similar results were also reported by Salem and coworkers for the adhesion of platelets [30]. They indicated that the hydrogel films could provide a suitable environment to promote and enhance the platelet adhesion regardless to the LiCl used.

3.3.4 Evaluation of agave hydrogel films.

As demonstrated, the agave hydrogel shows better cytotoxic properties depending upon the several forms of the hydrogels. Therefore, it is very meaningful to relate hydrogel nature and cytotoxic properties, when the hydrogel properties were shown in Table 3.1, the hydrogel film properties could be changed in the different content of LiCl varied in a range of 4 to 12 wt% concentration. There was a tendency on the films being swollen in PBS. So, the value of the water content percentage was in the range of 239% to 325%, when the LiCl concentration was from 4 to 12 wt%. Mechanical properties of tensile strength and elongation of the hydrogel films showed that the addition of the LiCl increased the strength and elongation values. The values of tensile strength were varied from 50 N/mm² to 66 N/mm² in the cases of 12wt% and 4wt% of the LiCl, respectively. Figure 3.5 shows viscoelastic data for the agave hydrogel films prepared from different LiCl concentration. It was observed that the deformation of hydrogel film prepared with 12 wt% of LiCl was lower than those made with 4 wt% of LiCl. This could be attributed to the

increment of cellulose aggregates at higher concentration of LiCl. It has been postulated that in the DMAc/LiCl system a macrocation $[DMAc\text{-}LiCl\text{-}DMAc\text{-}Cl^-]_n$ is formed [31]. This macrocation interact with cellulose fibers and acts as cross-linker.it is well known that the elastic response to the deformation only occurs under momentary deformation. However, under a prolonged deformation, it cannot recover its original shape because the polymer chains have flowed. When the amount of LiCl increased, the polymer chains in the network kept the chains strands from moving away. Apparently, the viscoelasticity data implied that the hydrogel film prepared at 4 wt% and 6 wt% of LiCl expressed softness nature relative with that of 12 wt% of LiCl, in the deformation during the strain sweep measurements. Since the hydrogels prepared from lower LiCl concentration proved soft nature, these facts could be atribuited to the change in the hydrogel microstructure depending upon the LiCl concentration.

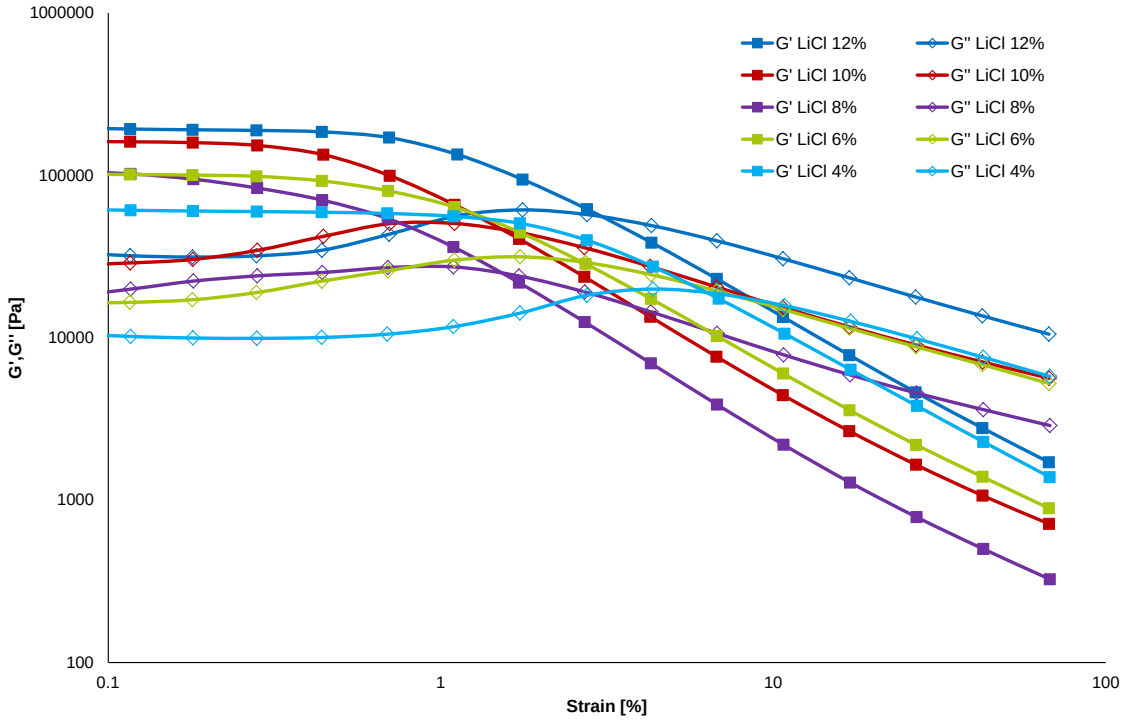

Figure 3.5. Viscoelasticity of cellulose hydrogels films of different LiCl contents for strain - G', G'' plots at 37°C.

Therefore, AFM observation was performed for the hydrogel films. Figure 3.6 shows the AFM images (20 mm x 20 mm) of the film sample prepared with (a) and (c) 4 wt% and (b) and (d) 12 wt% of LiCl, including fiber width and cross-section for the films of (c) 4 wt%, (d) 12 wt% of LiCl contents. The roughness areas showed a highly-ordered fiber pattern with the periodic size of 150-300 nm, due to the agave cellulose aggregated in the hydrogel film with 4 wt% of LiCl. It was presented that the effect of the aggregation of the cellulose networks in the film was apparently changed with the LiCl concentration. For example, the surface roughness in the hydrogel films decreased from 7.9 to 4.1 nm, as the samples were prepared with the 4 wt% and 12 wt% of LiCl, repectively. This was evidence of the formation of aggregate fibers in the films. As it was observed in the reflectance optical microscope images showed in Figure 3.3, the formation of aggragates due to the presence of the macrocation influenced the order or the cellulose fibers in the DMAc solution depending of the content of LiCl. This influenced the cytocompatibility due to the enhancement of the interaction between the celulose fibers the effecting the swelling and softness of the hydrogel films and concequenly protein adsorption and cell adhesion.

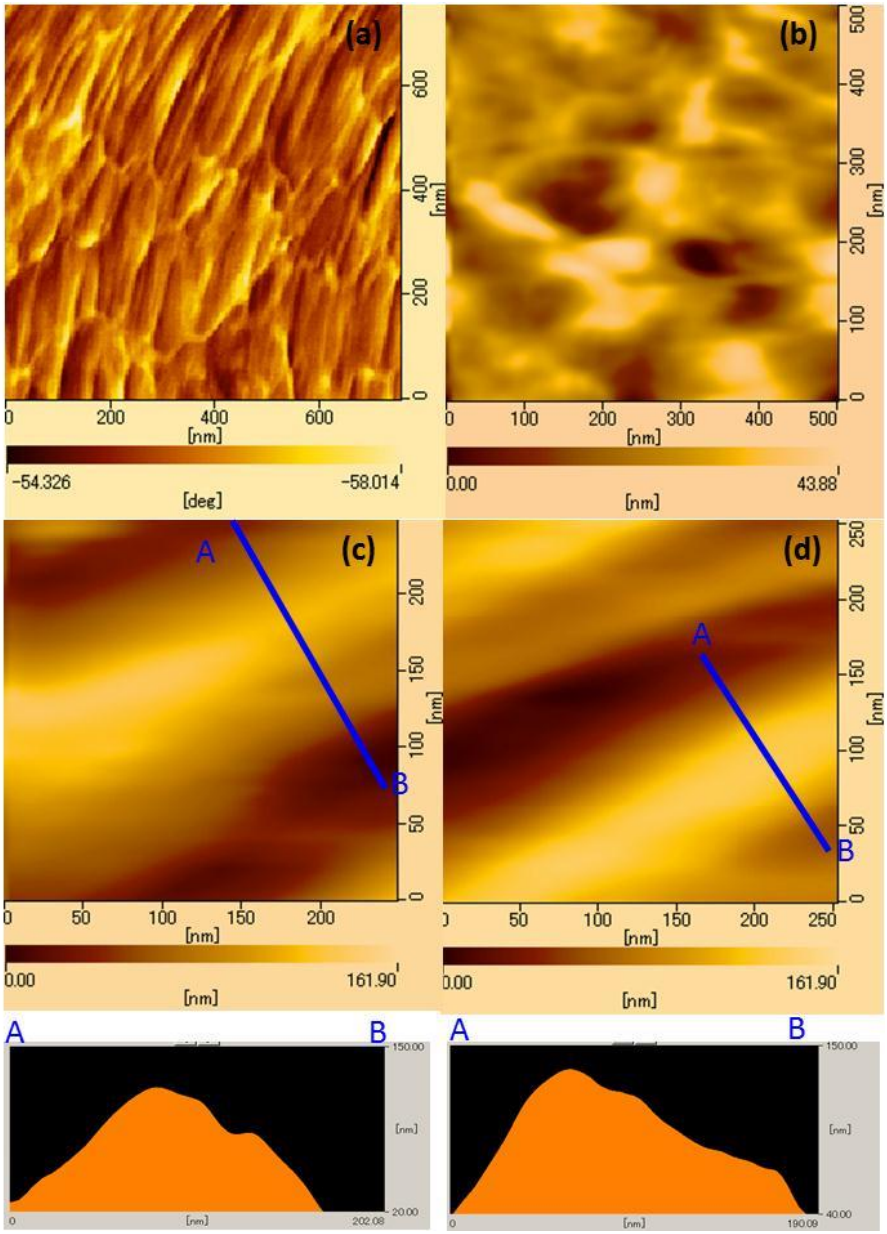

Figure 3.6. AFM images (a) Agave hydrogel film containing 6 wt% of LiCl, (b) Agave hydrogel film containing 12 wt% of LiCl, (c) fiber width in agave hydrogel film with 4 wt% of LiCl, and cross-section, (d) fiber width of agave hydrogel film containing 12 wt% of LiCl and cross-section.

3.4. Conclusion

Hydrogel films prepared from agave fibers were obtained by phase inversion of the DMAc solution with LiCl. The cellulose hydrogel film had better mechanical properties, although there was no chemical crosslinking. Depending on the LiCl concentration, these hydrogel films exhibited lower protein adhesion and higher coagulation time for the biocompatibility. Even though, very good cytocompatibility was resulted in the hydrogel films relative to reference PS dish. It was proved that the LiCl acted to be dense networks of the agave cellulose segments. Thus, the hydrogel forms influenced in vitro cyto and biocompatibility. These results indicated that the hydrogel films became leading biomaterials as candidate in tissue engineering.

3.5 References

[1] Yamaoka, H.; Ogasawara, T.; Nishizawa, H.; Takahashi, T.; Nakatsuka, T.; Koshima, I.; Nakamura, K.; Kawaguchi. H.; Chung, U.; Takato, T.; Hoshi, K. Cartilage tissue engineering using human auricular chondrocytes embedded in different hydrogel materials. *J. Biomed. Mater. Res. A,* **2006,** *78*, 1.

[2] Langer, R.; Vacanti, J. P. Tissue engineering. *Science.* **1993**, *260*, 920.

[3] Sionkowske, A. Current research on the blends of natural and synthetic polymers as new biomaterials: Review. *Prog. Polym. Sci.* **2011**, *36*, 1254.

[4] Jiang, T.; Wang, G.; Qiu, J.; Luo, L.; Zhang, G. Preparation and biocompatibility of polyvivyl alcohol-smal intestinal submucosa hydrogel membranes. *J. Meb. Biol. Eng.* **2009**, *29*, 102.

[5] Lydon, M.; Minett, T. Cellular interactions with synthetic polymer surfaces in culture. *Biomaterials.* **1985**, *6*, 396.

[6] De Bartolo, L.; Morelli, S.; Bader, A.; Drioli, E. Evolution of cell behavior related to physic-chemical properties of polymeric membranes to be used in bioartificial organs. *Biomaterials.* **2002**, *23*, 2485.

[7] Thomas, B. H.; Fryman, C.; Liu, K.; Mason, J. Hydrophilic-hydrophobic hydrogels for cartilage replacement. *J. Mech. Behav. Biomed. Mater.* **2009**, *2*, 588.

[8] Chen, H.; Yuan. L.; Song, W.; Wu, Z.; Li, D. Biocompatible polymer materials. Role of protein-surface interactions. *Prog. Polym. Sci.* **2008**, *33*, 1059.

[9] Nair, L. S.; Laurencin, C. T. Biodegradable polymers as biomaterials. *Prog. Polym. Sci.* **2007**, *32*, 762.

[10] Gibson, L. J. Biomechanics of cellular solids. *J. Biomech.* **2005**, *38*, 377.

[11] Liu, X.; Ma, L.; Mao, Z.; Gao, C. Chitosan-based biomaterials for tissue repair and regeneration. *Adv. Polym. Sci.* **2011**, *244*, 81.

[12] Lloyd, L. L.; Kennedy, J. F.; Methacanon, P.; Paterson, M.; Knill, C. J. Carbohydrates polymers as wound management aids. *Carbohydr. Polym.* **1998**, *37*, 315.

[13] Vazquez, M. I.; De Lara, R.; Benavente, J. Chemical surface diffusional, electrical and elastic characterization of two different dense regenerated cellulose membranes. *J. Colloid. Interface. Sci.* **2008**, *328*, 331.

[14] Edgar, K. J.; Buchanan, C. M.; Debenham, J. S.; Rundquist, P. A.; Seiler, B. D.; Shelton, M. C.; Tindall, D. Advances in cellulose ester performance and application. *Prog. Polym. Sci.* **2001**, *26*, 1605.

[15] Dupont, A. L.; Egasse, C.; Morin, A.; Vasseur, F. Comprehensive characterization of cellulose and lignocellulose degradation products in aged papers: Capillary zone electrophoresis of low molar mass organic acids, carbohydrates, and aromatic lignin derivatives. *Carbohydr. Polym*. **2007**, *68*, 1.

[16] Saika, C. N.; Goswami, T.; Ghosh, A. C. Esterification of high α cellulose extracted from hibiscus cannabinus. *L. Ind. Crops. Prod.* **1995**, *4,* 233.

[17] Svensson, A.; Nicklasson, E.; Harrah, T.; Panilaitis, B.; Kaplan, D. L.; Brittberg, M.; Gatenholm, P. Bacterial cellulose as a potential scaffold for tissue engineering of cartilage. *Biomaterials*. **2005**, *26*, 419.

[18] Ruozi, B.; Parma, B.; Crace, M. A.; Tosi, G.; Bondioli, L.; Vismara, S.; Forni, F.; Vendelli, M. A. Collagen based modified membranes for tissue engineering: influence of type and molecular weight of GAGs on cell proliferation. *Int. J. Pharm.* **2009**, *378*, 108.

[19] Stamatials, D. T.; Papendurg, B. J.; Girones. M.; Saiful, S.; Bettahalli, S. N. M.; Schmitmeter, S.; Wessling, M. Medical applications of membranes: Drug delivery, artificial organs tissue engineering. *J. Memb. Sci.* **2008**, *38*, 1.

[20] Hoenich, N. A. Update on the biocompatibility of hemodialysis membranes. *Hong Kong J. Nephrol.* **2004**, *6*, 74.

[21] Puppi, D.; Chiellini, F.; Piras, A. M.; Chiellini, E. Polimeric materials for bone and cartilage repair. *Prog. Polym. Sci.* **2010**, *35*, 403.

[22] Sikareepaisan, P.; Ruktanonchai, U.; Supaphol, P. Preparation and characterization of asiaticoside-loaded alginate films and their potential for use as effectual wound dressings. *Carbohy. Polyms*. **2011**, *83*, 1457.

[23] Filho, G. R.; Ribeiro, S. D.; Meireles, C. da S.; Da silva, L. G.; Ruggiero, R.; Junior, M. F. F.; Cerqueira, D. A.; Assuncao, R. M. N.; Zeni, M.; Polleto, P. Release of doxycycline through cellulose acetate symmetric and asymmetric membrane produced from recycled agroindustrial residue: sugarcane bagasse. *Ind. Crop. Prod.* **2011**, *33*, 566.

[24] Li, Y.; Mai, Y. W.; Ye, L. Sisal fibre and its composites: a review of recent developments. *Compos. Sci. Technol*. **2000**, *60*, 2037.

[25] Iñuguez-Covarrubias, G.; Lang, S. E.; Rowel, R. M. Utilization of by-products from the tequila industry. Part 1: potential value of agave tequilana webber azul leaves. *Bioresour. Technol*. **2001**, *77*, 25.

[26] Iñuguez-Covarrubias, G.; Diaz-Teres, R.; Sanjuan-Dueñas, R.; Anzaldo-Hernandez, J.; Rowel, R. M. Utilization of by-products from the tequila industry. Part 2: potential value of agave tequilana webber azul leaves. *Bioresour. Technol*. **2001**, *77*, 101.

[27] Pokhrel, D. T.; Viroraghavan, T. Treatment of pulp and paper mill wastewater a review. *Sci. Total. Environ.* **2004**, *333*, 37.

[28] Walkowiak, B.; Kesy, A.; Michalec, L. Microplate reader- a convenient tool in studies of blood coagulation. Thromb Res. **1997**, *87*, 95.

[29] Tamada, Y; Ikada, Q. Effect of preadsorbed proteins on cell adhesion to polymer surface. *J. Colloid. Interface. Sci.* **1993**, *155*, 334.

[30] Salem, A. K.; Tendler, S. J.; Roberts, C. J. Interactions of 3T3 fibroblasts and endothelial cells with defined pore features. J. Biomed. Mater. Res. **2002**, *61*, 212.

[31] Sjoholm, E.; Gustafsson, K.; Eriksson, B.; Brown, W.; Colmsjo, A. Aggregation of cellulose in lithium chloride/*N,N*-dimethylacetamide. Carbohydr Polym **2000**, *41*, 153.

Chapter 4

Bamboo Fibers Elaborating Cellulose Hydrogel Films for Medical Applications

Abstract: Bamboo fibers were used as source to prepare cellulose hydrogel films for cell cultivation scaffold. The preparation of cellulose solutions was carried out by three different dissolving methods with NaOH-based and NaOH/urea aqueous solutions and DMAc/LiCl solution. Several hydrogel films were elaborated and their properties were compared to evaluate the effect of the dissolving method. It was found that tensile strength of the resultant hydrogel films increased from 21 to 66 N/mm^2 when DMAc/LiCl was used insted of the NaOH/urea to dissolve bamboo fibers. The same tendency was observed in the obtained elongation values. Moreover, a remarkable difference in fibroblast cell cultivation was observed in higher cell density, when DMAc/LiCl method was used. The obtained results with DMAc/LiCl also were seen to be higher than the reults for PS dish used as control. However, low cytocompatibility was observed when NaOH and NaOH/urea methods were used. The obtained results showed that hydrogel films elaborated with cellulose solution prepared with DMAc/LiCl method exhibited good cytocompatibility for the cell cultivation scaffold. In addition to bamboo, this chapter presents fibroblast growing in several cellulose hydrogels made of agave, kenaf and conifer dissolving in DMAc/LiCl system.

4.1 Introduction

As reported, scientists have devoted much energy to the development of novel hydrogels for tissue engineering. This has a purpose in natural polymers like cellulose occurring in attractive strategy for producing scaffolds for tissue regeneration [1,2]. More recently, fibroblast compatibility was reported on scaffold hydrogel films prepared from agave tequilana weber bagasse for tissue regeneration [3]. However, little is known about the method for elaborating hydrogel films by using cellulose. It is known that cellulose is the most important renewable resource on the earth. Natural fibers as bamboo can be renewable and cheaper for the preparation of hydrogels [1-5]. However, the dissolution of cellulose without chemical modification or derivation is difficult to achieve because of the stiffness and close chain packing caused by numerous inter-and intra-molecular hydrogen bonds present in cellulose. Therefore, cellulose still has not reached its potential in many areas for all its availability [6-8]. The most general solvents for dissolving cellulose are unsuitable. More common than not, cellulose needs to be activated or made accessible to be dissolved. In addition, the dissolving methods generate hazardous environmental pollution. Moreover, it was found that chemical modification or derivatization methods might affect the cytotoxicity of the obtained films for medical applications [9-12]. Thus, identifying new solvent systems for cellulose processing would help to reduce these toxicity problems. Some powerful non-derivatizing organic solvents for cellulose have been developed and used for preparing regenerated cellulose films and fibers during the last two decades, such as n-methylmorpholine-n-oxide and ionic liquids [13-15]. In addition to solvents mentioned previously, NaOH-based aqueous systems have been one focus of cellulose solvents research because of they can lead to environmentally friendly, simple, and economic process. Moreover, some limitations of NaOH-based aqueous systems have been observed on the

preparation of solutions from wood pulps [15-18]. This due to the intermolecular hydrogen bonds present in cellulose. The effectively destruction of intermolecular hydrogen bonding, is essential for successful applications of cellulose. Intermolecular hydrogen bonding of polysaccharides can be broken by using urea. Interestingly, NaOH and especially urea broke intermolecular hydrogen bondings of polysaccharides, loading to enhance water-solubility. The addition of organic compounds such as urea, thiourea to NaOH solution could have substantial impact on cellulose solubility [19-20].

One of the most useful solvent systems to emerge over the last two dacates is *N*,*N*-dimethyl acetamide with lithium chloride (DMAc/LiCl). DMAc/LiCl has become the solvent of choice for high-molecular weight cellulose analysis, as well as for the determination of solution characteristics of a number of other polysaccharides [21-23].

The purpose of this study was to compare the preparation method of cellulose solutions from bamboo fibers by NaOH-based aqueous, NaOH/urea and DMAc/liCl systems to elaborate hydrogel films for fibroblast cell cultivation.

4.2 Experiments

4.2.1 Materials

Bamboo fibers were provided from Hokuetsu Kishu Paper Mill CO. Sodium hydroxide and urea was purchased from TCI (Tokyo, Japan). Tripsin-M-ethylenediaminetetraacetate (Trypsin-EDTA) was purchased from Gibco (Tokyo, Japan) and formaldehyde (37 vol% aqueous solution) was from Wako Co., Ltd. NIH3T3 mouse embryonic fibroblast cells were also

purchased from BioResource Center (Japan).

4.2.2 Preparation of cellulose solutions

NaOH-based aqueous method: the cellulose fibers (1 g) were washed and swollen in ethanol followed by water according to exchange solvent technique. Then, cellulose fibers were dissolved in sodium hydroxide aqueous 9 wt%. The suspension was stirred for 10 h and then frozen at -20°C to become a solid state. After being frozen in about 15 h, the solid mass was taken out the freezer and thaw at ambient condition [24].

NaOH/urea method: cellulose fibers (1 g) were dissolved in urea aqueous solution (14 wt%) pre-cooled to 0°C with stirring for 1 min. Then, urea aqueous solution (24 wt%) pre-cooled to 0°C was added immediately with stirring vigorously for 2 min. The solution was kept at 0°C during 12 h and left at room temperature until the solution became liquid again [20].

DMAc/LiCl method: cellulose fibers (1 g) were treated by three steps of solvent exchange. First, fibers were suspended in 300 mL of distilled water and stirred overnight, after water was removed, ethanol (300 mL) was added to the swelled fibers and the mixture was stirred for 24 h. Then, ethanol was removed and DMAc was added and then stirred for 24 h. Then, DMAc (previously dried with potassium hydroxide) was added to the swelled cellulose fibers to obtain 1 wt% solution, and LiCl (6 wt%) was added. The mixture was stirred at room temperature for 3 days until a viscous solution was obtained [14].

4.2.3 Preparation of hydrogel films

NaOH-based aqueous method: the obtained solution (10 g) was cast on the glass plate and heated at 70°C. Then, distilled water was poured into the glass plate to gently wash the semi-membrane

obtained and reduce the alkaline and remove the insoluble cellulose. After washing, a second drying process was carried out at 75°C until a dried membrane was obtained. Second washing step was done to enhance the mechanical properties. Finally, a third drying step was carried out at 75°C until a dried membrane was obtained.

NaOH/urea aqueous method: the obtained solution (10 g) was poured on a glass plate and coagulated with isopropanol overnight. The resulting film was washed by ethanol 3 times.

DMAc/LiCl method: 10 g of cellulose solution were poured into a glass plate tray (10 cm diameter) and kept for 12 h in a container filled with 20 mL of ethanol as coagulant. The resulting film was washed by ethanol 3 times and then submerged in water for 12 h.

The films obtained for the different dissolving methods were submerged in 100 mL of distilled water and placed in a shaking bath at 25°C for 24 h to remove traces of chemical compounds, distilled water was changed each 2 h. Finally, the hydrogel films were immersed in distilled water for 12 h and kept in phosphate buffered saline (PBS) at 4°C in a plastic container.

4.2.4 Evaluation of hydrogel films

Before the preparation of the hydrogel films, shear viscosity of the obtained cellulose solutions was measured by a B type viscometer at 25°C. Water contents of the resultant hydrogel films were determined by weighing the wet and dry samples by following. Samples of 5 mm diameter were cut from cast films, dried in a vacuum oven and weighed. The samples were then swollen in PBS for 36 h and blotted lightly with filter paper to remove excess PBS. The weight of the swelled samples was then determined. The percent of equilibrium water content (EWC) was calculated based on $EWC= W_h-W_d/W_h \times 100$, where W_h is the weight of the hydrated sample and

W_d is the dry weight of the sample. For each specimen, four independent measurements were determined and averaged [25].

Tensile strength and elongation of the hydrogel films were measured on LTS-500-S20 (Minebea, Japan) with universal testing machine equipped with a 2.5 kN cell. Strips (50 x 10 x 1 mm) were cut from cast films with a razor blade. Strain was recorded by means of Zwick Makrosense clip-on displacement sensors. One set of samples (five strips each) was measured and each set was repeated 3 times. Only samples which ruptured near mid-specimen length were considered for calculation of tensile strength. The values of the tensile strength and elongation were calculated by using the following:

Tensile strength (N/mm^2) = Maxilum Load/ cross-section area.

Elongation (%) = ((Final length (mm) – Initial length (mm))/ (Initial length (mm)) x 100

Water contact angle (WCA) measurements were carried out by using a contact angle goniometer (Kyowa Interface Science). Samples of 2 x 2 cm were cut from cast films. Samples were stuck on a glass slide and mounted on the goniometer. A total of 3μL of distilled water was dropped on the airside surface of the film at room temperature. And the values of the contact angle were measured after 10 seconds and at least eight measurements were averaged for each prepared film to obtain a reliable value.

SAXS experiments were conducted using synchrotron radiation at beamline BL-10C of the Photon Factory. The scattered X-ray was collected for 60 sec with a 2-dimensional pixel detector (DECTRIS, PILATUS 300K-W). The scattering angle was calibrated by using silver behenate (d_{001}=5.888 nm). The scattering vector was defined as $q=(4\pi/\lambda)\sin(\theta/2)$, where θ and λ are the scattering angle and the wavelength of the incident X-ray, respectively. SAXS measurements

were performed for the hydrogel to investigate the aggregation state of cellulose molecular chains.

Information on the structure of cellulose was obtained from the SAXS profiles by OZ equation [22].

$$I(q) = I(0/1+q^2\zeta^2)$$

Where ζ is the correlation length and I/0 is the scattered intensity at q=0.

4.2.5 Cytotoxicity of hydrogel films

Hydrogel films circles with 30 mm diameter were used for cell seeding purposes. The samples were sterilized with 70 and 50 wt% of aqueous ethanol for 30 min and then, rinsed twice with PBS for 30 min. Finally, the hydrogel films were swelled in Dulbecco´s modified eagle medium (DMEM) for 2 h before seeding procedure. The NIH3T3 mouse embryonic fibroblast cells were cultured at 37°C in 95 wt% of relative humidity and 5 wt% of CO_2 environment. The culture medium was in 90 wt% of DMEM supplemented with 10 wt% of fetal bovine serum (FBS) and 1 wt% of penicillin/streptomycin. The cells were seeded (cell density $8x10^3$ cm^2) on the hydrogel films and tissue culture grade polystyrene dish (PS dish) was used as control. The cells were used for imaging and characterization purpose after 4, 24, 48 and 72 h of culture. The sample image was obtained using an inverse microscope (Olympus CKX41, Japan). Approximately, 50 cells were analyzed per image. For each sample, five images were analyzed to obtain an unbiased estimated of the cell morphology. The results presented herein were based on three independent experimental runs. The measurements were assessed statically using a one-way

analysis of variance (ANOVA) test followed by Student´s t Test with a significance criterion of $p<0.05$.

4.3 Results and Discussion

4.3.1 Results with different solvents

4.3.1.1 Preparation of hydrogel films

Figure 4.1 shows shear viscosity of the obtained cellulose solutions. The white cellulose fibers from bamboo were used (Fig. 4.2a)The cellulose solutions made with bamboo fibers varying the dissolving method showed a significant difference in shear viscosity value around 107 Cp, 109 Cp, and 165 Cp for NaOH-based aqueous method, NaOH/urea aqueous method and DMAc/LiCl method, respectively. The change could be attributed to the effect on the cellulose fibers by the chemical compounds used in the different methods. McCormick et. al., reported that compounds such as sodium hydroxide tend to affect changes in the molecule: the remaining cellulose is either degraded, its crystallinity has been altered and/or it is not absolutely pure [26]. It was also observed that shear viscosity value was higher in the cellulose solution prepared by DMAc/LiCl method. This could be due to it has been reported that the DMAc/LiCl method can dissolved cellulose with a molecular weight of more than 10^6 under ambient conditions without severe degradation or other undesirable reaction.

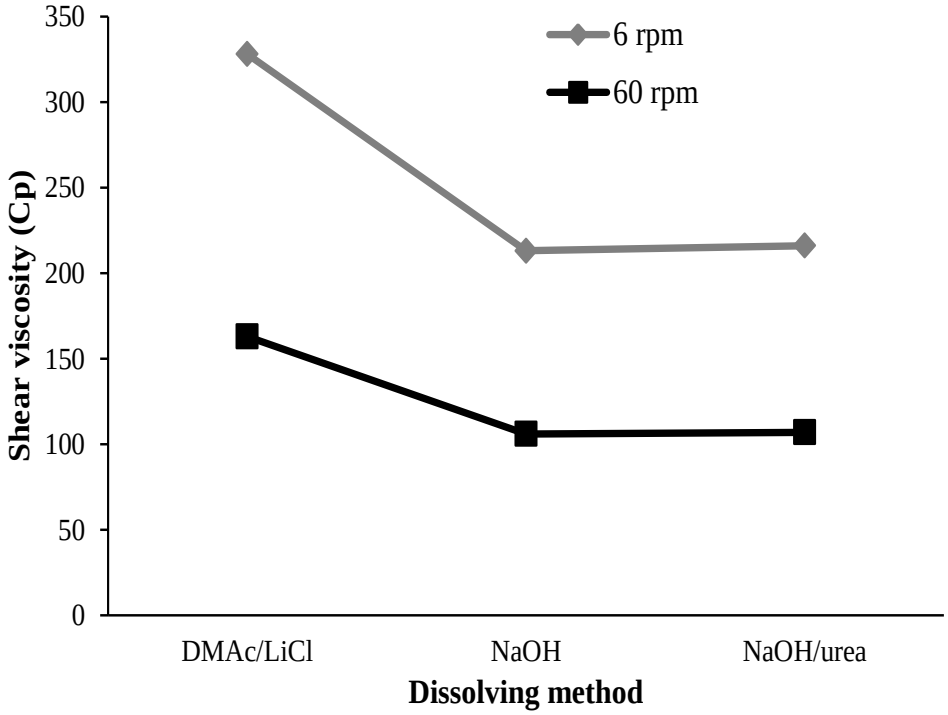

Figure 4.1. Shear viscosity of hydrogel films elaborated with cellulose solution prepared with different dissolving method. Shear viscosity was measured at 6 and 60 rpm at 25°C.

It was seen that a remarkable difference in appearance was observed in the obtained hydrogel films. All the cellulose solutions prepared from bamboo fibers (Fig. 4.2a) by different dissolving method were transparent. On the other hand, the hydrogel film elaborated with cellulose fibers dissolved by NaOH/Urea method showed a white color and low transparency (Fig. 4.2b). Lower white color was observed in hydrogel film prepared with cellulose fibers dissolved by NaOH-based aqueous method (Fig. 4.2c). In addition, only a highly transparent and color less hydrogel film was obtained when DMAc/LiCl method was used for the preparation of cellulose solution (Fig. 2d).

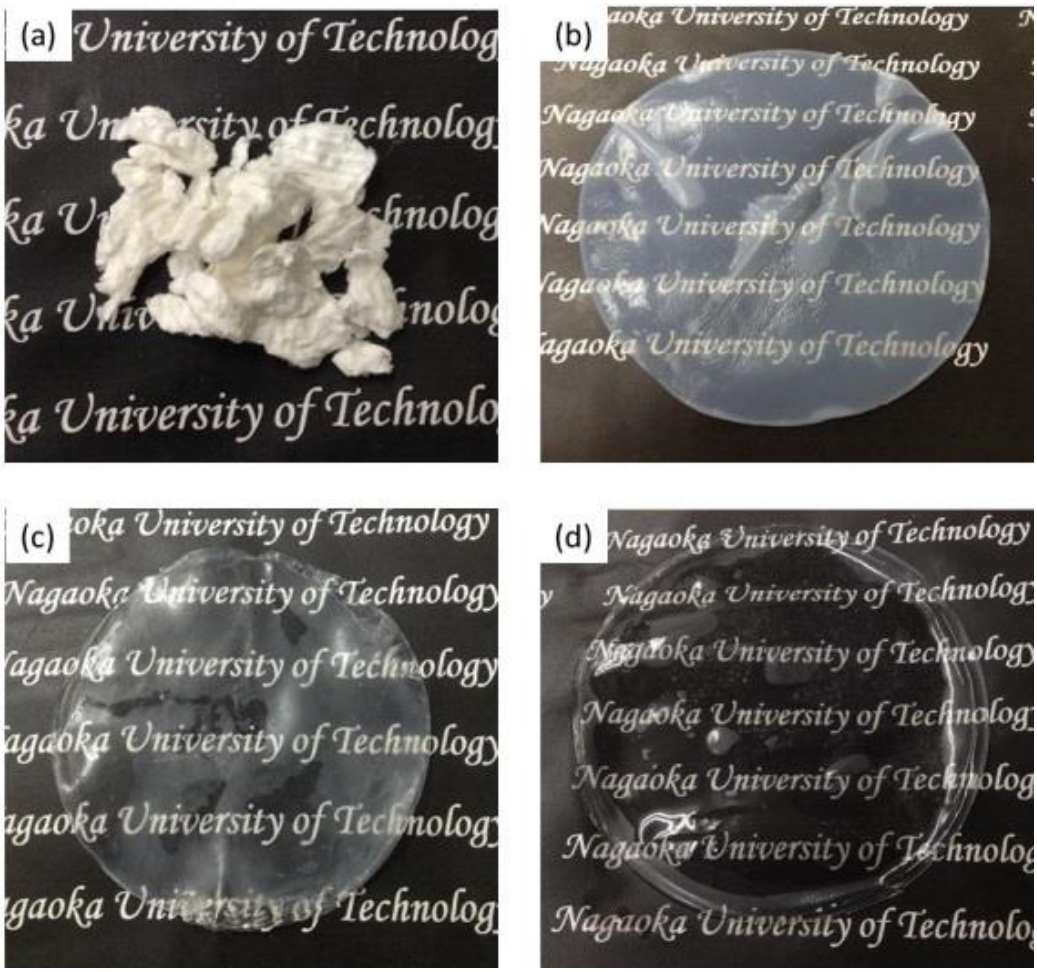

Figure 4.2. Cellulose fibers and hydrogel films for (a) bamboo fibers, (b) film obtained when NaOH/urea and, (c) film obtained when NaOH method, were used and (d) for film obtained when DMAc/LiCl was used.

Table 4.1 also lists hydrogel film properties, as equilibrium water content at room temperature for 36 h. The water content decreased from 31.2 % to 10.9 % when the dissolving method was change from DMAc/LiCl to NaOH/urea for the preparation al cellulose solution. This could be attributed the effect of NaOH on the cellulose fibers. Thus, when DMAc/LiCl method was used for the preparation of cellulose solution, water molecules were capable of penetrating and

interacted easily into the obtained hydrogel films. For uniaxial tensile testing, the hydrogel samples (50x10x1mm) were placed between two clamps and the film was then pulled away. Table 4.1 shows that higher elongation and tensile strength was observed in the films elaborated with cellulose solution prepared with DMAc/LiCl method. Tensile and elongation values increased from 21 to 66 N/mm^2 and from 8 to 33.5%, in the cases of NaOH/urea and DMAc/LiCl, respectively. Water contact measurements showed that the surface of films obtained with cellulose solutions prepared with NaOH were more hydrophilic with a contact angle around 32° compared with the hydrophilic behave observed on the surface of hydrogel films elaborated with cellulose solution prepared with DMAc/LiCl with contact value around 61°.

Table 4.1. Properties of hydrogel films.

Dissolving method	EWC (%)	Elongation (%)	Tensile strength (N/mm^2)	WCA (degree)
DMAc/LiCl	312	33.5	66	61
NaOH	141	13	27	35
NaOH/urea	109	8	21	32

4.3.1.2 Cytotoxicity of hydrogel films

If the present hydrogels would be applied for healing repair as scaffold, another important issue to consider is fibroblast growing on the hydrogel surface [3]. In order to observe such behavior, phase-contrast light microscope images were used. Figure 4.3 shows cell density of the hydrogel

films prepared.

A remarkable difference was observed when the dissolving method for the preparation of cellulose solutions was changed (ANOVA, $p<0.05$). Moreover, the number of adherent cells on the hydrogel films was higher when DMAc/LiCl was used, this was significant (Student´s t-test, $p<0.05$, n=6). This results were significant comparing NaOH and NaOH/Urea method (Student´s t-test, $p<0.05$, n=6). After 72 h of cultivation cell density on hydrogel films elaborated with cellulose solution prepared with DMAc/LiCl method showed an increased. This increase was significant comparing with PS dish results (Student´s t-test, $p<0.05$, n=6). These results were consistent with the reported by Salem, et. al., they observed higher cell density on surface with a contact angle around 60° [27] as the observed on hydrogel films elaborated with cellulose solution prepared with DMAc/LiCl method.

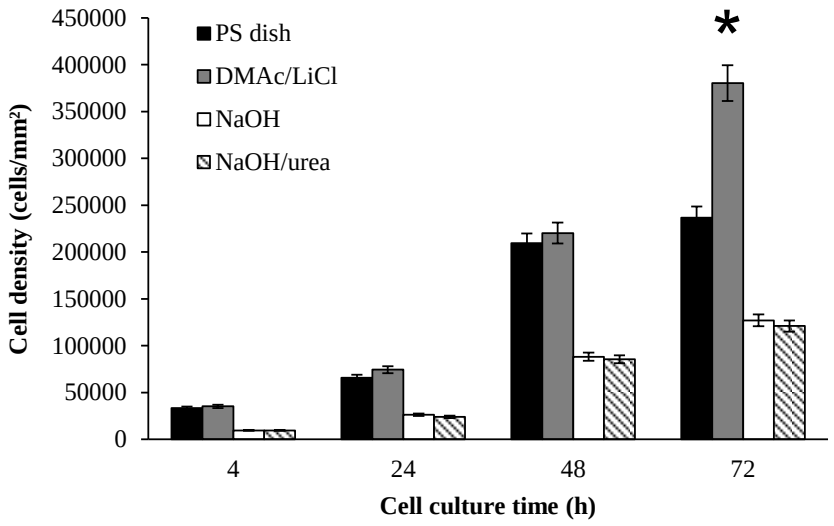

Figure 4.3. Cell number on the hydrogel films surfaces as function of culture time. The dissolving method for the preparation of cellulose solution was varied. An asterisk indicates statistically significant different from PS dish used as control ($p<0.05$). Mean ± SEM ($n=6$).

As shown in Figure 4.4, phase-contrast light microscope images revealed a remarkable difference on fibroblast pattern in the morphology for PS dish (a-c) used as control and the hydrogel films (d-l). The Hydrogel films obtained in the DMAc/LiCl system was used for cases of (d-f). The adherent cells showed longer axis shape of the grown adherent cells as compared with those adhered on the PS dish at the same condition (a-c). Moreover, the boundaries of the adherent cells on the cellulose films obtained when DMAc/LiCl method was seemed to be clear tightly adhesion at 4h for (d) on the hydrogel surface showing a diffuse shape on the cultivated cell edge. In addition, anisotropic shape was observed in the first 4h of cell culture. It was also noticed that the anisotropic shape increased in the adherent fibroblast cells after 72 h (d) of culture time passed [3]. These results revealed that the hydrogel films obtained from DMAc/LiCl solution had higher cytocompatibility rather than the PS dish used. On the other hand, the cellulose obtained in the NaOH method was used as (g-i) adherent fibroblast cells showed lower anisotropic shape as compared to PS dish at 4 h. In addition, no significant difference on the number of adherent fibroblast cells and less change in morphology was observed during the 72 h. When the NaON/urea was used as (j-l), the adherent cells had also less anisotropic shape, but round shape was observed at 4 h. The boundaries of the fibroblast cells seemed to show poor adhesion of the cellulose films and to be less remarkable difference in the observed at 72h. These results showed that the low cytocompatibility of the hydrogel films obtained by the NaOH and NaOH/urea methods. This could be atribuited to the lower water attachment rather than the sample surface of the DMAc/LiCl for the NaOH and NaOH/urea films. It has been reported for the silicon scaffolds that lower contact angle values and low mechanical properties affected fibroblast adhesion [27].

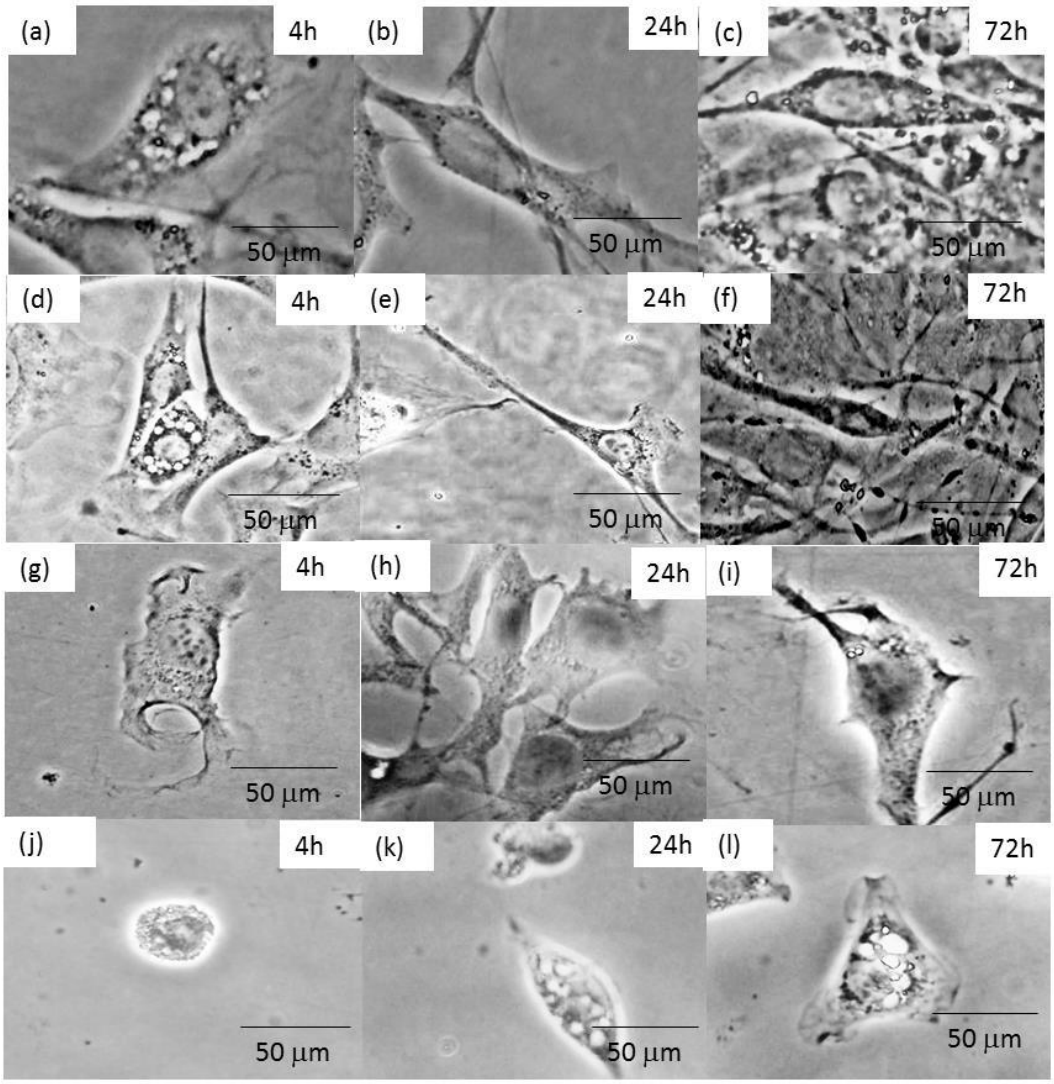

Figure 4.4. Phase-contrast light images, (a-c) PS dish used as control, (d-f) DMAc/LiCl method, ((g-i) NaOH method and (j-l) NaOH/urea method. The time culture was 4, 24 and 72 h.

4.3.2 Results with different fiber

4.3.2.1 Evaluation of hydrogel films

Table 4.2 shows that a significant difference in the properties of the hydrogels prepared with agave fibers compared with the hydrogel films prepared with kenaf and conifer fibers. The agave films showed the higher water content, elongation and tensile strength value. In addition, the difference observed in the obtained values with 6 and 12 wt% of LiCl was higher compared with the other fibers. Water content was significant higher in hydrogel films prepared with agave fibers. In addition, films prepared with 12 wt% of LiCl showed higher contact angle. The adsorption of plasma protein, like in the case of FBS, was higher in the films prepared with agave fibers, suggesting better cytocompatibility in the hydrogel films prepared with agave fibers and 6 wt% of LiCl.

Table 4.2 Properties of hydrogel films

Cellulose fiber	LiCl Content (wt%)	Water Content (%)	Contact angle	Protein adsorption (mg/μm²) PBS	FBS
Agave	6	296	51	9	35
	12	239	64	23	28
Kenaf	6	262	57	13	26
	12	252	61	24	29
Conifer	6	239	59	15	27
	12	232	63	21	28
Bamboo	6	223	61	20	26
	12	239	63	21	28

The obtained SAXS results showed differences in the structure of the hydrogels depending of the LiCl concentration and type of fiber used. Decreased of ζ value was observed when LiCl concentration increase from 6 to 12 wt%. The length ζ reflects the distance between the nearest neighboring chain in the network [22].

A remarkable difference of the obtained results for agave hydrogels was observed compared with kenaf and conifer. In the case of kenaf and conifer, small increment of the aggregates size and decrease of the distance between the aggregates was observed when LiCl concentration increased from 6 to 12 wt%. On the other hand, change of aggregates size and the distance between them was more evident in agave hydrogels.

Figure 4.5 shows the Zimm plots of the prepared cellulose solutions. The obtained results showed difference in the properties of the hydrogel films whith the LiCl concentration and the type of fiber was changed. The ζ changed when the LiCl concentration was changed from 6 to 12 wt%. The length ζ reflects the distance between the nearest neighboring chain in the network [22]. A remarkable difference in the agave Zimm plot was observed compared with the Kenaf and Conifer Zimm plots. These results suggest that the fiber structure of the fibers used is different and this affects the properties of the obtained hydrogel films. It has been reported that in the LiCl/DMAc system a macrocation is formed. This macrocation interact with the cellulose molecules in the fibers. This interactions lead to the formation of aggregates depending of the concentration of LiCl. For these reasons the length of ζ decreased with the increase of LiCl concentration. These results explain the difference obtained in the cyto and biocompatibility properties previously described.

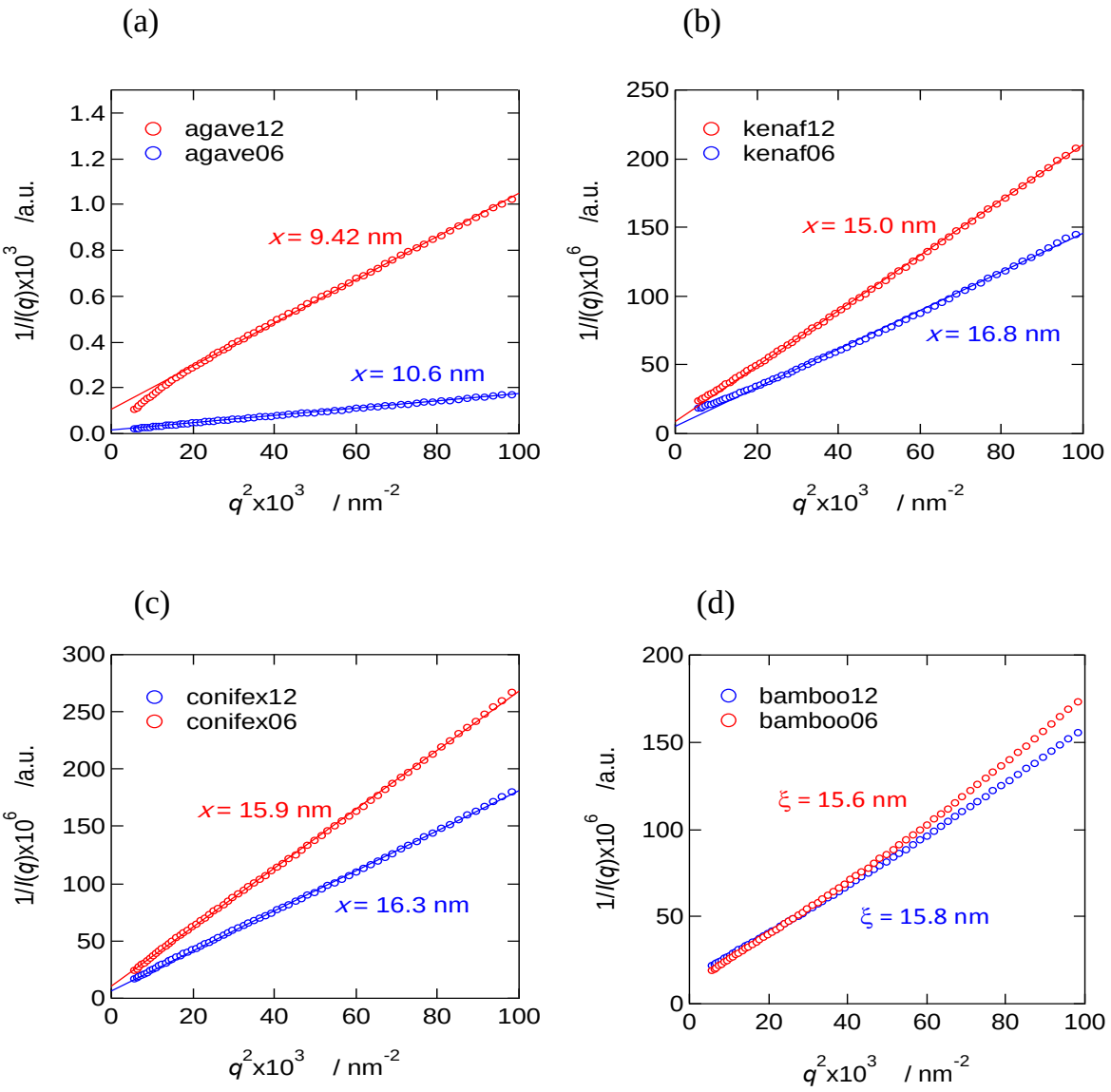

Figure 4.5 Zimm plot of 1 wt% cellulose in LiCl/DMAc solutions of (a) agave, (b) Kenaf, (c) conifer and (d) bamboo. Line shows an OZ equation given by Equation $1(q)=1(0)/(1+q^2\zeta^2)$. LiCl concentration used was 6 and 12 wt%.

This could be attributed to the difference of the structure of the fibers used and the different interaction of them with the LiCl/DMAc solution and the formed macrocation of the system. It has been reported that in the LiCl/DMAc system a macrocation is formed. This macrocation interact with the cellulose molecules in the fibers. This interactions lead to the formation of aggregates depending of the concentration of LiCl [14].

4.3.2.2 Evaluation of fibroblast adhesion on hydrogel films.

To evaluate cell adhesion on the hydrogel films fibroblast NIH 3T3 cells were used. The cells were seeding on the hydrogel films and tissue culture polystyrene dish (PS dish) at a density of 8 x 10^3 cell cm^{-2}. The culture time was varied from 1 to 14 days. Phase contrast images were used to determinate cell density and morphology of the adherent cells. The measurements were assessed statistically using a one-way analysis of variance (ANOVA) test followed by Student's Test with a significance criterion of $p<0.05$. The hydrogel film surfaces showed 90%-confluent adhesion state at 48 h. Figure 4.6 shows that all the samples revealed differences in the number of adherent cells on the hydrogel films. After 1 day of culture time the number of adherent cells showed significant increment on the surface of the agave films prepared with 6 wt% of LiCl. This tendency was also observed after 14 days of culture time. There was no significant difference in the cell density observed on the hydrogel films prepared with kenaf and conifer fibers, even thought when the concentration of LiCl used was 6 and 12 wt%. As it was expected, the same tendency observed in the mechanical and cytocompatibility properties was observed in the cell density.

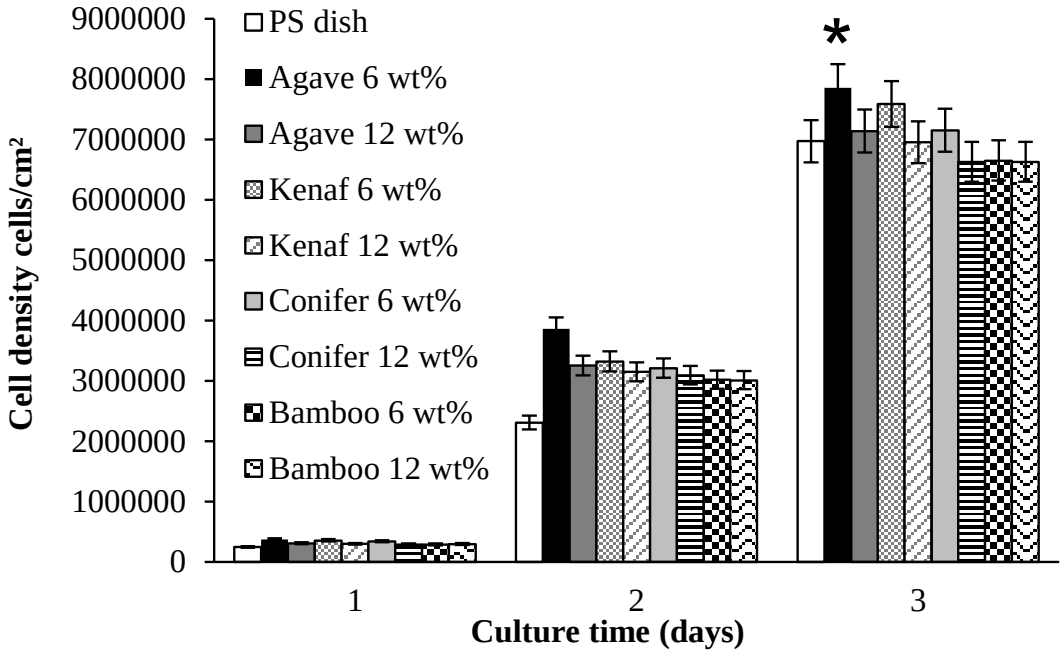

Figure 4.6. Cell number on hydrogel films as function of culture time. The LiCl concentration and the fiber tipe was varied. An asterisk indicates statistically significant difference from PS dish used as control (p<0.05).

The results revealed that all the hydrogel samples used showed better cytocompatibility than the PS dish used as control. Nevertheless, difference was observed when the LiCl concentration was changed, especially in the case of agave hydrogel films. These results confirm the expected suppress of fibroblast adhesion due the decrease of serum protein adsorption. Moreover, the higher cell adhered number was observed on agave films with contact angle around 50°, this results are consistent with the reported by Salem et. al. [27] and Tamada et. al. [28].

In addition, cell morphology results are shown in Figure 4.7 It was observed that the values of cell area (Fig. 4.7a), aspect ratio (Fig. 4.7b) and length of the long axis (Fig. 4.7c) were higher in the agave films. No significant difference was observed in the morphology of bamboo films. At 24 h of culture time, aspect ratio and long axis showed difference compared with PS dish used as control. In fact, all the hydrogel films showed higher results than the PS dish. These results were consistent with the reported by Salem et. al. [27] they observed diminished of the aspect ratio on surface with contact angle around 65°, like in the case of kenaf and conifer hydrogel films. In addition, it was reported that because adhesion and spreading of anchorage-dependent cells are prerequisite for cell viability and proliferation, [27,28] the reduction of the aspect ratio on surface with higher contact angle might be expected to result in lower cell densities, especially at early timepoints in the culture time.

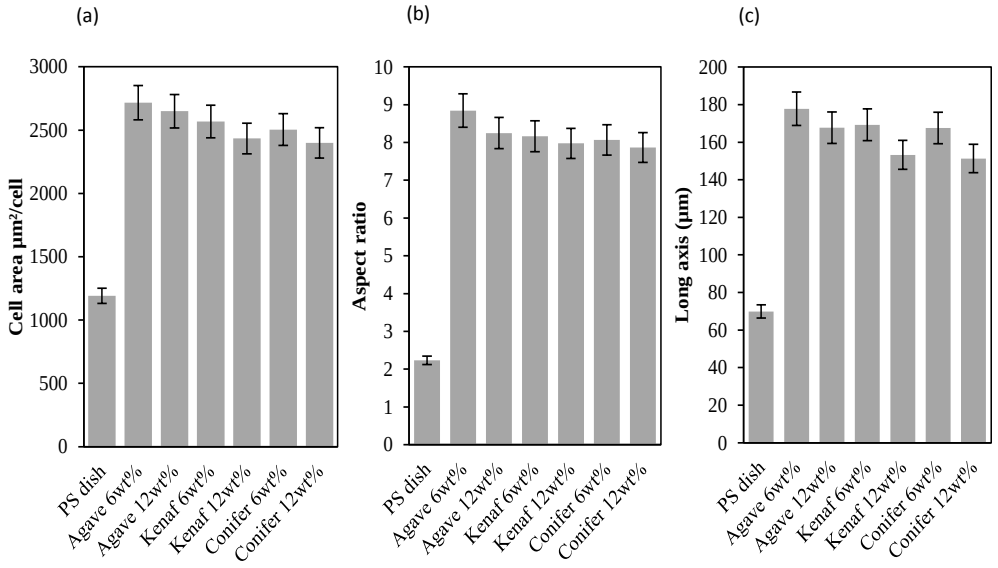

Figure 4.7. Effect of variation of LiCl concentration and type of fiber for the preparation of hydrogel films on (a) cell area, (b) aspect ratio and (c) length of long axis.

Figures 4.8 and 4.9 shows remarkable difference of cell spreading on surface elaborated with 6 and 12 wt% of LiCl, respectively. Figure 4.8 shows optical microscope images of (a) PS dish, (b) kenaf with 6 wt% of LiCl and (c) conifer with 6 wt% of LiCl after 24 h of cell culture time. When the images were compared higher number of adherent cells was observed in the hydrogel films. It was not possible to observe any spreading pattern of the adherent cells in kenaf or conifer hydrogel films as the ordered cell spreading observed on agave films in our previous report [3].

Moreover, when 12 wt% was used difference on cell spreading was observed as shown in Figure 4.9. With the increment of LiCl concentration cell spreading on the hydrogel surface appeared as domains as shown in Figure 5b for kenaf and Figure 5c for conifer. In both cases, cell spreading with domain shape remained. This domain shape was also observed on agave films prepared with 12 wt% of LiCl in our previous report [3]. In fact, when agave fibers were used for the preparation of the hydrogel films, remarkable difference were observed between 6 and 12 wt% of LiCl. When 6 wt% of LiCl was used, patterns in cell spreading were observed. On the other hand, these patterns were not observed on kenaf or conifer films. This could be due to difference of number and distance between cellulose aggregates observed in agave, kenaf and conifer, as it was showed in SAXS results. In kenaf and conifer the aggregates size is higher and space between cellulose aggregates is lower therefore, domain shape was observed on cell spreading.

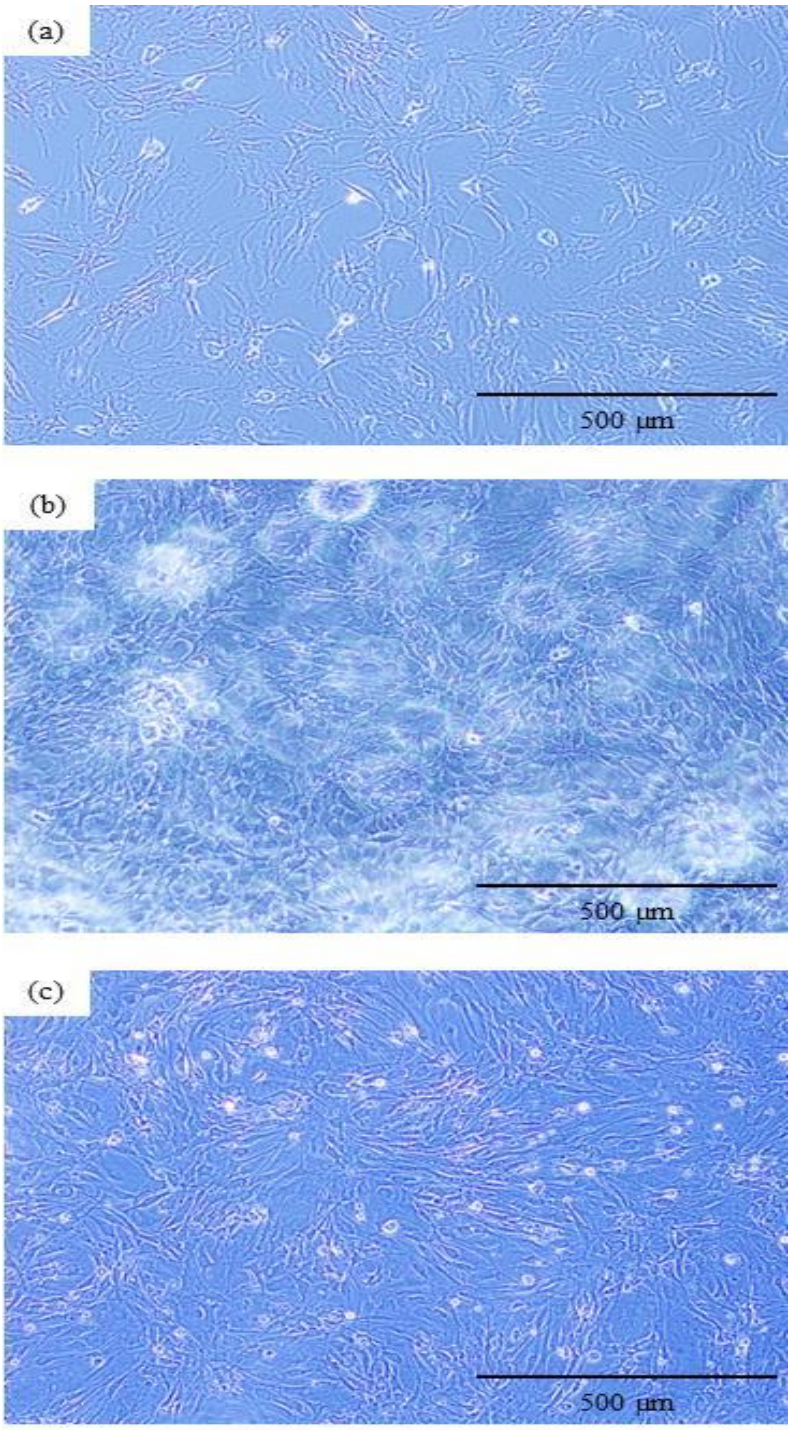

Figure 4.8. Adherent cell on (a) PS dis, (b) kenaf and (c) conifer film, the 6 wt% of LiCl concentration was used. The cell culture time was 1 day.

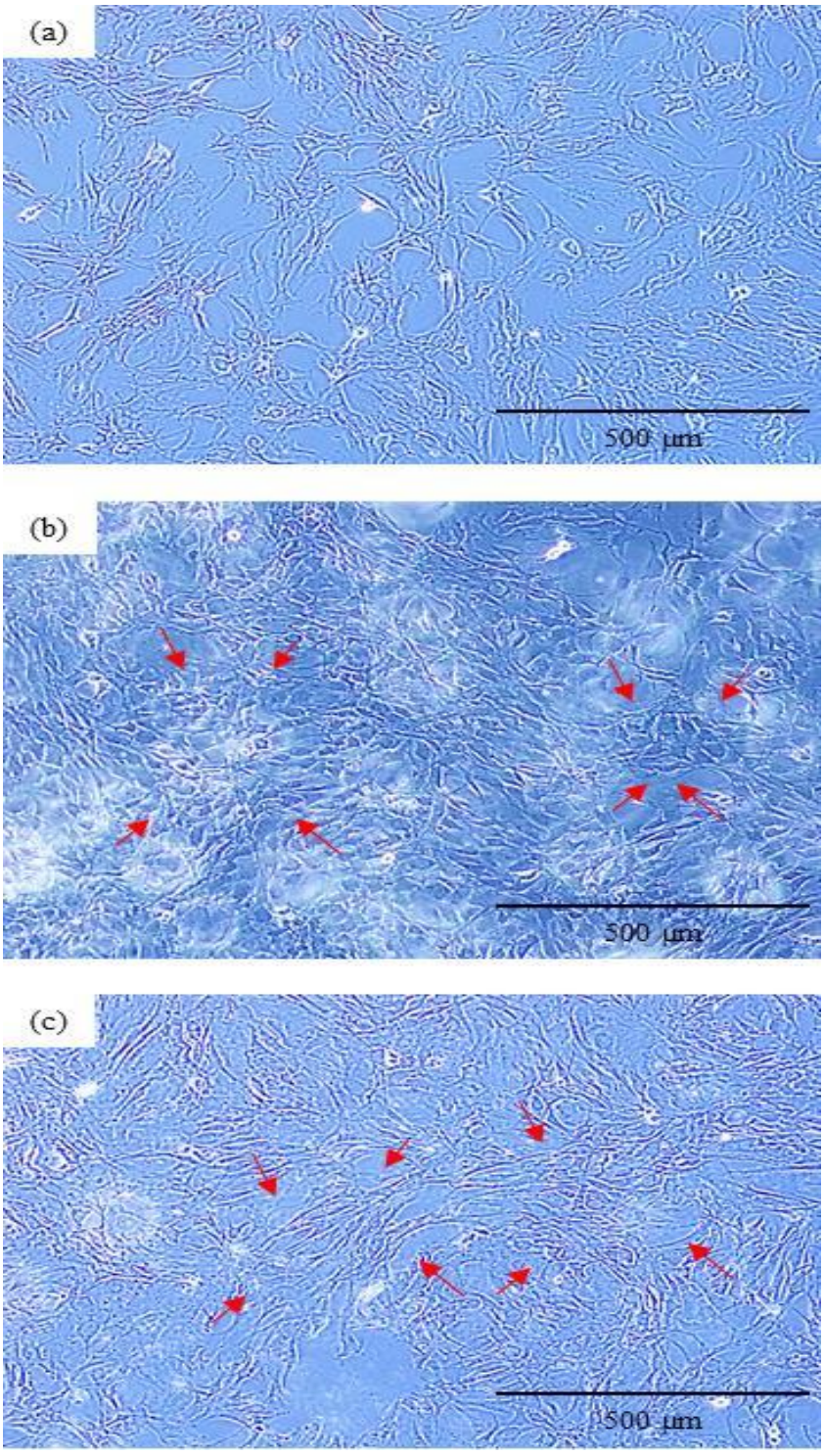

Figure 4.9. Adherent cell on (a) PS dis, (b) kenaf and (c) conifer film, the 12 wt% of LiCl concentration was used. The cell culture time was 1 day.

Figure 4.10 shows fluorescence dyeing of adherent cells on hydrogel films. In Figure 4.10 the cell organelles such as nucleus and cytoskeleton could be observed. The actin proteins could be used to observed the adhesion of fibroblast on the hydrogel films. Figure 4.11 shows dyeing fibroblast adhered on hydrogel films prepared with 6 and 12 wt% of LiCl. Remarkable difference in the spreading pattern was observed when the LiCl content was varied. Figure 4.11a shows more ordered and aligned cell spreading compared with the non-ordered cell spreading observed on films prepared with 12 wt% of LiCl.

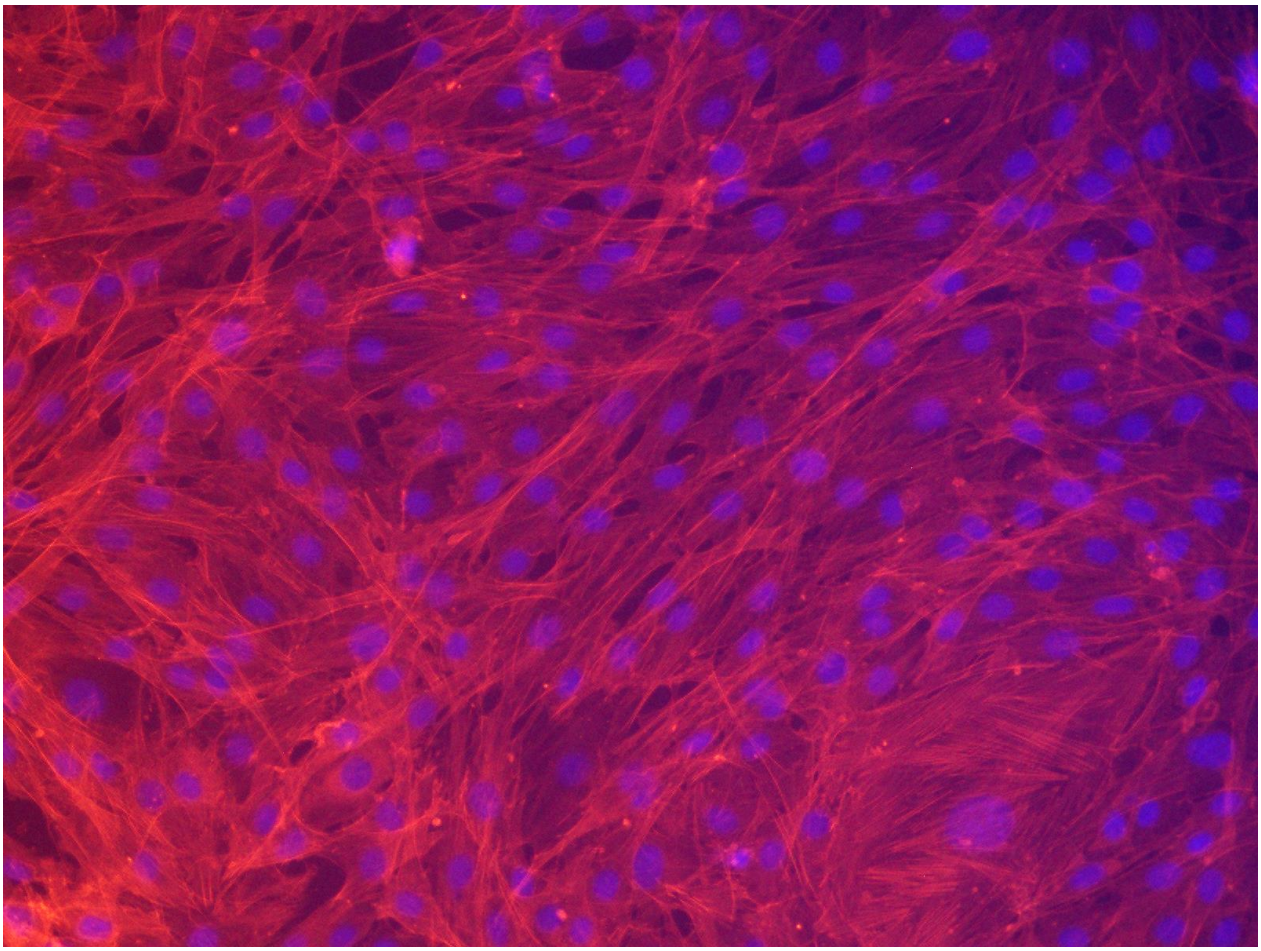

Figure 4.10. Fluorescence dyeing of adhered cell on hydrogel films after 24h of cell culture time at 37°C.

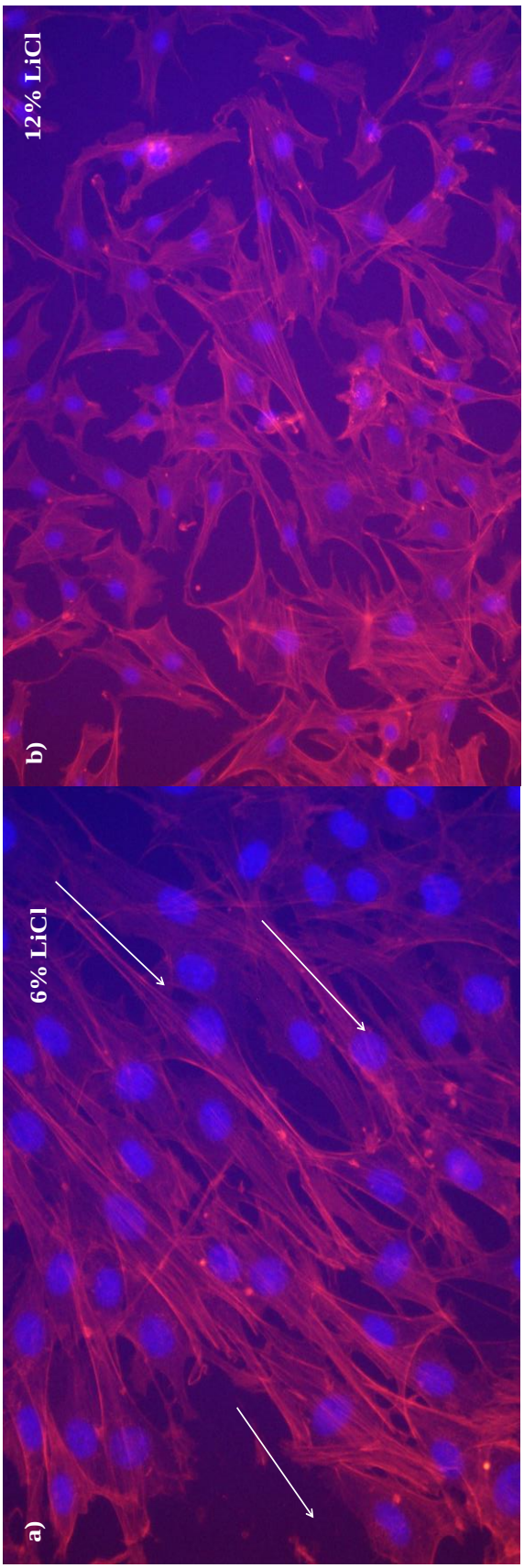

Figure 4.11. Fluorescence dyeing of adhered cells on hydrogel films prepared with different LiCl content after 4h of cell culture time.

4.4 Conclusions

Cellulose hydrogel films from bamboo fibers dissolved by three different methods were obtained. Depending of the dissolving method used, hydrogel film exhibited lower tensile strength, elongation and contact angle in the case of NaOH and NaOH/urea systems. On the other hand, very good cytocompatibility was observed in the hydrogel films elaborated with DMAc/LiCl solution. It was proved that the dissolving method used for the preparation of the cellulose solution affects the properties of the obtained films. These results suggest that hydrogel films elaborated with cellulose solution prepared with DMAc/LiCl showed better possibility of usage for tissue engineering scaffold. Depending on the LiCl and type of fiber used, these hydrogels exhibited different bio and cytocompatibility. All the obtained hydrogel films presented higher cytocompatibility compared with PS dish used as control. It was proved that LiCl acted to be dense networks of the cellulose segments, according with the SAXS results. These results indicated that the property of the hydrogel films affects the adhesion and spreading of the fibroblast cells.

4.5 References

[1] F. A. Muller, L. Muller, I. Hofman, P, Greil, M. M. Wenzel and R. Staudenmaier, "Cellulose Based Scaffold Materials for Cartilage Tissue Engineering," Biomaterials, Vol 27, 2006, pp. 3955-3963.

[2] H. Hoenich, "Cellulose for medical Applications: Past, Present, and Future," *Bioresources*, Vol 1, No. 2, 2006, pp. 270-280.

[3] K. L. Tovar-Carrillo, M. Tagaya, T. Kobayashi, "Fibroblast Compatibility on Scaffold Hydrogels Prepared from Agave Tequilana Weber Bagasse for Tissue Regeneration," *Industrial & Engineering Chemistry Research*, Vol, 33, 2013, pp.11607-11613.

[4] W. Deoliveira and W. G. Glasser, "Hydrogels from Polysaccharides. 1. Cellulose Beads for Chromatographic," *Journal of Applied Polymer Science,*Vol, 60, 1996, pp. 63-73.

[5] H. Saito, A. Sakurai, M. Sakakibara and H. Saga, "Preparation and Properties of Transparent Cellulose Hydrogels," *Journal of Applied Polymer Science,* Vol, 90, 2002, pp. 3020-3025.

[6] S. Zhang, F. X. Li and J. Y, Yu, "Preparation of Cellulose/Chitin Blend Bio-Fibers *Via* Direct Dissolution," *Cellulose Chemistry and Technology,* Vol, 43, No. 9-10, 2009, pp. 393-398.

[7] C. F. Liu, R. C. Sun, A. P. Zhang and J. L. Ren, "Preparation of Sugarcane Bagasse Cellulosic Phthalate Using an Ionic Liquid as Reaction Medium," *Carbohydrate Polymers,* Vol. 68, 2007, pp. 17-25.

[8] M. Abe, Y. Fukaya and H. Ohno, "Fast and Factible Dissolution of Cellulose with Tetrabutylphosphonium Hydroxide Containing 40 wt% Water," *ChemComm*, Vol, 48, 2012, pp. 1808-1810.

[9] L. Yan and Z. Gao, "Dissolving of Cellulose in PEG/NaOH aqueous Solution," *Cellulose*, Vol, 15, 2008, pp. 789-796.

[10] J, Vitz, T. Erdmenger, C. Haensch and U. S. Schubert, "Extended Dissolution Studies of Cellulose in Imidazolium Based Ionic Liquids," *Green Chemistry*, Vol, 11, 2009, pp. 417-424.

[11] E. Sjoholm, K, Gustafsson, B. Pettersson and A. Colmsjo, "Characterization of the Cellulosic Residues from Lithium Chloride/N,N-dimethylacetamide Dissolution of Softwood Kraft Pulp," *Carbohydrate Polymers*, Vol, 32, 1997, pp. 57-63.

[12] A. Ostlund, D. Lundberg, L. Nordstierna, K. Holmberg and M. Nyden, "Dissolution and Gelation of Cellulose in TBAF/DMSO Solutions: The Roles of Fluoride Ions and Water," *Biomacromolecules*, Vol, 10, 2009, pp. 2401-2407.

[13] B. Lindman, G. Karlstrom and L. Stigsson, "On the Mechanism of Dissolution of Cellulose," *Journal of Molecular Liquids*, Vol, 156, 2010, pp. 76-81.

[14] A. M. Striegel, "Theory and Applications of DMAc/LiCl in the Analysis of Polysaccharides," *Carbohydrate Polymers*, Vol, 34, 1997, pp. 267-274.

[15] S. Zhang, F. X. Li, J. Y. Yu, Y. L. Hsieh, "Dissolution behavior and Solubility if Cellulose in NaOH Complex Solution," *Carbohydrate Polymers*, Vol, 81, 2010, 668-674.

[16] A. Isogai and R. H. Atalla, "Dissolution of Cellulose in Aqueous NaOH Solutions," *Cellulose*, Vol, 5, 1995, pp. 309-319.

[17] S. Zhang, F.X. Li, J. Y. Yu and G. L. Xia, "Dissolved State and Viscosity Properties of Cellulose in a NaOH Complex Solvent," *Cellulose Chemistry and Technology*, Vol, 43, 2009, pp. 241-249.

[18] H. Jin, C. Zha and L. Gu, "Direct dissolution of Cellulose in NaOH/thiourea/urea Aqueous Solution," *Carbohydrate Research*, Vol, 342, 2007, pp. 851-858.

[19] J. Behin, F. Mikanikl and Z, Fadael, "Dissolving Pulp (alpha-cellulose) from Corn Stalk by Kraft Process," *Iranian Journal of Chemistry Engineering*, Vol, 5, No. 3, 2008, pp. 14-28.

[20] J. Zhou and L. Zhang, "Solubility of Cellulose in NaOH/urea Aqueous Solution," *Polymer Journal*, Vol, 32, 2000, pp. 866-870.

[21] L.A. Ramos, D. L. Morgado, O. A. El Seoud, V. C. da Silva, E. Frollini, "Acetylation of Cellulose in LiCl-N,N-dimethylacetamide: First Reporto n the Correlation Between the Reaction Effiency and the Aggregation Number of Dissolved Cellulose," *Cellulose*, Vol, 18, 2011, pp. 385-392.

[22] D. Ishii, D. Tatsumi and T. Matsumoto, "Effect of Solvent Exchange on the Supramolecular Structure, the Molecular Mobility and the Dissolution Behaviour of Cellulose in LiCl/DMAc," *Carbohydrate Research*, 343, 2008, pp. 919-928.

[23] N.G.Wanhg, J.Kim, Y. Chen, S. R. Yun and S. K. Lee, "Electro-Active-Paper Actuator Made with LiCl/Cellulose Films: Effect of LiCl content," *Macromolecular Research*, Vol, 14, 2006, pp. 624-629.

[24] H. Qi, Q. Yang, L. Zhang, T. Liebert and T. Heinze," The Dissolution of Cellulose in NaOH-based Aqueous System by two-step Process," *Cellulose*, Vol, 18, 2011, 237-245.

[25] K. Mequanint, A. Patel and D. Bezuidenhout, "Synthesis, Swelling Behaviour, and Biocompatibility of Novel Physically Cross-Linked Polyurethane-block-Poly(glycerol methacrylate) Hydrogels," *Biomacromolecules,* Vol, 7, 2006, pp. 883-891.

[26] T. R. Dawsey and C. L. McCormick, "The Lithium Chloride/Dimethylacetamide Solvent for Cellulose: a Literature Review," *Journal of Macromolecular Science, Part C: Polymers Reviews,* Vol, 30, 1990, pp. 405-440.

[27] Salem, A. K.; Tendler, S. J.; Roberts, C. J. Interactions of 3T3 fibroblasts and endothelial cells with defined pore features. *Journal of Biomedical Materials Research,* Vol, 61, 2002, pp. 212-218.

[28] Y. Tamada, Q, Ikada, Effect of preadsorbed proteins on cell adhesion to polymer surfaces. *J. Colloid Interface Sci,* Vol, 155, 1993, pp. 334-339.

Chapter 5

Wooden pulp cellulose hydrogels having cyto and biocompatible properties

Abstract: Pulp fibers were used as source to develop cellulose hydrogel films. Using dimethylacetamide/lithium chloride (DMAc/LiCl) system was possible to obtain flexible and transparent hydrogel films without chemical crosslinking. LiCl content was varied from 4 to 12 wt%. It was found that tensile strength of the resultant hydrogels was changed from 48 to 67 N/mm^2 and the elongation changed from 16.4 to 41.5%, with the increment of LiCl content from 4 to 12 wt%, respectively. In addition, when the NIH 3T3 fibroblast cells were used for cell adhesion assays, the growing cells showed better density and aspect ratio on the hydrogel films. The cell grown area on the hydrogel surface was significantly higher than the observed on the commercial PS dish used as control. These presented that the cellulose hydrogel films prepared from wooden pulp exhibited good cytocompatibility for application of tissue engineering.

5.1 Introduction

Hydrogels have been the primarily choice for a large number of researchers for many applications in regenerative medicine due to their unique biocompatibility [1-5]. Such attractive work show that hydrogels can serve as scaffolds and provide structural integrity to tissue constructs. The functional obligation of the tissue scaffold is to maintain cellular proliferation.

Therefore, finding a critical design for hydrogel in regenerative medicine is considered still in the transition on the healing process [6-10]. In addition, functionality in the scaffold and the emergent tissue during scaffold biodegradation is still remaining as a future development in research. So far, both natural and synthesized polymers have been used as supporting matrix for tissue repair and regeneration. Synthetic polymers as polyurethane, Poly (ethylene glycol), Poly (lactic), and poly(lactic-co-glycolic acid) have been intensively explored [6-9] for such candidate in biocompatible hydrogels. Previous experimental results using hydrogels prepared with synthetic polymers displayed their poor capacities to maintain cellular proliferation. As a consequence, there is a growing interest among researches to focus in natural polymers for their non-toxic and biocompatibity properties. Polymers of natural origin area have attractive options, mainly due to their similarities with extracellular matrix (ECM) as well as chemical versatility and biological performance. It is well known that the widely considered natural polymers include collagen, chitosan, chitin, starch, and cellulose and their excellent biocompatibility and safety is a result of their biological characteristics [10-13]. For example, such biodegradability and weak antigenicity have made collagen and chitosan a primary source of interest in medical applications for drug delivery, burns/wounds, and tissue engineering including skin replacement, bone substitute, and artificial blood vessels [9-14]. However, it might sound that polymers of natural origin were found to have some disadvantages as high cost, hydrophilicity affecting drug delivery, enzymatic degradation, mechanically brittle and weak properties in the bulk films [14-16]. Despite this, cellulose is regarded as the most common biopolymer in nature and one of the useful and sustainable biopolymer [17-22]. The excellent biocompatibility and safety of cellulose make this biopolymer an important source in modern medical applications. In general, biodegradable biomaterials are desirable in tissue engineering to be replaced by newly formed

tissue upon regeneration. There are however applications in tissue engineering where non-degradable materials are desirable as, replacement for cartilage, ophthalmic applications, and wound dressing to name a few. In the case of wound dressing, when the wound closes or fully heals, then the material falls off. Hydrogels provide a moist wound covering conductive to healing, and also protect the wound from infection. A disadvantage of many hydrogel networks, however, is their lack of strong mechanical properties [22-23]. The excellent biocompatibility and safety of cellulose make the biopolymer an important source in modern medical applications as the case of wound dressing, in which a material to maintain a moist environment at the wound interface, acting as a barrier to microorganisms and remove excess exudates and promote wound healing is needed [22-24]. Several approaches have been done to elaborate cellulose hydrogels and physical cross-linking and chemical cross-linking have been used to fabricate cellulose-based hydrogels. In the case of physical cross-linked gels, there is no covalent bonding formation or breakage and the cross-linked network is formed through ionic bonding, hydrogen bonding, or associated polymer-polymer interaction. In general, chemical cross-linked hydrogels are prepared through cross-linking two or more kinds of polymer chains with a functionalized cross-linker or under UV light [23]. Nevertheless, there are very few academic works on this topic relating with cyto and biocompatibility. Since even fewer are known to deal with effective applications of cellulose for hydrogel materials [25-26], most of the academic works have been reported preparation of biomaterials using cellulose derivatives or cellulose powder but none using cellulose fibers from waste product for biomedical applications. We report firstly here cellulose hydrogel films showing very good mechanical properties and bio and cytocompatibilities. In the present study, pulp fibers were used to elaborate hydrogels films, even though several approaches have been made previously in order to elaborate films using cellulose

fibers. Until the present day, no research has been conducted to study such cellulose hydrogels. Therefore, this work focuses in the preparation method and properties of mechanical and cyto and biocompatibility characteristics on the cellulose hydrogel films. When the hydrogel films were prepared by phase inversion, it was found that these properties depended upon LiCl content in the DMAc solution. Thus, evidence on broad *in vitro* cyto and biocompatibility presented that the hydrogels are very useful for medical applications, especially in tissue engineering.

5.2 Experiments

5.2.1 Materials.

Pulp cellulose fibers were provided from Hokuetsu Kishu Paper Mill CO. Solvent, DMAc, and other chemicals were obtained as mentioned before. For protein adsorption studies, bicinchoninic acid (BCA) kit was purched from Sigma Aldrich (Tokyo, Japan). Fetal bovine serum (FBS, Cell Culture Bioscience), bovine serum albumin (BSA, Sigma Aldrich), phosphate-buffered saline (PBS, Dullbecco Co., Ltd) were used. Trypsin-0.053 M-ethylenediaminetetraacetate (trypsin-EDTA) was purchased from Gibco (Tokyo, Japan) and formaldehyde (37 vol% aqueous solution) was from Wako Co., Ltd. NIH 3T3 mouse embryonic fibroblast cells were also purchased from BioResource Center (Japan).

5.2.2 Preparation of hydrogel films.

The pulp cellulose solutions in DMAc-LiCl system were prepared by following with modification of report [27-29] at different LiCl concentration from 4 to 12 wt%. The pulp cellulose fibers were firstly treated with water, ethanol, and finally DMAc by stepwise solvent exchange processes. The pulp cellulose fibers (1 wt%) were suspended in 300 mL of distilled water and left overnight to allow swelling of the fibers. Then, water was removed by an adapter glass filter under vacuum. On following process, ethanol (300 mL) was added to the swelled fibers and the mixture was stirred for 24 h with 2 rpm. After ethanol was removed by filtration, the pulp fibers were added in 300 mL of DMAc solution, which also was included a LiCl content ranging from 4 to 12 wt% of concentration. Finally, the solution was left overnight under stirring condition. As a result, transparent pulp solutions were successfully obtained. The preparation of the cellulose hydrogel films by phase inversion of the transparent solution to gelatinous solid was carried out as followed. A weighed amount of the cellulose solution was poured into a glass tray (10 cm diameter) and kept for 12 h in a container filled with 30 mL of ethanol as coagulant. The resulting films were wasted by ethanol 3 times and then, the cellulose films were submerged in 100 ml of distilled water and placed in shaking bath at 25°C to remove remain DMAc, distilled water was changed each 2 h. Pulp hydrogel films were kept in shaking bath for 12 h. Finally, the hydrogel films were immersed in distilled water over night and kept in phosphate buffered saline (PBS) at 4°C in a plastic container. This procedure was repeated 3 times.

5.2.3 Evaluation of hydrogel films.

Before the phase inversion process, shear viscosity of the cellulose DMAc solutions containing different LiCl concentration was measured by a B type viscometer at 25°C. Water

contents of the resultant hydrogel films were determined by weighing the wet and dry samples by following procedure. Samples of 5 mm diameter disks were cut from cast films, dried in a vacuum oven, and weighed. The samples were then swollen in phosphate buffered saline (PBS) for 36 h and blotted lightly with filter paper to remove excess water. The weight of the hydrated samples was then determined. The percent EWC of hydrogels was calculated based on EWC= $W_h - W_d / W_h \times 100$. Where W_h is the weight of the hydrated samples and W_d is the dry weight of the sample. For each specimen, four independent measurements were determined and averaged [30].

Tensile strength and elongation of the hydrogel films were measured on a LTS -500N - S20 (Minebea, Japan) with universal testing machine equipped with a 2.5 kN cell. Strips with a length of 50 mm and a width of 10 mm were cut from cast film with a razor blade. Strain was recorded by means of Zwick Makrosense clip-on displacement sensors. One set of samples (five strips each) was measured and each set was repeated 3 times. Only samples which ruptured near mid-specimen length were considered for the calculation of tensile strength. The values of the tensile strength and elongation were calculated.

Viscoelasticity of the hydrogel films with 2 cm in diameter and having 5 mm of thickness was determined by Auto Paar- Reoplus equipment (Anton Paar Japan, Tokyo) in wet conditions at 37°C.

For measurements of atomic force microscopy (AFM), samples were dried under vacuum overnight and images were recorded using Nanopics 1000, NPX 100 (Seiko Instruments Inc. Tokyo Japan). FT-IR spectroscopy was applied to examine component in wet hydrogel samples by using a FT-IR 4100 series (Jasco Corp), Japan. The thin hydrogel film was set up in a CaF_2 window (30 mm diameter; thickness 2 mm, Pier Optics Co. Ltd). Then, 2 μL of distillated water

was dropped to the film. Then, another window was pressed to cover the wet film. For measurement of scanning electronic microscope (SEM), after the hydrogel film sample was dried, samples were coated with a gold layer. The SEM images were recorded using JSM-5310LVB (JEOL, Japan) with a magnification of 5000 in magnitude.

5.2.4 In vitro biocompatibility experiments

Protein adsorption. Quantitative single protein adsorption experiments in PBS were determined by bicinchoninic acid assay[30]. Bovine serum albumin (BSA) and fetal bovine serum (FBS) were used. Protein concentration of serum proteins was 1 mg/mL. Hydrogel disks, 5 mm in diameter, were equilibrated in PBS for a period of 24 h and then immerged in 1 mL of PBS containing known serum proteins for 4 h at 37°C. Following the adsorption experiments, the hydrogel disks were rinsed 3 times then transferred into a plastic tube containing 5 mL of 2-wt% aqueous solution of sodium dodecyl sulfate (SDS) and shaken for 4 h at room temperature to elute the proteins adsorbed to the hydrogels. During screening experiments, we determine that an elution time of 4 h removed all adsorbed proteins. The amount of adsorbed proteins was calculated from the concentration of proteins in the SDS solution read at 562 nm and calibration curve prepared from pure sample was used. Four repeats (3 disks per repeat) were measured and the average value was taken.

Clotting experiments. Clotting experiments were performed in a microplate reader instrument Multiskan Go (Thermo Scientific) [31]. The instrument could maintain a chosen temperature during the experiment period. Samples were shaken only once, for 20 s (low speed just before the first reading). Hydrogel disks 5 mm in diameter were cut from cast films. Temperature 37°C was set and readings were repeated every 30 s. Readings were performed with a 545 nm filter

and were recorded in a computer memory for further evaluation. 100 μL of platelet poor plasma (PPP) was mixed with 100 μL of PBS and 100 μL of water in a 96 well flat-bottom microplate. The sample surfaces in a microplate have to be free from air-bubbles in order to get well reproducible curves. Controls for 100% PPP and PBS were observed during the whole period of measurements. Immediately before the reading, calcium chloride (50 μL) was added. The clotting agents were injected to the exanimated samples with a multichannel pipette. The collected data were finally evaluated using a computer program.

Platelet adhesion. Platelet adhesion experiments were conducted using hydrogel disks of 5 mm diameter were equilibrated with PBS overnight. A total of 0.6 mL of PRP was transferred to 24-well culture plates, and the PBS equilibrated hydrogels were placed into the PRP containing wells. Incubation was carried out at 37°C for 2 h after which the hydrogel disks were removed and rinsed with 1 mL of PBS to remove loosely attached platelets. Platelet counting was estimated by photometric method using plastic cuvettes, with 10 mm optical path. The measurements were performed at λ=800 nm. The formula for platelet count calculation is as follows:

$$N\ (10^8/mL) = (6.23/2.016\text{-}k*\lambda*E/800 - 3.09) * R$$

Where N is the estimated platelet count per milliliter, R is the examined sample dilution, λ is the used wavelength, E is the measured extinction of the sample and k is a geometrical factor equal 1 for 10 mm optical path. The equation was tested and is correct for measurements performed for λ ranged from 600 to 800 nm. PRP was diluted ten times for each measurement and the instrument was set for zero with the reference sample-plasma or buffer, both free from

platelets. On following this, the hydrogel films were rinsed for three times with PBS (37ºC) and the adhered platelet were fixed with 1 ml of 2.5 wt% glutaraldehide/PBS at 4ºC for 2 h. Finally, the hydrogel films were immersed into the PBS for 5 min and dehydrated twice as followed. The first dehydration was carried out with a series of ethanol/PBS mixtures with increasing ethanol concentrations (25, 50, 75, and 100 wt%) for 15 min in each mixture. The second dehydration was performed with of iso-amyl actetate/PBS mixtures with increasing iso-amyl acetate concentrations (25, 50, and 100 wt%) for 15 min. After freeze-drying the treated samples, the platelet-attached films were coated with a gold layer for the SEM measurements.

5.2.5 Cytotoxicity of hydrogel films.

Hydrogel films circles with 30 mm diameter were used for cell seeding purposes. The samples were sterilized with 70 and 50 wt% of aqueous ethanol in twice for 30 min and then, rinsed twice with the PBS for 30 min. Finally these were swelled in DMEM for 2 h before starting the seeding procedure. The NIH 3T3 mouse embryonic fibroblast cells were cultured at 37°C in 95 wt% of relative humidity and 5 wt% of CO_2 environment.

The culture medium was in 90 wt% of DMEM supplemented with 10 wt% FBS and 1 wt% penicillin/streptomycin. The cells were seeded on the hydrogel films and the tissue culture polystyrene dish (PS) with 35 x 10 mm size for the cell density of $8x10^3$ cm^{-2}.

The cells were used for imaging and characterization purposes after 14 days of culture. The sample image was obtained using an inverse microscope (Olympus CKX41, Japan) and was then analyzed for cell elongation and directionality using cellsens software digital imaging software.

To measure cell area, the cell boundaries were marked by the PC operation. Also aspect ratio, long axis and cell density were measured from for the image data. Approximately, 50 cells were analyzed per image. For each sample, five images were analyzed to obtain an unbiased estimation of the cell morphology. The results presented herein were based on three independent experimental runs.

5.3 Results and Discussion

5.3.1 Preparation of hydrogel films.

Figure 5.1 shows pictures of (a) pulp cellulose fibers, (b) transparent dry hydrogel, and (c) the wet film. In order to prepare hydrogel films of the pulp fibers (b), the fibers (a) were dissolved in DMAc solution having 4-12 wt% of LiCl after solvent exchange between water, ethanol, and DMAc. Shear viscosity of the obtained transparent DMAc solution of pulp cellulose was measured, when the LiCl content was changed.

Table 5.1 shows shear viscosity of the DMAc solutions containing different contents of LiCl, as measured at 6 and 60 rpm. It was noticed that when the amount of LiCl increased in the solution, both values of shear viscosity measured at 6 and 60 rpm increased. The obtained results at 6 and 60 rpm did not show significant difference, meaning that the pulp cellulose in the DMAc solution had less hydrogen bonding between the cellulose chains.

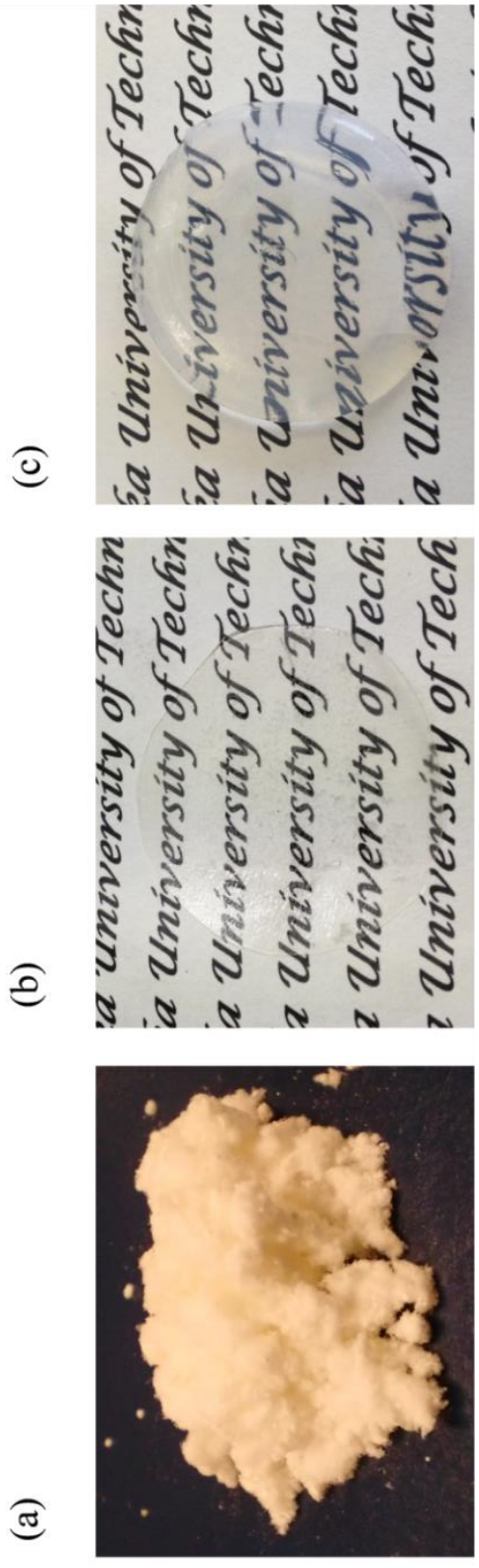

Figure 5.1. Cellulose fibers and films. (a) Pulp fibers, (b) pulp hydrogel film in dry condition, (c) pulp hydrogel film in wet conditions. The samples in (b) and (c) were prepared from DMAc solution containing 4 wt% of LiCl.

As the viscosity was increased at higher LiCl concentrations, similar phenomena were also presented in references [32-33], indicating that the LiCl added formed a macrocation with cellulose fibers in the DMAc solution. Therefore, in the present work, when the LiCl content increase in the DMAc solution, the interaction cellulose fiber-solvent and interactions fiber-fiber increased due to the increasing of the macrocation form by the DMAc/LiCl system reaching to a point in which aggregates form. Base on this, it was reasonable to consider that the increased viscosity was caused by the macrocation effect with the LiCl.

Table 5.1. Properties of pulp cellulose hydrogel films in wet conditions

Samples	Water Content (%)	Elongation (mm)	Tensile strength (N/mm²)	Shear viscosity (Cp) 6 rpm	60 rpm
Pulp-LiCl-4%	336	8.21	0.51	203	200
Pulp-LiCl-6%	302	13.77	0.48	411	407
Pulp-LiCl-8%	268	15.26	0.62	621	617
Pulp-LiCl-10%	254	19.84	0.66	985	979
Pulp-LiCl-12%	240	20.65	0.67	1426	1422

In order to analyze de surface of the cellulose films aggregated in the hydrogel films AFM measurements for dried samples were carried out. Figure 5.2 shows the AFM images (20 mm x 20 mm) including cross-section for the films of (a) 4 wt%, (b) 8 wt%, and (c) 10 wt% of LiCl contents. It was observed that the presence of the macrocation in the cellulose networks affects the surface roughness in the hydrogel samples increasing from 5.9 to 8.3 nm for the samples with 4 wt% and 8 wt% of LiCl, respectively. In addition, in the case of 12 wt% LiCl the roughness of the film significantly decreased to be 4.1 nm as shown in the film cross-section (c). This could be attributed to the formation of cellulose aggregate in the films due to the macrocation affecting

the shape of the valleys of the AFM views comparing samples with lower and higher LiCl content. It is known that at 6 wt% of LiCl on DMAc/LiCl system promote an arrangement of cellulose fibers increasing the interaction between the fibers, on the other hand at higher LiCl content fiber arrangement is affected due to the increased of cellulose aggregates forming domains and changing valleys shape and lowing roughness of the surface.

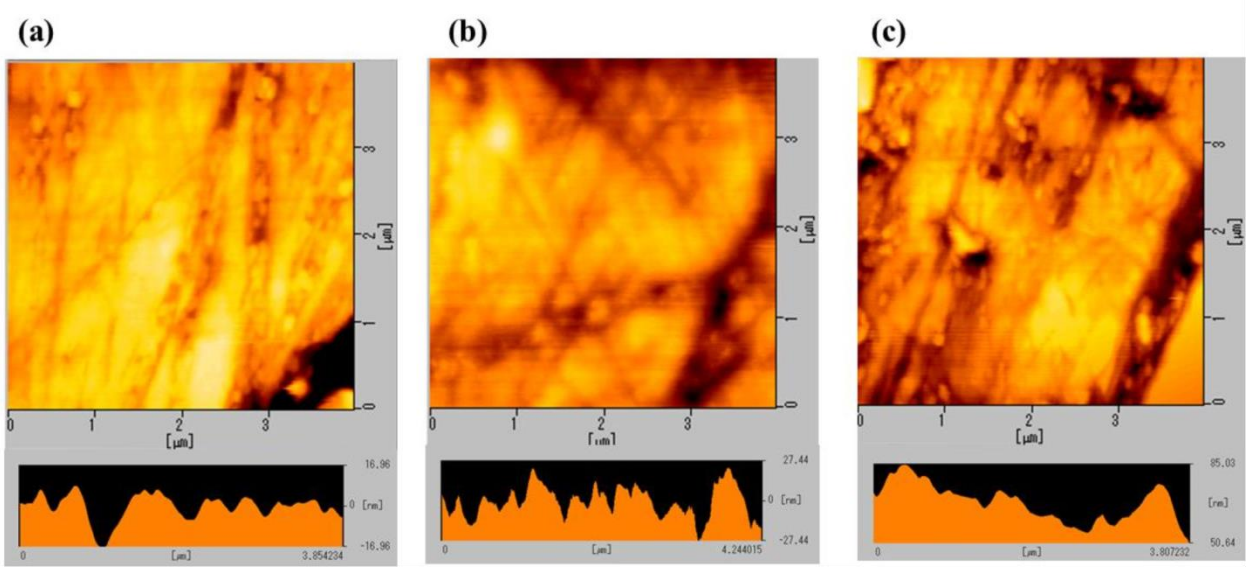

Figure 5.2. AFM images of the hydrogel film surface. The LiCl concentration was changed in (a) 4 wt%, (b) 8 wt%, and (c) 12 wt% for DMAc solution.

Table 5.1 also lists hydrogel film properties, as equilibrium water content at room temperature for 72 h. The values of water content decreased from 32.6% to 19.98% with the increment of the LiCl content from 4 to 12 wt%, respectively, in the DMAc solution. The LiCl dependence on the water content of the films might be due to the increment of the amount of the formed macrocation. Therefore, in the microenvironment of the celluloses, it was reasonable for consideration that the diminished water contents of the hydrogel films were due to the effect of LiCl on the cellulose networks. Thus, when the LiCl content was lower, water molecules were

capable of penetrating and interacted easily into the hydrogel films because of lower density on the cellulose networks. Therefore, water contents in the film became higher when the LiCl was lower. It was noted that the hydrogel films had very soft and flexible shape even though there was no chemical crosslinking treatment. For uniaxial tensile testing, the sample hydrogels (50 mm x 10 mm) were placed between two clamps and the hydrogel film was then pulled away. Table 1 shows that higher elongations were observed in the films in comparation with 12 wt% of LiCl content relative to that of 4 wt%. As shown in Table 5.1, the tensile strength and elongation values incresead from 51 N/mm² to 67 N/mm² in the cases of 4wt% and 12wt% of the LiCl, respectively. This might be attribuited to the increase of LiCl in the DMAc solution, which could enhance the interaction between pulp fibers. As reported in research [29], the cellulose could form intermolecular aggregation by interaction through hydrogen bonds in DMAc/LiCl solution and affect the stiffness of the resultant sample films. The effect thus could improve the resistance to the applied force in the higher LiCl case increasing the elongation value of the hydrogel films [29,32].

In the case of viscoelasticity measurements, it was known that the viscoelastic response to the deformation occurred only under momentary deformation. Therefore the present work performed viscoelastic measurement in the hydrogel film. Figure 5.3 shows G’ and G’’ plots on each strain (%) for the hydrogel films. It was observed that the deformation of hydrogel film prepared with 12 wt% of LiCl was lower than the observed on those prepared with 4 wt% of LiCl. This might be due to increment of the interactions cellulose-macrocation and fiber-fiber in the DMAc/LiCl system. The data showed that the tendency is more significant at higher LiCl content in the DMAc solution. However, it seems that the hydrogel films prepared with lower LiCl content showed soft nature in the deformation during the strain sweep measurements. Under prolonged

deformation condition, the hydrogel film could recover into their original shapes. Actually, the hydrogels prepared from lower LiCl concentration proved soft nature.

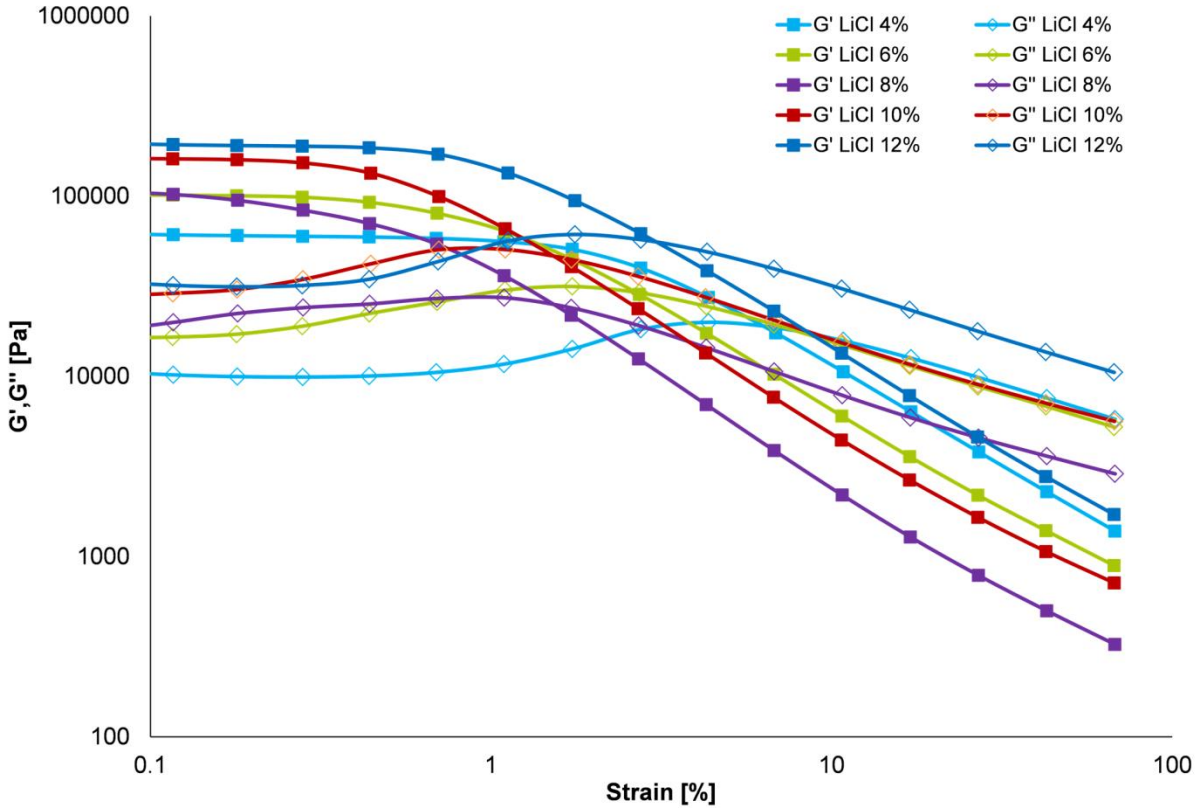

Figure 5.3. Viscoelasticity of cellulose hydrogels films of different LiCl contents for strain - G', G'' plots at 37°C.

In order to evaluate the wet condition of the hydrogel films, FT-IR measurements were carried out. The hydrogel films were dried under vacuum for 24 h at room temperature and then small amount of water droplet was added to be swelled on the CaF_2 window. Figures 5.4 show FT-IR spectra of their samples prepared from 4 to 12 wt% of LiCl concentration for (a) wet and (b) dry film condition. The FT-IR spectra of the films had strong peaks around 3550 and 3200

cm^{-1} attribuited to)-H band stretching. In addition, the peaks around 1150, 1160, 1120, 1059, and 1035 cm^{-1} refered to C-OH, C-O-C, and C-C ring bands, CH_2 and OH groups, respectively [34]. It was notice that the intensity of O-H band stretching increased in pulp hydrogel films in wet conditions. This phenomena meant that water bound to the OH group of the pulp fibers in the network. In the water band around 1400 cm^{-1}, in wet condition, the center peak sightly shift, this suggested that water molecules interacted with the pulp cellulose fibers.

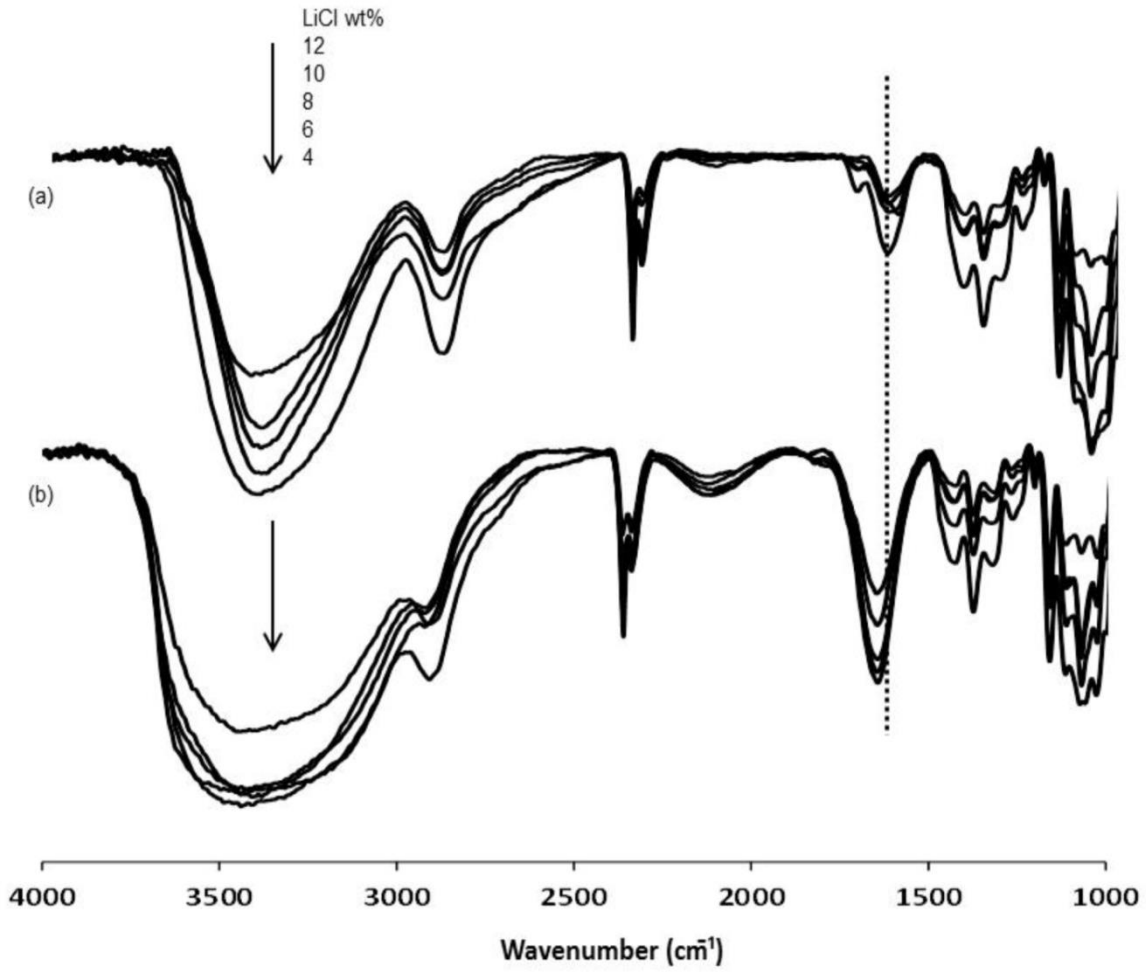

Figure 5.4. FT-IR spectra of pulp cellulose hydrogel films in dry (a), wet (b) conditions. These spectra were for the films prepared from different LiCl condition.

5.3.2 Evaluation of biocompatibility of hydrogel films.

Figure 4.1 shows pictures of (a) pulp cellulose fibers, (b) transparent dry hydrogel, and (c) the wet film. It is known that such hydrophilic hydrogel shows to have better tendency for biocompatibility including protein interaction with the scaffold. Such protein adsorption is the first stage of the interactions between substrate and the body. Therefore, it is interesting in the present work to study protein adsorption on the hydrogel films for BSA and FBS serum proteins. Figure 5 shows adsorption of BSA and FBS examined *in vitro* for each hydrogel film. As prepared by different LiCl content in the DMAc solution, the amounts of BSA on the hydrogels films increased with the increase of the LiCl contents. However, the results observed in the FBS expressed opposite tendency related to those of the BSA. It was known that BSA tended to bind onto hydrophobic surface, meanwhile FBS preferred to hydrophilic surface [35,36]. In the present work, the BSA adsorption tended to suppress cell adhesion, as the LiCl concentration was higher. The obtained results showed that FBS adsorption became higher in all cases. In these cases, it could be considered that the predominant adsorption of BSA and FBS might be due to hydrogel nature depending upon the LiCl contents. Base on the obtained results with FBS, it would be expected that the hydrogel films prepared with lower LiCl concentration might promoted such cellular adhesion.

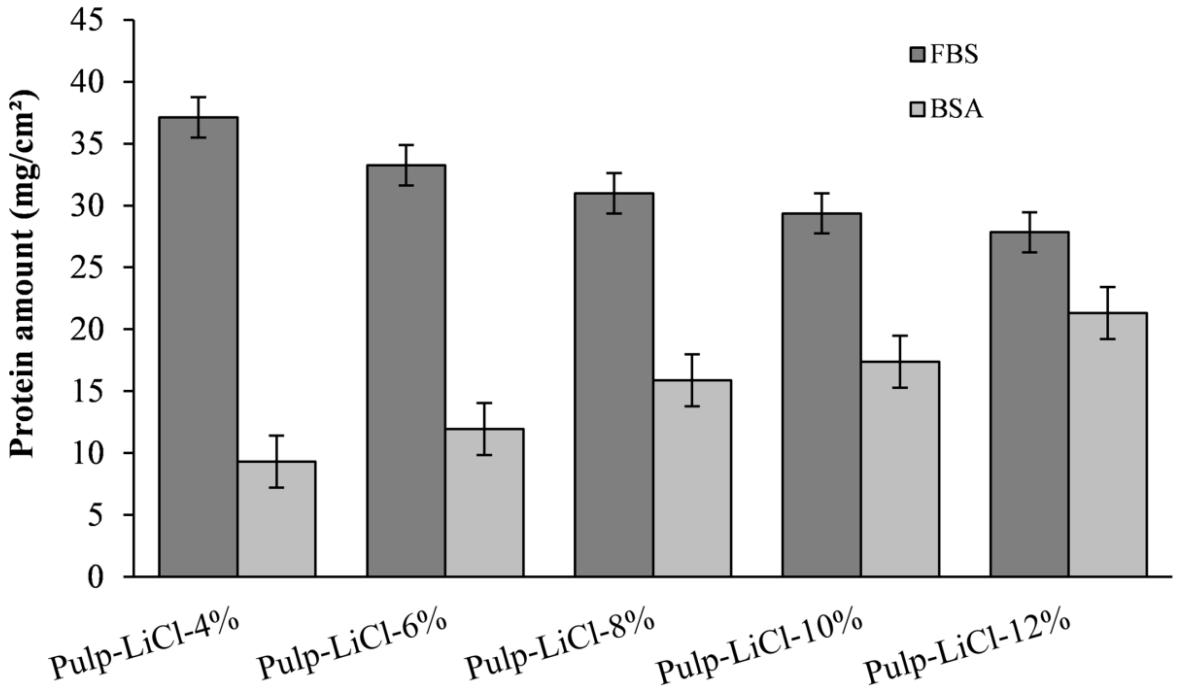

Figure 5.5. Protein adhesion of hydrogel films prepared from DMAc solution containing different LiCl concentration.

Furthermore, blood compatibility of the hydrogel films was studied as shown in Figure 5.6 (a). Herein, after the hydrogel samples were in contact with platelet poor plasma (PPP), the time of cloth formation was measured. The results demostrated that the time of the cloth formation was affected by the LiCl contents in the DMAc solution. As seen, the value of the time of cloth formation increased with the decrease of the LiCl content used.

This phenomenon could be supported with the obtained results of the FBS adsorption as shown in Figure 5.5. In protein adsorption capacity of the hydrogel films, it was easy to consider that the fibrinogen adsortion might be enhancing to form a fibrin rich cloth. Moreover, the incubated hydrogel disks in PRP were analyzed by SEM. Platelet adhesion results for these pulp hydrogels are shown in Figure 5.6 (b) and the typical SEM photographs are shown in Figure 5.6 (c-e). Platelet deposition behaviour showed that pulp hydrogels had good blood-contact properties. The number of adhered platelet showed a tendency to decreased with increasing of LiCl content. These results seem to be related to the properties of hydrogel surface investigated by AFM. As shown in Figure 5.6 (c-e), the SEM images revealed that results in platelet adhesion was lightly supressed at lower LiCl content in the DMAc solution. In addition, higher number of platelet was observed on the surface of samples prepared with 12 wt% of LiCl. Similar results were also reported (Salem, et al., 2002) for the adhesion of platelets. They indicated that the hydrogel films could provide a suitable environment to promote and enhance the platelet adhesion regardless to the LiCl used.

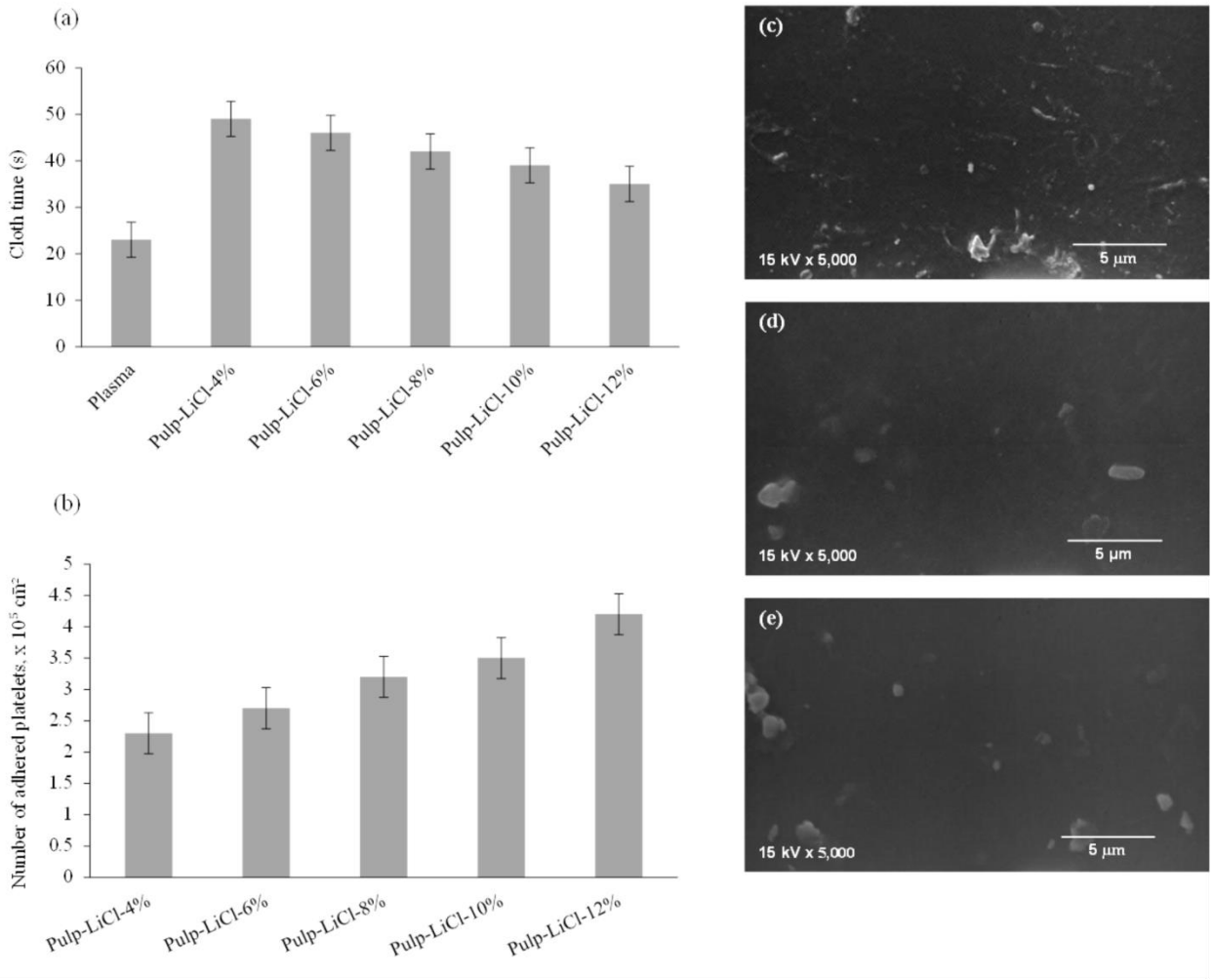

Figure 5.6. (a) Cloth time of cellulose hydrogel films prepared from DMAc solution containing different LiCl concentration, (b) Protein adhesion of hydrogel films prepared from DMAc solution containing different LiCl concentration. SEM images of the hydrogel film surface treated with platelet adhesion. The LiCl concentration was changed in (c) 4wt%, (d) 10 wt%, and (e) 12wt% for the DMAc solution.

5.3.3 Cell density on hydrogel films

If the present hydrogel would be applied for healing repair as scaffold, another important issue to consider is fibroblast growing on the hydrogel surface. In order to observe such behaviour for the hydrogel films, phase-contrast light microscope images were used. Cell morphology of adherent fibroblast on pulp hydrogels was analyzed to determine the effect of LiCl content on cell adhesion and morphology. NIH 3T3 cells adhered and proliferated well on all surfaces. The cell density on the hydrogel films were evaluated by counting adhered fibroblast on the hydrogel surface. Figure 5.7 shows cell density of NIH 3T3 for pulp cellulose hydrogels. In all cases, the obtained results showed that cell densities in the hydrogel films were higher than the observed on PS dish used as control surface. With the increment of culture time cell density gradually increase. After 72 h passed, the amounts of the cell density in the 4 wt% LiCl were actually higher. In addition, fibroblast was found to have a maximum adhesion on the surface of hydrophilic and soft films [35]. According with the results obtained by Grinnell et al [14], fibroblast preferred soft surface for proliferation. In the present work, the difference in the cell density between the hydrogels prepared with 4 wt% and 12 wt% of LiCl seemed to be related to the samples softness. Thus, as appeared in the viscoelastic data (Figure 5.3), the soft hydrogel film prepared from lower LiCl showed higher cell density. In the case of lower content of LiCl, the softness and stiffness of the films might regulate the adhesion between cellular-extracellular matrix molecules. Additionally, cell culture time was extended to 7 and 14 days and after this time no cytotoxic or decreased in cell density was found.

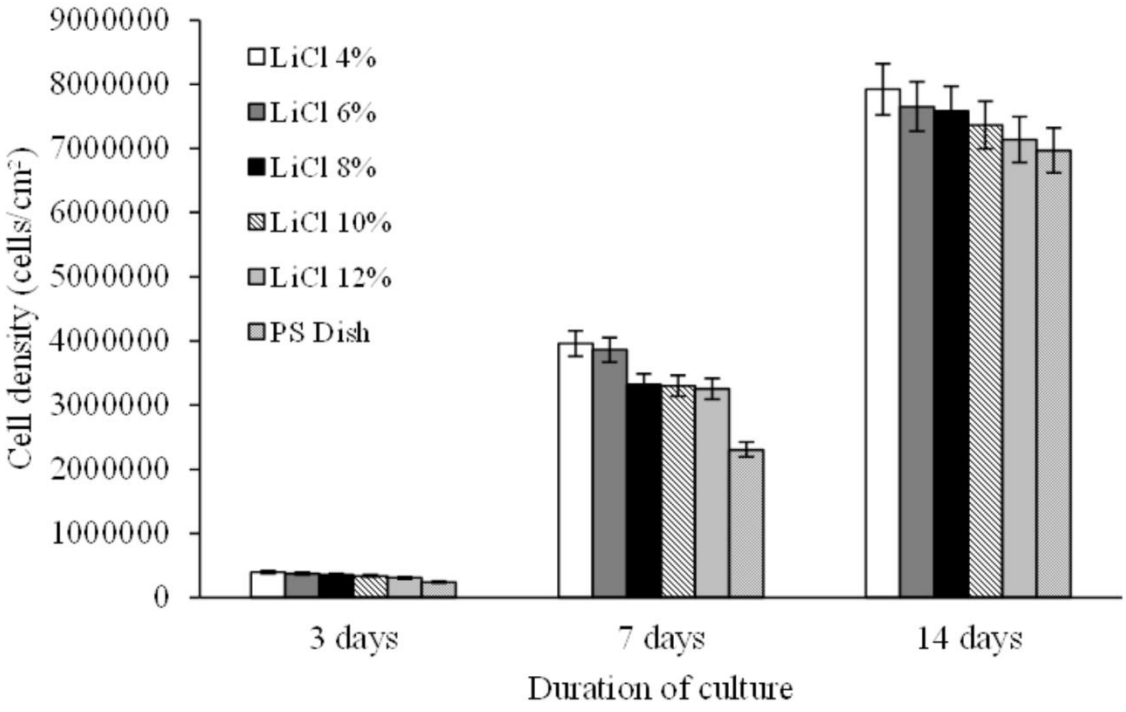

Figure 5.7. Cell density of pulp cellulose hydrogel films films prepared from DMAc solution containing different LiCl concentration. The error bars indicate the standard error ±. Significant difference ($P<0.05$).

3.3.4 Cell morphology on hydrogel films

In addition, cell morphology results showed that cell area, aspect ratio, and the length of the long axis were sensitive to LiCl content, as shown in Figure 5.8. In particular, all three parameters showed higher results in smooth surfaces. Projected cell area (j), aspect ratio (k), and length of the long axis (l) decreased systematically with the increment of LiCl content. Diminished projected cell area is consistent with [36] reported smaller projected areas for MC3T3-E1 pre-osteoblasts on less smooth surfaces. Two plausible explanations for diminished cell spreading on samples with higher LiCl content are related to the role of focal adhesion complexes in mediating cell adhesion to biomaterials. Focal adhesion contains clusters of integrin transmembrane adhesion receptors that bind the EMC proteins (e.g., fibronectin,

collagen) adsorbed to biomaterial surface. Consequently, it is plausible that the change of the roughness on the film surface undermine cell spreading and morphology by limiting the number of integrin receptors engaged in cell adhesion.

As shown in Figure 5.8, results of cell morphology on the hydrogels films revealed a remarkable difference on fibroblast pattern in the morphology for the hydrogel films and commercial PS dish (a-c). For example, in the hydrogel film for the 4 wt% LiCl (d-f), the fibroblast surely adhered and grew on the hydrogel film, as observed in the images. After 4 hours of cell culture, the image (b) showed longer axis shape of the grown cells as compared with those adhered on the PS Dish at the same condition. Moreover, the boundaries of the adhered cells on cellulose films seemed to be tightly adhered on the hydrogel surface, showing a diffuse shape on the cultivated cell edge. In addition, anisotropic shape was observed in the first hours of the cell culture, when the hydrogel films were used in the scaffold on the cell growing. Relative to the hydrogel film, the fibroblast shape observed on PS dish (a) was mainly round at 4 hours, as seen in (g). This indicated that the cell seems not to be tightly adhered to the surface of the commercial dish. Comparing with fibroblast shape shown in (b) and (g) for the hydrogels films, these demonstrated a much cytocompatibility to the hydrophilic and soft surface of the hydrogel films. When the LiCl was increased in the DMAc solution to be 12 wt%, the resultant hydrogels films showed lower aspect ratio, long axis and cell density. This might be due to the decreased swelling and softness of the sample film by the formation of macrocation in the film. These results revealed that the hydrogel films made of pulp cellulose provided a better surface for fibroblast growing.

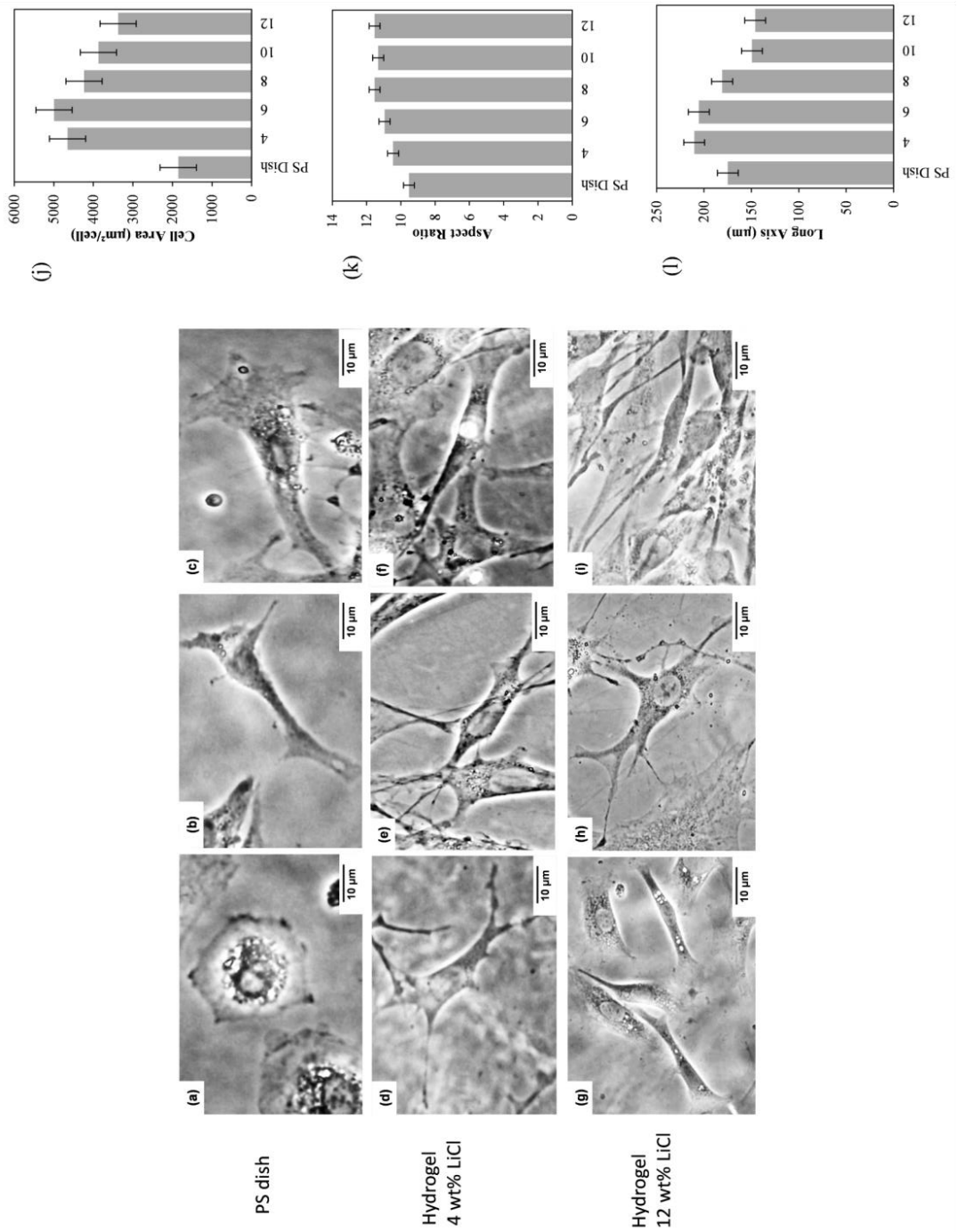

Figure 5.8. Phase-contrast light images of hydrogel films (a-f) and commercial PS Dish as control (g-i). Hydrogel films prepared from 4 wt% LiCl (a-c) and 12 wt% LiCl ((d-f). The cell culture time was 4 hours (a,d,g), 24 hours

5.4. Conclusion

Hydrogel films prepared from pulp fibers were obtained by phase inversion of the DMAc solution with LiCl. The cellulose hydrogel film had better mechanical properties, although there was no chemical crosslinking. Depending on the LiCl concentration, these hydrogel films exhibited lower protein adhesion and higher coagulation time for the biocompatibility. In addition, very good cytocompatibility was resulted in the hydrogel films prepared at 4 wt% of LiCl. It was proved that the LiCl acted to be dense networks of the cellulose segments and the hydrogel condition influenced in vitro cyto and biocompatibility. These results suggest that these hydrogel films prepared from wooden pulp may have the possibility of usage for biomaterial.

5.5 references

[1] Slaughter B.V., Khurshid, S.S., Fisher, O, Z., Khademhosseine, A., & Peppas, N.A. (2009). Hydrogels in regenerative medicine. *Advanced Materials, 21, 3307.*

[2] Langer, R. (1995). Biomaterials and biomedical engineering. *Chemical Engineering Science, 50, 4109.*

[3] Uchiyama, T., Watanabe, J., & Ishihara, K. J. (2002). Biocompatible polymer alloy membrane for implantable artificial pancreas. *Membrane Science, 208, 39.*

[4] Xu, F., Wang, Y., Jiang, X., Tan, H., Li, H., & Wang, K. J. (2012). Effects of different biomaterials: Comparing the bladder smooth muscle cells on waterborne polyurethane poly-lactic-co-glycolic acid membranes. *Kaohsiung Journal of Medical Sciences, 28, 10.*

[5] Nair, L. S., & Laurenoin, C. T. (2007). Biodegradable polymers as biomaterials. *Progress in Polymer Science, 32, 762.*

[6] Sionkowska, A. (2011). Current research on the blends of natural and synthetic polymers as new biomaterials: Review. *Progress in Polymer Science, 36, 1254.*

[7] Silva, M. R., & Castro, M. C. R. (2002). New dressings, including tissue engineered living skin. *Clinics in Dermatology, 20, 715.*

[8] Nho, Y. C., & Kwon, O. H. (2003). Blood compatibility of AAc, HEMA, and PEGMA-grafted cellulose films. *Radiation Physics and Chemistry, 66, 299.*

[9] Henich, N. A. & Kotopodis, K. P. (2002). Clinical characterization of a new polymeric membrane for use in renal replacement therapy. *Biomaterials, 23, 3853.*

[10] Barbosa, M. A., Granja, P. L., Barrias, C. C., & Amaral, I. F. (2005). Polysaccharides as scaffolds for bone regeneration. *ITBM-RBM, 26, 212.*

[11] Castillo-Briceno, P., Bihan, D., Nilges, M., Hamaia, S., Meseguer, J., Garcia-Ayala, A., Farndale, R. W., & Mulero, V. (2011). A role for specific collagen motifs during wound healing and inflammatory response of fibroblasts in the teleost fish gilthead seabream. *Molecular Immunology, 48, 826.*

[12] Jayakumar, R., Prabaharan, M., Sudheesh Kumar, P. T., Nair, S. V., & Tamara, H. (2011). Biomaterials base on chitin and chitosan in wound dressing applications. *Biotechnology Advances, 29, 322.*

[13] Liu, X., Ma, L., Mao, Z., & Gao, C. (2011). Chitosan-Based biomaterials for tissue repair and regeneration. *Advanced Polymer Science, 244, 81.*

[14] Grinnell, F., & Bennette, M. H. J. (1981). Fibroblast adhesion on collagen substrata in the presence and absence of plasma fibronectin. *Journal of Cell Science, 48, 19.*

[15] Lamprecht, F. F., Groth, T., Albrecht, T., Paul, D., & Gross, U. (2000). Development of membranes for the cultivation of kidney epithelial cells. *Biomaterial, 21, 183.*

[16] Hoenich, N. A. (2004). Update on the biocompatibility of hemodialysis membranes. Hong Kong Journal of Nephrology, *6*, 74.

[17] Muller, F. A., Muller, L., Hofmann, I., Greil, P., Wenzel, M, M., & Staudenmaier, R. (2006). Cellulose based scaffold materials for cartilage tissue engineering. *Biomaterials, 27, 3955.*

[18] Sannino, A., Demitri, C., & Madaghiele, M. (2009). Biodegradable cellulose based hydrogels: Design and applications. Materials, *2*, 353.

[19] Zhang, S., Li, F. X., & Yu, J. Y. (2009). Preparation of cellulose/chitin blend bio-fibers via direct dissolution. *Cellulose Chemistry and Technology, 43, 393.*

[20] Trovatti, E., Freire, C. S. R., Pinto, P. C., Almeida, I. F., Costa, P., Silvestre, A. J. D., Neto, C. P., & Rosado, C. (2012). Bacterial cellulose membranes applied in topical and transdermal delivery of lidocaine hydrochloride and ibuprofen: In vitro diffusion studies. *International Journal of Pharmaceutics, 1, 83.*

[21] Fricain, J. C., Granja, P. L., Barbosa, M. A., Jeso, B., Banthe, N., & Baquey, C. (2002). Cellulose phosphates as biomaterials. In vitro biocompatibility studies. *Biomaterials, 23, 971.*

[22] Chong, C. & Zhang, L. (2011). Cellulose-based hydrogels: Present status and application prospects. *Carbohydrate Polymers, 84, 40.*

[23] Seal, B. L., Otero, T.C., & Panitch, A. (2001). Polymeric biomaterials for tissue and organ regeneration. *Materials and Science Engineering R, 34, 147.*

[24] Hoenich, N. (2006). Cellulose for medical applications: Past, present, and future. *Bio resources, 2, 270.*

[25] Saito, H., Sakurai, A., Sakakibara, M., & Saga, H. (2003). Preparation and properties of transparent cellulose hydrogels. *Journal of Applied Polymer Science, 90, 3020.*

[26] Deoliveira, W., & Glasser, W. G. (1996). Hydrogels from polysaccharides. 1. Cellulose beads for chromatographic. *Journal of Applied Polymer Science, 60, 63.*

[27] Lindma, B., Karlstrom, G., & Stigsson, L. (2010). On the mechanism of dissolution of cellulose. *Journal of Molecular Liquids, 156, 76.*

[28] Pokhnel, D., & Viraraghava, T. (2004). Treatment of pulp paper mill wastewater a review. *Science of the Total Environment, 333, 37.*

[29] Striegel, A. M. (1997). Theory and applications of DMAc/LiCl in the analysis of polysaccharides. *Carbohydrate Polymers, 34, 267.*

[30] Mequanint, K., Patel, A., & Bezuidenhout, D. (2006). Synthesis, swelling behavior,and biocompatibility of novel physically cross-linked polyurethane-block-poly(glycerol methacrylate) hydrogels. *Biomacromolecules, 7, 883.*

[31] Walkowiak, B., Kesy, A., & Michalec, L. (1997). Microplate reader a convenient tool in studies of blood coagulation. *Thrombosis Research, 87, 95.*

[32] Sjoholm, E., Gustafsson, K., Eriksson, B., Brown, W., & Colmsjo, A. (2000). Aggregation of cellulose in lithium chloride/*N_N*-dimethylacetamide. Carbohydrate Polymers, *41*, 153.

[33] Ishii, D., Tatsumi, D., & Matsumoto, T. (2008). Effect of solvent exchange on the supramolecular structure, the molecular mobility and the dissolution behavior of cellulose in LiCl/DMAc. *Carbohydrate Research, 343, 919.*

[34] Kacurakova, M., Capek, P., Sasinkova, V., Wellner, N., & Ebringerova, A. (2000). FT-IR study of plant cell wall model compounds: pectic polysaccharides and hemicelluloses. *Carbohydrate Polymers, 43, 195.*

[35] Tamada, Y., & Ikada, Q. (1993). Effect of preadsorbed proteins on cell adhesion to polymer surfaces. *Journal of Colloid Interface Science, 155, 334.*

[36] Salem, A. K., Stevens, R., Pearson, R. G., Davies, M. C., Tendler, S. J. B., Roberts C. J., Williams, P. M., & Shakesheff, K. M. Interactions of 3T3 fibroblasts and endothelial cells with defined pore features. (2002). *Journal of Biomedical Materials Research, 61, 212.*

Chapter 6

Biohydrogels interpenetrated with hydroxyethyl cellulose and wooden pulp for biocompatible materials

Abstract: Biohydrogel interpenetrated films of wooden pulp cellulose and hydroxyethyl cellulose (HEC) was prepared and their biomedical properties were investigated. Our purpose was to obtain new material combining the nontoxicity and biocompatibility in wooden pulp cellulose films by interpenetration of HEC. It was found that the increment of HEC content affects the mechanical properties of the hydrogel from 10 to 50 wt% content of HEC. *In vitro* biocompatibility tests showed that protein adsorption, clotting time, and platelet adhesion were affected with the increment of HEC. All the obtained hydrogels showed better cytocompatibility than the reference on tissue culture grade polystyrene dish. However, HEC content seemed to decrease fibroblast cell densities due to its effect on the film properties, showing different pulp aggregation. In conclusion, the cell densities on hydrogel were significantly changed depending upon the HEC interpenetration.

6.1 Introduction

The principles and techniques of material science, cellular and molecular biology has been substantiated for cell proliferation with an ultimate aim of repair and regeneration of damaged tissues such as cartilage, tendons, blood vessels, skin, and many others. Hydrogels are polymeric networks constructs possessing an inherent water absorbing property. Their soft and rubbery

nature makes them suitable for drug delivery and tissue applications [1-5]. Various biochemical and physical properties of hydrogels such as the functional groups, chemical composition, hydrophilic-lipophilic balance, surface morphology, roughness and presence of adherent proteins are essential for regulation of cell interaction and extra cellular membrane (ECM) development. For inclusion of all these desired features in a single system, double component system interpenetrating polymeric network (IPN) based on biopolymers can serve as suitable matrix [6-10]. Interpenetrated hydrogels consist of double chemical networks, and they can be called a physical gel if a network alone does not form a gel but the HEC dissolution was not observed by the interpenetration which leads to a gel formation, like in the case of HEC [11-16]. Biopolymeric components provide substantial biological clues to the ECM proteins and also help in regulating degradation behavior of the system. Such strategy has proved great success by including all the desired features in a single system. As a consequence, there is a growing interest among researches to focus in natural polymers for their non-toxic and biocompatibility properties [15-20]. For example, Cellulose is regarded as the most common biopolymer in nature and as one of useful and sustainable biopolymer [21-26]. The excellent biocompatibility and safety of cellulose make the biopolymer an important source in modern medical applications [21-23]. However, because of difficulty in the hydrogel fabrication; cellulose has few reports in such application. Therefore, it is important to deal with effective applications of cellulose for hydrogel materials films. In the present paper, cellulose hydrogel film composed with pulp fibers and HEC were used to elaborate hydrogels films in order to study cell response to surface topography. In terms of tissue engineering, the ideal scaffolds provide a framework and initial support for the cells to attach, proliferate and differentiate, and form an extracellular matrix (ECM). It should be noted that scaffold surface topography and chemistry (wettability, softness and stiffness,

roughness) have been shown to significantly influence cell behaviors such adhesion, growth and differentiation, and to affect the bioactivity of scaffolds used for *in vivo* regeneration applications. In addition, changes in protein adsorption, topographical features, and stiffness across a substrate can all lead to guided migration of cells [27-30]. Studies have been carried out to determinate the effect of the scaffold topography on cell adhesion founding that NIH 3T3 cells accumulated preferentially on stiffer regions of substrates [27-34].

This work focuses on the preparation methods and properties of mechanical and cyto and biocompatibility characteristics on the hydrogel films containing different content of HEC. Thus, evidence of cyto and biocompatibility presented that the cellulose hydrogels could be a candidate for medical applications, especially for *in vitro* tissue engineering.

6.2 Experiments

6.2.1 Materials

Pulp cellulose fibers were provided from Hokuetsu Kishu Paper Mill CO. *N, N,* dimethylacetamide (DMAc) was purchased from TCI (Tokyo, Japan) and stored for more than 5 days with potassium hydroxide before use. Lithium chloride (LiCl) was dried at 80°C for 12 h in a vacuum oven. Hydroxyethyl cellulose (HEC) was purchased from TCI (Tokyo, Japan) Ethanol was purchased from Nacalai Tesque. Inc (Tokyo, Japan). For protein adsorption studies, bicinchoninic acid (BCA) kit was purched from Sigma Aldrich (Tokyo, Japan). Fetal bovine serum (FBS, Cell Culture Bioscience), bovine serum albumin (BSA, Sigma Aldrich), phosphate-buffered saline (PBS, Dullbecco Co., Ltd) were used. Trypsin-0.053 M-ethylenediaminetetraacetate (trypsin-EDTA) was purchased from Gibco (Tokyo, Japan) and formaldehyde (37 vol% aqueous solution) was purchased from Wako Co., Ltd. For cell culture

experiments, NIH3T3 mouse embryonic fibroblast cells were also purchased from BioResource Center (Japan).

6.2.2 Preparation of interpenetrated hydrogel films

The procedure of preparation of the interpenetrated hydrogel films was described as followed. The pulp/HEC cellulose solutions (1 wt%) in DMAc-LiCl system were prepared with modification of reports [35-36]. Pulp and HEC were firstly treated with water, ethanol, and finally DMAc by stepwise solvent exchange processes. After the solvent exchange process, the pulp/HEC solutions were prepared by varying HEC contents from 10 to 50 wt% and LiCl content were adjusted to be at 4 wt% and then these were stirred for 72 h. It is important to remark that 100% of HEC did not form hydrogel and was dissolved in water, no hydrogel films were obtained with HEC concentration higher than 50 wt%. This was due to strong dissolution of HEC. The obtained solutions were designed with P100HE0, P90HE10, P80HE20, P70HE30, P60HE40 and P50HE50 and the pulp/HEC contents in the DMAc solutions were 100/0, 90/10, 80/20, 70/30, 60/40 and 50/50 (g/g), respectively. As a result, transparent solutions were successfully obtained. The obtained hydrogel films of each pulp/HEC solution were prepared as followed. A weighed amount of the cellulose solution was poured into a glass tray (10 cm diameter), and then coagulated in ethanol. The resulting films were washed with ethanol 3 times and then, the cellulose films were submerged in 50 mL of distilled water and placed in shaking bath for 24 h at 25°C to remove the remained traces of the reagents. Finally, the hydrogel films were then immersed in distilled water over night and kept in phosphate buffered saline (PBS) at 4°C in a plastic container. This procedure was repeated 2 times.

6.2.3. Evaluation of interpenetrated hydrogel films.

Equilibrium water contents (EWC) of the resultant hydrogel films were determined by weighing the wet and dry samples as follow procedure. Samples (5 x 5 mm) were cut from cast films, dried in vacuum oven, and weighted. The samples were swollen in distillated water for 36 h. Then, film samples were removed and wrapped with filter paper to remove excess water. The weight of hydrated samples was determined. The percent EWC of hydrogels was calculated based on EWC= $W_h - W_d / W_d \times 100$. Where W_h is the weight of the hydrated samples and W_d is the dry weight of the sample. For each specimen, four independent measurements were determined and averaged [36].

Tensile strength and elongation of the hydrogel films were measured by a LTS -500N - S20 (Minebea, Japan) with universal testing machine equipped with a 2.5 kN cell. Briefly, each sample was cut in the form of a strip measuring approximately 1 mm x 10 mm x 50 mm. These sheets were uniaxially deformed along their longest axis. Strain was recorded by means of Zwick Makrosense clip-on displacement sensors. One set of samples was measured at five strips each and each set was repeated 3 times. Only samples which ruptured near mid-specimen length were considered for the calculation of tensile strength. The values of the tensile strength and elongation were calculated.

For measurements of atomic force microscopy (AFM), samples (20 mm x 20 mm) were dried under vacuum oven overnight. The images were recorded using Nanocute-AFM, Nano Navi IIs (Tokyo, Japan) by tapping mode. FT-IR spectroscopy was used to examine chemical functional groups in dry and wet hydrogel samples and HEC powder by using a FT-IR 4100 series (Jasco Corp), Japan. The thin hydrogel film having about 20 μm of thickness was set up in a CaF_2 window (30 mm diameter; thickness 2 mm, Pier Optics Co. Ltd). Then, 2 μL of distillated water

was dropped to the film. Then, another window was pressed to cover the wet film. For measurement of scanning electronic microscope (SEM), after the hydrogel film sample was dried, samples were coated with a gold layer. The SEM images were recorded using JSM-5310LVB (JEOL, Japan) with a magnification of 5000 in magnitude.

.

6.2.4. In vitro biocompatibility.

For the protein adsorption experiments, quantitative single protein adsorption experiments in PBS were determined by bicinchoninic acid assay (Micro BCA Protein Assay Reagent Kit, Aldrich) [35]. The hydrogels films (5 mm x 5 mm) were incubated in phosphate buffered saline (PBS) solution for 24 h then, immerged in 1 mL of the PBS solution containing BSA (1mg/mL) and incubated for 4 h at 37°C. For fetal bovine serum (FBS) experiments, 1 mL of Dulbecco's modified Eagle's medium (DMEM) enriched with 10 vol% of FBS was used. Following the adsorption experiments, the hydrogel samples were rinsed 3 times (10 min each) in PBS to remove loosely bound protein. The samples were then transferred into a glass tube containing 2 mL of aqueous sodium dodecyl sulfate (SDS) with 2 wt% concentration and shaken for 2 h at room temperature to elute the proteins adsorbed to the hydrogels. During screening experiments, it was confirmed that an elution time of 2 h removed all adsorbed proteins. Finally, the amount of adsorbed protein was calculated from the concentration of proteins in the SDS solution for measuring absorbance at 562 nm. The calibrated curve was prepared from pure sample of the target proteins measured. Four repeats (3 samples per repeat) for each hydrogel sample were measured and the average value was taken. For the measurement of the coagulation time, a modified Lee-White method was used. In the Lee White Clotting Time (LWTC) tests, the hydrogel films (5 mm x 5 mm) were incubated with 0.2 mL of platelet poor plasma (PPP) at

37°C in a plastic tube. At least, three measurements were averaged. Simultaneously, with addition of $CaCl_2$, the time was started and the solution was mixed well. After 20 s, the time of clot formation was recorded with a chronometer. The tests were repeated three times for each sample. For the platelet adhesion measurements, all of the appliance, reagents, and films (5 mm x 5 mm) were sterilized with ethanol 75 vol% for 3 h before the experiments. Then, the samples were immersed into BSA for 24 h and placed in disposable plastic tubes and 200 μL of platelet rich plasma (PRP) was dropped into each tube and incubated at 37°C for 90 minutes. On following this, the hydrogel films were rinsed three times with PBS and the adhered platelet were fixed with 1 mL of 2.5 vol% glutaraldehyde/PBS for 2 h. Finally, the hydrogel films were immersed into PBS for 5 min and dehydrated twice as followed. The first dehydration was carried out with a series of ethanol/PBS mixtures with increasing ethanol concentrations (25, 50, 75, and 100 wt%) for 15 min in each mixture. The second dehydration was performed with iso-amyl acetate/PBS mixtures with increasing iso-amyl acetate concentrations (25, 50, and 100 wt%) for 15 min. After freeze-drying the treated samples, adherent platelets were coated with a gold layer for the SEM measurements.

6.2.5. Cell culture and cell seeding.

Hydrogel films circles with 30 mm of diameter were used for cell seeding purposes. The samples were sterilized with 70 and 50 vol% of ethanol twice for 30 min and then, rinsed twice with the PBS for 30 min. Finally, the hydrogel films were swollen in DMEM for 1 h before starting the seeding procedure. The NIH 3T3 mouse embryonic fibroblast cells were cultured at 37°C in 95 wt% of relative humidity and 5 wt% of CO_2 environment. The culture medium was in 90 wt% of DMEM supplemented with 10 wt% FBS and 1 wt% penicillin/streptomycin. The cells

were seeded onto hydrogel films and tissue culture grade polystyrene dish (PS dish) at a density of $8x10^3$ cm^{-2} and maintained in 2 mL of medium. Cells were analyzed 4, 24, 48 and 72 h after seeding to characterize cell morphology and cell number. The measurements were assessed statistically using a one-way analysis of variance (ANOVA) test followed by the Student's t Test with a significance criterion of $p < 0.05$.

6.2.6. Cell morphology

Cell morphology was determined by image analysis of adherent fibroblast. Images were obtained using an Olympus CKX41 inverse microscope. The images were then imported into cellsens and the cell outline was determined using a variance edge detection algorithm. From this outline the projected cell area, aspect ratio and length were measured. Length was calculated from the mayor axis, and aspect ratio was calculated as the ratio of mayor to minor axes of the ellipse equivalent. Morphological analysis was limited to isolated cells.

6.3 Results and Discussion

6.3.1. Preparation of interpenetrated hydrogel films.

Table 6.1 lists properties of wet interpenetrated hydrogel films. In the case of water content measurements, samples were immersed in distilled water and reached to the equilibrium after 36 h. Figure 6.1 shows pictures of hydrogel film P100HE0 and P50HE50 in (a, c) dried and (b, d) wet conditions. Water content value increased from 37% to 50% with the increment of HEC in P100HE0 and P50HE50, respectively.

Table 6.1. Properties of hydrogel membranes of Pulp/HEC.

Sample	Water Content (%)	Contact Angle (°)	Tensile Strength (N/mm²)	Elongation (mm)
P100HE0	336	51	48	12
P90HE10	346	46	44	11
P80HE20	355	41	40	9
P70HE30	371	39	38	8
P60HE40	385	35	36	7
P50HE50	396	34	32	6

Mean ± standard deviation (SD) for $n \geq 30$ units.

This result confirmed that the HEC interpenetration into the pulp fiber could enhance water accessibility. As shown in the obtained values of contact angle, it was observed a tendency related to HEC content. At higher HEC content, water molecules were capable to penetrate and interacted easily into the interpenetrated hydrogel films. It was noted that the interpenetrated hydrogel films had very soft and flexible shape, although there was no chemical crosslinking treatment. For uniaxial tensile testing, the sample hydrogels (10 mm x 50 mm) were placed between two clamps in wet condition.

Table 6.1 shows tensile strength and elongation values for the hydrogel films. In the case of P100HE0 and P50HE50, the tensile strength values decresead from 48 N/mm² to 32 N/mm² and the elongation value decreased from 12.3% to 6.0%, respectively. This might be attribuited to the presence of HEC in the interpenetrated network, which could diminish the interaction between pulp fibers. This could explain the decrease of the stiffness of the films prepared with different contents of HEC.

The observed higher tensile value in the case of P100HE0, could be attribuited to the interaction of cellulose fibers with the macrocation formed in the DMAc/LiCl system. It has been postulated that in the DMAc/LiCl system a macrocation $[DMAc\text{-}LiCl\text{-}DMAc\text{-}Cl^-]_n$ is formed. This macrocation interacts with cellulose molecules and acts as crossliker [37,38]. In reference 39, the presence of aggregates was confirmed due to the interaction of the formed macrocation and cellulose molecules. To observe the cellulose fiber arrangement of the hydrogel films, AFM measurements were carried out in wet conditions.

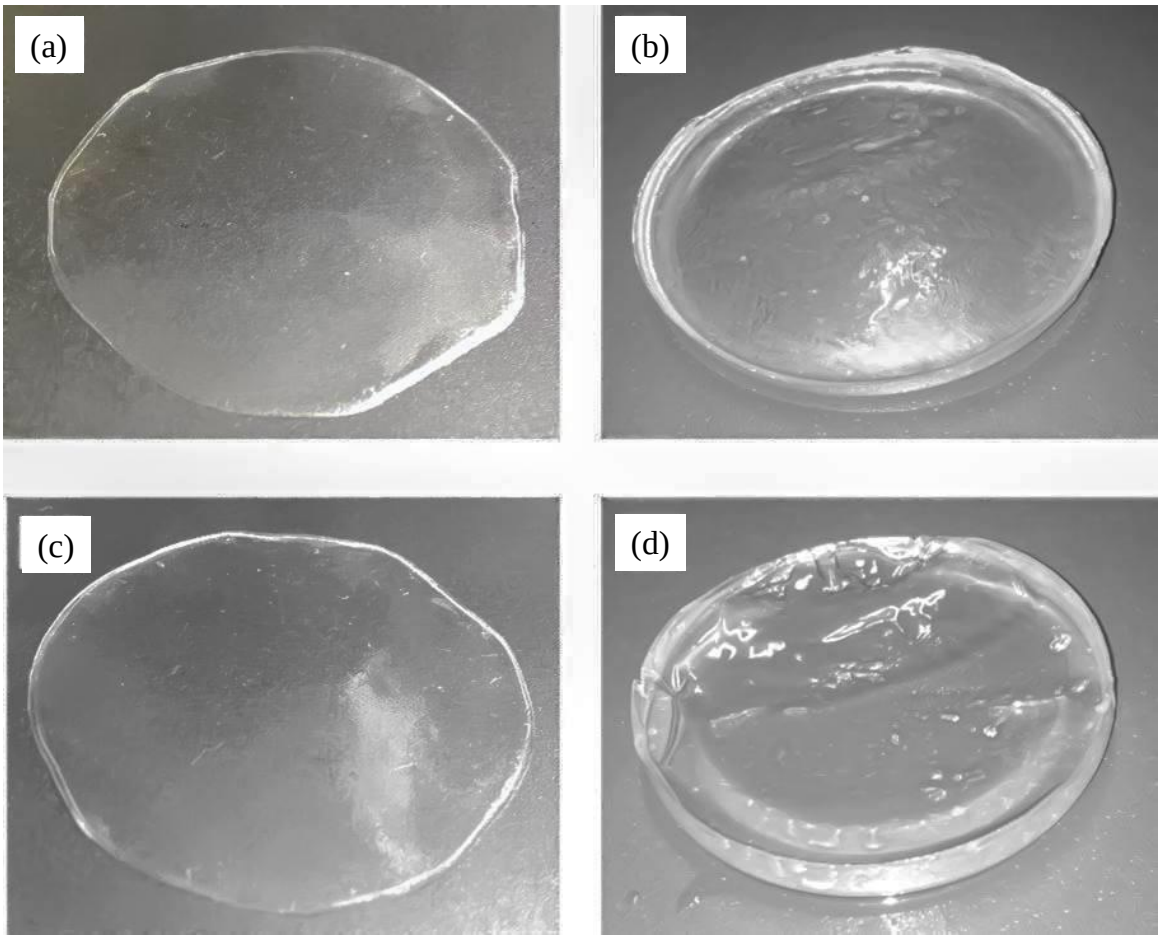

Figure 6.1. Representative hydrogel films photograph images of P100HE0 (a) dry and (b) wet condition, and P50HE50 (c) dry and (d) wet condition.

Figure 6.2 shows the AFM images (20 mm x 20 mm) including topographic and phase-shift images of the films. The arrangement view observed in sample P100HE0 was destroyed to be fine round structure with size about 80 nm in the case of sample P50HE50 due to the increment of HEC content. The observation strongly suggests diminish of interaction of pulp cellulose in the hydrogel films, due to the stiffness aggregation was affected by addition of HEC. The obtained AFM topographic images revealed that the addition of HEC changed the ordered

structure of pulp fibers by interpenetration and increased the space between the fibers. Figure 6.2 (f) showed that the morphology shape of the pulp and HEC domains changed to be about 50 nm size with round shape. The surface roughness (Rrms) of the samples decreased from 7.3 ± 0.83 nm to 4.3 ± 0.93 nm for the P50HE50 and P100HE0, respectively. This change was an evidence of the interference of HEC with the interpenetrated interaction into the aggregated pulp fibers changing valleys shape and roughness of the surface. In the case of P100HE0, AFM topographic images showed aggregated fibers on the same direction due to dense interaction with each cellulose fiber. Therefore, as mentioned in Table 6.1, it is reasonable to obtain higher tensile strength and elongation in the hydrogel film P100HE0. Figure 6.3 shows viscolelasticity of the interpetrated hydrogel films. Hydrogels films prepared varying HEC from 10 to 50 wt% in the DMAc solution were tested. It was observed that the deformation of P100HE0 was lower than the observed on the P50HE50. This could be attributed to the presence of HEC in the interpenetrated matrix which increased the deformation of the hydrogel reducing the interaction of pulp fibers, and decreasing the stiffness of the sample. The elastic response to the deformation only occurs under momentary deformation. However, under a prolonged deformation, it cannot recover its original shape because the polymer chains have flowed. When the amount of HEC decreased, the polymer chains in the network kept the chains strands from moving away.

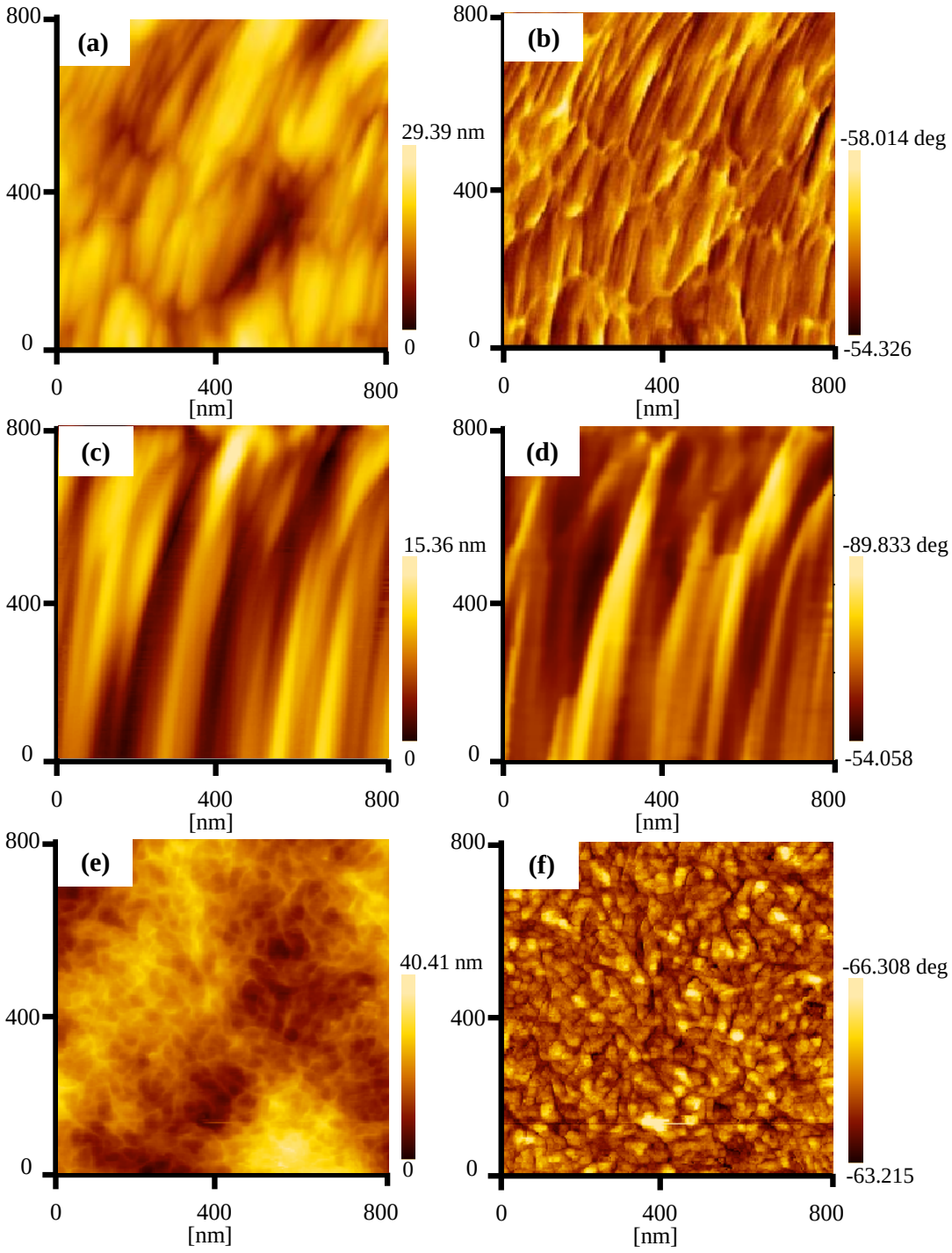

Figure 6.2. AFM images (a, c, e) topographic and (b, d, f) phase-shift images of hydrogel film (a, b) P100HE0, (c, d) P90HE10 and (e, f) P50HE50.

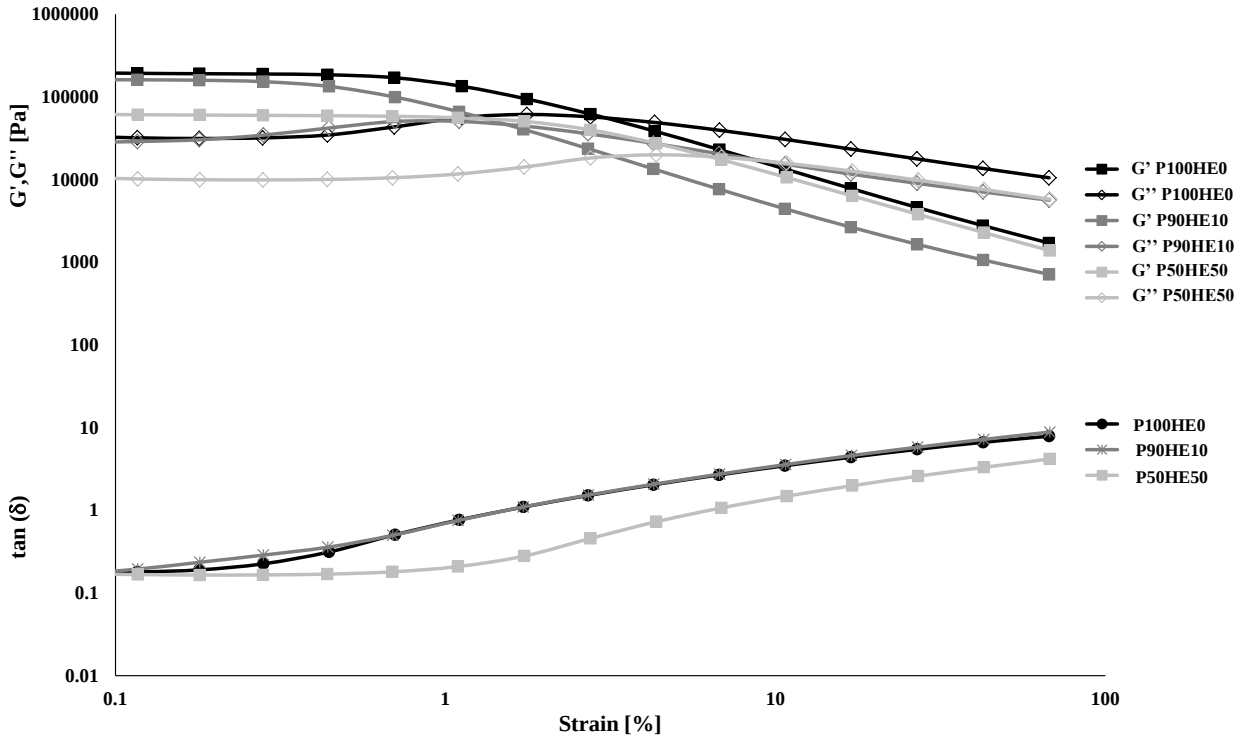

Figure 6.3. The viscoelasticity of strain G', G'' plots at 25°C of the hydrogel films with different HEC contents.

FT-IR measurements of interpenetrated films in dry and wet conditions were carried out. Figure 4 shows FT-IR spectra of HEC, P100HE0, P90HE10 and P50HE50 in (a) dry and (b) wet films. The FT-IR spectra of the films had strong peaks around 3550 and 3200 cm^{-1} attribuited to O-H band stretching. In addition, the peaks around at 1150, 1160, 1120, 1059, and 1035 cm^{-1} refered to C-OH, C-O-C, and C-C ring bands, CH_2 and OH groups, respectively [40]. It was noticed that the intensity of O-H band stretching increased in P90HE10 and P50HE50 films in wet condition. This phenomenon meant that water bound to the OH group of the pulp and HEC in the interpenetrated network. This change was slightly observed in HEC used as control, due to the higher interaction of water molecules with the network of the hydrogel. In the O-H stretching region, in the dry P100HE0, the center peak of the O-H stretching band appeared at 3424 cm^{-1}, however, in the case of wet film the center peak appeared at 3458 cm^{-1},. In P90HE10 similar shift was observed, however, the extent was lower in P100HE0. In addition, the center peak was slighly shifted to 1601 and 1628 cm^{-1}, wet films P90HE10 and P50HE50, respectivily. Moreover, the difference in shape of the obtained peaks between dry and wet films is clear in 3000-3800 cm^{-1} region. Broad peaks were observed in wet films compared with the narrow peaks observed in dry films. Moreover, the intensity of peaks around 1601 and 1628 cm^{-1} increased for wet films P90HE10 and P50HE50, respectively. This suggested that water molecules interacted with the pulp cellulose and HEC.

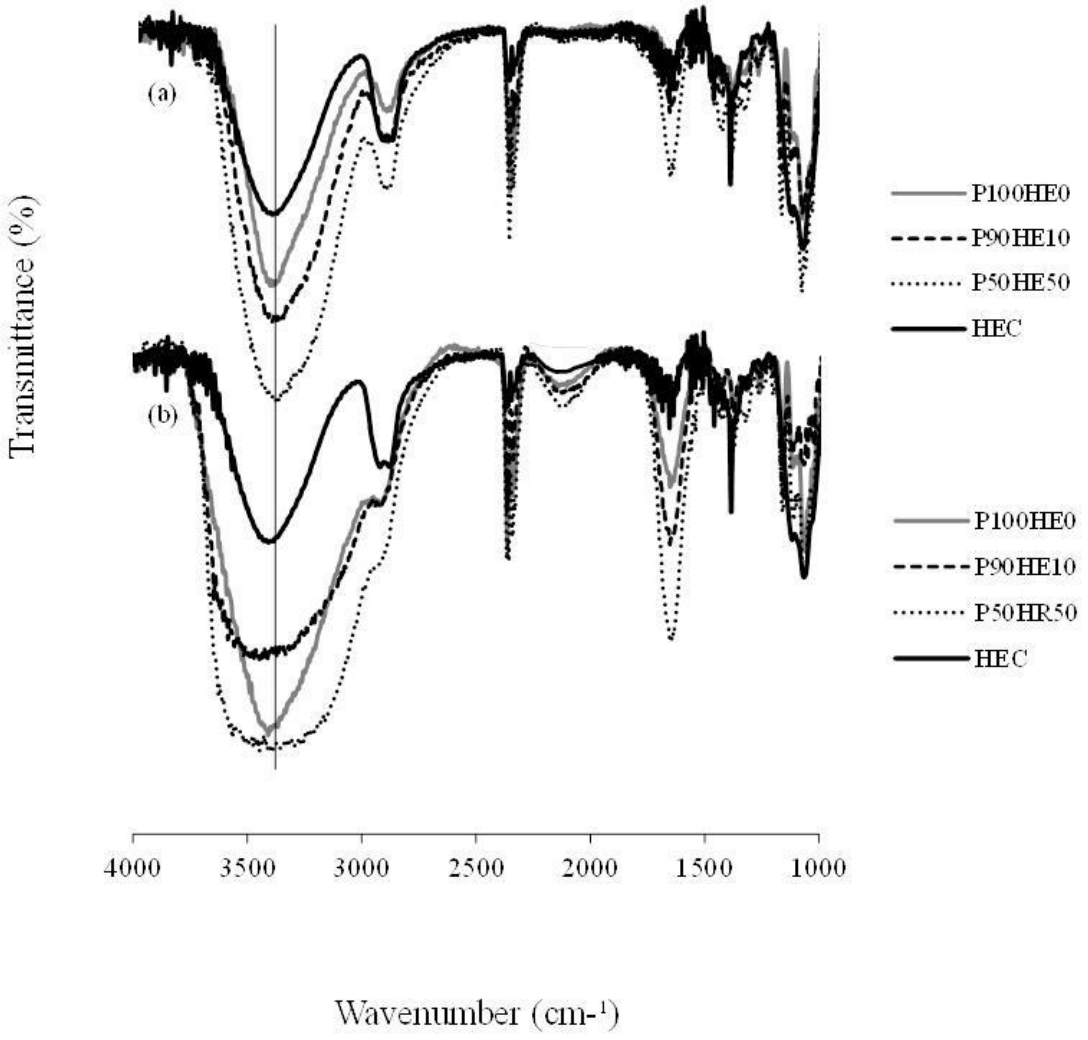

Figure 6.4. FT-IR spectra of the hydrogel films in dry (a) and wet (b) conditions prepared with different HEC contents. The spectra of HEC were measured in dry film, which was prepared from water evaporation of the aqueous solution and in wet film containing a few μL of water droplets for swelling of the dry films.

6.3.2 In vitro biocompatibility.

The protein adsorption data for the current hydrogels films are presented in Figure 6.5. When an artificial material is exposed to cells suspended in a culture medium supplemented with FBS, proteins in the serum are rapidly adsorbed onto its surface before the subsequent cell adhesion behavior. The results showed differences in protein adsorption values as HEC increased. These differences were significant (ANOVA, $p < 0.05$). In the case of BSA, P100HE0 showed higher adsorption value compared to the other samples, the addition of HEC decrease the adsorption value compared to P100HE0, this was significant (Student's t-test, p = < 0.05, n = 6). The adsorption value increased in the case of FBS when HEC content increased from 0% to 50% (Student's t-test, p = < 0.05, n = 6). It was known that the BSA proteins has stronger adsorption on hydrophobic surface, meanwhile FBS preferred hydrophilic surfaces [27-34,42-44]. In the present work, the BSA adsorption tended to suppress the cell adhesion as the HEC concentration was higher. In these cases, it could be considered that the changes in adsorption of BSA and FBS might be due to hydrogel nature depending upon the HEC contents. It has been reported that, the early BSA adsorption onto the surface could suppress cell adhesion, but when the hydrogel film is exposed to cells suspended in a culture medium supplemented with FBS, proteins in the serum area rapidly adsorbed onto the surface before the cells adhere. These adsorbed proteins determine the subsequent cell adhesion behavior contrasting the effect of BSA [44]. Based on the obtained results for serum proteins adsorption, it would be expected that the hydrogel films having higher HEC contents might induced less cellular adhesion.

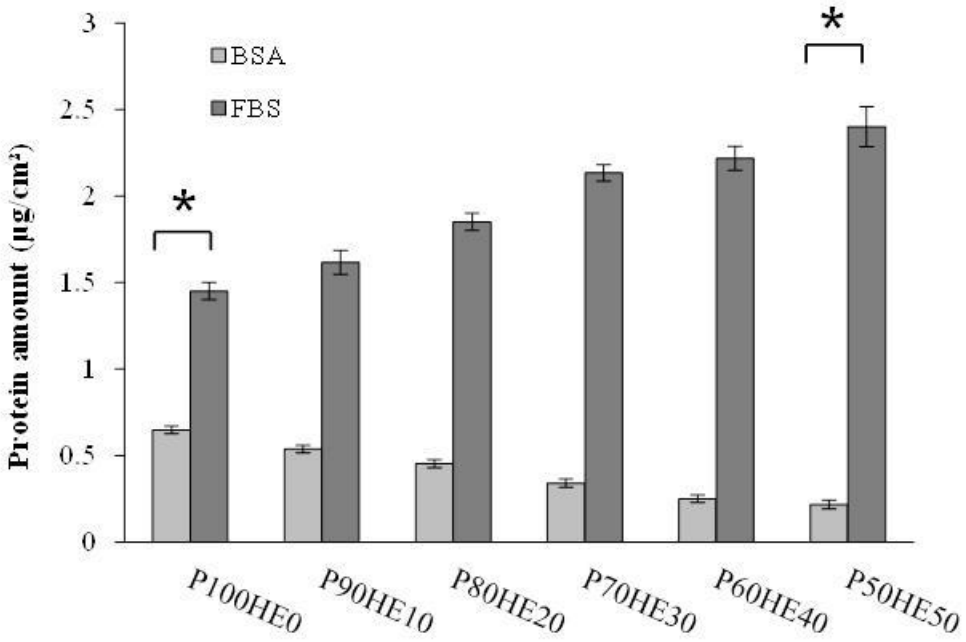

Figure 6.5. Protein adsorption of hydrogel films prepared from DMAc solution containing different HEC concentration. An asterisk indicates statistically significant ($p < 0.05$). Mean ± SEM ($n = 6$).

Figure 6.6 shows the clotting time measurements by using PPP in the test of hydrogel films varying HEC content. The obtained results showed that when HEC content was varied differences in clotting time was observed. These differences were significant (ANOVA, $p = < 0.05$). A slight increase of clotting time was observed as the HEC increased comparing P100HE0 and P90HE10 showing significant difference (Student's t-test, p = < 0.05, n = 3). P50HE50 showed of all the tested samples the higher clotting time (Student's t-test, p = < 0.05, n = 3). This

phenomenon could be supported with the results of the FBS protein adsorption as shown in Figure 6.5. In protein adsorption capacity of the hydrogel films, it was easy to consider that the fibrinogen adsortion might be suppressed to form a fibrin rich clot. In the case of the affinity of the material surface blood components should become important issue. Therefore, comparison of adherent platelet number on hydrogel surfaces gives us important results.

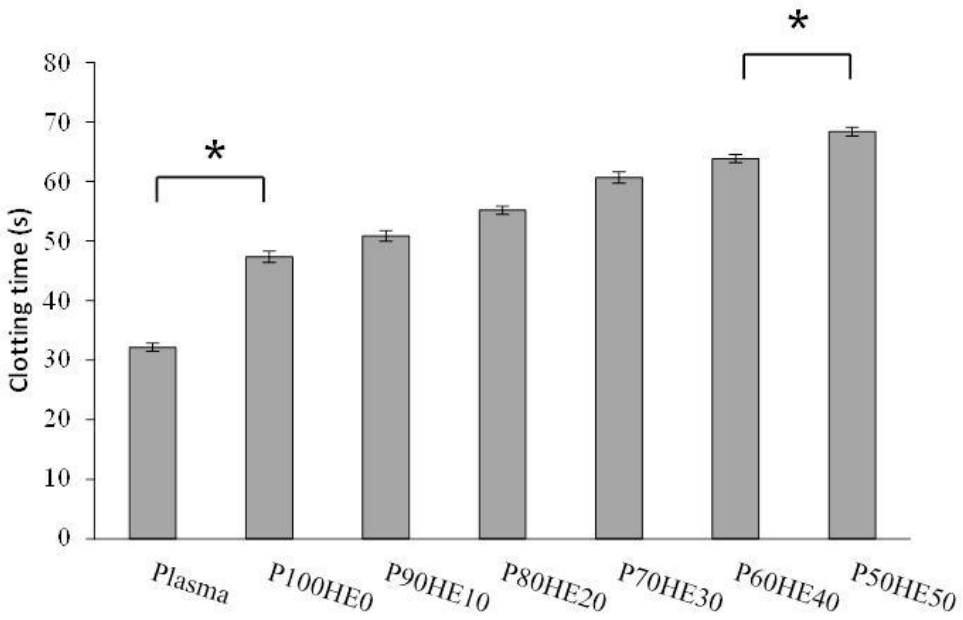

Figure 6.6. Clotting time of cellulose hydrogel films prepared from DMAc solution containing different HEC concentration. An asterisk indicates statistically significant ($p < 0.05$). Mean ± SEM ($n = 3$).

Figure 6.7 shows that all the hydrogels in the presence of HEC induced less platelet adhesion than PS dish used as control. Platelet adhesion is a desirable condition in our obtained hydrogels. There was a tendency of the number of adherent platelet to decrease with increasing of the HEC

content in the P50HEC50. This results seems to be related to the properties of the hydrogels surface as shown by AFM. Similar results were also reported by Korematsu et al. [41] for the adhesion of platelets.

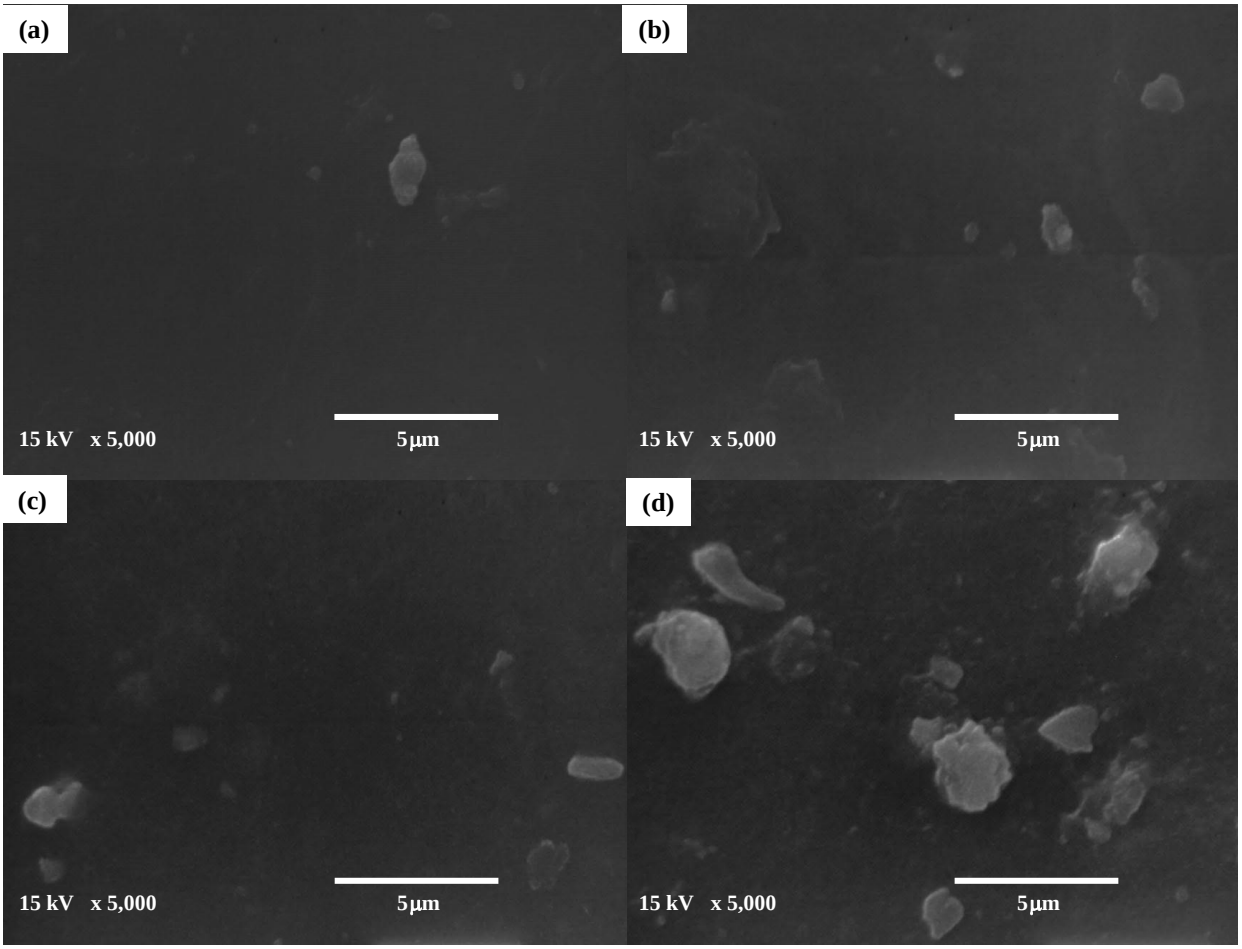

Figure 6.7. SEM photographs of platelet adhered on the surface of pulp/HEC hydrogels. The HEC content was changed in (a) P50HEC50, (b) P90HE10, (c) P100HE0, and (d) tissue culture grade polystyrene dish (PS dish) used as control.

6.3.3. Cell density on hydrogel films.

For wound healing repair films, another important factor to consider is fibroblast adhesion on the hydrogel surface. In order to observe such behaviour for the hydrogel films, phase-contrast light microscope images of fibroblasts on the hydrogel films surface were acquired to determine the effect of HEC on cell density. Figure 6.8 shows that all the samples revealed differences in the number of adherent cells on hydrogel films as HEC decreased, these differences were significant (ANOVA, $p < 0.05$). After 4 hours of cultivation the number of adherent cells showed slight difference compared with PS dish used as control. This was significant in all the hydrogel samples after 24, 48 and 72 hours of incubation (Student's t-test, $p < 0.05$, n = 6). An increase in the number of adherent cell was observed as HEC decreased. This increase was significant after 48 and 72 hours of incubation (Student's t-test, $p = < 0.05$, n = 6). These differences were observed between P100HE0 and P50HE50 after 48 hours of cultivation (Student's t-test, $p = < 0.05$, n = 6). In the case of P90HE10 and P80HE20 a slight decrease in the number of adherent cells was seen after 48 hours of cultivation, these differences were only significant after 72 hours of cultivation compared with P100HE0 (Student's t-test, $p = < 0.05$, n = 6). The results revealed that all the hydrogel samples used showed better cytocompatibility than the tissue culture grade polystyrene dish (PS dish) used as control. These results confirm the expected suppression of fibroblast adhesion with the increment of HEC based on protein adsorption results, obtained due to the significant decrease of contact angle. Moreover, higher cell number was observed on hydrogel surface with higher contact angle. Similar results were obtained by Tamada et al. [42] and Salem et al. [43] observing that fibroblast adhered better to stiffer surfaces with a contact angle around 52°. It was found that the softness and stiffness of the scaffold might regulate the adhesion between cellular-extracellular matrix molecules as well as surface wettability. [44]

Based on this, the observed difference in cell density between P100HE0 and P50HE0 could be attributed to the change on water content, contact angle, and the decrease of the hydrogel stiffness due to the presence of HEC.

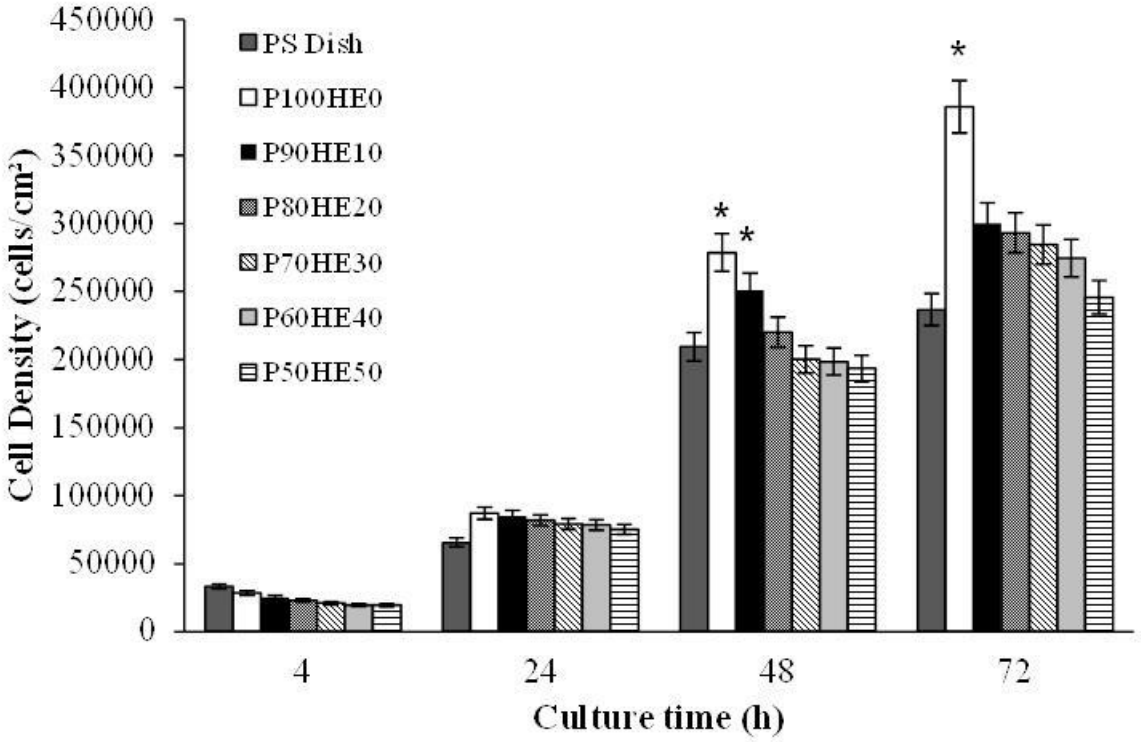

Figure 6.8. Cell number on interpenetrated pulp HEC hydrogel surfaces as function of culture duration. An asterisk indicates statistically significant different from the tissue culture grade polystyrene dish (PS dish) used as control ($p < 0.05$). Mean ± SEM ($n = 6$).

Figure 6.9 shows adhesion of fibroblast on hydrogel films after cell culture time of 24 h. The obtained results showed remarkable difference on the adherent fibroblast on the hydrogel films depending of the HEC contents. It is known that as the HEC content increased in the film, the stiffness of the film decreased affecting migration of cells, a phenomenon known as mechanotaxis. Similar results were obtained by Lin et al. [45] and Kidoaki et al. [46]. They observed that fibroblasts migrated preferentially towards stiffer surfaces. This could explain the observed decrease of cell density on Figure 6.8. As appeared in the viscoelastic data (Figure 6.3), the hydrogel film P100HE0 might become to have better cytocompatibility. In the case of higher content of HEC, the softness and stiffness of the films might regulate the adhesion between cellular- extracellular matrix molecules reducing the interaction of these molecules with the fibroblast diminishing cell density.

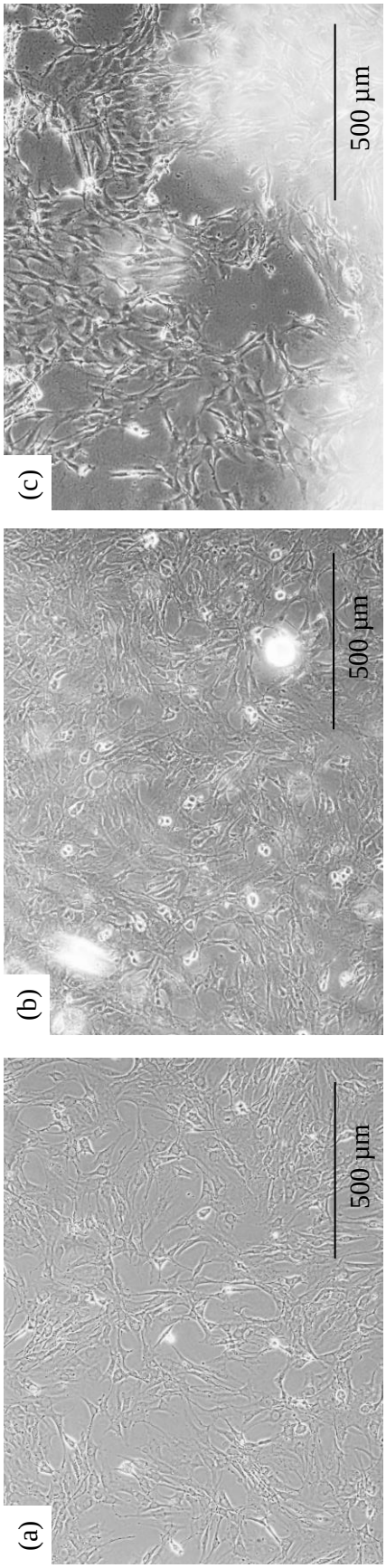

Figure 6.9. Phase-contrast light images of (a) PS dish used as control, (b) P100HE0, (c) P50HE50. The cell culture was 24 h.

6.3.4. Cell morphology on hydrogel films

As shown in Figure 6.10, results of cell morphology on the hydrogels films revealed a remarkable difference of adherent fibroblast on the tissue culture grade polystyrene dish (PS dish) (a-c) and hydrogel films (d-i). For example, in the case of P100HE0 (d-f), the fibroblast surely adhered and grown on the hydrogel film, as observed in the images. Figure 6.10 (d) showed longer axis shape of the cells compared with those adhered on the PS dish at the same condition at the first 4 h of cell culture time. Moreover, the boundaries of the adhered cells on P100HE0 films seemed to be tightly adhered on the hydrogel surface. In addition, anisotropic shape of adherent fibroblast was noted in comparison with the diffuse cell shape on P50HE50 (Figure 6.10 (g)) also, the mainly round cell shape on the PS dish was observed on Figure 6.10 (a). The obtained results after 4 h of cell culture revealed that P100HE0 film provide better substrate for cell adhesion than the PS dish and P50HE50. This is important because it was observed that at early culture time the fibroblast could tightly adhere to the surface enhancing them spreading on the surface. Films P50HE50 showed lower aspect ratio, long axis and cell density. This could be attributed to the interference of HEC to the ordered fiber in the pulp cellulose films as observed in Figure 2(f). This changed the surface roughness affecting cultivation growing on the adherent cells. These results revealed that, even though the obtained results showed that all the prepared hydrogels had better cytocompatibility than the PS dish, better results were obtained without the addition of HEC. Therefore, these results strongly suggest the clinical possibility for applying for tissue repairing.

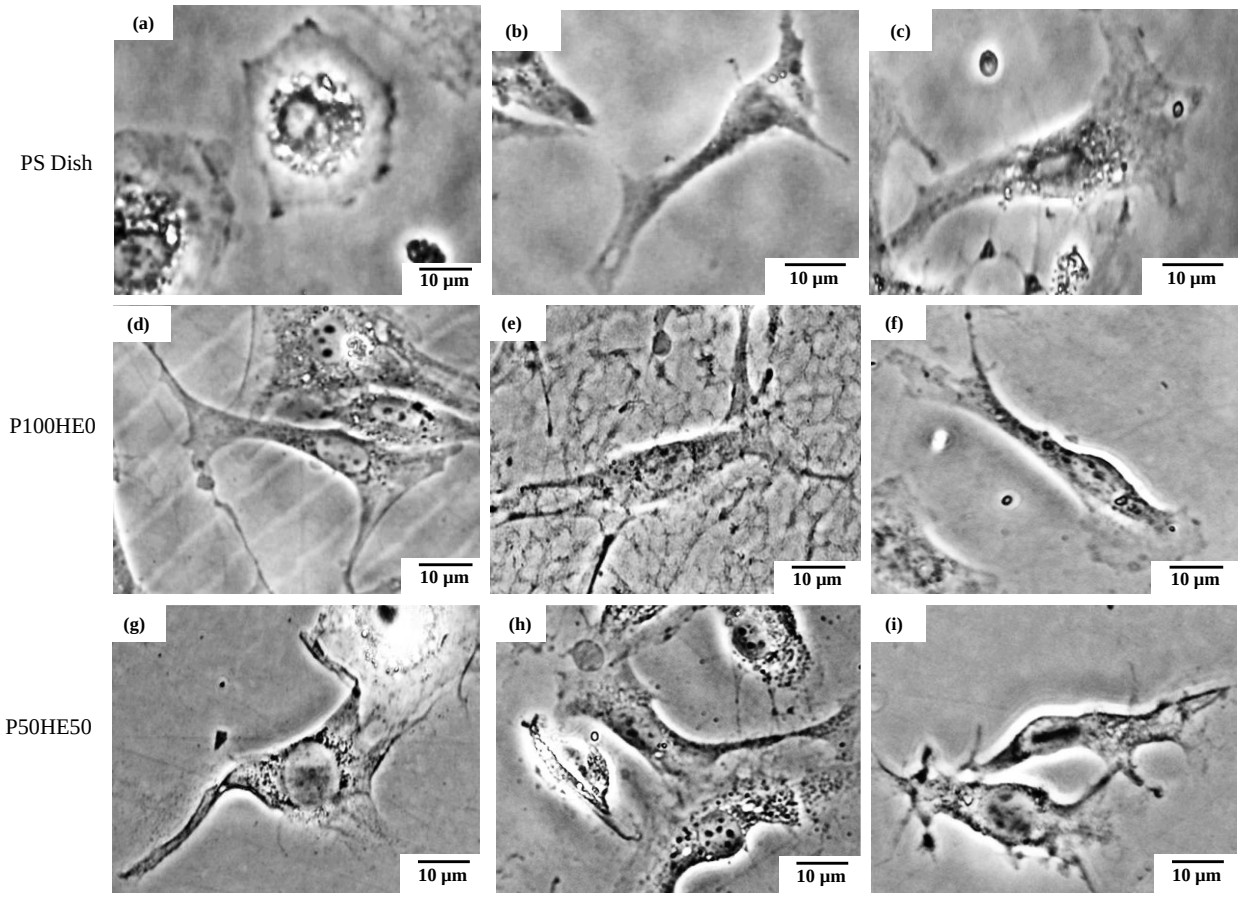

Figure 6.10. Phase-contrast light images of (a-c) tissue culture grade polystyrene dish (PS dish) as control, (d-f) hydrogel films P100HE0 (g-i) P50HE50. The cell culture was (a,d,g) 4 h, (b,e,h) 24 h and (c,f,i) 48 h.

6.4. Conclusion

Hydrogel films prepared from pulp fibers interpenetrated with HEC were obtained by phase inversion of the DMAc solution. The interpenetrated hydrogel film had better mechanical properties without chemical crosslinking, although the hydrogel contained higher water in the films. It was proved that the HEC acted to interfere with the interpenetrated interaction into the

aggregated pulp fibers. Depending on the HEC content, these hydrogel films exhibited lower protein adsorption and higher clotting time. The platelet adhesion observed on films with higher HEC content decreased. Moreover, films with lower HEC showed better cytocompatibility. In addition, all the obtained films showed better cytocompatibility than the tissue culture grade polystyrene dish (PS dish) used as control however lower HEC seems to improve cyto and biocompatibility.

6.5 References

[1] Slaughter, B.V., Khurshid, S.S., Fisher, O, Z., Khademhosseine, A. & Peppas, N.A. Hydrogel in Regenerative Medicine. *Adv. Mater*. **2009**, *21*, 3307.

[2] Langer, R. Biomaterials and biomedical engineering. *Chem. Eng. Sci.* **1995**, *50*, 4109.

[3] Qiu, Y. & Park, K. Environmental-sensitive hydrogel for drug delivery. *Adv. Drug. Deliv. Rev*. **2001**, *53*, 321.

[4] Drury, J. L. & Mooney, D. Hydrogel for tissue engineering: scaffold design variables and applications. *Biomaterials.* **2003**, *24*, 4337.

[5] Uchiyama, T., Watanabe, J. & Ishihara, K. Biocompatible polymer alloy membrane for implantable artificial pancreas. *J. Membrane Sci.* **2002**, *208*, 39.

[6] Xu, F., Wang, Y., Jiang, X., Tan, H., Li, H. & Wang, K. J. Effects of different biomaterials: comparing the bladder smooth muscle cells on waterborne polyurethane of poly-lactic-co-glycolic acid membranes. Kaohsiung *J. Med. Sci.* **2012**, *28*, 10.

[7] Nair, L. S. & Laurenoin, C. T. Biodegradable polymers as biomaterials. *Prog. Polym. Sci.* **2007**, *32*, 762.

[8] Sionkowska, A. Current research on the blends of natural and synthetic polymers as new biomaterials: review. *Prog. Polym. Sci.* **2011**, *36*, 1254.

[9] Vlierberghe, S. V., Dubruel, P. & Shacht, E. Biopolymer-Based hydrogels as scaffolds for tissue engineering applications: A review. *Biomacromolecules.* **2011**, *12*, 1387.

[10] Jeong, G. S., Kwon, G. H., Kang, A. R., Jung, B. Y., Park, Y., Chung, S. & Lee, S. H. Microfluidic assay of endothelial cell migration in 3D interpenetrating polymer semi-network HA-Collagen hydrogel. Biomed. *Microdevices.* **2011**, *13*, 717.

[11] Jaiswal, M., Koul, V., Dinda, A. K., Mohanty, S. & Jain, K. G. Cell adhesion and proliferation studies on semi-interpenetrating polymeric networks (semi-IPNs) of polyacrylamide and gelatin. J. Biomed. Mater. Res. Part B. *Appli. Biomater.* **2011**, *98B*, 342.

[12] Liu, W., Deng. C., McLauglin, C. R., Fagerholm, P., Lagali, N. S., Heyne, B, Scaino, J. C., Watshy, M. A., Kato, Y., Munger, R., Shinozaki, N., Li, F. & Griffith, M. Collagen-phosphorylcholine interpenetrating network hydrogels as corneal substitutes. *Biomaterials.* **2009**, *30*, 1551.

[13] Vashist, A., Gupta, Y. K. & Ahmad, S. Interpenetrating biopolymer network based hydrogels for an effective drug delivery system. *Carbohyd. Polym.* **2012**, *87*, 1433.

[14] Kajjary, P. B., Manjeshwar, L. S. & Aminabhavi, T. M. Semi-Interpenetrating polymer network hydrogel blend microspheres of gelatin and hydroxyethyl cellulose for controlled release of theophylline. *Ind. Eng. Chem. Res.* **2011**, *50*, 7833.

[15] Peng, Z.; Chen.F. Hydroxyethyl cellulose-based hydrogels with various pore sizes prepared by freeze-drying. *J. Macromol. Sci., Phys.* **2010**, *2*, 340.

[16] (16) Maleki, A.; Kjøniksen, A. L.; Knudsen, K. D.; Nyström, B. Dymanic and structural behavior of hydroxyethyl cellulose hydrogels ontained by chemical gelation. *Polym. Int.* **2006**, *55*, 365.

[17] Silva, M. R. & Castro, M. C. R. New dressings, inclusing tissue-engineering living skin. *Clin. Dermatol*. **2002**, *20*, 715.

[18] Jayakumar, R., Prabaharan, M., Sudheesh Kumar, P. T., Nair, S. V. & Tamara, H. Biomaterials base on chitin and chitosan in wound dressing applications. *Biotechnol. Adv.* **2011**, *29*, 322.

[19] Muzzarelli, R. A. A. Chitins and chitosans for repair of wounded skin, nerve, cartilage and bone. *Carbohyd. Polym*. **2011**, *76*, 167.

[20] Castillo-Briceno, P., Bihan, D., Nilges, M., Hamaia, S., Meseguer, J., Garcia-Ayala, A., Farndale, R. W. & Mulero, V. A role for specific collagen motifs during wound healing and inflammatory response of fibroblast in the teleost fish gilthead seabream. *Mol. Immunol.* **2011**, *48*, 826.

[21] Muller, F. A., Muller, L., Hofmann, I., Greil, P., Wenzel, M, M. & Staudenmaier, R. Cellulose-based scaffold materials for cartilage tissue engineering. *Biomaterials.* **2006**, *27*, 3955.

[22] Hoenich, N. Cellulose for medical applications: past, present, and future. *Bio resources*. **2006**, *2*, 270.

[23] Sannino, A., Demitri, C. & Madaghiele, M. Biodegradable cellulose-based hydrogels: design and applications. *Materials.* **2009**, *2*, 353.

[24] Zhang, S., Li, F. X. & Yu, J. Y. Preparation of cellulose/Chitin blends bio-fibers via direct dissolution. *Cell. Chem. Technol*. **2009**, *43*, 393.

[25] Granja, P. L., De Jeso, B., Bareille, R., Rouais, F., Baquey, C. & Barbosa, M. A. Cellulose phosphates as biomaterials. In vitro biocompatibility studies. React. *Funct. Polym*. **2006**, *66*, 728.

[26] Chong, C. & Zhang, L. Cellulose-based hydrogels: present status and application prospects. *Carbohyd. Polym*. **2011**, *84*, 40.

[27] Lo C. M., Wang H. B., Dembo, M. & Wang, Y. L. Cell movement is guided by rigidity of substrate. *Biophys J*. **2000**, *79*, 144.

[28] Mandeville, J. T., Lawson, M. A. & Maxfield, F. R. Dynamic imaging of neutrophil migration in three dimensions: mechanical interaction between cells and matrix. *J. Leukoc. Biol.* **1997**, *61*, 188.

[29] Rajnicek, A., Britland, S. & McCaig, C. Contact guidance of CNS neuritis on grooved quartz: influence of groove dimensions, neuronal age and cell type. *J. Cell. Sci.* **1997**, *110*, 2905.

[30] Choquet, D., Felsenfeld, D. P. & Sheetz, M. P. extracellular matrix rigidity causes strengthening of integrin-cytoskeleton linkages. *Cell.* **1997**, *88*, 39.

[31] Wang, H. B., Dembo, M., Hanks, S. K. & Wang Y. L. Focal adhesion kinase is involved in mechanosensing during fibroblast migration. *Proc. Natl. Acad. Sci. USA*. **2001**, *98*, 11295.

[32] Grinnell, F. & Feld, M. K. Fibronectin adsorption on hydrophilic and hydrophobic surfaces detected by antibody binding and analyzed during cell adhesion in serum-containing medium. *J. Biol. Chem*. **1982**, *257*, 4888.

[33] Grinnell, F. & Bennette, M. H. Fibroblast adhesion on collagen substrata in the presence and absence of plasma fibronectin. *J. Cell. Sci.* **1981**, *48*, 19.

[34] Baxter, L.C., Frauchiger, V., Textor, M., Gwynn, I. & Rochards, R. G. Fibroblast and osteoblast adhesion and morphology on calcium phosphate surfaces. *Eur. Cell. Mater*. **2002**, *4*, 1.

[35] Lindma, B., Karlstrom, G. & Stigsson, L. On the mechanism of dissolution of cellulose. *J. Mol. Liq*. **2010**, *156*, 76.

[36] Mequanint, K., Patel, A. & Bezuidenhout, D. Synthesis, swelling behavior, and biocompatibility of novel physically cross-linked polyurethane-block-poly(glycerol methacrylate) hydrogels. *Biomacromolecules*. **2006**, *7*, 883.

[37] Sjoholm, E., Gustafsson, K., Eriksson, B., Brown, W. & Colmsjo, A. Aggregation of cellulose in lithium chloride/N,N-dimethylacetamide. *Carbohyd. Polym*. **2000**, *41*, 153.

[38] Striegel, A. M. Theory and applications of DMAc/LiCl in the analysis of polysaccharides. *Carbohyd. Polym*. **1997**, *34*, 267.

[39] Ishii, D.; Tatsumi, D.; Matsumoto, T.; Murata, K.; Hayashi, H.; Yoshitani, H. Investigation of structure of cellulose in LiCl/DMAc solution and its gelation behaviour by small-angle X-ray scattering measurements. *Macromol. Biosci.* **2006**, *6*, 293.

[40] Wang, W., Wang, J., Kang, Y. & Wang. A. Synthesis, swelling and response properties of a new composite hydrogel based on hydroxyethyl cellulose and medical stone. *Composites:B.* **2011**, *42*, 809.

[41] Korematsu, A., Takemoto, Y., Nakaya, T. & Inoue, H. Synthesis, characterization and platelet adhesión of segmented polyurethanes grafted phospholipid analogous vinyl monomer on surface. *Biomaterials*. **2002**, *23*, 263.

[42] Tamada, Y. & Ikada, Q, Effect of preadsorbed proteins on cell adhesion to polymer surface. *J. Coll. Interf. Sci*. **1993**, *155*, 334.

[43] Salem, A. K., Tendler, S. J. & Roberts, C. J. Interactions of 3T3 fibroblasts and endothelial cells with defined pore features. J. Biomed. Mater. Res. **2002**, *61*, 212.

[44] Arima, Y.; Iwata, H. Effect of wettability and surface functional groups on protein adsorption and cell adhesion using well-defined mixed self-assembled monolayers. *Biomaterials.* **2007**, *28*, 3074.

[45] Lin, X. & Helmke, B. P. Micropatterned structural control suppresses mechanotaxis of endothelial cells. *Biophys. J*. **2008**, *95*, 3066.

[46] Kidoaki, S. & Matsuda, T. Microelastic gradient gelatinous gels to induce cellular machanotaxis. *J. Biotech*. **2008**, *133*, 225.

Chapter 7

Summary

Natural polymers have been applied in medical fields for decades. Since 1980s there was an explosion of interest in tissue engineering as an emerging field. Tissue engineering involves cell seeding on a scaffold followed by culturing in vitro prior implantation. Recently, natural polymers as cellulose are gaining interesting in the scientific community as a potential polymer for the preparation of scaffolds.

In the present work, waste fibers were used to obtain a biomass hydrogel and then the hydrogel films could be applied as scaffold on tissue regeneration. Base on this background, the research in waste fibers as cellulose source could apply in sustainable waste product for tissue regeneration. As a frontier research, the present work in natural cellulose polymer can provide important evidence on tissue regeneration. The elaboration of hydrogel films from waste fibers and cytotoxic nature was firstly reported in the present, showing possibility in tissue regeneration application.

Therefore, before demonstration of these interesting data, in **Chapter 1** a brave introduction of hydrogels and cellulose and scaffolds for biomedical applications has been mentioned. In **Chapter 2**, it showed that effect of sodium hypochlorite treatment of agave tequilana weber bagasse fibers for the preparation of cyto and biocompatible hydrogel films. It was observed that the chemical treatment had a significant influence in the properties of the obtained films. In addition, it was noted that shear viscosity of the agave solutions increased with the increment of the concentration of NaOCl used during the treatment of the agave fibers. In the case of the hydrogel films, it was proved that the NaOCl concentration used for the agave fiber treatment

strongly affected the mechanical properties of the hydrogel films. It was concluded that the cytotoxicity and biocompatibility properties were remarkably influenced by the degree of the NaOCl concentration used the treatment. Thus, the presence of lignin was due to the soft chemical treatment of agave fibers retarded the formation of the interaction hydrogen bonding networks of the resultant cellulose in the hydrogel film. This might be influenced in the protein adsorption for the fibroblast cells at initial stage.

In **Chapter 3**, Agave fibers were used to elaborate a transparent and flexible cellulose hydrogel films used as scaffold for tissue regeneration and tested by *in vitro* assays with NIH 3T3 fibroblast cells. The cellulose hydrogel film had better mechanical properties, although there was no chemical crosslinking. Depending on the LiCl concentration, these hydrogel films exhibited lower protein adhesion and higher coagulation time for the biocompatibility. Even though, very good cytocompatibility was resulted in the hydrogel films relative to reference PS dish. It was proved that the LiCl acted to be dense networks of the agave cellulose segments. Thus, the hydrogel forms influenced in vitro cyto and biocompatibility.

In **Chapter 4**, Bamboo fibers were used as source to prepare cellulose hydrogel films for cell cultivation scaffold. The preparation of cellulose solutions was carried out by three different dissolving methods with NaOH-based and NaOH/urea aqueous solutions and DMAc/LiCl solution. Cellulose hydrogel films from bamboo fibers dissolved by three different methods were obtained. Depending of the dissolving method used, hydrogel film exhibited lower tensile strength, elongation and contact angle in the case of NaOH and NaOH/urea systems. On the other hand, very good cytocompatibility was observed in the hydrogel films elaborated with DMAc/LiCl solution. It was proved that the dissolving method used for the preparation of the cellulose solution affects the properties of the obtained films. These results suggest that hydrogel

films elaborated with cellulose solution prepared with DMAc/LiCl showed better possibility of usage for tissue engineering scaffold. Depending on the LiCl and type of fiber used, these hydrogels exhibited different bio and cytocompatibility. All the obtained hydrogel films presented higher cytocompatibility compared with PS dish used as control. It was proved that LiCl acted to be dense networks of the cellulose segments, according with the SAXS results. These results indicated that the property of the hydrogel films affects the adhesion and spreading of the fibroblast cells.

In **Chapter 5**, pulp fibers were used as source to develop cellulose hydrogel films using DMAc/LiCl system to obtain flexible and transparent hydrogel films without chemical crosslinking. LiCl content was varied from 4 to 12 wt%. The cellulose hydrogel film had better mechanical properties, although there was no chemical crosslinking. Depending on the LiCl concentration, these hydrogel films exhibited lower protein adhesion and higher coagulation time for the biocompatibility. In addition, very good cytocompatibility was resulted in the hydrogel films prepared at 4 wt% of LiCl. It was proved that the LiCl acted to be dense networks of the cellulose segments and the hydrogel condition influenced in vitro cyto and biocompatibility.

In **Chapter 6**, Biohydrogel interpenetrated films of wooden pulp cellulose and hydroxyethyl cellulose (HEC) was prepared and their biomedical properties were investigated. The interpenetrated hydrogel film had better mechanical properties without chemical crosslinking, although the hydrogel contained higher water in the films. It was proved that the HEC acted to interfere with the interpenetrated interaction into the aggregated pulp fibers. Depending on the HEC content, these hydrogel films exhibited lower protein adsorption and higher clotting time. The platelet adhesion observed on films with higher HEC content decreased. Moreover, films with lower HEC showed better cytocompatibility. In addition, all the obtained films showed

better cytocompatibility than the tissue culture grade polystyrene dish (PS dish) used as control however lower HEC seems to improve cyto and biocompatibility.

List of Achievements

1. Industrial & Engineering Chemistry Research (I&EC), 52, (2013), 11607-11613. **Fibroblast Compatibility on Scaffold Hydrogels Prepared from Agave Tequilana Weber Bagasse for Tissue Regeneration**, Karla L. Tovar-Carrillo, Satoshi Sugita Sueyoshi, Motohiro Tagaya, and Takaomi Kobayashi.

2. Journal of Materials Science and Chemical Engineering, 1, (2013), 7-12. **Bamboo Fibers Elaborating Cellulose Hydrogel Films for Medical Applications**, *Karla Lizette Tovar-Carrillo*, Motohiro Tagaya, Takaomi Kobayashi.

3. Industrial & Engineering Chemistry Research (I&EC), **Biohydrogels interpenetrated with hydroxyethyl cellulose and wooden pulp for biocompatible materials**, Karla L. Tovar-Carrillo, Motohiro Tagaya, and Takaomi Kobayashi. doi. Org/10.102/ie403257a *In press* (2014).

Other Related Papers

1. Proceedings IMRC 2013, **Biopolymer Hydrogels Regenerated from Agave Tequilana Waste for Cytocompatible Materials**, Takaomi Kobayashi, Karla L. Tovar-Carrillo, Motohiro Tagaya.

Presentation in International Conference and Symposium

1. Karla Tovar; Jorge Contreras, Rosa Saucedo, Takaomi Kobayashi, Kyoko Uemura, Kazuki Nakasone, Armando Zaragoza. "Surface characterization of hydroxyethyl cellulose: Polyvinyl alcohol hydrogels development by regeneration of adipose tissue". **2010 International Chemical Congress of Pacific Basin Societies (PACIFICHEM 2010)**, December 15-20 (Honolulu, Hawaii, USA).

2. Karla, T.; Tagaya, M.; Kobayashi, T. "Preparation of Pulp/Hydroxyethyl Cellulose Composite Gels and the Application for Biomaterials" [Session: GIGAKU & Material Design] **The 1st International GIGAKU Conference in Nagaoka (IGCN)**, February 2012 (Nagaoka, Niigata, Japan).

3. Karla, T.; Tagaya, M.; Kobayashi T. "Study of Biomaterial Sheets Made of Pulp/Hydroxymethyl Cellulose for a Purpose of Biocompatibility" **5th Symposium on Japan-Mexico USA Consortium for Technological Engineering**, November 2011 (University of Guanajuato, Gto., Mexico).

4. Karla Tovar, Motohiro Tagaya, Takaomi Kobayashi. "Preparation and cytocompatible properties of agave tequilana cellulose films for biomaterial applications". **The 2nd Joint symposium CU-NUT, Octuber 2012** (Faculty of Science, Chulalongkorn University Bangkok, Thailand).

5. Karla L. Tovar-Carrillo, Motohiro Tagaya, Takaomi Kobayashi. "Utilization of agave Bagasse for highly-cytocompatible cellulose membranes". **第 61 回高分子学会北陸支部研究発表会**. November 2012 (Fukui, Japan).

6. 長岡技科大工,羽多野千尋, Tovar-Carrillo Karla L,"多賀谷基博,小林高臣　海苔由来ポルフィランハイドロゲルの線維芽細胞の親和性評価". **第 61 回高分子学会北陸支部研究発表会**. November 2012 (Fukui, Japan).

7. Karla, T.; Tagaya, M.; Kobayashi, T. "Cytocompatible Agave Tequilana Cellulose Used as Scaffold Films for Tissue Regeneration" [Session: GIGAKU & Material Design] **The 2st International GIGAKU Conference in Nagaoka (IGCN)**, June 21-23, 2012 (Nagaoka, Niigata, Japan).

8. Karla, T.; Tagaya, M.; Kobayashi, T. "Comparation of Cyto and Biocompatible Properties of Hydrogel Prepared from Agave Tequilana, Sugarcane and Bamboo Cellulose for Medical Applications". **第 62 回高分子学会北陸支部研究発表会**.November 15, 2013 (Nagaoka, Niigata, Japan).